

Carbohydrate Metabolism in *Archaea*: Current Insights into Unusual Enzymes and Pathways and Their Regulation

Christopher Bräsen, Dominik Esser, Bernadette Rauch, Bettina Siebers

Molecular Enzyme Technology and Biochemistry, Biofilm Centre, Faculty of Chemistry, University of Duisburg-Essen, Essen, Germany

SUMMARY	91
INTRODUCTION	91
MODIFICATIONS OF THE EMBDEN-MEYERHOF-PARNAS PATHWAY IN ARCHAEA	92
Glucose Phosphorylation	94
ADP-dependent glucokinase	94
ROK hexokinase	95
Other archaeal sugar kinases	95
Phosphoglucose Isomerase	98
Phosphoglucose isomerase/phosphomannose isomerase	98
Cupin-type phosphoglucose isomerase	100
Phosphofructokinase	100
Pyrophosphate-dependent phosphofructokinase	100
ADP-dependent phosphofructokinase	100
ATP-dependent phosphofructokinase (PFK-B)	101
Fructose-1,6-Bisphosphate Aldolase (Catabolic)	101
Triosephosphate Isomerase	102
Glyceraldehyde 3-Phosphate Oxidation	103
Glyceraldehyde-3-phosphate:ferredoxin oxidoreductase	104
Nonphosphorylating glyceraldehyde-3-phosphate dehydrogenase	104
Glyceraldehyde-3-phosphate dehydrogenase (phosphorylating) (catabolic)	105
Phosphoglycerate Kinase	106
Phosphoglycerate Mutase	107
2,3-Bisphosphoglycerate cofactor-dependent phosphoglycerate mutase	107
Cofactor-independent phosphoglycerate mutase	107
Enolase	108
Phosphoenolpyruvate Conversion to Pyruvate	108
Pyruvate kinase	108
MODIFICATIONS OF THE ENTNER-DOUDOROFF PATHWAY IN ARCHAEA	109
Glucose Dehydrogenase	110
Gluconate Dehydratase	113
2-Keto-3-Deoxygluconate Kinase	114
2-Keto-3-Deoxy-(6-Phospho)Gluconate Aldolase [KD(P)GA]	114
GAP Conversion	115
Glyceraldehyde dehydrogenase/(glycer)aldehyde:ferredoxin oxidoreductase	115
Glycerate Kinase	116
GLUCONEOGENESIS	116
Phosphoenolpyruvate Synthetase	116
Pyruvate:Phosphate Dikinase	117
Phosphoenolpyruvate Carboxykinase	117
Glyceraldehyde-3-Phosphate Dehydrogenase/Phosphoglycerate Kinase	119
Bifunctional Fructose-1,6-Bisphosphate Aldolase/Phosphatase	119
PENTOSE DEGRADATION PATHWAYS IN ARCHAEA	120
Pentose Oxidation and Xylose Dehydrogenase/Arabinose Dehydrogenase	122
C ₅ Sugar Acid Dehydration and Xylonate Dehydratase/Arabinonate Dehydratase	125
2-Keto-3-Deoxyxylonate Dehydratase/2-Keto-3-Deoxyarabinonate Dehydratase	126
α-Ketoglutarate Semialdehyde Dehydrogenase	126
2-Keto-3-Deoxyxylonate (KDX)/2-Keto-3-Deoxyarabinonate (KDA) Cleavage	127
Conversion of Glycolaldehyde to Malate	127

(continued)

Address correspondence to Christopher Bräsen, christopher.braesen@uni-due.de, or Bettina Siebers, bettina.siebers@uni-due.de.

Copyright © 2014, American Society for Microbiology. All Rights Reserved.

doi:10.1128/MMBR.00041-13

PENTOSE SYNTHESIS PATHWAYS IN ARCHAEA	127
Hexulosephosphate Synthase/Phosphohexulose Isomerase.....	129
Ribose-5-Phosphate Isomerase.....	129
Transketolase.....	132
Alternative Pathways for C ₅ -C ₃ Interconversion.....	132
METABOLIC AND REGULATORY CHARACTERISTICS OF WELL-STUDIED ARCHAEOAL MODEL ORGANISMS.....	132
Regulation at the Transcript Level.....	132
Regulation at the Protein Level.....	133
Metabolic Thermoadaptation.....	133
<i>Thermococcales</i> (<i>Pyrococcus furius</i> and <i>Thermococcus kodakarensis</i>).....	134
Growth conditions.....	134
Sugar transport	134
Sugar metabolism	135
(i) The modified EMP pathway	135
(ii) Gluconeogenesis	135
Energetics.....	137
Regulation at the protein level.....	137
Regulation at the gene level.....	137
Transcriptional regulator TrmB in <i>Thermococcales</i>	138
TrmB-like regulators in <i>Thermococcales</i>	139
(i) TrmB-like regulators in <i>Tco. kodakarensis</i>	139
(ii) TrmB-like regulators in <i>Pyrococcus furius</i>	140
In vivo function of TrmB and TrmB-like regulators in <i>Pyrococcus</i>	140
<i>Sulfolobus solfataricus</i>	140
Growth conditions.....	140
Sugar transport	143
Sugar metabolism	143
(i) The promiscuous branched ED pathway	143
(ii) Significance of both ED branches	144
(iii) Gluconeogenesis	144
Energetics.....	144
Regulation	144
(i) Regulation at the enzyme level by allosteric effectors.....	144
(ii) Regulation at the translational level.....	145
(iii) Regulation at the posttranslational level by protein phosphorylation.....	145
(iv) Regulation at the gene/transcript level	146
Transcriptional regulators of the central carbohydrate metabolism.....	146
<i>Thermoplasmatales</i> (<i>Thermoplasma acidophilum</i> and <i>Picrophilus torridus</i>)	147
Growth conditions.....	147
Sugar (glucose) metabolism	147
Energetics.....	147
First insights into regulation at the protein and gene levels.....	147
<i>Thermoproteus tenax</i>	148
Growth conditions.....	148
Sugar transport	148
Sugar (glucose) metabolism	148
(i) The modified EMP pathway	148
(ii) The branched ED pathway.....	150
(iii) Gluconeogenesis	150
Energetics.....	150
Regulation at the protein and gene levels.....	150
(i) Regulation at the enzyme level by allosteric effectors.....	150
(ii) Regulation at the gene/transcript level	151
<i>Haloarchaea</i> (<i>Haloferax volcanii</i> , <i>Haloarcula marismortui</i> , and <i>Halobacterium salinarum</i>)	152
Growth conditions.....	152
Sugar transport	152
Sugar metabolism	152
(i) Different degradation pathways for glucose and fructose	152
(ii) Glucose-fructose diauxie.....	154
Energetics.....	154
Regulation at the gene and protein levels.....	154
Glycerol-mediated catabolite repression	155
Transcriptional regulator GlpR	155
<i>Halobacterium salinarum</i>	155
(i) TrmB-like transcriptional regulator	155
Methanogens	156

(continued)

Growth conditions.....	156
Sugar (endogenous glycogen) metabolism	157
Energetics.....	157
Regulation at the gene and protein levels.....	157
CONCLUSION.....	159
ACKNOWLEDGMENTS.....	159
REFERENCES.....	159

SUMMARY

The metabolism of *Archaea*, the third domain of life, resembles in its complexity those of *Bacteria* and lower *Eukarya*. However, this metabolic complexity in *Archaea* is accompanied by the absence of many “classical” pathways, particularly in central carbohydrate metabolism. Instead, *Archaea* are characterized by the presence of unique, modified variants of classical pathways such as the Embden-Meyerhof-Parnas (EMP) pathway and the Entner-Doudoroff (ED) pathway. The pentose phosphate pathway is only partly present (if at all), and pentose degradation also significantly differs from that known for bacterial model organisms. These modifications are accompanied by the invention of “new,” unusual enzymes which cause fundamental consequences for the underlying regulatory principles, and classical allosteric regulation sites well established in *Bacteria* and *Eukarya* are lost. The aim of this review is to present the current understanding of central carbohydrate metabolic pathways and their regulation in *Archaea*. In order to give an overview of their complexity, pathway modifications are discussed with respect to unusual archaeal biocatalysts, their structural and mechanistic characteristics, and their regulatory properties in comparison to their classic counterparts from *Bacteria* and *Eukarya*. Furthermore, an overview focusing on hexose metabolic, i.e., glycolytic as well as gluconeogenic, pathways identified in archaeal model organisms is given. Their energy gain is discussed, and new insights into different levels of regulation that have been observed so far, including the transcript and protein levels (e.g., gene regulation, known transcription regulators, and posttranslational modification via reversible protein phosphorylation), are presented.

INTRODUCTION

Archaea were established as the third domain of life besides *Bacteria* and *Eukarya* only 30 years ago (1, 2). To date, most cultivable species are adapted to extreme environments, where they constitute the dominant majority, or harbor unique metabolic capabilities like methanogens. The so-called “extremophiles” thrive in hostile habitats characterized by extremes of temperature, pH, salt, or combinations thereof. However, metagenomic/environmental molecular biology approaches revealed that *Archaea* are ubiquitous and widely distributed in moderate habitats and play a major role in geochemical cycles (3–5).

Archaea exhibit a mosaic character, as they share some typical bacterial and eukaryotic properties. Their unicellular life-style, lack of organelles, cell size and shape, as well as DNA structure (e.g., one circular chromosome, operon structures, and plasmids) resemble those of *Bacteria*, whereas most mechanisms involved in information processing (e.g., replication, transcription, repair, and translation) are generally regarded as less complex versions of the respective eukaryotic equivalents (6–12). However, *Archaea* also possess unique archaeal features, most notably the unique

archaeal membrane lipids composed of isoprenoid chains ether linked to *sn*-glycerol 1-phosphate head groups (i.e., dibiphytanylethers or biphytanylethers) rather than fatty acids ester linked to *sn*-glycerol 3-phosphate, as found in *Bacteria* and *Eukarya* (13). In addition, murein, the typical peptidoglycan of bacterial cell walls, is absent in *Archaea*, and, for example, pseudomurein (e.g., *Methanospaera* and *Methanothermus*), S-layer proteins (e.g., *Thermoproteus* spp. and *Sulfobolales*), or no cell envelopes (e.g., *Thermoplasmatales*) are found.

With respect to their life-style and metabolic complexity, *Archaea* resemble *Bacteria* and lower *Eukarya*, and chemolithoautotrophic, chemoorganoheterotrophic, as well as phototrophic (aerobic/anaerobic) growth has been reported (14, 15). However, this metabolic complexity in *Archaea* is accompanied by the absence of many “classical” pathways known for *Bacteria* and *Eukarya*. Instead, *Archaea* are characterized by the presence of unique pathways, e.g., methanogenesis, and/or by some unusual, modified-pathway versions of the classical routes. This especially applies to central carbohydrate metabolism (CCM). Only modified variants of classical sugar degradation pathways such as the Embden-Meyerhof-Parnas (EMP) pathway and the Entner-Doudoroff (ED) pathway have been identified in *Archaea*. The pentose phosphate pathway (PPP) is present only partly (if at all), and pentose degradation significantly differs from that known for bacterial model organisms such as *Escherichia coli*. Particularly, the modifications and distinct features of the sugar degradation pathways cause fundamental consequences for the underlying regulatory principles.

Notably, the vast majority of metabolic conversions and, thus, intermediates found in the glycolytic and also gluconeogenic pathways for glucose-to-pyruvate interconversion are conserved in all three domains of life, highlighting government by thermodynamic and chemical constraints (e.g., flux rates/short pathways) (16). However, in *Archaea*, the enzymes involved in their conversion often share no similarity with their bacterial and eukaryotic counterparts and represent members of new enzyme families. Accordingly, by using a comparative genomics approach, the “central core and variable shell” of archaeal genomes were established, and several missing links in archaeal central metabolism were identified, which are conserved in bacterial and eukaryotic metabolism (17, 18). These identified “gaps” in archaeal central metabolic pathways are the product of nonhomologous gene replacement. In the meantime, many of these pathway holes have been closed by the identification of the respective candidates by using comparative genomics-based approaches and/or classical biochemistry.

Today, 267 archaeal genome sequences have been completed (as of December 2013) (Genome Online Database [GOLD] [<http://genomesonline.org/>]), and six main archaeal phyla have been proposed: *Crenarchaeota*, *Euryarchaeota*, *Nanoarchaeota*, *Thaumarchaeota*, *Korarchaeota*, and the recently proposed *Aigarchaeota*.

The two largest and first-established phyla are the *Euryarchaeota* and the *Crenarchaeota* (2). The *Euryarchaeota* comprise all methanogens and extreme halophiles and some thermoacidophiles and (hyper)thermophiles, whereas the *Crenarchaeota* contain only (hyper)thermophilic species (2). The *Nanoarchaeota* comprise only two species so far: *Nanoarchaeum equitans*, which can be grown only in coculture with the crenarchaeote *Ignicoccus hospitalis*, and Nst1, where the likely host is a member of the *Sulfolobales* (Acd1) (19, 20). The *Korarchaeota* instead contain only uncultivated hyperthermophilic, anaerobic *Archaea*, and the heterotrophic organism “*Candidatus Korarchaeum cryptofilum*” is the first proposed member of this group (21, 22). Members of the *Thaumarchaeota* are both thermophiles and mesophiles and thrive in very different environmental niches (e.g., freshwater, soil, ocean, and hot springs) (23, 24). All members of this phylum characterized so far (e.g., *Nitrososphaera gargensis*, *Nitrosopumilus maritimus*, and *Cenarchaeum symbiosum*) are chemolithoautotrophic ammonia oxidizers, which was thought to be performed solely by *Betaproteobacteria* and *Gammaproteobacteria* (24). HWCG1 is the only identified member of the *Aigarchaeota* so far (25). However, whether the *Aigarchaeota* are indeed a new archaeal phylum or a deeply branching thaumarchaeal lineage is still a matter of debate (26).

Whereas the carbohydrate metabolism of members of the *Crenarchaeota* and *Euryarchaeota* has been studied in considerable detail, only little information is available for the remaining archaeal phyla. In *Archaea*, sugar degradation was first investigated in aerobic extreme halophiles, such as *Halobacterium* sp. and *Halocula*, and thermophilic acidophiles, e.g., the euryarchaeon *Thermoplasma acidophilum* and the crenarchaeon *Sulfolobus solfataricus*. In the early 1990s, anaerobic hyperthermophiles, including the fermentatively growing euryarchaeon *Pyrococcus furiosus* and the crenarchaeon *Thermoproteus tenax*, growing on sugars by means of sulfur respiration, were also extensively investigated, and these studies have been extended to other anaerobic hyperthermophiles such as members of the *Euryarchaeota* (*Thermococcus* spp. and *Archaeoglobus fulgidus*) and the *Crenarchaeota* (*Desulfurococcus amylolyticus* and the [micro]aerophilic/aerobic organisms *Pyrobaculum aerophilum* and *Aeropyrum pernix*). Also, the most acidophilic organism known to date, the moderately thermophilic euryarchaeon *Picrophilus torridus*, has been investigated, and the role of sugar-metabolizing routes in some methanogenic organisms, such as *Methanococcus maripaludis* and *Methanocaldococcus jannaschii*, have been addressed.

By using ¹³C nuclear magnetic resonance (NMR) analyses, the question of pathway utilization, i.e., whether the EMP pathway, the ED pathway, or both routes are utilized for sugar degradation in the respective organisms, and to which extent, has been addressed. With classical biochemical techniques like enzyme measurements in crude extracts, native protein purification, as well as comparative genome analyses and with molecular biological methods like recombinant expression of candidate enzymes, the pathways could be reconstructed. The enzymes involved in the pathways have been identified and characterized, and the structures of more and more of the archaeal enzymes involved in sugar metabolism have been determined. Also, “genetic toolboxes” for a number of archaeal model organisms, e.g., *Haloferax volcanii*, *Thermococcus kodakarensis*, *Sul. solfataricus*, *Sulfolobus acidocaldarius*, and *Pyr. furiosus*, as well as methanogens such as *Methanococcus* spp. and *Methanosa*cina spp. have been established, and

the physiological significance of genes could be studied by mutant construction (for reviews and literature, see references 27 and 28). Furthermore, transcriptomic (microarray analyses and deep sequencing in combination with reverse transcription-quantitative PCR [qRT-PCR]), proteomic, and metabolomic as well as systems biology approaches were also used for *Archaea*, facilitating the investigation of pathway regulation and underlying principles.

The aim of this review is to present the current understanding of sugar degradation pathways and their regulation in *Archaea*. In order to give an overview of the complexity, this review is subdivided into two parts. The first part focuses on pathway modification with respect to unusual archaeal biocatalysts, their structural and mechanistic characteristics, and their regulatory properties in comparison to their classic counterparts from *Bacteria* and *Eukarya*. In the second part, an overview focusing on hexose metabolic pathways, i.e., glycolysis as well as gluconeogenesis, identified in archaeal model organisms is given. Their energy gain is discussed, and new insights into the different levels of regulation that have been observed so far, including the transcript and protein levels (e.g., gene regulation, known transcription regulators, and posttranslational modification [PTM] via reversible protein phosphorylation), are presented (for previous reviews in the field of archaeal central carbohydrate metabolism, see references 14 and 29–37) (see Fig. 1 and 12 for the most frequently used abbreviations for enzymes and metabolic intermediates).

MODIFICATIONS OF THE EMBDEN-MEYERHOF-PARNAS PATHWAY IN ARCHAEA

The EMP pathway can be regarded as an evolutionarily optimized pathway for the conversion/oxidation of glucose to 2 molecules of pyruvate, yielding ATP as well as reducing equivalents and intermediates as precursors for cellular building blocks. Pathway optimization means that product formation is achieved in the fewest possible steps with overall exergonism to drive the whole process. The aim is to ensure the highest possible effectivity/fluxes on the one hand and to enable the highest possible energy/ATP yields on the other hand. These purposes are achieved under the consideration of chemical and mechanistic feasibilities as well as the physicochemical properties of intermediates with respect to, e.g., stability, permeability, polarity, and toxicity (16, 38).

In the classical EMP pathway, glucose is phosphorylated to glucose 6-phosphate (G6P) either by ATP-dependent hexokinase (HK)/glucokinase (GLK) or, in many *Bacteria*, by the action of the phosphoenolpyruvate (PEP) phosphotransferase system (PTS). G6P is then isomerized to fructose 6-phosphate (F6P) via phosphoglucose isomerase and is again phosphorylated to form fructose 1,6-bisphosphate (F1,6BP), a key intermediate of the EMP pathway, by phosphofructokinase. F1,6BP is cleaved to dihydroxyacetone phosphate (DHAP) and glyceraldehyde 3-phosphate (GAP), catalyzed by F1,6BP aldolase. DHAP is converted to GAP via triosephosphate isomerase (TIM), and GAP is oxidized to 1,3-bisphosphoglycerate (1,3BPG) through the action of glyceraldehyde-3-phosphate dehydrogenase (GAPDH), yielding NAD(P)H. The phosphate moiety from the acid anhydride 1,3BPG is transferred to ADP, yielding ATP in the first step of substrate-level phosphorylation within the pathway, catalyzed by phosphoglycerate kinase (PGK). The resulting 3-phosphoglycerate (3PG) is further converted to 2-phosphoglycerate (2PG) and the phosphoenolester PEP via phosphoglycerate mutase (PGAM) and enolase (ENO). From PEP, the phosphate moiety is again transferred

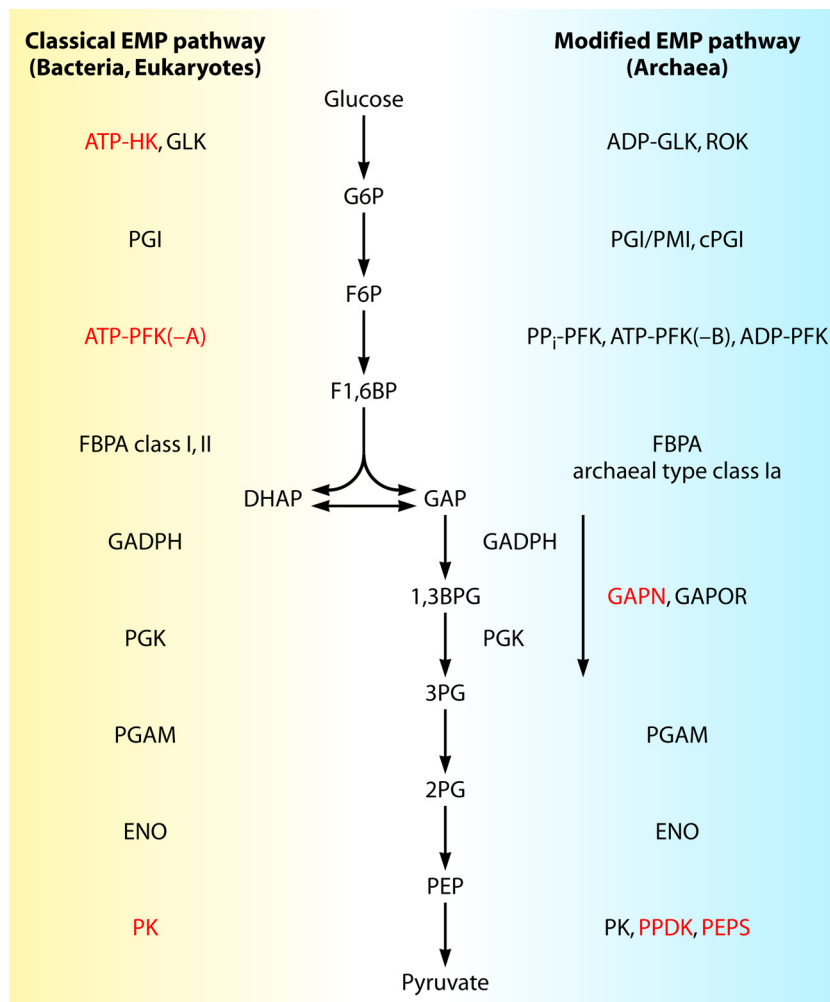


FIG 1 Glucose degradation via the EMP pathway known for most *Bacteria* and *Eukarya* (classical) and the modified EMP versions reported for *Archaea*. Allosterically regulated enzymes are depicted in red. Abbreviations: ENO, enolase; FBPA, fructose-1,6-bisphosphate aldolase; GADPH, glyceraldehyde-3-phosphate dehydrogenase; GAPN, nonphosphorylating GAPDH; GAPOR, GAP:Fd oxidoreductase; GLK, glucose kinase; HK, hexokinase; PEPS, PEP synthetase; PFK, phosphofructokinase; PGI, phosphoglucomutase; PGAM, phosphoglycerate mutase (dPGAM, 2,3-bisphosphoglycerate [2,3BPG] cofactor independent); PGK, phosphoglycerate kinase; PGAM, phosphoglycerate mutase (dPGAM, 2,3-bisphosphoglycerate [2,3BPG] cofactor independent); PK, pyruvate kinase; PPDK, pyruvate:phosphate dikinase; ROK, hexokinase of the repressor protein, open reading frame, sugar kinase family; G6P, glucose 6-phosphate; F6P, fructose 6-phosphate; F1,6BP, fructose 1,6-bisphosphate; DHAP, dihydroxyacetone phosphate; GAP, glyceraldehyde 3-phosphate; 1,3BPG, 1,3-bisphosphoglycerate; 3PG, 3-phosphoglycerate; 2PG, 2-phosphoglycerate; PEP, phosphoenolpyruvate.

to ADP via substrate-level phosphorylation to finally form pyruvate in the pyruvate kinase (PK)-catalyzed reaction (for an overview, see Fig. 1). Thus, the conversion of 2 mol GAP to pyruvate yields 4 mol ATP in the PGK and PK reactions, and 2 mol ATP has to be invested for phosphorylation of glucose and F6P in the preparatory phase of glycolysis, resulting in a net yield of 2 mol ATP per mol glucose oxidized to pyruvate. Within this pathway, phosphorylation from glucose to G6P and from F6P to F1,6BP as well as pyruvate formation from PEP represent irreversible steps, and the enzymes involved are accordingly the main points of allosteric regulation. Also, these irreversible reactions, especially the PK and phosphofructokinase (PFK) reactions, have to be bypassed during gluconeogenesis. This is usually accomplished by PEP synthetase (PEPS), pyruvate:phosphate dikinase (PPDK), or the pyruvate carboxylase/PEP carboxykinase (PCK) enzyme couple for the PK reaction and fructose bisphosphatase (FBPase) for the PFK reaction.

Due to its comparatively high energy yield of maximally 2 mol ATP/mol of glucose, the utilization of the EMP pathway is particularly advantageous for organisms with an anaerobic or facultatively anaerobic life-style gaining energy mainly by fermentative metabolism from sugars/glucose. Accordingly, by using ¹³C NMR studies in combination with enzyme measurements in crude extracts, the anaerobic hyperthermophiles, the *Euryarchaeota Pyrofurosus* and *Thermococcus* spp., and the crenarchaeon *Desulfurococcus* fermentatively growing on sugars have been shown to degrade glucose 100% via modified EMP pathways. Also, the crenarchaeon *Tpt. tenax*, growing on glucose using sulfur reduction, metabolizes the sugar 85% via an EMP pathway modification (39, 40). For the anaerobic, euryarchaeal sulfate reducer *Arc. fulgidus* as well as the microaerophilic *Crenarchaeota Pyb. aerophilum* and *Aer. pernix*, modified EMP versions have also been described on the basis of enzyme analyses (41, 42). Underlining the optimized properties of the EMP pathway and the thermodynamic, kinetic,

and mechanistic constraints under which the pathway evolved, glucose degradation via these modified EMP pathway versions in *Archaea* basically proceeds via the same intermediates known for the classical EMP pathway in *Bacteria* and *Eukarya*, also highlighting the ancestral character of the pathway. However, although catalyzing the same conversions, the enzymes in archaeal EMP pathway versions differ remarkably (see Fig. 1 for a comparative illustration of the classical EMP pathway and the modified archaeal versions). The pathway modifications occur mainly in the upper part of the archaeal pathways, involving ADP-, PP_i-, or ATP-dependent kinases, distinct from the classical enzymes in *Bacteria* and *Eukarya*. Also, the phosphoglucose isomerases as well as the fructose-1,6-bisphosphate aldolases in *Archaea* differ from their bacterial and eukaryotic counterparts. The most striking difference in archaeal pathways, especially in (hyper)thermophiles, is the direct and irreversible oxidation of GAP to 3PG, catalyzed either by NAD(P)⁺-dependent nonphosphorylating glyceraldehyde-3-phosphate dehydrogenase (GAPN) or, mainly in anaerobes, by ferredoxin (Fd)-dependent glyceraldehyde-3-phosphate oxidoreductase (GAPOR). Both enzymes omit the formation of 1,3-bisphosphoglycerate and the production of ATP via substrate-level phosphorylation, with considerable consequences for pathway energetics. Reduced ferredoxin (Fd_{red}) can serve as an electron donor in anabolic reactions instead of or at least in combination with NAD(P)H. The utilization of ferredoxin also allows for additional energy conservation via H₂ generation by means of membrane-bound hydrogenase, which is especially advantageous under anaerobic conditions. Despite the energetics, the EMP pathway modifications in *Archaea* also strongly influence their regulation. The classical sites of allosteric regulation in *Bacteria* and *Eukarya*, i.e., particularly HK and ATP-PFK (PFK-A) (see below), are replaced in archaeal pathways. Also, the archaeal PKs show strongly altered (if any) regulatory properties (see below). Instead, as known so far, GAPN, mainly found in (hyper)thermophilic *Archaea*, represents the main site of allosteric regulation.

As outlined below, the unusual enzymes in the archaeal pathway modifications represent mostly examples of nonhomologous gene replacements rather than novel inventions (30). In contrast to the modifications in the upper part of the archaeal EMP variants, the enzymes in the lower part, with the exception of catabolic GAPOR and GAPN, i.e., TIM, PGAM, ENO, and PK, are homologous to their classical counterparts in *Bacteria* and *Eukarya*. Also, the GAPDH/PGK couple, which is present in *Archaea* (except for extreme halophiles and some methanogens) exclusively for anabolic purposes (see Gluconeogenesis, below), corresponds well to its classical counterparts. Furthermore, the phylogenies of these universally distributed enzymes show distinct archaeal clusters, whereas the bacterial and eukaryotic proteins appeared to be more closely related and less distinct, presumably due to an endosymbiotic origin and lateral gene transfer events, respectively. The universal distribution and homology of the enzymes of the lower part of the glycolysis pathway in combination with their low evolutionary rates have been taken as a strong indication that the EMP pathway evolved in the gluconeogenic direction (43).

In the following sections, we describe step by step the archaeal biocatalysts of the upper and the lower shunts of the EMP pathway in comparison to their bacterial and eukaryotic counterparts, with special reference to structural and mechanistic characteristics (Table 1 gives an overview of all the enzymes involved in the modified

archaeal EMP pathway versions as well as the classical EMP pathway from *Bacteria* and *Eukarya*).

Glucose Phosphorylation

The first step in the modified EM pathways of *Archaea* is the phosphorylation of glucose to glucose 6-phosphate. In *Bacteria*, this process is coupled to transport via the PEP phosphotransferase system or is catalyzed by glucose and ATP-specific glucokinases, whereas in *Eukarya*, this reaction is catalyzed by ATP-specific hexokinases, which usually show broad substrate specificity for a variety of other sugars, like fructose, mannose, and galactose (44, 45). Conversely, the bacterial ATP-dependent glucokinases show a pronounced specificity for their respective sugar substrates (for literature, see reference 46). Both the eukaryotic hexokinases as well as the bacterial glucokinases constitute distinct families within the actin-like ATPase domain superfamily. Members of this superfamily share a similar overall fold consisting of a large domain (five-stranded mixed β sheet faced by five α helices on one side of the sheet) and a small domain (five-stranded mixed β sheet surrounded by three α helices, two on one side and one on the other side of the sheet). The active site is located at the domain interface, and upon substrate binding, the conformation changes to its closed state through domain movement (44). On the basis of crystal structures (47–49) and the results of mutagenesis studies (50), the catalytic mechanism for sugar kinases from the actin-like ATPase domain superfamily has been proposed to involve a conserved Asp (i.e., Asp657 in human hexokinase I) that abstracts the proton from the 6-hydroxyl group of glucose as a catalytic base. This enables a nucleophilic attack of the γ-phosphorus of ATP on the activated 6-oxygen of glucose, finally yielding G6P (see Fig. 3). The positive charges of Arg539 and a Mg²⁺ ion are proposed to stabilize the reaction intermediate. These catalytic residues are structurally conserved in the sugar kinases of the actin-like ATPase domain superfamily. In *Archaea*, two different mechanisms of glucose phosphorylation have been described.

ADP-dependent glucokinase. In *Euryarchaeota* such as *Pyr. furiosus*, *Thermococcus litoralis*, and *Arc. fulgidus*, glucose phosphorylation is carried out by ADP-dependent glucokinases (ADP-GLKs). These enzymes show high specificity for glucose (51–55) and belong to the ribokinase superfamily. Conversely, in the *Crenarchaeota* *Tpt. tenax*, *Pyrobaculum islandicum*, *Pyb. aerophilum*, *Aer. pernix*, and *Des. amylolyticus*, this process is ATP dependent (ADP forming), involving an ATP-dependent hexokinase with a broad hexose substrate spectrum, as shown for the enzymes of *Aer. pernix* and *Tpt. tenax* (40, 41, 46, 55). These ATP-dependent archaeal hexokinases belong to the ROK (repressor protein, open reading frame, sugar kinase) family (see below). Whereas classical eukaryotic hexokinases represent monomeric, and sometimes dimeric, proteins (subunit size of ~50 or 100 kDa), and the bacterial ATP-dependent glucokinases are dimers composed of ~30-kDa subunits, the archaeal ADP-GLKs have been biochemically characterized as monomeric enzymes (subunit of ~50 kDa) (44–46, 51, 53–56).

Archaeal ADP-GLKs prefer ADP as the phosphoryl donor and additionally also utilize CDP but not GDP, IDP, or UDP (57). The *Arc. fulgidus* enzyme appears to be specific for ADP (51, 53, 54). The bifunctional ADP-GLK/PFK from *Mca. jannaschii* also utilizes GDP (40%) in addition to ADP (100%) and, less efficiently, CDP (14%) (58). The crystal structures of archaeal ADP-GLKs from *Pyr. furiosus*, *Pyrococcus horikoshii*, and *Tco. litoralis* have

been solved, identifying the archaeal ADP-GLKs as members of the ADP-dependent sugar kinase family within the ribokinase superfamily (59–61). The basic fold of ADP-GLK is composed of one large domain and an additional small domain, with the active site located at the domain interface (Fig. 2A). The nucleotide binding site lies within the large domain, and the sugar binding site lies in a cleft between both domains. The larger domain consists of a twisted 11- to 12-stranded β sheet flanked on both faces by 13 α helices and 3 β_{10} helices, forming an α/β 3-layer sandwich. The smaller domain, which covers the active site, forms an α/β two-layer structure containing 5 to 7 β strands and 4 α helices on the far side of the active-site cleft of the sheet (56, 59–61). The large domain represents the ribokinase core fold, which typically consists of an eight-stranded β sheet surrounded by eight α helices, three on one side and five on the other side of the sheet (57). Upon sugar binding, the small domain undergoes a conformational change, closing the active site (59, 61). Although the “classical” hexokinases in *Eukarya* have been described to possess a similar two-domain architecture and to follow a comparable catalytic mechanism, there are no similarities between ADP-GLKs and hexokinases either on the sequence level or in the fold of both domains (44, 45, 57). ADP-GLKs contain two sequence motifs, i.e., GXGD and NXXE, highly conserved in members of the ribokinase superfamily and involved in catalysis (57). The aspartate residue of the GXGD motif has been proposed to act in sugar binding and as a general base during the catalytic cycle (proton abstraction from the acceptor hydroxyl group) (57, 59) (Fig. 3). Asparagine and glutamate of the NXXE motif are proposed to be involved in bivalent metal cation and nucleotide binding (57, 62). ADP-GLKs depend strictly on bivalent metal ions, which coordinate proper nucleotide binding and positioning of the phosphate groups for the phosphoryl transfer reaction (51, 53, 54, 57, 62). Recently, a third motif (HXE), with a highly conserved glutamate involved in metal ion coordination, has been identified. Furthermore, binding of a second metal ion to another conserved sequence motif in ADP-dependent sugar kinases with regulatory implications has been proposed (62). However, all of the ADP-dependent sugar kinases, including those from *Archaea* reported so far, did not show any regulatory properties like cooperativity or allosteric control, thus differing from eukaryotic hexokinases, which represent one of the sites of allosteric control in the classical EMP pathway (56).

ROK hexokinase. The second mechanism of glucose phosphorylation in *Archaea* is catalyzed by ATP-dependent kinases with broad sugar substrate specificity, as described for *Aer. pernix* and *Tpt. tenax*, which convert several other sugars in addition to glucose, such as fructose, mannose, and 2-deoxyglucose (46, 55). These ~35-kDa monomeric enzymes exhibit the two signature patterns of the ROK family [LIVM]-x₍₂₎-G-[LIVMFCT]-G-X-[GA]-X-G-X₍₃₋₅₎-[GATP]-X₍₂₎-G-[RKH] and C-X-C-GX₍₂₎-G-X-[WILV]-E-X-[YFVIN]-X-[STAG] (46). The ROK kinases constitute one family within the superfamily of actin-like ATPase domain proteins also comprising the hexokinase family and the ATP-dependent glucokinase family (see above) (44). In addition to the archaeal ROK hexokinases, several ROK sugar kinases have been characterized (e.g., from *Thermotoga maritima*), and crystal structures (e.g., from *Thermus thermophilus*, *Bacillus subtilis*, and *Streptomyces griseus*) have been reported (63–65). In contrast to the monomeric archaeal ROK kinases, the bacterial ROK sugar kinases represent homodimers (*Tmt. maritima*

and *Bac. subtilis*) or homotetramers (*The. thermophilus* and *Str. griseus*). Since most bacterial ROK kinases were shown to be specific for their respective sugar substrates, it has been discussed that the broad substrate spectrum might be a characteristic feature of archaeal ROK sugar kinases (63). However, the *The. thermophilus* ROK sugar kinase also converts mannose in addition to glucose (64). Although no crystal structures of archaeal ROK kinases are available, the structures from *Bacteria* revealed a two-domain architecture and fold similar to those described for hexokinases and ATP-dependent glycerate kinases (ATP-GKs), with both substrates binding in the cleft between both domains (64, 66). From the amino acid sequence similarities, comparable structures might also be expected for the archaeal ROK kinases. The archaeal ROK hexokinase activities appeared to be dependent on bivalent metal ions (46, 55), and in the crystal structures of bacterial ROK kinases, a bound Zn²⁺ ion in a zinc finger motif has been observed (64, 66). This zinc ion interacts with residues that in turn are involved in substrate binding, and thereby, this zinc ion helps to position the sugar substrate for catalysis. The catalytic mechanism of the ROK kinases seems to be similar to that described for ATP-GLK and HK (65). Although a similar mechanism was also proposed for ADP-dependent kinases (see above), there are no structural or sequence similarities between both enzymes, and also, the mechanism of metal ion dependency appears to be different (46, 50) (Fig. 2A and C and 3). In the crystal structure of the *Bac. subtilis* ROK fructokinase, no drastic conformational changes have been observed upon substrate binding.

Other archaeal sugar kinases. For *Sulfolobus tokodaii*, a hexokinase from the actin-like ATPase domain superfamily has been purified, and the encoding gene has been identified (67). The 64-kDa dimeric enzyme (subunits of 32 kDa) showed a broad substrate spectrum, converting mannose, glucosamine, N-acetylglucosamine (GlcNAc), and 2-deoxyglucose in addition to glucose, with a preference for ATP as the phosphoryl donor. ADP showed an inhibitory effect on the enzyme. The crystal structure of *Sul. tokodaii* HK (StHK) showed a hexokinase-like fold (Fig. 2C) and exhibited some sequence similarities with mammalian GlcNAc kinases, although the latter enzymes are specific for GlcNAc (49). Homologs of this *Sul. tokodaii* hexokinase with sequence similarities of >50% were identified only in *Sulfolobus* species. Due to their fold and since these *Sulfolobus* enzymes seem to belong to neither the ROK nor the glucokinase family, it has been discussed that they represent new members of the hexokinase family with a unique substrate specificity.

In halophilic *Archaea*, a modified version of the EMP pathway is used for the degradation of fructose, in which the substrate is phosphorylated to fructose 1-phosphate (F1P) via ketohexokinase (KHK). F1P is further phosphorylated by 1-phosphofructokinase (1-PFK) to F1,6BP, which is then cleaved to DHAP and GAP by fructose bisphosphate (FBP) aldolase (FBPA). DHAP and GAP are converted to pyruvate by classical EMP pathway enzymes (68–70). The KHK from *Haloarcula vallismortis* catalyzing the first step in this EMP pathway modification, i.e., the ATP-dependent phosphorylation of fructose to fructose 1-phosphate, has been purified and characterized (71, 72). The native molecular mass was determined to be 100 kDa, but the subunit composition and sizes could not unambiguously be established. F1P-forming KHKs are known mainly from *Eukarya*. These enzymes belong to the PFK-B family, as revealed by sequence and structural analyses, and represent ~70-kDa dimeric proteins composed of a single ~35-kDa sub-

TABLE 1 Overview of enzymes involved in the classical EMP pathway in *Bacteria* and *Eukarya* as well as in the modified EMP pathway versions in *Archaea*

Enzyme	EC no.	Abbreviation	Reaction	Protein superfamily(ies) (according to the SCOP database)	Protein family(ies)	Distribution
Hexokinase	2.7.1.1	HK	Hexose + ATP → hexose 6-phosphate + ADP	Actin-like ATPase superfamily	Hexokinase family	<i>Eukarya</i>
ATP-dependent glucokinase	2.7.1.2	ATP-GLK	Glucose + ATP → glucose 6-phosphate + ADP	Actin-like ATPase superfamily	Glucokinase family	<i>Bacteria</i>
ADP-dependent glucokinase	2.7.1.147	ADP-GLK	Glucose + ADP → glucose 6-phosphate + AMP	Ribokinase superfamily	ADP-dependent sugar kinase family	<i>Archaea</i> (mainly anaerobic <i>Euryarchaeota</i>)
ROK hexokinase	2.7.1.1	ROK-HK	Hexose + ATP → hexose 6-phosphate + ADP	Actin-like ATPase superfamily	ROK family	<i>Archaea</i> (<i>Crenarchaeota</i>), <i>Bacteria</i>
Ketothexokinase	2.7.1.3	KHK	Fructose + ATP → fructose 1-phosphate + ADP	Protein sequence in <i>Archaea</i> unknown; eukaryote ribokinase superfamily	PFK-B	Halophilic <i>Euryarchaeota</i> , <i>Eukarya</i>
Hexokinase	2.7.1.1	HK	Hexose + ATP → hexose 6-phosphate + ADP	Actin-like ATPase superfamily	Probably BadF/BadG/BcrA/ BcrD ATPase family	<i>Crenarchaeota</i> (<i>Sulfolobus</i>)
Phosphoglucose isomerase	5.3.1.9	PGI	Glucose 6-phosphate ⇌ fructose 6-phosphate	PGI superfamily (SIS domain superfamily)	PGI family	<i>Eukarya</i> , <i>Bacteria</i> , halophilic <i>Euryarchaeota</i> , methanogenic <i>Euryarchaeota</i> (<i>Methanococcus</i>)
Phosphoglucosidase/phosphomannose isomerase	5.3.1.9/5.3.1.8	PGI/PMI	Glucose 6-phosphate/mannose 6-phosphate ⇌ fructose 6-phosphate	PGI superfamily (SIS domain superfamily)	PGI/PMI family	Anaerobic <i>Euryarchaeota</i> (including <i>Methanosaicina mazae</i>), some <i>Bacteria</i> (<i>Ensifer meliloti</i> , <i>Salmonella Typhimurium</i>), horizontal gene transfer
Cupin-type phosphoglucose isomerase	5.3.1.9	cPGI	Glucose 6-phosphate ⇌ fructose 6-phosphate	Cupin superfamily	cPGI family	<i>Eukarya</i> , <i>Bacteria</i>
ATP-dependent phosphofructokinase	2.7.1.11	ATP-PFK	Fructose 6-phosphate + ATP → fructose 1,6-bisphosphate + ADP	Phosphofructokinase superfamily (known as PFK-A)	Phosphofructokinase family (known as PFK-A)	<i>Archaea</i> , (mainly anaerobic <i>Euryarchaeota</i>), glycoxygen-forming methanogens
ADP-dependent phosphofructokinase	2.7.1.146	ADP-PFK	Fructose 6-phosphate + ADP → fructose 1,6-bisphosphate + AMP	Ribokinase superfamily	ADP-dependent sugar kinase family	<i>Crenarchaeota</i> (<i>Aeropyrum pernix</i> , <i>Desulfurooccus amylolyticus</i>)
ATP-dependent phosphofructokinase	2.7.1.11	PFK-B	Fructose 6-phosphate + ATP → fructose 1,6-bisphosphate + ADP	Ribokinase superfamily	PFK-B family	<i>Crenarchaeota</i> (<i>Thermoproteus tenax</i>), some <i>Bacteria</i> , <i>Eukarya</i> (protists, plants)
PP _i -dependent phosphofructokinase	2.7.1.90	PP _i -PFK	Fructose 6-phosphate + PP _i ⇌ fructose 1,6-bisphosphate + P _i	Phosphofructokinase superfamily (known as PFK-A), forming a distinct subfamily	Phosphofructokinase family (known as PFK-A), forming a distinct subfamily	<i>Eukarya</i>
Fructose-1,6-bisphosphate aldolase class I	4.1.2.13	FBPA I	Fructose 1,6-bisphosphate ⇌ dihydroxyacetone phosphate + glyceraldehyde 3-phosphate	Aldolase superfamily [(βα) ₈ barrel fold]	Class I aldolase family	<i>Archaea</i> , <i>Bacteria</i>
Archaeal type class I fructose-1,6-bisphosphate aldolase	4.1.2.13	FBPA IA	Fructose 1,6-bisphosphate ⇌ dihydroxyacetone phosphate + glyceraldehyde 3-phosphate	Aldolase superfamily [(βα) ₈ barrel fold]	Class I aldolase family	<i>Archaea</i> , <i>Bacteria</i>
Fructose-1,6-bisphosphate aldolase class II	4.1.2.13	FBPA II	Fructose 1,6-bisphosphate ⇌ dihydroxyacetone phosphate + glyceraldehyde 3-phosphate	Aldolase superfamily [(βα) ₈ barrel fold]	Class II FBP aldolase family	Halophilic <i>Euryarchaeota</i> , <i>Bacteria</i> , fungi
Triosephosphate isomerase	5.3.1.1	TIM	Dihydroxyacetone phosphate ⇌ glyceraldehyde 3-phosphate	Triosephosphate isomerase superfamily [(βα) ₈ barrel fold]	Triosephosphate isomerase family	<i>Eukarya</i> , <i>Bacteria</i> , <i>Archaea</i>
Glyceraldehyde-3-phosphate dehydrogenase (phosphorylating)	1.2.1.13 (NADP ⁺), 1.2.1.12 (NAD ⁺)	GAPDH	Glyceraldehyde 3-phosphate + NAD(P) ⁺ + P _i ⇌ 1,3-bisphosphoglycerate + NAD(P)H + H ⁺	N-terminal domain NAD(P) binding domain, Rossman fold-like domain superfamily; C-terminal glyceraldehyde 3-phosphate dehydrogenase-like, C-terminal domain superfamily	GAPDH N- and C-terminal domain families, respectively	<i>Eukarya</i> , <i>Bacteria</i> , halophilic <i>Euryarchaeota</i> , glycoxygen-degrading methanogens (catabolic and anabolic), all other <i>Archaea</i> (only anabolic)
Phosphoglycerate kinase	2.7.3.2	PGK	1,3-Bisphosphoglycerate + ADP ⇌ 3-phosphoglycerate + ATP	Phosphoglycerate kinase superfamily	Phosphoglycerate kinase family	<i>Eukarya</i> , <i>Bacteria</i> , halophilic <i>Euryarchaeota</i> , glycoxygen-degrading methanogens (catabolic and anabolic), all other <i>Archaea</i> (only anabolic)

Glyceraldehyde-3-phosphate dehydrogenase (nonphosphorylating)	1.2.1.9	GAPN	Glyceraldehyde 3-phosphate + NAD(P) ⁺ → 3-phosphoglycerate + NAD(P)H + H ⁺	ALDH-like superfamily	(Hyper)thermophilic <i>Archaea</i>
Glyceraldehyde-3-phosphate:ferredoxin oxidoreductase	1.2.7.6	GAPOR	Glyceraldehyde 3-phosphate + Fd _{ox} → 3-phosphoglycerate + Fd _{red} ^a	Aldehyde:ferredoxin oxidoreductase, N- and C-terminal domain superfamily	Anaerobic <i>Archaea</i> , some anaerobic (hyper)thermophiles in addition to GAPN
2,3-Bisphosphoglycerate-dependent phosphoglycerate mutase	5.4.2.1	dPGAM	3-Phosphoglycerate ⇌ 2-phosphoglycerate	Phosphoglycerate mutase-like superfamily	Cofactor-dependent phosphoglycerate mutase family
2,3-Bisphosphoglycerate-independent phosphoglycerate mutase	5.4.2.1	iPGAM	3-Phosphoglycerate ⇌ 2-phosphoglycerate	Alkaline phosphatase superfamily; 2,3-bisphosphoglycerate-independent phosphoglycerate mutase, substrate binding domain superfamily	Vertebrates, yeasts, <i>Bacteria</i> , mainly thermoacidophilic <i>Archaea</i> and <i>Methanosaicina</i> spp.
Enolase	4.2.1.11	ENO	2-Phosphoglycerate ⇌ phosphoenolpyruvate	Enolase-like, N- and C-terminal domain superfamily	Eukarya, <i>Bacteria</i> , <i>Archaea</i>
Pyruvate kinase	2.7.1.40	PK	Phosphoenolpyruvate + ADP → pyruvate + ATP	PEP:pyruvate domain superfamily; pyruvate kinase beta-barrel domain-like superfamily	Eukarya, <i>Bacteria</i> , <i>Archaea</i>
Pyruvate:phosphate dikinase	2.7.9.1	PPDK	Pyruvate + ATP + P _i ⇌ phosphoenolpyruvate + AMP + PP _i	Glutathione synthetase ATP binding domain-like superfamily (N-terminal domain) (ATP grasp fold); phosphohistidine domain superfamily (central domain); phosphoenolpyruvate/pyruvate domain superfamily (C-terminal domain) (TIM barrel fold)	Eukarya, <i>Bacteria</i> , <i>Archaea</i>

^a Fd_{ox}, oxidized ferredoxin; Fd_{red}, reduced ferredoxin.

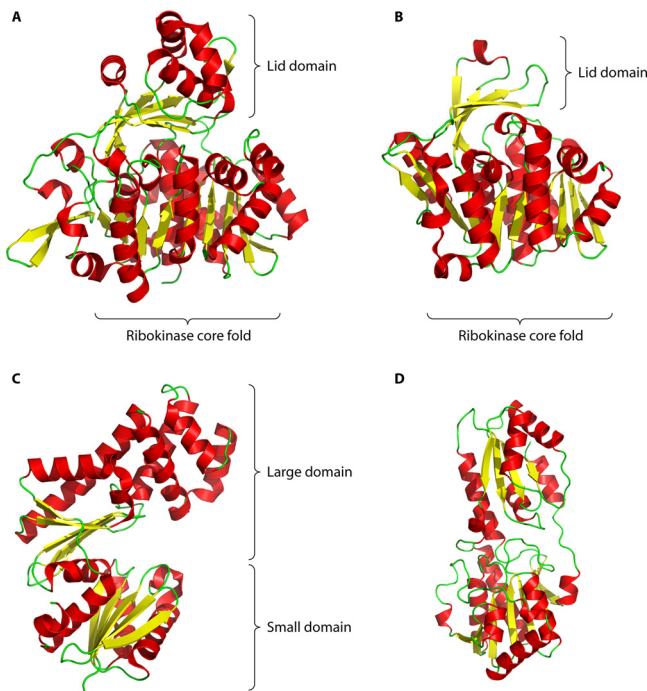


FIG 2 Ribbon representation of the crystal structures of the monomers of the different sugar kinases found in *Archaea*. (A) ADP-GLK from *Pyr. furiosus* (PDB accession number 1U4A) (59) as a representative of the ADP-dependent sugar kinase family within the ribokinase superfamily also comprising ADP-PFKs as well as the promiscuous ADP-GLK/PFK from *Mca. jannaschii*. (B) KDGK from *Sul. solfataricus* (PDB accession number 2VAR) (122) as a member of the ribokinase superfamily, exhibiting the PFK-B fold like the ATP-dependent PFKs present in, e.g., *Des. amylolyticus* and *Aer. pernix*. (C) HK from *Sul. tokodaii* (PDB accession number 2E2N) (49) as a member of the actin-ATPase domain-like superfamily also comprising ROK hexokinases and classical HKs from *Eukarya* and *Bacteria*. (D) Classical phosphofructokinase from *E. coli* (PDB accession number 6PFK) (101) as a member of the PFK-A family, to which also the PP_i-dependent PFK from *Tpt. tenax* belongs. All illustrations of crystal structures were prepared by using the Pymol Molecular Graphics System, version 1.3 (Schrödinger, LLC).

unit (73). In contrast to the PFK-B kinases (see below), evidence that a phosphoenzyme intermediate is involved in the haloarchaeal KHK catalytic cycle has been reported and no antigenic cross-reactivity using antibodies raised against haloarchaeal KHK could be detected with mammalian KHK from different rat tissues (72). These findings suggest that a novel, nonhomologous enzyme is involved in fructose phosphorylation in halophilic *Archaea*. However, the haloarchaeal KHK-encoding gene has not been

identified and, since fructose was shown to be transported into the cells and phosphorylated by a PTS (see below) in *Hfx. volcanii*, the activity of KHK might not be required. Nevertheless, in *Halocarcula marismortui*, KHK activity seems to be induced during growth on fructose (70).

Phosphoglucose Isomerase

Phosphoglucose isomerases (PGIs) catalyze the interconversion of the aldose G6P to the ketose F6P in both the classical EMP pathway in *Bacteria* and *Eukarya* as well as the modified versions in *Archaea*. This reaction is an intramolecular redox reaction/electron rearrangement in which an aldehyde (C-1 in G6P) is reduced and the hydroxyl group at C-2 is oxidized to a ketone. This is accompanied by a proton rearrangement. Conventional PGIs of *Eukarya* and *Bacteria* from a variety of sources have extensively been investigated, and the crystal structures have been reported for several organisms (e.g., pig, rabbit, human, and the bacterium *Bacillus stearothermophilus*). The conserved amino acids proposed to be involved in substrate binding and/or catalysis have been identified (for literature, see reference 74). PGIs from mammalian sources exhibit the properties of a cytokine involved in cell migration and proliferation (75, 76). Conventional PGIs are homodimeric proteins (~120 kDa), and each subunit (~60 kDa) comprises two domains. The active center located at the domain interface is made up of residues from both subunits. The conventional PGIs belong to the PGI family within the PGI superfamily of proteins (SIS [sugar isomerase] domain superfamily in the SCOP database) (45, 77–80). In *Archaea*, homologs of these classical bacterial and eukaryotic PGIs have been identified only in halophiles and some methanogens, and the enzyme from *Mca. jannaschii* has been characterized (81). Instead, PGI activity in all other *Archaea* is associated with two other protein families.

Phosphoglucose isomerase/phosphomannose isomerase. PGIs have been purified from *Aer. pernix*, *Tpt. tenax*, and *Pyb. aerophilum* as well as from the modified ED pathway utilizer *Tpl. acidophilum* (see below). The coding sequences show low but detectable sequence similarities to the classical PGIs, especially in those residues involved in catalysis (82–84). However, in contrast to the G6P/F6P-specific conventional PGIs, the corresponding enzymes show promiscuous PGI and phosphomannose isomerase (PMI) activities, converting both G6P and mannose 6-phosphate (M6P) to F6P. Similar to the classical PGIs, the archaeal PGI/PMIs are dimers and show a two-domain structure. Each domain shows an $\alpha\beta\alpha$ sandwich fold, which is built around a parallel β sheet, five stranded in the N-terminal domain and four stranded in the C-terminal domain (Fig. 4). However, with a subunit size of ~35

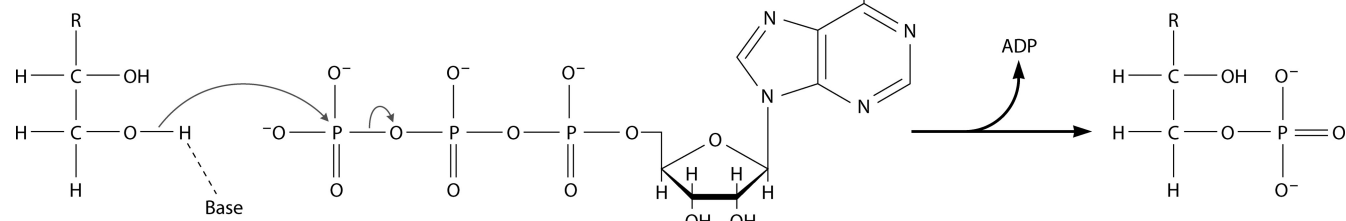


FIG 3 Proposed reaction mechanism catalyzed by sugar kinases, including base-mediated proton abstraction from the acceptor hydroxyl group followed by nucleophilic attack on the γ -phosphate group of ATP.

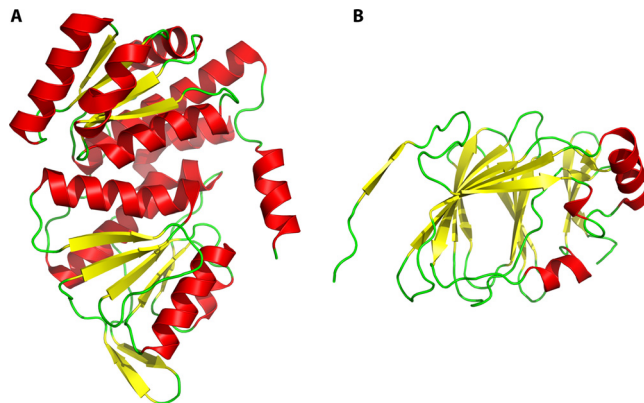


FIG 4 (A) Crystal structure of the monomer of PGI/PMI from *Pyb. aerophilum* (PDB accession number 1X9H) (87), which shows the PGI superfamily fold. Both PGI/PMIs and classical PGIs constitute distinct families within the PGI superfamily. (B) Monomer of cPGI from *Pyr. furiosus* (PDB accession number 2VAR) (96), which shows the small barrel formed by two β sheets, typical of the cupin superfamily.

kDa and a native molecular mass of ~ 70 kDa, PGI/PMIs are by far smaller (85, 86). The multistep reaction mechanism carried out by both conventional PGI and PGI/PMI enzymes is proposed to include (i) the ring opening of the closed circular form of the sugar phosphate; (ii) the isomerization reaction of the open-chain form of the substrate, including an $\sim 180^\circ$ rotation of the C-3–C-4 bond; (iii) subsequent general base (Glu203 in *Pyb. aerophilum* PGI/PMI)-catalyzed proton transfer from C-2 to C-1 via a *cis*-enediolate intermediate (Fig. 5); and, finally, (iv) the ring closure of the isomerized product. However, for the conversion of M6P by PGI/PMI, an additional rotation around the C-2–C-3 bond of the substrate is required directly after the C-3–C-4 rotation. This proposed second rotation is sterically hindered in classical PGIs by a conserved glutamine residue, whereas in promiscuous *Pyrobaculum* PGI/PMI, glutamine is replaced by the smaller threonine, leaving more space in the active site to facilitate the C-2–C-3 rotation of the M6P substrate (87). On the one hand, the similar core fold of PGI compared to that of PGI/PMI, the reaction mechanism, and the concomitant sequence conservation in functionally important residues clearly group the archaeal PGI/PMIs together with conventional PGIs into the same protein superfamily. On the other hand, the low overall sequence similarity accompanied by structural and mechanistic alterations facilitating the broader sub-

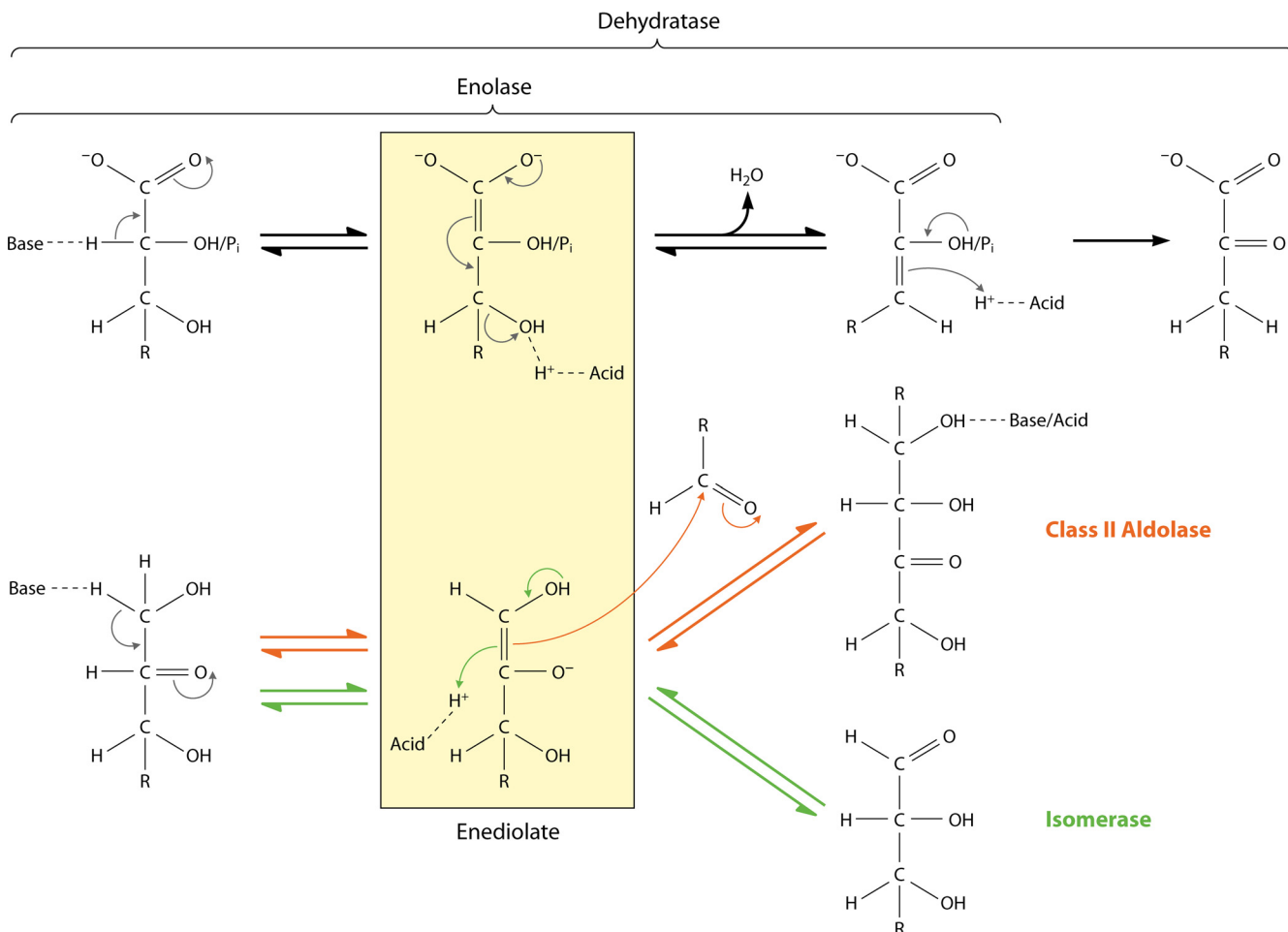


FIG 5 Schemes illustrating the proposed reaction mechanisms for dehydratases, enolases, class II aldolases, and isomerases, all proceeding via an enediolate intermediate (highlighted by the box).

strate spectrum define the conventional PGIs and the PGI/PMI enzymes as discrete protein families within the same superfamily (82, 83, 86).

Cupin-type phosphoglucose isomerase. PGI activity in the anaerobic *Euryarchaeota Pyr. furiosus*, *Tco. litoralis*, *Arc. fulgidus*, and *Methanoscincina mazei* has been shown to be catalyzed by metal-containing enzymes specific for G6P/F6P (74, 88–90). The coding sequences did not show any homology to conventional PGIs but were instead identified as members of the novel cupin-type PGI (cPGI) family within the cupin superfamily, which harbors functionally diverse members of all three domains of life. cPGIs are monomeric or homodimeric enzymes composed of identical ~25-kDa subunits, which is far smaller than the subunit size of conventional PGIs (~60 kDa [see above]). Crystal structure analyses of *Pyr. furiosus* cPGI (PfcPGI) revealed a cupin fold (*cupa*, Latin for small barrel) basically consisting of two β sheets forming a small barrel, which contains the metal ion as well as the substrate binding site (91, 92) (Fig. 4). In contrast to conventional PGIs, cPGI activity is strictly dependent on bivalent metal ions such as Fe^{2+} and Ni^{2+} (74, 93). Two different catalytic mechanisms, proceeding via (i) a carbocation and a subsequent hydride shift and (ii) a *cis*-enediolate intermediate with a conserved glutamate residue (E97) as a base catalyst, as described above, have been proposed (94–96). In both proposed mechanisms, the metal dependence is explained by the coordination of the substrate in the active site not being involved directly in catalysis (95). More recently, a third mechanism, via a zwitterionic intermediate involving both a proton and a hydride shift, was proposed by Wu et al., which could solve the contradiction between the former two mechanisms (97). However, with the missing sequence similarity/homology, the metal dependence, and the completely different overall fold, cPGI clearly represents a different and novel type of metal-dependent PGI and, thus, a convergent line of PGI evolution (74). cPGIs have also been identified in some *Bacteria*, such as *Ensifer meliloti* and *Salmonella enterica* serovar Typhimurium, which has been explained by lateral gene transfer from *Euryarchaeota*, i.e., *Thermococcales* and *Archaeoglobales*, respectively (74).

Phosphofructokinase

In the classical EMP pathway in *Bacteria* and *Eukarya*, the phosphorylation of F6P to F1,6BP catalyzed by 6-phosphofructokinase (PFK) represents the major control point of glycolysis. These classical PFKs from *Bacteria* and *Eukarya* belong to the phosphofructokinase A (PFK-A) family (98). Bacterial PFKs from the PFK-A family are usually tetramers composed of single 35-kDa subunits (99, 100). Each subunit comprises two domains, a large and a smaller 3-layered $\alpha\beta\alpha$ sandwich domain (101). Bacterial PFK-A enzymes are allosterically regulated by PEP (inhibition) and ADP (activation) (101). Eukaryotic PFKs from the PFK-A family show more complex architecture and regulation. The subunits are approximately twice as large and presumably originated from their bacterial homologs via a gene duplication event (102). Eukaryotic PFKs are regulated by more effectors, such as fructose 2,6-bisphosphate (F2,6BP), citrate, F1,6BP, AMP, cyclic AMP (cAMP), P_i , and 3-phosphoglycerate in addition to PEP and ADP. The Mg^{2+} -dependent phosphoryl transfer mechanism of ATP-dependent PFKs from the PFK-A family, finally yielding a phosphoester bond, involves a nucleophilic attack by the hydroxyl oxygen at C-1

of F6P on the γ -phosphate of ATP, facilitated by Asp127 (*E. coli* enzyme) acting as a base (100, 103).

In *Archaea*, the phosphorylation of F6P is catalyzed by different enzymes, which vary with respect to their phosphoryl donors PP_i , ADP, and ATP. Notably, all archaeal PFKs possess no allosteric properties.

Pyrophosphate-dependent phosphofructokinase. In the cre-narchaeon *Tpt. tenax*, a PP_i -dependent PFK (PP_i -PFK) has been identified and characterized as a 100-kDa homodimeric (or homotrimeric) protein composed of identical 37-kDa subunits (104, 105). *Tpt. tenax* PP_i -PFK is specific for its substrates F6P/ PP_i and F1,6BP/ P_i and requires Mg^{2+} ions for activity. In contrast to the irreversibility of the classical ATP-PFK reaction, PP_i -PFK operates reversibly, also catalyzing the P_i -dependent dephosphorylation of F1,6P, thereby substituting for the FBPase reaction (105). PP_i -PFKs have also been described for some *Bacteria* as well as some protists and higher plants (106, 107). Sequence analyses and phylogenetic studies grouped *Tpt. tenax* PP_i -PFK into the PFK-A family, comprising three distinct phylogenetic groups of PFKs. Group I represents the classical, allosterically regulated ATP-PFKs from *Bacteria* and *Eukarya*. Group II comprises PP_i -PFKs from higher plants, protists, and some *Bacteria*, which are dimeric proteins composed of larger subunits (~60 kDa). The small-subunit (~40-kDa) PP_i -PFKs from *T. tenax* and also from, e.g., *Amycolatopsis methanolicus* (fungus) as well as ATP-PFK from *Str. coelicolor* comprise group III. PP_i -PFKs have also been characterized from (hyper)thermophilic *Bacteria* such as *Tmt. maritima* and *Dictyoglomus thermophilum* (phylum *Dictyoglomi*) (108, 109). Sequence and structural analyses revealed that many of the residues important for substrate binding and catalysis in classical ATP-PFK from, e.g., *E. coli* and *Bac. stearothermophilus* are also conserved in PP_i -PFKs, and a similar reaction mechanism has been proposed (106, 107) (see Fig. 2 for structure illustration of *E. coli* PFK-A). The PP_i specificity is assumed to be achieved by some subtle structural and sequence alterations compared to classical ATP-PFK (106). However, to date, structural information is not available for either *Tpt. tenax* PP_i -PFK or other group III small-subunit (PP_i -)PFK enzymes.

ADP-dependent phosphofructokinase. In the hyperthermophilic *Euryarchaeota Thermococcus zilligii*, *Pyr. furiosus*, and *Arc. fulgidus*, F6P phosphorylation to F1,6P was shown to be catalyzed by ADP-dependent PFKs (ADP-PFKs) (42, 52, 110–114). ADP-dependent PFKs have also been identified in glycogen-forming mesophilic and thermophilic methanogenic *Archaea* (115), and the enzyme from *Mca. jannaschii*, which represent the only ADP-dependent sugar kinase homolog in this organism, was shown to be promiscuous, converting both glucose and F6P (see “ADP-dependent glucokinase,” above) (58). ADP-PFKs are composed of an ~50-kDa subunit and were characterized as tetrameric (*Tco. zilligii* and *Pyr. furiosus*) or monomeric (promiscuous) (ADP-GLK/PFK of *Mca. jannaschii*). The *Arc. fulgidus* enzyme turned out to be active as both a dimer and a tetramer (114). Analyses of the available crystal structure of *Pyr. horikoshii* ADP-PFK suggested that the enzyme might be a monomer *in vivo* (116). With the exception of the bifunctional *Mca. jannaschii* ADP-GLK/PFK, all characterized ADP-PFKs are specific for F6P. Although the nucleotide substrate specificity of ADP-PFKs appears to be broader than that described for ADP-GLKs (e.g., in *Pyr. furiosus* ADP-PFK, ADP could partly be replaced by GDP, ATP, or GTP [111], and the *Pyr. horikoshii* enzyme accepted UDP with nearly

the same efficiencies as ADP [116]), the highest catalytic efficiencies are achieved with ADP. ADP-PFKs require bivalent metal ions, preferentially Mg²⁺, for activity. The only crystal structure of an ADP-PFK available so far has been reported for *Pyr. horikoshii* (116). The enzyme shares approximately 30% sequence identity with ADP-GLKs from *Thermococcales* and also shares a very similar overall structure (a large α/β sandwich domain with a ribokinase core fold and a small α/β sandwich domain), grouping the ADP-PFKs together with ADP-GLK in the protein family of ADP-dependent sugar kinases within the ribokinase superfamily (see Fig. 2 for an illustration). Also, most of the residues important for substrate binding and catalysis in ADP-GLKs are conserved in ADP-PFKs (57). The catalytically essential base catalyst (Asp440 in *Pyr. furiosus* ADP-GLK) is also highly conserved in ADP-PFK (Asp433 in *Pyr. horikoshii* ADP-PFK), and mutation completely abolishes PFK activity, indicating a similar catalytic mechanism. Both ADP-GLK and ADP-PFK are specific for their respective substrates, and some conserved amino acid substitutions were identified, which encounter different substrate specificities (116). Comparison of the sugar binding sites of ADP-GLKs and ADP-PFKs with that of the promiscuous *Mca. jannaschii* enzyme converting both glucose and F6P (58, 117) revealed that most of the sugar binding residues are conserved throughout the ADP-dependent sugar kinases. The sugar specificity relies on only very few residues, i.e., one glutamate residue in ADP-GLKs (i.e., Glu88 in *Pyr. furiosus* ADP-GLK and Glu82 in *Mca. jannaschii* ADP-GLK/PFK) interacting with the C-2 hydroxyl group of glucose, which is substituted for Ala in ADP-PFKs, and two basic residues at the bottom of the sugar binding pocket (K158 and Arg191 in *Pyr. horikoshii* ADP-PFK) stabilizing the negative charge of the phosphate moiety of fructose 6-phosphate in ADP-PFKs (116, 117).

Phylogenetic analyses suggested that the ADP-GLKs from *Thermococcales* are more closely related to the ADP-PFKs from both *Thermococcales* and *Methanosaecinales*, whereas ADP-GLKs from *Methanosaecinales* are more distantly related to both groups. The promiscuous enzyme from *Mca. jannaschii* (and other *Methanococcales*) appeared to be deeply branching between both groups of ADP-PFKs. This tree topology was explained by a gene duplication event after the separation of *Thermococcales* and *Methanosaecinales*. ADP-PFKs were then acquired by the *Methanosaecinales* through lateral gene transfer from *Thermococcales*. However, the position of the bifunctional *Mca. jannaschii* enzyme indicated that it is not an ancestral form of both ADP-GLK and ADP-PFK but might represent a transition form in the evolution of ADP-PFK after gene duplication of ADP-GLK (57).

ATP-dependent phosphofructokinase (PFK-B). The third mechanism of F6P phosphorylation to F1,6BP is catalyzed by ATP-dependent phosphofructokinase. This has been described for *Aer. pernix* and *Des. amylolyticus* (118, 119). Both proteins are ~120-kDa tetramers composed of 33-kDa subunits. Both ATP-PFKs required divalent metal ions for activity and, in addition to ATP, could also utilize other nucleoside triphosphates as phosphoryl donors. However, ADP or PP_i could not serve as the substrate, clearly defining both enzymes as ATP dependent, in contrast to the ADP-PFKs and PP_i-PFKs described above. Whereas ATP-PFK from *Des. amylolyticus* turned out to be specific for F6P, the *Aer. pernix* enzyme accepted a variety of other phosphoryl acceptors as substrates, such as G6P, adenosine, fructose, ribose 5-phosphate (R5P), and ribose, with similar efficiencies. The N-terminal amino acid sequence of the enzyme purified from *Des.*

amylolyticus showed no sequence similarities to classical ATP-dependent PFKs but showed similarities to the *Aer. pernix* ATP-PFK. Sequence comparisons indicated that the *Aer. pernix* enzyme and, therefore, presumably also the *Des. amylolyticus* enzyme belong to the PFK-B family within the ribokinase superfamily, as for the ADP-dependent sugar kinases described above. A crystal structure of an archaeal ATP-PFK from the PFK-B family is not yet available.

However, the crystal structure of a PFK-B homolog from *Mca. jannaschii* was reported, which represents an ATP-dependent nucleoside kinase (MjNK) presumably involved in the nucleotide metabolism of this organism (120, 121). Based on the results obtained for MjNK, the substrate specificity of the archaeal ATP-PFKs was reexamined, revealing that the *Des. amylolyticus* enzyme is indeed a F6P-specific PFK, whereas the *Aer. pernix* enzyme exhibited a broad substrate spectrum, converting several nucleosides in addition to F6P, thus redefining the enzyme as ATP-PFK/NK, which might fulfill a dual function in glucose catabolism as well as in nucleotide metabolism in *Aer. pernix* (121). Also, the crystal structure of the 2-keto-3-deoxygluconate (KDG) kinase (KDGK), a PFK-B homolog operative in the modified ED pathway (see below), has been reported (122). In contrast to the PFK-B ATP-PFKs, MjNK and also *Sul. solfataricus* KDGK (SsoKDGK) represent homodimers, and each subunit is comprised of a central α/β fold representing the ribokinase core fold and a protruding lid domain. The central α/β fold of MjNK is composed of a central eight-stranded β sheet flanked by five α helices on one side and four on the other side. The protruding lid domain is made up of four strands. The lid folds back over the substrate binding site and thus shields the substrate from the solvent (120). Also, the KDG kinase from *Sul. solfataricus* shows a very similar structure (122) (Fig. 2B). Many of the catalytically important residues in the ribokinase superfamily proteins, including the ADP-GLKs described above, are also conserved in MjNK, and a similar reaction mechanism has been proposed, suggesting that the archaeal ATP-PFKs from the PFK-B family also share a similar mechanism (120).

As recently shown, 1-PFK, involved in the modified EMP pathway for fructose degradation in the halophilic archaeon *Hfx. volcanii*, also represents a PFK-B member (123). Enzyme characterization revealed an ~70-kDa homodimeric structure (38-kDa subunits), and sequence comparison showed considerable sequence identities with *E. coli* 1-PFK (FruK) (124). The previously characterized 1-PFK from *Har. vallismortis* has been reported to be a 70-kDa monomer; however, the encoding sequence has never been clearly identified (125).

Fructose-1,6-Bisphosphate Aldolase (Catabolic)

Fructose-1,6-bisphosphate aldolase (FBPA) (EC 4.1.2.13) catalyzes the reversible aldol cleavage in the β position to the carbonyl C atom of F1,6BP to yield GAP and DHAP. The electron rearrangement retains both electrons of the C-C bond at the hydroxyl carbon of DHAP, whereas the other hydroxyl carbon of the substrate is oxidized to a carbonyl group (C-1 of GAP). FBPA activity has been demonstrated in all sugar-metabolizing *Archaea* analyzed (40–42, 70, 105, 110, 126–132) and has been characterized in detail for *Haloflexax* species, *Tpt. tenax*, *Pyr. furiosus*, and *Tco. kodakarensis* (126, 130, 132, 133). Two classes of FBPA, which differ with respect to reaction mechanisms and distributions in the biosphere, have been identified (for literature, see reference

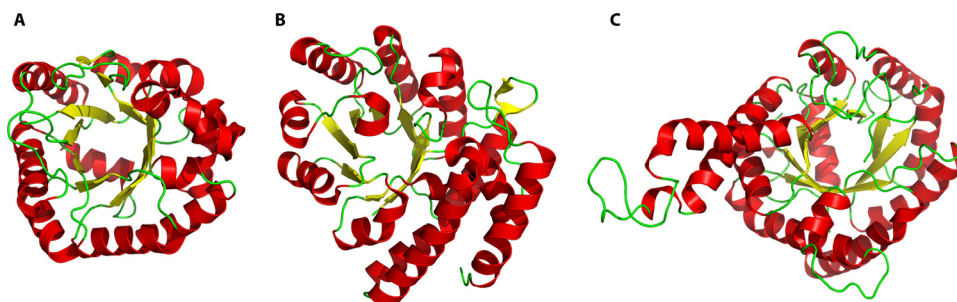


FIG 6 (A and B) Ribbon diagrams of the archaeal-type class I FBPA (PDB accession number 1OJX) (135) (A) and KD(P)GA (PDB accession number 2R91) (298) (B) from *Tpt. tenax*, both members of the class I aldolase family within the aldolase superfamily. (C) For comparison, the class II FBPA from *E. coli* is depicted (PDB accession number 1B57) (138), which also has been described for some halophilic *Archaea*. Class II aldolases constitute a distinct family within the aldolase superfamily. However, the figures show that all of these aldolases share a $(\beta/\alpha)_8$ TIM barrel fold.

134). Class I FBPA (FBPA I) utilizes a Schiff base reaction mechanism and was originally found in animals, plants, protozoans, and algae but has also been identified in *Bacteria* and *Archaea*. FBPA II uses divalent metal ions for catalysis and has been found in *Bacteria* and fungi. The class I FBPAs are grouped into two different enzyme families: one with only eukaryotic members and one with both bacterial and archaeal members (termed archaeal-type class I FBPA, or FBPA IA) (126). Several crystal structures have shown that eukaryotic FBPA I is an ~160-kDa homotetramer composed of ~40-kDa subunits, where the subunits adopt the fold of a parallel $(\beta\alpha)_8$ TIM barrel (see Fig. 6 for a comparative illustration of class I and class II aldolases). Although the archaeal FBPA I subunit also displays the $(\beta\alpha)_8$ barrel fold, its quaternary structure is that of a homodecamer, resulting from the dimerization of two identical pentamers (135). A decameric structure has also been reported for *Har. vallismortis* and *Tco. kodakarensis* (130, 133). Despite the lack of significant overall sequence identity, the structural similarity of the two types of FBPA I enzymes suggests a common ancestry and, thus, homology (135, 136). Together with the similar binding modes for Schiff base intermediates of the substrate DHAP, this strongly indicates a similar catalytic mechanism for the eukaryotic and the archaeal-type class I FBPAs. This mechanism is proposed to proceed via a ring-opening reaction, followed by nucleophilic attack of a catalytically essential lysine (Lys177 in *Tpt. tenax* FBPA [TtxFBPA]) on the carbonyl C atom of the substrate, leading to a covalent carbinolamine intermediate, which is then protonated and dehydrated, leading to the Schiff base (mediated by Tyr146 in TtxFBPA) (Fig. 7). A conserved aspartate residue is then believed to subtract a proton from C-4, thus mediating the cleavage into GAP and enzyme-bound DHAP (134). The archaeal-type class I aldolases also accept F1P, in addition to F1,6BP, as the substrate but with significantly reduced efficiencies.

Although these archaeal-type class I enzymes have been reported for most *Archaea*, including many extreme halophiles, and therefore might represent the typical archaeal FBPA (126, 137), for *Halofervax* species as well as some other haloarchaea, class II enzymes have been reported and characterized in detail (123, 132). These halophilic class II aldolases represent the only archaeal class II aldolases known so far. In contrast to the class I enzymes, the class II FBPA mechanism deduced from the crystal structure of the *E. coli* enzyme relies on bivalent metal ions. The cleavage mechanism of F1,6BP has been proposed to proceed via an enediolate intermediate (Asp109 as a general base in the *E. coli* en-

zyme), and through proton donation to C-1 involving a conserved Glu residue (Glu182 in the *E. coli* enzyme), DHAP is formed (138). In the case of the dimeric *E. coli* enzyme, which exhibits an $(\alpha/\beta)_8$ barrel fold, a Zn²⁺ ion coordinates the proper binding of the carbonyl C atom during catalysis, and a conserved Arg (Arg331) binds the GAP moiety of the substrate. In accordance with the *E. coli* enzyme, the halophilic class II aldolases are 100-kDa homodimers (50-kDa subunits), share the conserved residues involved in catalysis, and were described to prefer Fe²⁺ or Mn²⁺ instead of Zn²⁺ as a bivalent metal ion. Phylogenetic analyses revealed that the haloarchaeal sequences form a distinct third subfamily within the class II FBPA family, and it has been speculated that haloarchaea acquired these enzymes from *Bacteria* in a horizontal gene transfer event (123, 132). The archaeal class I aldolases have been proposed to represent early descendants of an ancient lineage separated very early from the lineages of classical class I and class II aldolases (126).

Triosephosphate Isomerase

Triosephosphate isomerases (TIMs) are universally distributed in all three domains of life and catalyze the reversible isomerization of DHAP to GAP, representing an electron and proton rearrangement similar to that described above for the PGI-catalyzed reaction. TIM activity has been detected in crude extracts of many archaeal species (40–42, 70, 105, 128), and TIM sequences have been identified in apparently all archaeal genomes (36, 43). Detailed characterizations have been reported for the enzymes from *Pyrococcus woesei*, *Pyr. furiosus*, *Methanothermus fervidus*, and *Tpt. tenax* (139–144). The crystal structures have been solved for the enzymes from *Pyr. woesei*, *Tpt. tenax*, and *Mca. jannaschii* (145–148). The archaeal TIM sequences are shorter, by ~20 amino acids, than those of their bacterial/eukaryotic counterparts, comprising ~230 amino acids and ~250 to 260 amino acids, corresponding to ~24 kDa and 28 kDa, respectively (36, 139). The characterized hyperthermophilic archaeal TIM proteins represent homotetramers, whereas the mesophilic TIMs from *Bacteria* and *Eukarya* are homodimers. Since the fused TIM/PGK from the hyperthermophilic bacterium *Tmt. maritima* is also a tetramer (149), and TIM from the mesophilic archaeon *Methanobacterium bryantii* is a homodimer, there appears to be a correlation between oligomerization and thermostability. Therefore, TIMs became one of the model systems to study thermostability of proteins, especially the stabilizing mechanism, through higher oligomerization states (146, 147). However, the TIM from the hyperthermo-

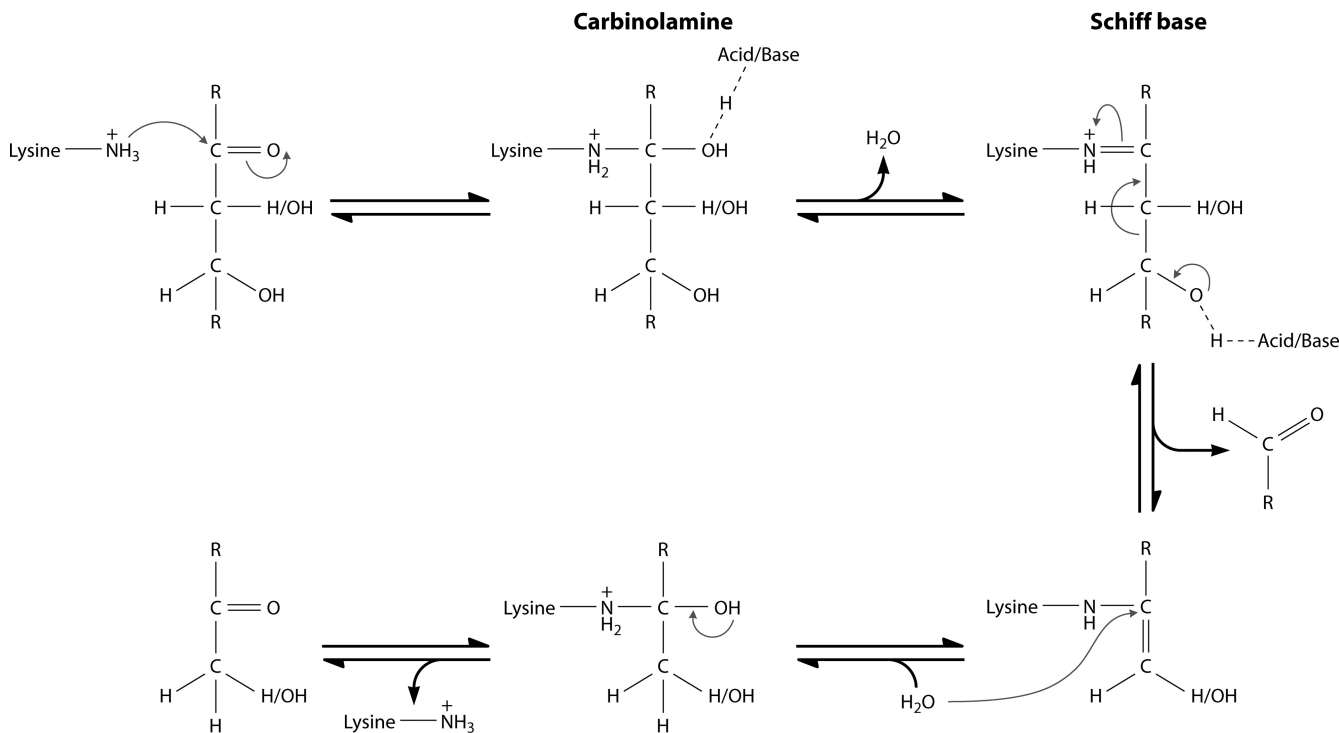


FIG 7 Schiff base mechanism catalyzed by FBPA and KD(P)GA in the course of the modified sugar degradation pathways in *Archaea*. The first step is the nucleophilic attack of the catalytically essential lysine at the carbonyl C atom, yielding the carbinolamine intermediate, which is then dehydrated to the Schiff base, followed by base-mediated cleavage of the substrate. $-H/OH$ means that in this position, the substituent is either a hydroxyl group (as in fructose converted by FBPA) or a hydrogen atom [as in 2-keto-3-deoxy sugar acids converted by KD(P)GA]. The bifunctional FBPA/ase from gluconeogenesis in *Archaea* catalyzes a similar reaction in the first part of the conversion of GAP and DHAP to F6P (for a more detailed discussion, see Gluconeogenesis, below).

phile *Tpt. tenax* was found to exist in an equilibrium between inactive dimers and active tetramers, which is shifted to the tetrameric state through a specific interaction with glycerol-1-phosphate dehydrogenase. This observation was interpreted in physiological terms as a need to reduce the formation of thermolabile metabolic intermediates (GAP and DHAP) (140, 147). TIMs are the archetypical $(\beta/\alpha)_8$ barrel proteins or TIM barrels (Fig. 8): an 8-fold repeat of strand-turn-helix-turn units assembled into a cylinder of eight parallel β strands surrounded by a layer of eight α helices. The active site is located at the carboxyl end of the barrel (45, 146–148). The enzyme follows an enediolate intermediate mechanism (Glu144 [*P. woesei* numbering] acid/base catalyst) (150, 151). His96 stabilizes the intermediate, and a highly conserved and also catalytically essential lysine (Lys14) also fulfills a stabilizing role, interacting with the phosphate group of the substrate. Phylogenetic analyses revealed that archaeal TIMs form a distinct subgroup within the TIMs from all three domains of life, clearly separated from the bacterial and eukaryotic TIMs, which seem to be more closely related to each other than to the archaeal sequences (43).

Glyceraldehyde 3-Phosphate Oxidation

In the classical EMP pathway for sugar degradation in *Eukarya* and *Bacteria*, the GAPDH/PGK couple catalyzes the reversible P_i -dependent oxidation of glyceraldehyde 3-phosphate (GAP) with the concomitant generation of ATP via substrate-level phosphorylation in two steps, with 1,3BPG as an intermediate. In most sugar-utilizing (hyper)thermophilic *Archaea* analyzed so far, GAP

oxidation is carried out in one step without 1,3BPG formation and, thus, without coupling of the oxidation of GAP to 3PG with the synthesis of ATP via substrate-level phosphorylation. Hence, the reaction catalyzed by either ferredoxin-dependent glyceraldehyde-3-phosphate:ferredoxin oxidoreductase (GAPOR) or NAD(P)⁺-dependent nonphosphorylating glyceraldehyde-3-phosphate dehydrogenase (GAPN) is irreversible in *Archaea*. Only mesophilic extreme halophiles growing at the expense of sugars rely on the GAPDH/PGK couple for GAP oxidation in the modified EMP and ED pathways utilized for fructose and glucose degradation, respectively (70, 123, 152). Also, in most methanogens, neither GAPOR nor GAPN has been identified, which might reflect the inability of most methanogenic species to degrade sugars (36, 153). However, some methanogens have been described to use glycogen as a storage compound, thus requiring a GAP-oxidizing system. GAPOR homologs have been identified in *Mco. maripaludis* and *Mca. jannaschii*, and for *Mco. maripaludis*, GAPOR, in addition to GAPDH/PGK, has been characterized in detail (153, 154). In addition, in *Tpl. acidophilum*, initially thought to degrade glucose exclusively via the nonphosphorylative ED branch involving glyceraldehyde (GA) dehydrogenase (GADH) oxidizing nonphosphorylated GA instead of GAP, no GAPN or GAPOR homologs could be identified (153). However, an aldehyde dehydrogenase (ALDH) paralog, which might utilize GAP as the substrate, has been found in the genome (32). From the distribution of GAP-oxidizing enzymes in *Archaea*, it might be concluded that GAPN is found mainly in (hyper)thermophiles

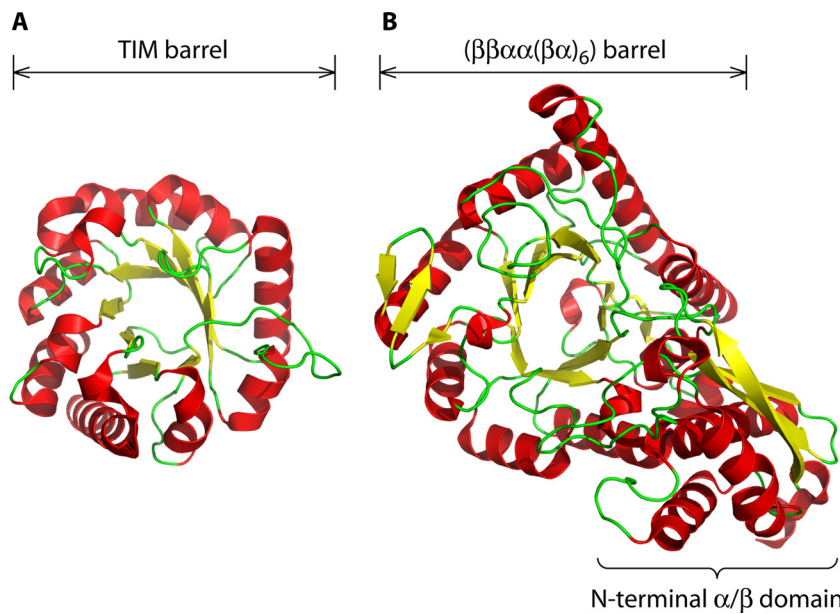


FIG 8 Comparative illustrations of the classical triosephosphate isomerase (TIM) barrel fold present in TIM (here from *T. tenax* [PDB accession number 1W0M]) (147) and the modified $\beta\beta\alpha\alpha(\beta\alpha)_6$ barrel fold from the enolase superfamily members (here from the putative enolase of *Mca. jannaschii* [PDB accession number 2PA6]) (229), comprising, besides ENOs, dehydratases used in the degradation of hexoses and pentoses in Archaea (see Fig. 5 for the reaction mechanism of isomerases and enolases).

and that anaerobic *Archaea* acquired GAPOR, in the case of an aerobic (hyper)thermophiles mostly, in addition to GAPN (153). For *Tco. kodakarensis*, it was shown that both GAPOR and GAPN are essential for glycolytic growth and that the reduced ferredoxin produced by GAPOR is indispensable for energy production under anaerobic conditions, whereas GAPN provides NADPH for anabolic purposes (175).

Glyceraldehyde-3-phosphate:ferredoxin oxidoreductase. GAPOR irreversibly converts GAP to 3PG in a ferredoxin-dependent manner, and activity has been detected in *Pyr. furiosus*, *Thermococcus* species, *Arc. fulgidus*, *Pyb. aerophilum*, *Des. amylolyticus*, *Tpt. tenax*, and *Mco. maripaludis* (40, 42, 128, 154, 156–158). The enzymes from *Pyr. furiosus*, *Pyb. aerophilum*, and *Mco. maripaludis* have been characterized in detail (41, 154, 156, 159–161). GAPORs represent ~65- to 70-kDa monomers and are highly specific for GAP as the substrate. Fd cannot be substituted by NAD(P)⁺. They belong to the aldehyde:Fd oxidoreductase (AOR) family of enzymes, all of which contain two pterins as cofactors, one tungsten atom, and at least four iron atoms in a [4Fe:4S] cluster; *Pyr. furiosus* GAPOR was reported to contain one tungsten and six iron atoms (160, 162). Meanwhile, all five paralogs of the AOR family in *Pyr. furiosus*, including GAPOR, formaldehyde:Fd oxidoreductase (FOR), AOR, and two further AORs (i.e., WOR4 and WOR5), were characterized. These enzymes function in the oxidation of a wide range of different aldehydes derived from degradation, e.g., of peptides and might also be involved in electron transport reactions (156, 160, 163–166). Also, a second AOR paralog was reported for *Pyb. aerophilum*, exhibiting a broad substrate spectrum and preferentially converting unsaturated and aromatic aldehydes (167). For *Pyb. aerophilum* GAPOR, the metal content has not been analyzed, but the amino acid residues assumed to take part in metal pterin cofactor and Fe/S cluster coordination, as deduced from the crystal structures of *Pyr. furiosus*

AOR and FOR, appear to be conserved (41, 164). However, *Mco. maripaludis* GAPOR was reported to contain molybdenum instead of tungsten (154). Although no crystal structure of a GAPOR itself is available, those of two members of the AOR enzyme family, the dimeric AOR and the tetrameric FOR from *Pyr. furiosus*, have been reported (168, 169). The basic fold of the subunit of both enzymes consists of three domains. Domain 1 is dominated by two central six-stranded β sheets, whereas domains 2 and 3 are predominantly helical. Domain 2 contains the [4Fe:4S] cluster binding sequence with three cysteines, and domain 3 provides the fourth cysteine for Fe/S cluster coordination. The tungstopterin cofactor is located in the center of the molecule, sandwiched by domain 1 on one side and domains 2 and 3 on the other side, which are all involved in cofactor binding (Fig. 9B). Most of these residues appear to be conserved in GAPORs. As a catalytic mechanism, a nucleophilic attack of a water molecule, activated by the tungsten atom, which changes its redox state from state IV to state VI, on the carbonyl group of the substrate is proposed. Electron transfer proceeds from the tungsten center via the pterin cofactor and the [4Fe:4S] cluster finally to the [4Fe:4S] cluster of ferredoxin (168, 170). However, the GAPOR characterized for *Sul. acidocaldarius* has been described to be different from the *Pyrococcus* and *Pyrobaculum* enzymes with respect to subunit composition and metal content (see below) (171).

Nonphosphorylating glyceraldehyde-3-phosphate dehydrogenase. GAPN catalyzes the NAD(P)⁺-dependent irreversible oxidation of GAP to 3PG. GAPN activity has been detected in extracts of *Tpt. tenax* and *Aer. pernix* (40, 41, 172) as well as in *Sul. solfataricus*, where it operates in the semiphosphorylative branch of the modified branched ED pathway (spED pathway) (153, 173) (see below). In addition, GAPN sequence homologs have been identified in *Pyr. furiosus* and *Tco. kodakarensis*. Also, a GAPN homolog has been identified in *Halobacterium salinarum* NRC-1

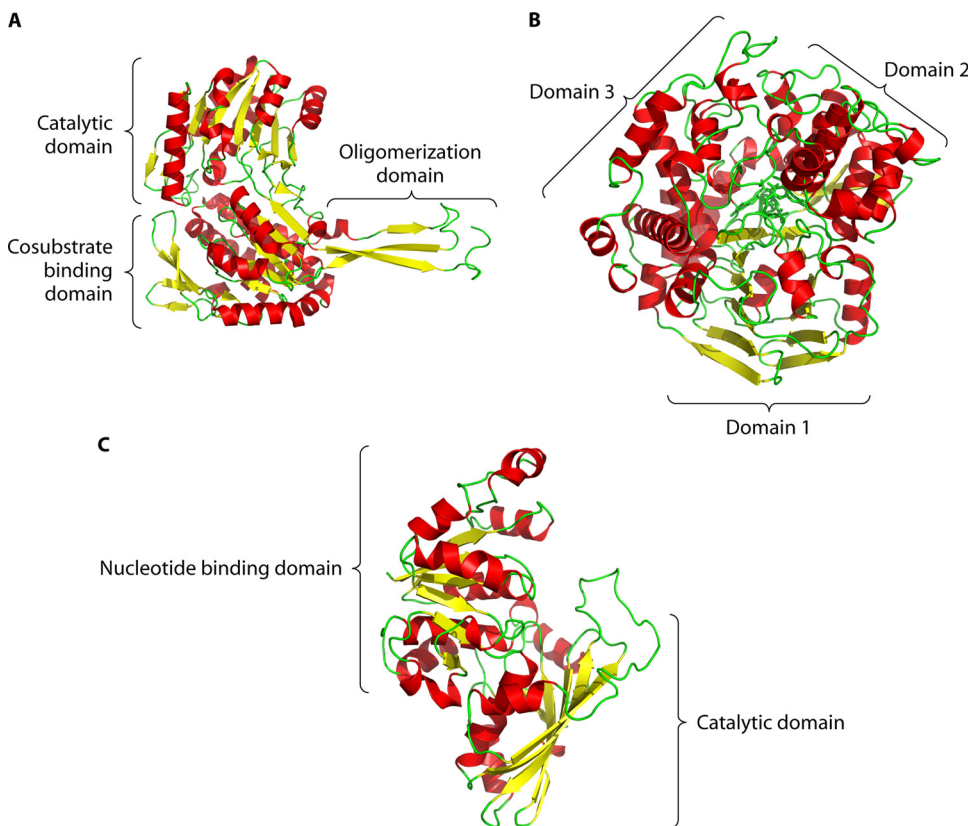


FIG 9 Ribbon representations of GAP-oxidizing enzymes in *Archaea*. (A) GAPN from *Tpt. tenax* (PDB accession number 1UXN) (174) showing the three-domain organization. GAPN is a member of the ALDH superfamily, also comprising the glyceraldehyde dehydrogenases from the npED branch in *Thermoplasma* spp. and α -ketoglutarate semialdehyde dehydrogenases from the pentose degradation pathway in *Sulfolobus* and *Haloferax*. (B) Aldehyde:ferredoxin oxidoreductase from *Pyr. furiosus* (PDB accession number 1AOR) (169), a representative of the AOR superfamily, to which the archaeal GAPORs also belong. The protein is organized in three domains, with the pterin cofactor and Fe/S cluster (depicted as a green stick model) binding site in the center between the three domains. (C) The classical GAPDH from *Sul. solfataricus* (PDB accession number 1B7G) (193) is shown operating exclusively in the anabolic/gluconeogenic direction, exhibiting the typical two-domain structure with an N-terminal Rossman fold nucleotide binding domain and a C-terminal catalytic domain.

(153), although so far, neither GAPN nor GAPOR activity has been detected in haloarchaea. The GAPNs from *Tpt. tenax*, *Tco. kodakarensis*, *Sul. solfataricus*, and *Sul. tokodaii* are 220-kDa homotetrameric (55-kDa subunit) enzymes not showing any similarity to classical phosphorylating GAPDHs. Instead, sequence and structural similarities identified them as members of the aldehyde dehydrogenase superfamily, in which they form a distinct subgroup (172). The characterized GAPNs exhibit dual cosubstrate specificity, converting both NAD⁺ and NADP⁺, with a clear preference for NADP⁺ (174). The enzymes show allosteric activation by G1P and in some cases F6P. *Tpt. tenax* GAPN exhibits a more extended allosteric potential, being additionally activated by ADP and AMP and inhibited by ATP, NADP⁺, NADPH, and NADH (153, 172, 175, 176). The GAPNs of *Tco. kodakarensis* and *Sul. tokodaii* showed remarkable substrate inhibition kinetics with GAP (175, 176). Thus, GAPN represents one of the main allosterically regulated glycolytic enzymes in *Archaea*, suggesting a pivotal role in the control of glycolysis at the level of GAP (172, 177, 178).

The crystal structure of *Tpt. tenax* GAPN was solved, and the overall fold of the GAPN monomer is similar to the structures of ALDHs described previously, consisting of three domains. The cosubstrate binding domain comprises a central parallel five-stranded β sheet surrounded by five helices and a small N-termi-

nal antiparallel β sheet. The catalytic domain adopts an α/β fold with a central parallel β sheet (Fig. 9A). This domain contains the active-site cysteine (Cys302) that is highly conserved in the ALDH superfamily, and the loop region is implicated in substrate specificity. The oligomerization domain is composed of three antiparallel β strands (174, 179). Activators are bound to a common binding site at the interface of the oligomerization domain and the cosubstrate binding domain, causing conformational changes which lead to the observed regulatory behavior of the enzyme. The negative regulatory effect of NADP⁺, NADPH, and NADH seems to be due to inhibitor binding to the cosubstrate binding site. The GAPN catalytic mechanism (as also proposed for other ALDHs) proceeds in two main steps. (i) In the acylation step, Glu268 activates Cys302 to form an active thiolate, followed by the nucleophilic attack of Cys302 on the substrate carbonyl to form a thiohemiacetal. Through hydride transfer to the cosubstrate NAD⁺, the enzyme-thioester is formed. (ii) In the deacylation step, a Glu268-activated water molecule attacks the thioester bond, and finally, the acid and the reduced cosubstrate are released (Fig. 10).

Glyceraldehyde-3-phosphate dehydrogenase (phosphorylating) (catabolic). A GAPDH operating in the catabolic direction in *Archaea* has been identified mainly in mesophilic haloarchaea and methanogens, with the exception of *Mco. maripaludis*, which also

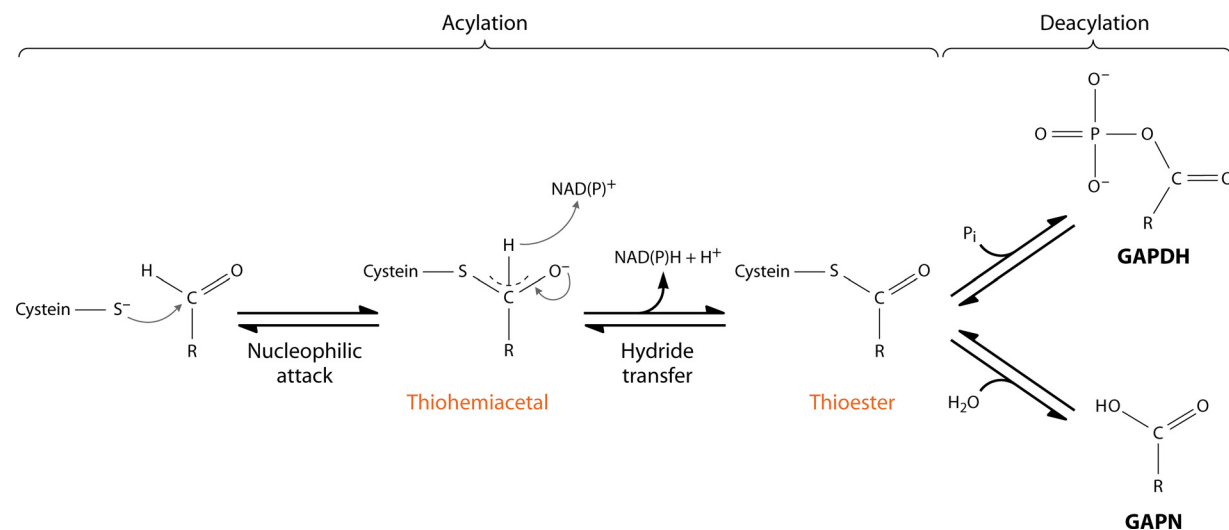


FIG 10 Proposed catalytic mechanism of classical phosphorylating GAPDH and nonphosphorylating GAPN with similar first acylation and hydride transfer steps and different deacylation steps, with phosphate as the acyl acceptor in GAPDH and water as the acyl acceptor in GAPN.

possesses a GAPOR (154). In mesophilic sugar-degrading haloarchaea, neither GAPN nor GAPOR activity could be detected, although a GAPN sequence homolog has been reported for *Halobacterium* NRC-1 (153). Instead, haloarchaea have been reported to utilize the GAPDH/PGK couple for the oxidation of GAP to 3PG (70, 131, 152, 180). In contrast to GAPN, classical GAPDH belongs to the glyceraldehyde-3-phosphate dehydrogenase-like C-terminal domain superfamily as well as to the NAD(P)⁺ binding Rossmann fold domain superfamily (N terminus) (according to the SCOP database) and catalyzes the oxidation of GAP to 1,3BPG via a two-step mechanism. The initial acylation step, including the nucleophilic attack of the catalytic cysteine residue on the aldehyde group, hydride transfer (facilitated by a histidine residue in GAPDHs), and the formation of the thioacyl enzyme intermediate as well as NAD(P)H, proceeds in a similar way as in GAPN enzymes (Fig. 10). However, GAPDH and GAPN differ in the second deacylation step. In phosphorylating GAPDH (type 2; TIGR01546), inorganic phosphate serves as the acyl acceptor, whereas in nonphosphorylating GAPN, the attack of the thioacyl enzyme intermediate is performed by an activated water molecule, leading to the formation of the respective nonactivated acid 3PG (181). Although GAPN and GAPDH have been described to consist of a nucleotide binding Rossmann-like fold and a catalytic domain, there is no sequence similarity between both enzymes, and also, the folds are distinct from each other (172, 182, 183). GAPDHs have been identified in all archaeal genomes analyzed so far and have been biochemically characterized in detail for a variety of Archaea, i.e., *Sul. solfataricus*, *Sul. tokodaii*, *Tpt. tenax*, *Tco. kodakarensis*, *Pyr. woesei*, *Har. vallismortis*, *Mtt. fervidus*, and *Mtb. bryantii* (131, 152, 176, 178, 184–191). The crystal structures are available for *Mca. jannaschii*, *Sul. solfataricus*, *Mtt. fervidus*, and *Pyr. horikoshii* (192–194). As for classical phosphorylating GAPDHs from Eukarya and Bacteria, the archaeal GAPDHs are ~150-kDa homotetramers composed of 36-kDa subunits. GAPDHs consist of two main domains (Fig. 9C): a nucleotide binding domain and a catalytic domain. A minor C-terminal domain composed of two helices is located at the junction between the nucleotide binding and catalytic domains. (This minor C-ter-

minal domain has also been described as part of the nucleotide binding domain.) The N-terminal nucleotide binding domain consists of a parallel β sheet surrounded by α helices in a classical Rossmann fold. The catalytic domain is composed of an antiparallel β sheet surrounded by α helices. This domain contains the active-site residues as well as the so-called S loop involved in nucleotide binding. In contrast to the eukaryotic/bacterial GAPDHs, which were described to be specific for NAD⁺, the archaeal GAPDHs show dual cosubstrate specificity for both NAD⁺ and NADP⁺. The archaeal and bacterial/eukaryotic GAPDHs share only weak sequence identities (15 to 20%), and the active sites and cofactor binding sites exhibit some subtle differences (193, 195–197). Nevertheless, since their structures and mechanisms are very similar, archaeal and eukaryotic/bacterial GAPDHs are grouped as distinct classes within the same protein superfamily. However, as discussed further below, the haloarchaea together with some glycogen-forming/utilizing methanogens seem to be the only archaeal organisms to date known to utilize the GAPDH/PGK couple in the catabolic direction. All other Archaea employ these enzymes exclusively for gluconeogenesis.

Phosphoglycerate Kinase

PGK sequences have also been identified in all archaeal genomes, and PGK activity has been found in crude extracts of several archaeal organisms, such as extreme halophiles, *Thermococcales*, *Sulfolobus*, *Thermoproteus*, *Desulfurococcus*, *Methanobacterium*, *Methanococcus*, *Methanothermus*, and *Methanothrix* (36, 40, 43, 70, 105, 127, 198–201). PGK catalyzes the transfer of phosphate from 1,3BPG to ADP in the first ATP-generating step of the classical EMP pathway. More detailed analyses have been carried out with several archaeal enzymes, including those from *Pyr. woesei*, *Mtt. fervidus*, and *Sul. solfataricus* (187, 199–205). The enzymes from *Mtt. fervidus* and *Pyr. woesei* represent homodimeric proteins (41-kDa subunits), whereas the enzyme from *Mtb. bryantii* shows a monomeric structure, as do most of the characterized PGKs from Bacteria and Eukarya. Furthermore, the PGKs from *Pyr. woesei* and *Mtt. fervidus* have been described to depend on monovalent cations such as K⁺ (201). However, so far, only one

archaeal PGK crystal structure, from *Pyr. horikoshii*, is available in the Protein Data Bank (PDB) (accession number 2CUN), but the structure has not been described in detail. Usually, PGK is composed of two similarly sized domains, both with a Rossman fold topology, termed the N-terminal domain, which binds the phosphoglycerate species 3PG and 1,3BPG, and the C-terminal domain, which binds the nucleotides ADP and ATP. The active site is located at the hinge region between both domains. For catalysis, a large domain movement from an open to a closed conformation takes place upon substrate binding, to bring the substrates into close proximity for phosphoryl transfer, which involves a nucleophilic attack of the oxygen atom of the β phosphate group of ADP on the phosphor atom of the C-1 phosphate group of 1,3BPG (for details and literature, see reference 206). As for GAPDH and TIM, PGK also appears to be well conserved and universally distributed in all three domains of life. However, as outlined above, archaeal organisms utilizing the GAPDH/PGK couple in the glycolytic direction for GAP oxidation and ATP generation are mainly extreme halophiles and some glycogen-forming methanogens. Due to the presence of GAPN or GAPOR, especially in (hyper)thermophiles, the GAPDH/PGK couple in *Archaea* usually operates exclusively in the gluconeogenic direction (see below), as deduced from mutational analyses and biochemical and regulatory properties (31, 175, 176, 178, 207, 208).

Phosphoglycerate Mutase

Phosphoglycerate mutase (PGAM) catalyzes the reversible interconversion of 3PG to 2PG, and PGAM activity has been detected in several archaeal organisms, including *Har. marismortui*, *Halorubrum saccharovorum*, *Pyr. furiosus*, *Thermococcus* spp., *Tpt. tenax*, *Arc. fulgidus*, *Pic. torridus*, *Mco. maripaludis*, *Mca. jannaschii*, *Methanothermobacter thermautotrophicus*, *Pyb. aerophilum*, and *Aer. pernix* (41, 70, 110, 198, 209). Generally, two types of PGAMs have been described for *Bacteria* and *Eukarya*: (i) the 2,3-bisphosphoglycerate (2,3BPG) cofactor-dependent enzymes (dPGAMs) and (ii) the cofactor-independent PGAMs (iPGAM). dPGAMs belong to the cofactor-dependent PGAM phosphoglycerate mutase-like superfamily and are known mainly from vertebrates, yeasts, and several *Bacteria*. In contrast, iPGAMs belong to the alkaline phosphatase-like superfamily and have been described in plants, nematodes, and many *Bacteria* (210, 211). Also, both types of PGAMs have been described in *Archaea*, including iPGAMs from *Pyr. furiosus* (212), *Pyr. horikoshii* (213), *Mca. jannaschii* (212, 214), *Sul. solfataricus* (215), and *Arc. fulgidus* (216) and dPGAM from *Tpl. acidophilum* (216).

2,3-Bisphosphoglycerate cofactor-dependent phosphoglycerate mutase. For *Archaea*, dPGAM of *Tpl. acidophilum* has been characterized in detail, and homologs were identified in several other archaeal species, especially in other thermoacidophiles such as *Sulfolobus*, *Thermoplasma*, *Picrophilus*, and *Ferroplasma* as well as *Methanosarcina* species and some halophiles (216). *Tpl. acidophilum* dPGAM represents a 46-kDa homodimer (23-kDa subunits) and is inhibited by vanadate, which is characteristic of dPGAM enzymes (216–218). This inhibition could be relieved by EDTA. *Tpl. acidophilum* dPGAM shows rather low sequence identities with other characterized dPGAMs. However, most of the functionally important residues appear to be conserved, including the family consensus pattern (210). Also, the secondary structural elements were predicted to be very similar to those deduced from the crystal structures from, e.g., *E. coli* (216, 219). dPGAMs are

tetramers, dimers, or sometimes monomers. Each subunit comprises a large α/β fold domain with a three-layer sandwich consisting of a largely parallel β sheet flanked on both sides by α helices and a small subdomain made up of two helices and one β strand (211). All dPGAM sequences, including that of *Tpl. acidophilum*, contain a conserved active-site histidine, which is phosphorylated during the catalytic cycle (211). The catalytic mechanism is initiated by 3PG binding to the enzyme's active site, which is phosphorylated at the conserved histidine by the 2,3BPG cofactor. The phosphate group is then transferred from the conserved His to the C-2 of 3PG to yield 2,3BPG as the reaction intermediate. After reorientation of the 2,3BPG intermediate in the active site, the phosphate group of C-3 is transferred back to the conserved histidine, the phosphoenzyme is regenerated, and 2PG is formed (211, 220). The archaeal dPGAMs seem to form a distinct subclass clearly separated from the bacterial and eukaryotic enzymes. The eukaryotic dPGAMs might have originated from *Bacteria* via horizontal gene transfer (216).

Cofactor-independent phosphoglycerate mutase. iPGAMs are structurally unrelated to dPGAMs and thus represent a convergent line of PGAM evolution. They belong to the alkaline phosphatase superfamily, which comprises a variety of metalloenzymes with diverse functions, such as phosphopen-tomutases (PPMs), alkaline phosphodiesterases, and sulfatases (221, 222). iPGAMs from *Pyr. furiosus*, *Mca. jannaschii*, *Sul. solfataricus*, and *Arc. fulgidus* have been characterized. The *Arc. fulgidus* enzyme is a 46-kDa monomer (bacterial iPGAMs also usually represent monomers), which, as for the iPGAM of *Sul. solfataricus*, is stimulated by Mn^{2+} ions or Co^{2+} (212, 215, 216). The *Mca. jannaschii* and *Pyr. furiosus* iPGAMs have been characterized as tetramers stimulated by Mg^{2+} (212). The crystal structure of the iPGAMs from *Tpl. acidophilum* and *Pyr. horikoshii* are available in the PDB (accession numbers 3KD8, 3IDD, and 2ZKT), but no detailed description has been published to date. However, the overall fold appears to be very similar to that described, e.g., for *Bac. stearothermophilus*, which consists of two domains of similar sizes connected only by two short loops. Each domain possesses a central, mostly parallel β sheet surrounded by 8 to 9 α helices. The cleft between both domains contains the active site with the 3PG substrate and two Mn^{2+} ion binding sites (in the *Bac. stearothermophilus* structure) (223, 224). The catalytic mechanism has been proposed to proceed via an intramolecular phosphoryl transfer from C-3 to C-2 of glycerate. From C-3, the phosphate moiety is first transferred to a conserved serine residue of the protein, forming a phosphoserine enzyme intermediate. The glycerate molecule is then repositioned/rotated, and an Asp residue abstracts a proton from C-2, facilitating an attack of the C-2 oxygen on the phosphor atom of the enzyme-bound phosphate group, resulting in the formation of 2PG. The two metal ions function in the coordination of the oxygen atoms of the phosphate group and the hydroxyl groups of the glycerate moiety and the serine residue. This proposed mechanism is in agreement with the finding that the characterized iPGAM from *Sul. solfataricus* autophosphorylates at this conserved serine residue (215).

Especially in thermoacidophiles and some methanogens, both iPGAM and dPGAM have been identified to be simultaneously present in one organism (216). In *E. coli*, which also harbors both

PGAM types, they are differentially expressed during growth (225).

Enolase

The reversible dehydration of 2PG to PEP is catalyzed by enolase (ENO). Enolase activity has been found in most of the Archaea investigated (in halophiles and members of the genera *Sulfolobus*, *Thermococcus*, *Thermoproteus*, *Pyrococcus*, *Archaeoglobus*, *Methanococcus*, *Pyrobaculum*, *Aeropyrum*, *Picrophilus*, and *Thermoplasma*) and has been characterized in some detail for *Pyr. furiosus* (40–42, 70, 105, 127, 128, 209, 226, 227). As for ENOs from *Eukarya* and *Bacteria*, the *Pyr. furiosus* enzyme represents a homodimer composed of 45-kDa subunits. For *Bacteria*, at least in some cases, octameric structures (i.e., a tetramer of dimers) have been described (228, 229). *Pyr. furiosus* ENO depends on Mg²⁺ ions for activity, which is common to all ENOs described so far (226). ENOs are abundant and highly conserved among all three domains of life (43, 230). They belong to the enolase superfamily and exhibit an eight-stranded α/β barrel fold [$\beta\beta\alpha\alpha(\beta\alpha)_6$] differing slightly from the TIM barrel topology [$(\beta\alpha)_8$] in the C terminus (Fig. 8). The N-terminal α/β domain consists of a three-stranded antiparallel β sheet surrounded by four α helices, which function in closing the active site during the catalytic cycle (45, 228, 229, 231). The active site is located at the C-terminal end of the barrel containing a highly conserved lysine residue. The first step of catalysis, i.e., proton abstraction from the C- α of the carboxylic acid, is common to all members of the enolase superfamily (230), resulting in an enolate intermediate. In enolases, a conserved lysine acts as a general base. In the second step, a glutamate donates a proton to the hydroxyl group at C-3, eliminating 1 molecule of water from the intermediate to yield PEP (228, 231) (Fig. 5). No crystal structures of enolases from archaeal sources have been reported. Only for *Mca. jannaschii* has the crystal structure of a putative enolase been described (PDB accession number 2PA6), indicating an octameric structure, but a detailed description remains to be published (229).

Phosphoenolpyruvate Conversion to Pyruvate

In *Archaea*, three mechanisms for the conversion of PEP to pyruvate and the concomitant synthesis of ATP via substrate-level phosphorylation have been described. Pyruvate kinase operates exclusively in the catabolic direction, whereas PEP synthetase and pyruvate:phosphate dikinase (PPDK) are known to catalyze mainly the anabolic direction and were reported to be involved in catabolism in only some cases (e.g., PEPS in *Tco. kodakarensis* and PPDK in *Tpt. tenax*). Therefore, here, i.e., in the context of hexose degradation, we focus on the description of the archaeal PKs and discuss PEPS and PPDK below (see Gluconeogenesis).

Pyruvate kinase. Pyruvate kinase is ubiquitous in all three domains of life and catalyzes an irreversible phosphoryl transfer from PEP to ADP to yield pyruvate and ATP, the last common step of glycolysis, found in the classical as well as the modified archaeal pathways for sugar degradation. In *Archaea*, PK activity has been detected in all sugar-degrading organisms, and PK sequences have been identified in nearly all archaeal genomes, with the exception of *Methanopyrus kandleri*, *Mba. thermautotrophicus*, and *Arc. fulgidus* VC16 (in sugar-degrading *Arc. fulgidus* strain 7324, both PK activity and the sequence have been identified) (40–42, 70, 105, 110, 127, 128, 209, 227, 232). Detailed biochemical studies on PKs in *Archaea* were reported for the enzymes from

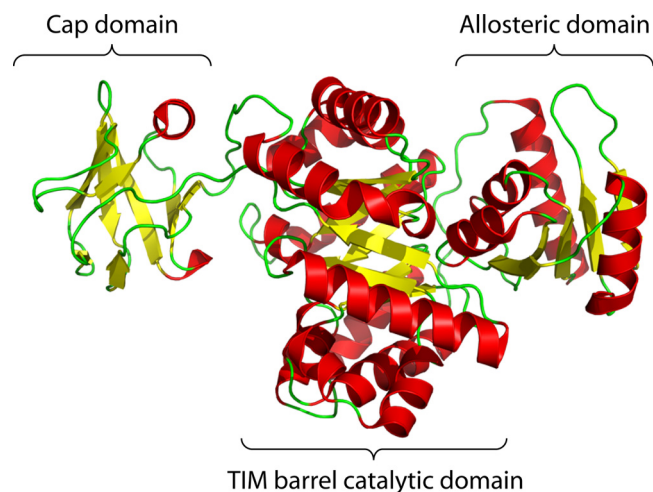


FIG 11 PK monomer crystal structure from *Pyb. aerophilum* (PDB accession number 3QTG) (244) shown as a ribbon diagram. As for classical PKs, the archaeal enzyme exhibits a three-domain structure, with a central TIM barrel catalytic domain flanked on one side by the cap domain and on the other side by the allosteric domain, where effector binding takes place.

Tpl. acidophilum, *Tpt. tenax*, *Arc. fulgidus* (strain 7324), *Aer. pernix*, and *Pyb. aerophilum* (232–235). As for their bacterial and eukaryotic counterparts, the archaeal PKs represent 200-kDa homotetrameric proteins composed of 50-kDa subunits and require divalent metal ions (Mg²⁺ and Mn²⁺) for activity. With the exception of the *Tpl. acidophilum* enzyme, archaeal PKs do not depend on the presence of monovalent cations like K⁺ or NH₄⁺, as described for many other PKs from *Bacteria* and *Eukarya*. This independence was attributed to the substitution of a conserved glutamate, which is highly conserved in the K⁺ sites of PKs stimulated by monovalent cations (232, 236). This glutamate is also present in the K⁺-dependent *Tpl. acidophilum* PK (233). Furthermore, most of the archaeal PKs exhibited positive cooperativity toward PEP and ADP, and the *Tpt. tenax* enzyme exhibited positive cooperativity toward PEP and Mg²⁺. From phylogenetic analyses, it has been concluded that the PK family is subdivided into two distinct branches (232, 235, 236), and it appears that this clustering is due to K⁺ dependence or independence (236).

The archaeal PK sequences show a high degree of similarity with their bacterial and eukaryotic counterparts, including the prosite consensus patterns for PKs (232, 235). PKs, as deduced from the crystal structures available from bacterial and eukaryotic sources and also recently from the crenarchaeon *Pyb. aerophilum* (PDB accession number 3QTG), share a very similar architecture (237–244) (Fig. 11). Each subunit consists of three domains: a central catalytic A domain with a classic (α/β)₈ barrel topology, a B domain comprising mainly a β sheet capping the catalytic domain, and a C domain with an α - β - α sandwich organization that contains the binding site for allosteric effectors. The eukaryotic proteins contain an additional small N-terminal domain, which is absent in prokaryotic enzymes. The active site, including a conserved lysine and glutamate residue, is located on the C-terminal side of the A domain (α/β)₈ barrel, facing the cleft between the A and B domains. The subunits interact mainly through the A domain (dimer formation) and the C domain (tetramer formation), and the interfaces are involved in the transmission of regulatory signals for cooperative behavior and allosteric regulation, respec-

tively (242, 244). The pyruvate kinase reaction is proposed to take place in two steps. The first step involves a phosphoryl transfer from PEP to ADP, forming an enolate intermediate and ATP, and the second step involves protonation of the enolate intermediate, forming pyruvate (243). A catalytically essential lysine residue, which is conserved among PKs, is proposed to promote the phosphoryl transfer step by stabilizing the pentavalent phosphate transition state. Most of the residues shown to be catalytically important for, e.g., the yeast enzyme are also conserved in the archaeal PK sequences.

One main feature of bacterial and eukaryotic PKs is the allosteric regulation by heterotrophic compounds such as F1,6BP, F2,6BP, AMP, or other sugar phosphates. Allosteric regulation by these classical effectors appears to be absent in most archaeal PKs; again, *Tpl. acidophilum* PK seems to be an exception, being activated by AMP (232, 235). The PK structure from *Pyb. aerophilum* revealed a phosphate ion binding site in a position comparable to that of the phosphate moiety of FBP in eukaryotic PKs. However, the binding site of the sugar moiety was shown to be occupied by a tyrosine in *Pyb. aerophilum* PK. Based on these results, docking experiments as well as kinetic analyses identified 3PG as a novel allosteric activator, which is bound to the C domain in a different mode compared to FBP binding in eukaryotic PKs (244). Thus, in *Pyb. aerophilum*, PK shows coordinated regulation with the irreversible GAPOR step in lower glycolysis, whereas classical PKs are regulated by the product of the irreversible PFK reaction in the upper part of the EMP pathway. This kind of allosteric regulation by a noncarbohydrate compound was discussed as a relic of a more ancient evolutionary stage preceding sugar metabolism. However, 3PG-mediated regulation seems not to be a common feature of archaeal PKs, since 3PG had no detectable effect on *Aer. pernix* and *Tpt. tenax* PKs due to missing structural features involved in 3PG binding.

MODIFICATIONS OF THE ENTNER-DOUDOROFF PATHWAY IN ARCHAEA

The main difference of the classical ED pathway, the second prominent glycolytic pathway known mainly for *Bacteria* and a few eukaryotic microorganisms, compared to the classical EMP pathway lies in the upper part of the reaction sequence. G6P is formed from glucose by ATP-dependent HK/GLK or by means of the PTS and subsequently oxidized to 6-phosphogluconate (6PG) via G6P dehydrogenase and 6-phosphogluconolactonase, which is then dehydrated to form the key intermediate of the pathway, 2-keto-3-deoxy-6-phosphogluconate (KDPG). KDPG is cleaved to pyruvate and GAP, catalyzed by KDPG aldolase, and GAP is further converted to a second molecule of pyruvate via the same reaction sequence as that in the lower shunt of the EMP pathway via GAPDH, PGK, PGAM, ENO, and PK (see Fig. 12 for an overview of the classical ED pathway and the modifications in *Archaea*). As a consequence of the initial oxidation of the carbonyl group of glucose, only 1 mol GAP is formed per mol glucose. The oxidation of GAP to pyruvate yields 2 mol ATP, and 1 mol ATP has to be invested for glucose phosphorylation. Thus, the net energy yield of this pathway is 1 mol ATP per mol glucose. The initial exergonic steps (i.e., carbonyl oxidation and sugar acid dehydration) not coupled to ATP production might enhance the effectiveness/flux of the pathway, and it has been discussed that the different glycolytic pathways might be seen as a trade-off between the “chemical motive force” of the whole process and its ATP yield. It

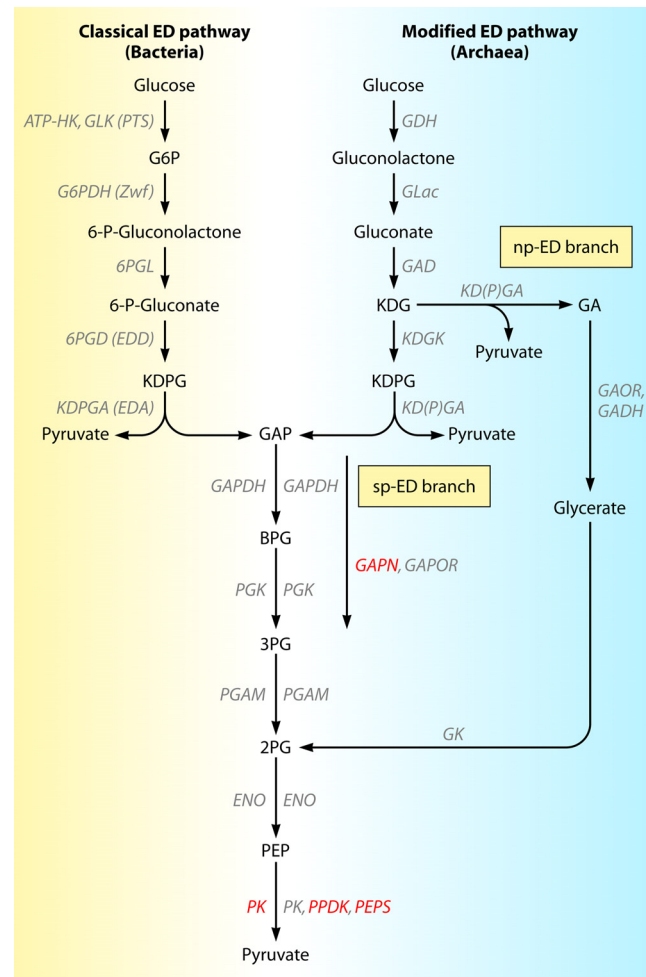


FIG 12 Glucose degradation via the Entner-Doudoroff (ED) pathways known for *Bacteria* (classical) and the modified branched versions reported for *Archaea*. The nonphosphorylative ED (npED) and the semiphosphorylative ED (spED) branches in *Archaea*, with phosphorylation at the level of glyceraldehyde and 2-keto-3-deoxygluconate (KDG), respectively, are shown. Abbreviations: 6PGD (EDD), gluconate-6-phosphate dehydratase; ENO, enolase; G6PDH (Zwf), glucose-6-phosphate dehydrogenase; GAD, gluconate dehydratase; GADH, glyceraldehyde dehydrogenase; GAOR, glyceraldehyde:ferredoxin oxidoreductase; GAPDH, glyceraldehyde-3-phosphate dehydrogenase; GAPN, nonphosphorylating GAPDH; GAPOR, GAP:Fd oxidoreductase; GDH, glucose dehydrogenase; GK, glyceraldehyde kinase; GLac, gluconolactonase; GLK, glucokinase; HK, hexokinase; KDGK, 2-keto-3-deoxygluconate kinase; KDPGA (EDA), 2-keto-3-deoxy-6-phosphogluconate aldolase; KD(P)GA, 2-keto-3-deoxy-(6-phospho)gluconate aldolase; PGK, phosphoglycerate kinase; PGL, 6-phosphoglucono-1,4-lactonase; PGAM, phosphoglycerate mutase (dPGAM, 2,3BPG cofactor dependent; iPGAM, 2,3BPG cofactor independent); PK, pyruvate kinase; PEPS, PEP synthetase; PPDK, pyruvate:phosphate dikinase; PTS, PEP-dependent phototransferase system; G6P, glucose 6-phosphate; GAP, glyceraldehyde 3-phosphate; 1,3BPG, 1,3-bisphosphoglycerate; 3PG, 3-phosphoglycerate; 2PG, 2-phosphoglycerate; PEP, phosphoenolpyruvate; KDG, 2-keto-3-deoxygluconate; KDPG, 2-keto-3-deoxy-6-phosphogluconate; GA, glyceraldehyde.

has also been argued that the protein cost of the ED pathway is lower, balancing the lower ATP yield or even making the ED pathway more effective than the EMP pathway under certain conditions (245). However, the lower ATP yield of the ED pathway has no or only minor consequences under conditions where the major source of energy is represented by the citric acid cycle (CAC) and

respiratory chain, especially under conditions of aerobiosis. Consequently, as shown by ^{13}C labeling experiments, several aerobic *Archaea*, especially extreme halophiles and thermoacidophiles, have been described to degrade glucose 100% via ED pathway versions. In *Tpt. tenax*, the modified EMP pathway, as described above, represents the main sugar-degrading pathway, converting 85% of the glucose. Nevertheless, 15% of the sugar is oxidized to pyruvate via a modified ED pathway, demonstrating that both the modified EMP pathway and a modified ED pathway operate in parallel in *Tpt. tenax* (39, 40, 70).

Modified ED pathway versions are known for all three domains of life: initially, for the ED pathway, two modified versions were reported: the semiphosphorylative ED (spED) pathway in extremely halophilic euryarchaea and several *Clostridium* species (70, 246, 247) and the nonphosphorylative ED (npED) pathway in thermoacidophilic organisms of the crenarchaeal genus *Sulfolobus* and the *Euryarchaeota Tpl. acidophilum* and, later on, *Pic. torridus* (33, 227, 248, 249). In *Eukarya*, the npED pathway version was identified in *Aspergillus* species (250). However, *Archaea* exclusively utilize ED pathway modifications, whereas in *Bacteria*, the classical pathway represents the predominant ED version, and modifications are restricted to a few species. In contrast to the classical ED pathway, in which glucose is first phosphorylated to glucose 6-phosphate, in the spED pathway of haloarchaea, glucose is directly oxidized to gluconate via glucose dehydrogenase (GDH). Gluconate dehydratase (GAD) converts gluconate to 2-keto-3-deoxygluconate (KDG). KDG is subsequently phosphorylated to 2-keto-3-deoxy-6-phosphogluconate (KDPG) by KDG kinase. KDPG is then cleaved to GAP and pyruvate by the action of the KDPG aldolase. GAP enters the lower common shunt of the EMP pathway, and in haloarchaea (as in the classical ED pathway known for *Bacteria*), the GAPDH/PGK couple catalyzes GAP oxidation to 3PG via 1,3BPG coupled to the synthesis of ATP via substrate-level phosphorylation. 3PG is further converted to 2PG by PGAM, and finally, via ENO and PK, a second molecule of pyruvate and also a second molecule of ATP are formed (70). Thus, due to the GAPDH/PGK couple, the spED pathway in extreme halophiles has the same ATP yield as the classical ED pathway in *Bacteria*. Only the site of phosphorylation changes from glucose to KDG.

The first two steps, i.e., glucose oxidation to gluconate and the subsequent dehydration to KDG, are also common to the npED pathway, as described for *Tpl. acidophilum* and *Pic. torridus* (248). However, in this ED variant, KDG is not phosphorylated but is directly cleaved into GA and pyruvate by a KDG aldolase, which was described to be specific for KDG not converting its phosphorylated derivative KDPG (see below) (209, 227). In *Thermoplasma* and *Picrophilus*, the resulting GA is further oxidized via GA dehydrogenase to glycerate. GA is then phosphorylated by glycerate kinase to yield 2PG and further converted to a second molecule of pyruvate by ENO and PK (248, 251–254). Due to bypassing phosphorylation at the level of KDG and also subsequent GAP oxidation, and since GA oxidation to glycerate is not coupled to ATP formation, the net ATP yield of the npED branch is zero (1 ATP invested for glycerate phosphorylation, and 1 ATP gained in the PK-catalyzed reaction).

However, more recent studies of the (hyper)thermophilic *Crenarchaeota Sul. solfataricus* P2 (DSM1617) and *Tpt. tenax* (Kra1; DSM2078) revealed that both ED pathway versions are operative in parallel, referred to as the branched ED pathway (173) (Fig. 12).

Later, bioinformatic studies also revealed that in most other ED pathway-utilizing *Archaea*, including halophiles and thermoacidophiles, homologs of both ED pathway branches are present, suggesting that the branched ED pathway might represent the common sugar degradation route in ED-utilizing *Archaea* (30, 32). Due to the presence of KDG kinase, in the branched ED pathway, KDG, formed by GDH and GAD, is either phosphorylated to KDPG by KDG kinase and then cleaved to GAP and pyruvate in the spED branch or directly cleaved to GA and pyruvate in the npED branch. KDG and KDPG cleavage in both pathway branches is catalyzed by the same bifunctional 2-keto-3-deoxy-(6-phospho)gluconate [KD(P)G] aldolase [KD(P)GA] (173, 255). In contrast to the haloarchaea, utilizing the reversible GAPDH/PGK couple for GAP oxidation, in other *Archaea*, GAP is oxidized in the spED branch via the unidirectional, nonphosphorylating GAPN and/or GAPOR (41, 153, 160, 172, 175). Both enzymes oxidize GAP directly to 3PG without coupling oxidation to the synthesis of ATP. 3PG is further converted to 2PG by PGAM. In the npED branch, GA, the product of KDG cleavage, is oxidized to glycerate by either GADH or glyceraldehyde:ferredoxin oxidoreductase (GAOR) (171, 248). Glycerate is then phosphorylated to 2PG via glycerate kinase (GK) (252–254, 256), which again enters the lower shunt of the EMP pathway (see above). 2PG, the intermediate of both the spED and npED branches, is finally converted via ENO and PK, and a second molecule of pyruvate is formed in both pathway branches (see Fig. 12 for a comparative illustration of the classical ED pathway and the archaeal modified ED pathway). Since in the spED branch of (hyper)thermophiles, GAP oxidation is also not coupled to ATP generation, the net ATP yield of the branched ED pathway is also zero.

However, the lower ATP yield of ED modifications is not that severe under aerobic conditions; the additional irreversible steps might drive the whole process more efficiently. Further on, the npED branch omits the formation of heat-labile intermediates like GAP and 1,3BPG and might thus be advantageous under thermophilic conditions (see below). The additional utilization of the spED branch seems to be energetically more favorable for anabolically necessary GAP synthesis (i.e., for pentose formation via F6P) and might also be seen as a mechanism of thermodadaptation, since otherwise, GAP has to be provided through the gluconeogenic sequence via heat-labile 1,3BPG at the expense of ATP cleavage (256) (Table 2 summarizes the enzymes involved in archaeal ED modifications as well as the classical ED pathway enzymes; see also below for further discussion).

Glucose Dehydrogenase

GDH catalyzes the first step in all archaeal ED pathway versions, i.e., the oxidation of D-glucose to D-gluconolactone using NAD⁺ and/or NADP⁺ as a cosubstrate. The enzyme has been characterized for a variety of organisms, such as *Sul. solfataricus*, *Tpl. acidophilum*, *Haloferax mediterranei*, *Tpt. tenax*, *Halobacterium salinarum*, *Sul. tokodaii*, and *Pic. torridus* (257–261). The characterized GDHs have been reported to be homotetramers or homodimers composed of ~40-kDa subunits. Most of the characterized GDHs show dual cosubstrate specificity, with a more or less pronounced preference for NADP⁺. The characterized GDHs from *Sul. solfataricus* (SsoGDH-1; SSO3003), *Pic. torridus*, and *Tpl. acidophilum* are promiscuous for the conversion of D-glucose and at least D-galactose (SsoGDH-1 additionally converts the pentoses D-xylose and L-arabinose) (255, 261–263). Conversely, the

TABLE 2 Overview of enzymes involved in the classical ED pathway in *Bacteria* as well as in the modified ED pathway versions in *Archaea*

Enzyme	EC no.	Abbreviation	Reaction	Protein superfamily(ies) (according to the SCOP database)	Protein family(ies)	Distribution
Glucose 6-phosphate dehydrogenase	1.1.1.49	G6PDH	D-Glucose 6-phosphate + NAD(P) ⁺ → D-glucono-1,5-lactone 6-phosphate + NAD(P)H + H ⁺	N-terminal domain NAD(P) binding Rossman fold-like domain superfamily; C-terminal glyceraldehyde-3-phosphate dehydrogenase-like, C-terminal domain superfamily	GADDH N-terminal domain family, glucose 6-phosphate dehydrogenase-like family (C-terminal domain)	<i>Bacteria, Eukarya</i>
Glucose dehydrogenase	1.1.1.47	GDH	D-Glucose + NAD(P) ⁺ → D-glucono-1,5-lactone + NAD(P)H + H ⁺	N-terminal GroES-like superfamily, C-terminal NAD(P) binding Rossman fold domain superfamily (known as the MDR superfamily)	Alcohol dehydrogenase, N-terminal domain-like and C-terminal domain-like (classical Rossman fold)	<i>Archaea, Bacteria</i>
6-Phosphogluconolactonase	3.1.1.31		D-Glucuno-1,5-lactone 6-phosphate + H ₂ O → 6-phospho-D-gluconate			
Glucuronolactonase	3.1.1.17		D-Glucuno-1,5-lactone H ₂ O → D-gluconate			
6-Phosphogluconate dehydrogenase	4.2.1.12	EDD	6-Phospho-D-gluconate → 2-keto-3-deoxy-6-phospho-D-gluconate + H ₂ O	LeuD/IIVD-like superfamily	IvD/EDD family	<i>Bacteria</i>
Glucuronate dehydrogenase	4.2.1.39	GAD	D-Gluconate → 2-keto-3-deoxy-D-gluconate + H ₂ O	Endolase-like N-terminal and C-terminal domain superfamily		<i>Archaea, Bacteria</i>
2-Keto-3-deoxy-D-gluconate kinase	2.7.1.45	KDGK	2-Keto-3-deoxy-D-gluconate + ATP → 2-keto-3-deoxy-6-phospho-D-gluconate + ADP	Ribokinase superfamily	PFK-B family	
2-Keto-3-deoxy-(6-phospho)-D-gluconate aldolase	4.1.2.14/4.1.2.21	KDG(P)GA	2-Keto-3-deoxy-(6-phospho)-D-gluconate ⇌ glyceraldehyde-(3-phosphate) + pyruvate	Aldolase superfamily [(βα) ₈ barrel fold]	Class I aldolase family (KDGA aldolase subfamily distinct from bacterial KDG aldolases and also from class I F1,6BP aldolases and archaeal-type class I F1,6BP aldolases)	<i>Bacteria, ED Pathway-utilizing Archaea</i>
2-Keto-3-deoxy-D-gluconate aldolase	4.1.2.14	KDGA	2-Keto-3-deoxy-D-gluconate ⇌ glyceraldehyde + pyruvate	Aldolase superfamily [(βα) ₈ barrel fold]	Class I aldolase family (distinct from the KDGA aldolase subfamily, bacterial KDG aldolases, and also class I F1,6BP aldolases and archaeal-type class I F1,6BP aldolases)	<i>Thermoacidophilic Eurarchaeota, Picromyces torridus, Thermoplasmata spp.</i>
Glyceraldehyde dehydrogenase	1.2.1.3	GADH	Glyceraldehyde + NAD(P) ⁺ H ₂ O → glycinate + ALDH-like superfamily		Thermoacidophilic Archaea	
Glyceradehyde-ferredoxin oxidoreductase	1.2.99.8	GAOR	Glyceradehyde + Fd _{ox} + H ₂ O → glycinate + Fd _{red} + H ⁺	Aldehyde oxidase/xanthine dehydrogenase superfamily	<i>Sulfolobus</i> spp.	
Glycerate kinase	2.7.1.165	GK	Glycerate	GckA/TudD-like superfamily (C-terminal domain, also known as the MOFRL superfamily)	GckA/TudD-like family	<i>Eukarya, Bacteria, Archaea</i>

GDH enzymes from *Tpt. tenax* and *Hfx. mediterranei* as well as a second GDH isoenzyme from *Sul. solfataricus* (SsoGDH-2; SSO3204) have been described to be more specific for D-glucose (39, 259, 264).

The crystal structures of GDH enzymes of three archaeal organisms, *Tpl. acidophilum*, *Hfx. volcanii*, and *Sul. solfataricus* (SsoGDH-1), have been reported (265–272). GDHs belong to the medium-chain dehydrogenase/reductase (MDR) superfamily, displaying a two-domain organization comprised of a central nucleotide binding domain flanked at the N and C termini by protein regions, which together make up the catalytic domain (273) (Fig. 13A). The nucleotide binding domain represents a typical Rossman fold comprised of a central six-stranded parallel β sheet surrounded by four α helices and contains the characteristic GX GXXG nucleotide binding motif (the third Gly is substituted for Ala in *Tpl. acidophilum* GDH [TacGDH]). A conserved, positively charged residue (Arg in SsoGDH-1 and *Hfx. volcanii* GDH [HfxGDH] and His in TacGDH) interacting with the phosphate moiety of NADP⁺ appears to encounter the dual cosubstrate specificity (266, 269, 274). The positively charged residue is apparently absent in NAD⁺-specific dehydrogenases of the MDR family, and the position two residues upstream is occupied by a negatively charged residue, hindering the binding of NADP⁺ (266, 269, 274).

The catalytic domain contains the binding sites of a structural zinc ion coordinated by four Cys residues in SsoGDH-1, three of which are also conserved in TacGDH. However, in HfxGDH, none of these coordinating residues is conserved, and accordingly, the structural zinc has not been detected in the crystal structures (270). Thus, the structural zinc identified in the other archaeal GDHs seems not to be functionally essential, as also described for other MDR family members (273, 275–277).

The catalytic zinc ion, however, is found in all archaeal GDH structures, and the coordinating residues Cys39 and H66 (SsoGDH-1 numbering) appear to be conserved throughout the protein family (except for HfxGDH, in which the Cys is substituted for Asp, which has been discussed as halophilic adaptation) (266, 269, 272, 274). A third residue coordinating the catalytic zinc has been identified from the HfxGDH and the SsoGDH structures to be Glu67, which is also highly conserved in all archaeal GDHs as well as in most alcohol dehydrogenase (ADH)-like enzymes for which a crystal structure is available. A fourth coordinating residue appears to be more variable and is usually a Glu/Asp (in archaeal GDH) or Cys (in other ADHs) but is substituted for Gln in SsoGDH-1 (i.e., Gln150). A further ligand is represented by a water molecule. The catalytic zinc binding site is localized at the active center at the bottom of a deep cleft separating both domains of the monomer. The catalytic mechanism is of an ordered Bi Bi type, with sequential binding of NADP⁺ prior to glucose, followed by an ordered release of first the gluconolactone and finally the reduced NADPH cosubstrate. NADP⁺ binding is accompanied by a conformational change of the loop connecting the α A helix and the β E strand, closing the active site, which reduces solvent accessibility (260, 272). Catalysis is proposed to basically proceed via an alkoxide intermediate through proton abstraction from the C-1 hydroxyl group of the substrate followed by hydride transfer from C-1 to NAD(P)⁺. The catalytic zinc-coordinating water molecule acts as the general base in proton abstraction (269, 272). During the catalytic cycle, the catalytic zinc ion appears to move within the active center, changing its coordination partners and coordination states, as deduced from the HfxGDH crystal structures.

This leads to subtle spatial rearrangements, bringing the reaction partners into the right position for the hydride transfer from C-1 to NADP⁺, finally leading to the formation of lactone and reduced NAD(P)H (272).

The crystal structures of SsoGDH-1 in complex with D-glucose and D-xylose, respectively, revealed that the majority of interactions between the enzyme and sugar substrate are formed with the hydroxyl groups at C-1, C-2, and C-3. In these positions, the glucose configuration is required for substrate binding. A change of the configuration, especially at positions C-2 and C-3, would lead to a nearly complete loss of substrate-enzyme interactions, whereas altered configurations at C-4 to C-6 have no or only minor effects on substrate binding. From this, the substrate specificity and, thus, the promiscuity of the enzyme for D-glucose, D-galactose, and D-xylose degradation have been explained (269). Biochemical and sequence analyses as well as homology modeling of SsoGDH-2 based on the SsoGDH-1 structure revealed some striking differences in the substrate binding residues. Particularly, the two amino acids Asn89 and His297 in SsoGDH-1 are substituted for Val93 and Glu294 in SsoGDH-2, respectively, and might encounter the higher specificity of SsoGDH-2 for glucose (259).

In contrast to the archaeal MDR family GDHs, the classical glucose 6-phosphate dehydrogenases (G6PDHs) (Zwf, encoded by the zwf gene in *E. coli* [278]), catalyzing the first oxidation step from G6P to 6PG in the classical ED pathway (and also in the oxidative part of the pentose phosphate pathway) of *Bacteria*, belong to the GAPDH-like C- and N-terminal domain superfamilies (SCOP database). G6PDH has been characterized, e.g., for *Tmt. maritima* (279), and the crystal structure has been reported, e.g., for the enzyme from *Leuconostoc mesenteroides* (280) (Fig. 13B). Both the *Tmt. maritima* and the *Leu. mesenteroides* G6PDHs represent homodimers with a subunit molecular mass of ~60 kDa. The *Leu. mesenteroides* G6PDH subunit comprises two domains, an N-terminal Rossman fold domain for coenzyme binding and a C-terminal large β/α domain composed of an antiparallel nine-stranded β -sheet, which contributes mainly to the active site located between both domains. However, catalysis also proceeds via proton abstraction from the C-1 hydroxyl (His240 general base), followed by hydride transfer to the coenzyme. His240 forms a catalytic dyad with Asp177, proposed to stabilize the positive charge that forms on His240 in the transition state (280).

It is commonly accepted that the product of the sugar dehydrogenase reaction is represented by the corresponding lactone (281). Also, the crystal structures of the archaeal sugar dehydrogenases acting on the closed circular form of the respective sugar substrates as well as, particularly, the HfxGDH structure in complex with the product gluconolactone confirm this finding for the archaeal dehydrogenases (269, 272). At ambient temperatures, spontaneous hydrolysis of these lactones to the corresponding straight-chain sugar acids, which then serve as substrates for the following dehydratase reaction, proceed only very slowly (282). Thus, lactone-hydrolyzing enzymes, i.e., lactonases, are required for the ring-opening reactions, especially under mesophilic conditions. Although this spontaneous lactone hydrolysis might proceed rapidly enough under elevated temperatures, in *Sul. solfataricus*, two genes encoding putative lactonases belonging to the SMP-30 (senescence marker protein 30) family have been identified, i.e., SSO3041 and SSO2705. However, these putative lacto-

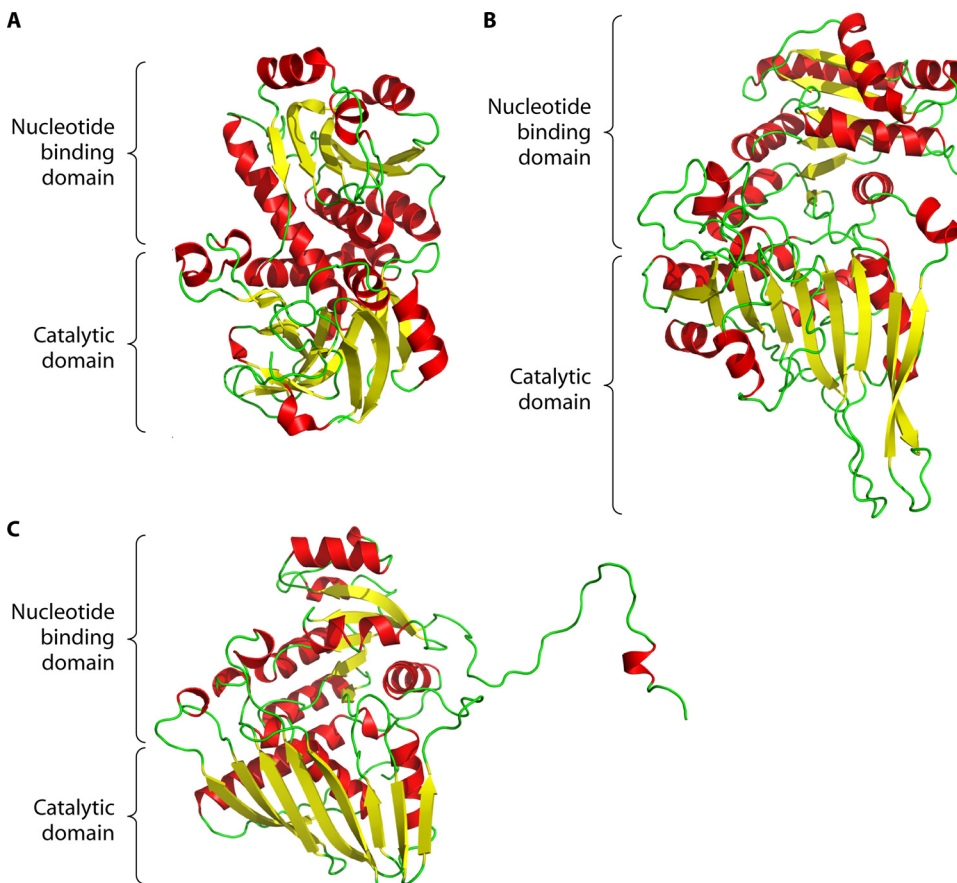


FIG 13 (A) Promiscuous GDH (PDB accession number 2CD9) (269) involved in hexose and pentose degradation in *Sul. solfataricus* exhibiting the typical two-domain dehydrogenase topology of the MDR superfamily members. (B) For comparison, the G6PDH structure from *Leuconostoc mesenteroides* (PDB accession number 1E7Y) (280), involved in the classical ED pathway, is shown. (C) The crystal structure of the *Zymomonas mobilis* glucose-fructose oxidoreductase is depicted (PDB accession number 1OFG) (349), which belongs to the same protein superfamily as the XDH described for *Hfx. volcanii*. For each protein, the ribbon representation of one monomer is shown.

nases appear not to be regulated in response to the carbon source and are not part of the identified pentose degradation gene clusters (283). However, interestingly, SSO3041 is colocalized with a GDH homolog (SSO3042) in the *Sul. solfataricus* genome. The recently crystallized gluconolactonase from *Xanthomonas campestris* as well as the xylonolactonases/arabinolactonases from *Azospirillum brasiliense* and *Caulobacter crescentus* belong to the same superfamily of SMP-30 proteins (284–286). In *Hfx. volcanii*, the putative SMP-30 D-xylonolactonase-encoding gene, HVO_B0030, harboring significant sequence identity to the lactonases from *Azo. brasiliense* and *Cau. crescentus*, was identified as part of the xylose degradation gene cluster, which is upregulated during growth on D-xylose (287). Although the enzyme activity was not confirmed, nor was an in-frame deletion mutant constructed, to confirm that this enzyme is essential for D-xylose degradation. The SMP-30 superfamily members appear not to be the only lactonases present in *Archaea*. For example, a putative xylonolactonase in *Har. marismortui* belongs to the β -lactamase superfamily (for literature, see reference 283), and the phosphotriesterase-like lactonases (e.g., from *Sulfolobus islandicus*) are amidohydrolase superfamily members (288). However, a sugar acid lactonase has so far not been characterized for *Archaea*.

Gluconate Dehydratase

The dehydration of gluconate to 2-keto-3-deoxygluconate (KDG) is carried out by GAD. GAD activity has been detected in *Sul. solfataricus*, *Sul. acidocaldarius*, *Tpl. acidophilum*, *Pic. torridus*, *Tpt. tenax*, as well as extremely halophilic *Archaea* (173, 227, 248, 249, 289, 290). The native enzyme was purified to homogeneity from *Sul. solfataricus* (SSO3198) and also from *Pic. torridus* (Pto0485) extracts, and the characterization revealed that both enzymes, like the GDHs, are promiscuous for the conversion of gluconate and galactonate (173, 209, 290). This supported the pathway promiscuity proposed for the modified ED pathway in *Sul. solfataricus*. In contrast to SsoGDH-1 also converting C₅ sugars, SsoGAD did not convert C₅ sugar acids like D/L-xylonate or D/L-arabinonate (289). For the breakdown of C₅ sugars, other dehydratases have been identified, i.e., xylonate dehydratase (XAD) (putatively SSO2665) and arabinonate dehydratase (AraD; SSO3124) (see below) (291). Sequence comparison revealed that SsoGAD (GnaD) belongs to the enolase-like superfamily, and it was predicted to contain typical enolase-like N- and C-terminal domains. Also, residues shown to be involved in metal ion coordination and catalysis in members of the superfamily appeared to be conserved in SsoGAD (173, 230, 289). This suggests that the

first step of the catalytic action, i.e., the abstraction of the proton from the C- α of a carboxylic acid to form an enolic intermediate (Fig. 5), common to all members of the superfamily is also carried out by GADs (230). This is also supported by the molecular properties of SsoGAD, reported to represent a 350-kDa homo-octamer composed of 44-kDa subunits (289). For other members of the enolase superfamily, octameric structures as well as the activating effect of bivalent cations such as Mg²⁺, Mn²⁺, Co²⁺, and Ni²⁺ observed for SsoGAD activity have also been reported (230). However, a crystal structure of an enolase superfamily protein has so far not been reported for *Archaea* (see Fig. 8 for the enolase fold). In contrast to the enolase superfamily GADs in *Archaea*, 6-phosphogluconate dehydratases catalyzing the dehydration step in the classical ED pathway in *Bacteria* belong to the IlvD (isoleucine valine biosynthesis)/EDD (Entner-Doudoroff dehydratase) family within the LeuD/IlvD-like superfamily of proteins (SCOP database) and are thus nonhomologous to the archaeal GADs at the sequence level and presumably also at the structural level. However, a detailed structural description of a classical 6-phosphogluconate dehydratase has also not been published so far, although a solved crystal structure from *Shewanella oneidensis* is available in the PDB (accession number 2GPA).

2-Keto-3-Deoxygluconate Kinase

Phosphorylating KDG to KDPG with ATP as the phosphoryl donor, KDG kinase represents the key enzyme of the spED pathway, and activity has been detected in extreme halophiles, *Tpt. tenax*, and *Sulfolobus* spp. (70, 173, 255). The KDGK gene is part of the ED gene cluster in *Tpt. tenax* and *Sul. solfataricus*, also encoding GAD, KD(P)G aldolase, and GAPN (*Sul. solfataricus*) or glucoamylase (*Tpt. tenax*) (173). Enzyme characterization revealed that in addition to GDH and GAD, KDGK in *Sul. solfataricus* is also promiscuous using KDG and 2-keto-3-deoxygalactonate (KDGal) as substrates (255, 292). SsoKDGK is a 70-kDa homodimeric enzyme (35-kDa subunits) and requires Mg²⁺ ions for activity. Sequence comparison as well as the crystal structure defined the enzyme as a member of the PFK-B family within the ribokinase superfamily (as also reported for the unusual ATP-dependent PFKs characterized for some EMP pathway-utilizing *Archaea* [see above]). Members of this family share a high degree of structural homology as well as a common catalytic mechanism (see above) (Fig. 3). As reported for other PFK-B family members, each monomer has a two-domain structure, with a major α/β domain, composed of 11 α helices positioned around a central β sheet formed by eight parallel and one antiparallel β -strand in KDGK, and a minor lid domain, comprising an antiparallel four-stranded β sheet and a small 3₁₀ helix (122) (Fig. 2B). The SsoKDGK structure was compared to the structure reported for the 2-keto-3-deoxygluconate-specific KDGK from *The. thermophilus* (TtKDGK) to gain insights into the structural determinants of the substrate promiscuity of SsoKDGK. From these comparisons, it was suggested that the active site in both enzymes turns out to be highly conserved and that particularly the protein substrate interactions at the O-1 carboxylate as well as the O-2, O-5, and O-6 of 2-keto-3-deoxygluconate are similar, whereas the main variation is around O-4. A shift in the position of a loop in the active center that carries Asp294 in SsoKDGK was observed. This reorientation of the loop allows this aspartate residue to interact with O-4 in both the C-4 epimers, KDG and KDGal, in SsoKDGK, whereas the position of the conserved aspartate residue in TtKDGK (i.e.,

Asp287) would disfavor binding of KDGal. Similarly, the reorientation of further residues, i.e., Thr90 and Leu104 in SsoKDGK as well as Thr89, Asn38, and Val101 in TtKDGK, has been observed, and it has been suggested that the sum of these rearrangements allows for the binding of 2-keto-3-deoxygalactonate in promiscuous SsoKDGK. It has been speculated that these subtle rearrangements might in turn be caused by sequence differences in other parts of the protein (122). Also, in *Tpl. acidophilum*, thought to utilize the npED pathway exclusively for glucose degradation, KDGK activity, and, thus, the key enzyme of the spED branch, has been detected. The enzyme has been purified from crude extracts and was characterized as a 260-kDa homo-octamer composed of 34-kDa subunits specific for the phosphorylation of KDG (293). The encoding gene has been identified, and sequence homologs of this novel kinase from the actin-like ATPase superfamily (BadF/BadG/BcrA/BcrD-like family) have been found in other thermoacidophilic *Euryarchaeota* from the *Thermoplasmatales*, including *Pic. torridus*, also reported to employ the npED route exclusively. This suggests that the branched ED pathway might also be operative in these organisms and thus might represent the common sugar degradation route in ED pathway-utilizing *Archaea*.

2-Keto-3-Deoxy-(6-Phospho)Gluconate Aldolase [KD(P)GA]

KD(P)GA catalyzes the reversible cleavage of KDG and KDPG, yielding pyruvate as well as GA and GAP, respectively, and has been detected in all archaeal ED pathway utilizers (40, 70, 158, 227, 248, 249). Initially, the enzyme from *Sul. solfataricus* was described as KDG aldolase converting only the nonphosphorylated substrates GA and pyruvate as well as KDG, respectively (257, 294). Also, the enzyme lacked facial selectivity, converting both KDG and KDGal to GA and pyruvate. However, later studies revealed that the aldolases from *Sul. solfataricus* and *Tpt. tenax* are also promiscuous for the conversion of the phosphorylated substrates KDPG and GAP (173). Thus, KD(P)G aldolase represents the key enzyme in both the npED and the spED branches of the branched ED pathway operative in *Sul. solfataricus* and *Tpt. tenax* (173). This has also been confirmed by another reinvestigation of *Sul. solfataricus* KD(P)G aldolase (255). In contrast, the aldolase characterized for *Pic. torridus* is specific for the nonphosphorylated compounds GA/pyruvate and KDG, respectively, and in conjunction with the apparent absence of KDPGA activity in cell extracts of *Pic. torridus*, it has been concluded that this organism exclusively utilizes the npED pathway for glucose degradation (209, 248). The crystal structures of the KD(P)G aldolases from *Sul. solfataricus*, *Sul. acidocaldarius*, and *Tpt. tenax* have been reported (295–298). They belong to the protein family of Schiff base-forming class I aldolases, in which the archaeal KD(P)G aldolases appear to belong to a distinct subgroup of enzymes (SCOP database). Also, the KDPG aldolases of the classical ED pathway in *Bacteria*, i.e., the Entner-Doudoroff aldolase (EDA) (278), crystallized, e.g., from *E. coli* (299, 300), *Pseudomonas putida* (301), and *Tmt. maritima* (300), belong to the Schiff base-forming class I aldolase family but represent a subgroup different from the archaeal KD(P)G aldolases (SCOP database). The bacterial enzymes show a classical ($\beta\alpha$)₈ TIM barrel fold and form trimeric structures. The archaeal KD(P)G aldolases are homotetrameric proteins, with each 33-kDa subunit exhibiting a classical ($\beta\alpha$)₈ TIM barrel fold with a C-terminal helical extension (Fig. 6B). The catalytic center with the Schiff base-forming catalytically essential

lysine [Lys155 in SsoKD(P)GA and Lys173 in the TtxKD(P)GA] is located near the center of the TIM barrel, close to the C terminus of the protein. As expected for the protein family, the catalytic mechanism is proposed to involve a Schiff base intermediate (Fig. 7). The substrate carboxyl group at C-1 then itself acts as a base [mediated by a conserved tyrosine residue, i.e., Tyr130 in SsoKD(P)GA] abstracting a proton from C-4 facilitating aldol cleavage to yield GA or GAP and the enzyme-bound pyruvate Schiff base, which is subsequently hydrolyzed to pyruvate and an unliganded enzyme (296). The archaeal KD(P)GAs exhibit high specificity for pyruvate as the donor substrate but show a greater flexibility concerning the aldehyde acceptor. This is reflected by the lack of facial selectivity, which has been explained by the solved crystal structures in complex with KDG and KDGal. Although the active site appears to be rigid, the enzymes are able to bind both substrate C-4 epimers, KDG and KDGal, where C-4 of the ligated C₆ substrate corresponds to C-1 of the aldehyde acceptor, i.e., GA(P). However, C-3 and C-4 of KDGal are shifted compared to KDG but still interact with the same residues of the enzyme [especially Tyr130 in SsoKD(P)GA]. This in turn seems to result in an altered spatial orientation of C-5 and C-6, which generally show a certain degree of flexibility in the structures. However, the binding interactions of the C-5 and C-6 groups of KDG and KDGal are different within the active site, and it has been concluded that substrate promiscuity is achieved by the incorporation of additional functionality while maintaining the rigidity and thus the stability of the active site (296).

Furthermore, the *Sulfolobus* and *Tpt. tenax* KD(P)GAs accept the phosphorylated and the nonphosphorylated acceptor substrates GAP and GA, respectively. This was found to be correlated with the presence of a newly identified phosphate binding motif comprised of two conserved Arg residues from two neighboring subunits of the tetramer. Such a phosphate binding motif was interestingly not found in nonphosphorylating KDGA (not accepting KDPG or GAP as the substrate) (297). In addition to the C₃ substrates GA and GAP, the *Sulfolobus* enzyme converts C₂ substrates like glycolaldehyde and glyoxylate as well as C₄ aldoses like D- and L-erythrose and threose. Acetaldehyde or propionaldehyde was not converted by the enzyme (297, 302). This substrate spectrum suggests that the C-5 hydroxyl of the ligated product (i.e., C-2 of the aldehyde acceptor substrate) is essential for binding, whereas C-6 is dispensable. Although the substrate binding pocket appears to be large enough, only very low activity has been observed with C₅ sugars, which has been suggested to be due to the predominantly closed circular conformation of these sugars and the concomitant inability of the enzymes to catalyze ring opening, thus preferring the open-chain form of the substrates (297). Interestingly, two additional aldolase paralogs were identified in *Sulfolobus solfataricus* (SulfoSYS Project [303]). The first analysis of the recombinant enzymes revealed that SSO3072 is specific for phosphorylated substrates (GAP and pyruvate) (D. Esser and B. Siebers, unpublished data), and SSO2274 shows significant similarity to the recently characterized KDG-specific *Pic. torridus* enzyme (209). These findings suggest that beside the promiscuous KD(P)G aldolase, two branch-specific enzymes are present. On the other hand, additional aldolase sequences were also identified in *Pic. torridus*, *Thermoplasma* spp., as well as *Ferroplasma acidarmanus*. These proteins show greater sequence homology to the characterized promiscuous KD(P)GAs from *Sulfolobus* and *Thermoproteus* (153, 209). This might indicate that in

these organisms, in addition to npED pathway-specific KDGA, a promiscuous KD(P)GA, and, thus, the spED branch, is also operative. This is supported by the finding of an active KDGK in *Thermoplasma* (see above) and further strengthens the idea of the branched ED pathway as a common sugar-degrading route in ED-utilizing Archaea.

GAP Conversion

GAP, the product of the aldol cleavage of KDPG in the course of the spED branch, is oxidized via two routes in *Archaea*, i.e., the GAPDH/PGK couple, found mainly in haloarchaea, as well as GAPN, which has been characterized in detail for *Sul. solfataricus* and *Tpt. tenax*. GAPOR (see above for a detailed description), representing the most common GAP-oxidizing mechanism in EMP-utilizing (hyper)thermophilic anaerobic *Archaea*, has so far not been identified in spED pathway branch-utilizing aerobic *Archaea*. Thus, only in the anaerobe *Tpt. tenax* do GAPN and GAPOR operate simultaneously in sugar degradation via both the modified EMP and the modified branched ED pathways, respectively (84). All three enzymes are described above in the section discussing the lower common shunt of the EMP pathway. Notably, in the *Thermoplasmatales*, i.e., *Tpl. acidophilum* and *Thermoplasma volcanium*, as well as in *Pic. torridus*, additional putative ALDH sequence homologs have also been identified (32). Although not characterized, it cannot be excluded that these enzymes might catalyze GAP oxidation. This might be a further indication of a functional spED branch in these organisms (84).

Glyceraldehyde dehydrogenase/(glycer)aldehydeferredoxin oxidoreductase. GA is a key intermediate of the npED pathway produced by the cleavage of KDG catalyzed by KD(P)G aldolase. In the *Euryarchaeota* *Tpl. acidophilum* and *Pic. torridus*, GA is oxidized to glycerate by a NADP⁺-dependent GADH. Activity has been detected in crude extracts, and the enzymes from both organisms have been characterized (227, 248, 304). Like GAPN, the GADHs are members of the aldehyde dehydrogenase (ALDH) superfamily (see Fig. 9A for the ALDH fold), represent 110-kDa homodimers (~55-kDa subunits) or 220-kDa tetramers, are specific for GA, and utilize exclusively NADP⁺ as a cofactor (248, 304). Although the branched ED pathway in *Sul. solfataricus* is operative, involving the spED and npED branches, and GA has been shown to be an intermediate of this pathway, no GADH activity could be detected. Furthermore, for none of the five ALDH superfamily paralogs identified in this organism by biochemical and bioinformatic analyses could catalytically relevant GADH activity be confirmed. Instead, these paralogs have been characterized as α-ketoglutaric semialdehyde dehydrogenase (α-KGSADH), GAPN, two succinic semialdehyde dehydrogenases (SSADHs), and methylmalonate semialdehyde dehydrogenases (MSDHs) (153, 283, 305). Although α-KGSADH showed some activity with GA in addition to α-ketoglutarate (α-KG) semialdehyde (KGSA), the catalytic efficiency and regulation strongly indicate a main function of α-KGSADH in pentose degradation (283) (see below). Also, the catalytic efficiency of the SSADHs for GA turned out to be far lower than for succinic semialdehyde, and a physiological function in amino acid and polyamine metabolism has been suggested (305). Thus, from the substrate specificity, kinetic properties, and regulation, a role of these ALDHs in glucose degradation could be excluded.

Instead, in *Tpt. tenax* and *Sulfolobus* spp., crude extract measurements and sequence comparisons indicated the presence of a

ferredoxin-dependent aldehyde oxidoreductase for GA oxidation to glycerate (84, 158). A molybdate-containing AOR from *Sul. acidocaldarius* with the highest activity toward GA was purified and characterized, and a function of this enzyme in sugar degradation was shown (171). *Sul. acidocaldarius* AOR (SaciAOR) is a 177-kDa heteromeric protein consisting of three subunits of 80.5 kDa (α), 32 kDa (β), and 19.5 kDa (γ). The enzyme contains flavin adenine dinucleotide (FAD), a molybdopterin cofactor, and two Fe_2S_2 clusters and thus differs significantly from the tungsten-containing monomeric *Pyr. furiosus* AOR described above, belonging to the AOR superfamily. In contrast, SaciAOR belongs to the aldehyde oxidase/xanthine dehydrogenase superfamily, which, however, seems to share some similarities in reaction mechanisms although exhibiting divergent folds (170, 306).

Glycerate Kinase

Glycerate kinase (GK) catalyzes the final step in the npED branch, i.e., the ATP-dependent phosphorylation of glycerate to 2PG yielding ADP. The GK enzymes from *Tpl. acidophilum*, *Pic. torridus*, *Pyr. horikoshii*, *Sul. tokodaii*, and *Tpt. tenax* have been characterized (252–254, 256, 307). They represent ~95-kDa homodimeric (*Sul. tokodaii*, *Pyr. horikoshii*, and *Pic. torridus*) or monomeric (*Tpl. acidophilum* and *Tpt. tenax*) proteins. The characterized GKs are specific for the formation of 2PG from D-glycerate and exhibit only low activity with L-glycerate; no other phosphoryl acceptors are utilized. GKs require divalent metal ions for activity and show a rather broad spectrum of phosphoryl donors, including ATP, GTP, CTP, and UTP and in some cases also ADP and pyrophosphate (*Pyr. horikoshii*) and even AMP (*Sul. tokodaii*). Only *Tpl. acidophilum* GK appeared to be specific for ATP. Additionally, GK from *Pyr. horikoshii* has been described to be activated by monovalent cations. *Sul. solfataricus* GK showed positive cooperativity with both substrates (glycerate and ATP) and also substrate inhibition. The physiological significance of this substrate inhibition remains unknown. However, evidence for an *in vivo* function of GK as a throttle valve regulating metabolic fluxes through either of the ED pathway branches has been provided (256). All archaeal GKs belong to the class II glycerate kinases (MORFL [multiorganism fragment with rich leucine] family), which have also been described for several *Bacteria* and *Eukarya*, where they function in formaldehyde assimilation via the serine cycle and in serine metabolism, respectively. The only crystal structure of a class II GK has been reported for *Tmt. maritima* (TM1585 [PDB accession number 2B8N]) (308). For *Pyr. horikoshii* (PD accession number 1X3L), the structure is available in the PDB but has not yet been described in detail. The *Tmt. maritima* structure revealed a monomer comprised of two dissimilar α/β domains. The N-terminal Rossman-like domain is composed of a central, six-stranded, parallel β sheet surrounded by 4 helices and an all-helical subdomain putatively providing the nucleotide binding site. The C-terminal domain exhibits a so-far-unknown fold containing a six-stranded, mixed β sheet surrounded by seven helices packed on both sides, which might be the substrate binding site. Several highly conserved amino acid residues from both domains have been identified, which might build up the active site suggested to be located in the cleft between both domains (308, 309). In addition to class II GK from the MORFL family, two further glycerate kinase classes are known. The class I GK enzymes (GK I superfamily [SCOP database]) are described mainly for *Bacteria* and for a few *Eukarya*, which are involved, e.g.,

in *E. coli* in allantoin (GK-1) as well as in glucarate and galactarate utilization (GK-2) (310). The crystal structure of the *Neisseria meningitidis* enzyme (PDB accession number 1TO6; PubMed identification is not available) has been solved and indicates no structural or sequence similarity to the class II enzymes (251, 252, 311). The class III GKs were first characterized for *Arabidopsis thaliana*, and homologs have been identified mainly in plants, some *Cyanobacteria*, and fungi, where they function in photospiration or glycerol metabolism (312; for details, see reference 252).

GLUCONEOGENESIS

Like in *Bacteria* and *Eukarya*, gluconeogenesis, i.e., the synthesis of G6P from pyruvate, in all *Archaea* proceeds via the reversible reactions of the EMP pathway catalyzed by ENO, PGAM, TIM, and PGI. In the modified versions of the EMP pathway in *Archaea*, there are three irreversible reactions (see above) which have to be bypassed during gluconeogenesis: (i) the PEP-to-pyruvate conversion catalyzed by PK, (ii) the GAP-to-3PG conversion catalyzed by GAPN and GAPOR (particularly in [hyper]thermophiles), and (iii) the reaction from F6P (F1P in halophiles) to F1,6BP catalyzed by ADP- or ATP-dependent PFKs. Reactions i and ii are bypassed through mechanisms known from the classical pathways in *Bacteria* and *Eukarya*, i.e., reaction i by phosphoenolpyruvate synthase, pyruvate:phosphate dikinase, or PEP carboxykinase and reaction ii by the classical GAPDH/PGK couple. However, the generation and dephosphorylation of F1,6BP to yield F6P, usually catalyzed by reversible FBPA and fructose bisphosphatase in *Bacteria* and *Eukarya*, differs in most *Archaea*, especially (hyper)thermophiles (and also some deep-branching *Bacteria*): the conversion of GAP and DHAP to F6P is carried out by one bifunctional enzyme, i.e., the fructose bisphosphate aldolase/phosphatase (FBPA/ase), without the release of the intermediate F1,6BP (see Table 3 for a summary of the gluconeogenic enzymes mentioned in the text).

Phosphoenolpyruvate Synthetase

The PK reaction is reversed by the action of PEPS catalyzing the ATP-dependent phosphorylation from pyruvate to PEP, yielding AMP and P_i . In *Bacteria*, e.g., in *E. coli* and *Salmonella Typhimurium*, PEPS has been reported to be essential for growth on pyruvate, lactate, and alanine (313, 314). PEPS has been identified in nearly all archaeal genomes except for *Thermoplasma* spp. Also, an important role of PEPS during autotrophic growth of *Mba. thermautotrophicus* has been reported, and PEPS activity has been detected in pyruvate-grown *Pyr. furiosus* (198, 315) and in obligate and facultative autotrophs such as *Ign. hospitalis* and *Methanospaera sedula*, respectively (316, 317). An unusual multimeric form of PEPS has been identified in *Staphylothermus marinus* but was not functionally characterized in detail (318, 319). From information on the thermodynamic, kinetic, and regulatory properties gained from detailed biochemical characterizations of archaeal PEPSs from *Mba. thermautotrophicus* and *Tpt. tenax*, an *in vivo* anabolic function in PEP synthesis was concluded (315, 320, 321). In contrast to this widespread and common function of PEPS in gluconeogenesis, mutational analyses of *Tco. kodakarensis* revealed that the enzyme is indispensable for glycolysis, i.e., during growth on maltooligosaccharides. This seems to also have been confirmed by the regulation of PEPS in *Pyr. furiosus* showing increased PEPS activity as well as increased transcription of the

encoding gene during growth on maltose (322). However, in other studies, PEPS appeared not to be significantly regulated in *Pyr. furiosus* at either the transcriptional or the activity level in response to glycolytic or gluconeogenic conditions, respectively (198, 207). An additional functional role of PEPS in gluconeogenesis is, however, also indicated by an impaired growth phenotype of a PEPS mutant of *Tco. kodakarensis* on pyruvate and the kinetic properties of the *Pyr. furiosus* enzyme showing higher catalytic efficiencies for pyruvate and ATP than for PEP and AMP (323, 324).

The archaeal PEPS characterized so far consists of a single 90-kDa subunit and forms multimeric aggregates in its native state, as described for the *Tpt. tenax* and *Sta. marinus* enzymes (318, 320). Also, the *Pyr. furiosus* enzyme has been reported to be an octamer with a tendency to form higher inactive aggregates (324). In contrast to the *Tpt. tenax* enzyme, those from *Mba. thermautotrophicus* and *Pyr. furiosus* were dependent on the presence of monovalent cations such as K^+ and NH_4^+ in addition to Mg^{2+} or Mn^{2+} (315, 324). Like the pyruvate:phosphate dikinases (PPDKs) (see below), PEPSs belong to the PEP-utilizing enzyme family containing the conserved signature pattern, as revealed by sequence comparison (PROSITE database accession numbers PS00370 and PS00742) (325, 326). Although no detailed structural description has been reported for a PEPS enzyme, the recently available structure of the *Nei. meningitidis* enzyme in the PDB (accession number 2OLS) indicates a three-domain architecture similar to that described for PPDKs (see below), with a central swiveling domain shuttling the phosphate moiety between the nucleotide and PEP binding sites. The two-step catalytic mechanism is initiated by nucleophilic substitution of the imidazole N-3 nitrogen of a conserved His residue at the β -phosphorus of ATP to yield AMP, P_i , and a phosphoenzyme intermediate (PEPS-P) phosphorylated at the conserved His. This step is followed by phosphoryl transfer from the enzyme-His-P intermediate to pyruvate to form PEP (327), as follows:

1. PEPS-His + ATP + $H_2O \leftrightarrow$ PEPS-His-P + AMP + P_i
2. PEPS-His-P + pyruvate \leftrightarrow enzyme-His + PEP

The sequence conservation of archaeal PEPS enzymes compared to their bacterial and eukaryotic counterparts suggests similar structures and mechanisms. In combination with the essential function in gluconeogenesis reported for PEPS in *Bacteria* and the high level of conservation of the enzyme in all three domains of life, together with its high abundance in *Archaea*, the findings point to a general gluconeogenic function of PEPS in *Archaea*. The additional glycolytic function of PEPS acquired in *Thermococcales* has been discussed as energetically favorable when ADP-dependent sugar kinases are used in the upper part of the modified EMP pathway for sugar degradation (323), since the AMP produced by the ADP-dependent sugar kinases is reconsumed by PEPS together with P_i to form ATP.

Pyruvate:Phosphate Dikinase

A second mechanism for PEP synthesis from pyruvate is represented by PPDK catalyzing the reversible ATP- and P_i -dependent formation of PEP from pyruvate, yielding AMP and PP_i . Compared to PEPS, PPDK is less distributed in *Archaea* and simultaneously present in a few organisms, such as *Tpt. tenax*, *Pyb. aerophilum*, *Sulfolobus* spp., and several methanogens, together with

PEPS (and PK) (32, 320). In *Thermoplasma* spp., which lack genes encoding PEPS, PPDK might represent the only PEP synthesis pathway from pyruvate. As outlined above, PPDK also belongs to the PEP-utilizing enzyme family, with the characteristic signature patterns and the three-domain organization comprising an N-terminal ATP binding domain, a C-terminal α,β barrel PEP-pyruvate binding domain, and the small central α,β fold swiveling domain, which shuttles the phosphoryl moiety between the two binding sites over a distance of ~ 45 Å. The phosphate residue is bound to a catalytically essential His residue in the swiveling domain, forming a phosphoryl-enzyme intermediate in the course of the catalytic cycle (328, 329). The catalytic mechanism is initiated by a nucleophilic substitution of the His imidazole N-3 nitrogen at the β -phosphorus of ATP to yield AMP and a pyrophosphorylated enzyme intermediate (PPDK-His-P β P γ). From the pyrophosphate intermediate, γP is transferred to P_i , yielding pyrophosphate and the phosphoryl-enzyme intermediate. This step is followed by phosphoryltransfer from the enzyme-His-P β intermediate to pyruvate to form PEP, and thus, finally, the P β phosphate is transferred from ATP to pyruvate in a three-step mechanism (see reference 329 and references therein):

1. PPDK-His + ATP \leftrightarrow PPDK-His-P β P γ + AMP
2. PPDK-His-P β P γ + $P_i \leftrightarrow$ PPDK-His-P β + P γP_i
3. PPDK-His-P β + pyruvate \leftrightarrow PEP + PPDK-His

In contrast to this PPDK three-step catalytic mechanism, a stable pyrophosphoryl-enzyme intermediate could not be determined in PEPS enzymes (327), probably due to spontaneous hydrolysis of the pyrophosphoryl-enzyme intermediate liberating the P γ of ATP and AMP already in the first partial reaction, resulting in the two-step mechanism described above. The archaeal PPDK from *Tpt. tenax*, like its bacterial counterparts, represents a 250-kDa homodimer (100-kDa subunits). It depends strictly on P_i in the anabolic direction and PP i in the catabolic direction, which distinguishes PPDK from PEPS (see above). *Tpt. tenax* PPDK turned out to be fully reversible, operating in both the catabolic and anabolic directions. From the kinetic constants, a slight preference of the enzyme for the catabolic direction was assumed (320). The enzyme has been characterized as being independent of monovalent cations. In contrast to *Tpt. tenax* PEPS, PPDK is not inhibited by AMP or ADP but by ATP at the protein level and is also not significantly regulated at the transcriptional level. From these enzyme properties, PPDK has been assumed to fulfill a role as a "standby" enzyme under both glycolytic and gluconeogenic growth conditions in *Tpt. tenax*, allowing quick adaptation to changing conditions (320).

Phosphoenolpyruvate Carboxykinase

Phosphoenolpyruvate carboxykinase (PCK) catalyzes the reversible ATP- or GTP-dependent decarboxylation of oxaloacetate to PEP and CO₂. In *Archaea*, PCK-encoding genes have been identified in *Thermococcales* and *Sulfolobales* as well as in *Aer. pernix* and *Thermoplasma* spp. (330). Enzyme activity has been detected in crude extracts of *Tco. kodakarensis* and *Met. sedula*, and a detailed characterization has been reported for the *Tco. kodakarensis* enzyme (317, 330). PCKs belong to the PEP carboxykinase-like superfamily, comprising two major classes, i.e., the ATP-dependent PCKs (ATP-PCKs) and the GTP-dependent PCKs. ATP-dependent PCKs are distributed mainly in *Bacteria*, yeasts, and plants,

TABLE 3 Overview of enzymes involved in gluconeogenesis in *Archaea*, *Bacteria*, and *Eukarya*

Enzyme	EC no.	Abbreviation	Reaction	Protein superfamily(ies) (according to the SCOP database)	Distribution
Phosphoenolpyruvate carboxykinase	4.1.1.32 (GTP), 4.1.1.49 (ATP)	PCK	Oxaloacetate + GTP \rightleftharpoons phosphoenolpyruvate + CO ₂ + GDP (ADP)	PEP carboxykinase N-terminal domain superfamily	<i>Eukarya, Bacteria, Euryarchaeota, Crenarchaeota</i>
Pyruvate-phosphate dikinase	2.7.9.1	PPDK	Pyruvate + ATP + P _i \rightleftharpoons phosphoenolpyruvate + AMP + PP _i	Glutathione synthetase ATP binding domain-like superfamily (N-terminal domain) (ATP grasp fold); phosphohistidine domain superfamily (central domain), phosphoenolpyruvate/pyruvate domain superfamily (C-terminal domain) (TIM barrel fold)	<i>Eukarya, Bacteria, Archaea</i>
Phosphoenolpyruvate synthase (pyruvate, water dikinase)	2.7.9.2	PEPS	Pyruvate + ATP + H ₂ O \rightleftharpoons phosphoenolpyruvate + AMP + P _i	From sequence comparisons, domain organization likely similar to that of the glutathione synthetase ATP-binding domain-like superfamily (N-terminal domain) (ATP grasp fold); phosphohistidine domain superfamily (central domain); phosphoenolpyruvate-pyruvate domain superfamily (C-terminal domain) (TIM barrel fold)	<i>Eukarya, Bacteria, Archaea</i>
Enolase	4.2.1.11	ENO	Phosphoenolpyruvate + H ₂ O \rightleftharpoons 2-phosphoglycerate	Enolase-like, N- and C-terminal superfamily	<i>Eukarya, Bacteria, Archaea</i>
2,3-Bisphosphoglycerate-independent phosphoglycerate mutase	5.4.2.1	iPGAM	2-Phosphoglycerate \rightleftharpoons 3-phosphoglycerate	Alkaline phosphatase superfamily, 2,3-bisphosphoglycerate-independent phosphoglycerate mutase; substrate binding domain superfamily	<i>Plants, nematodes, Bacteria, Archaea</i>
2,3-Bisphosphoglycerate-dependent phosphoglycerate mutase	5.4.2.1	dPGAM	2-Phosphoglycerate \rightleftharpoons 3-phosphoglycerate	Cofactor-dependent phosphoglycerate mutase family	<i>Vertebrates, yeasts, Bacteria, mainly thermoacidophilic Archaea and Methanotrichia spp.</i>
Phosphoglycerate kinase	2.7.3.2	PGK	3-Phosphoglycerate + ATP \rightleftharpoons 1,3-bisphosphoglycerate + ADP	Phosphoglycerate kinase superfamily	<i>Eukarya, Bacteria, Archaea</i>
Glyceraldehyde-3-phosphate dehydrogenase (phosphorylating)	1.2.1.13 (NADP ⁺), 1.2.1.12 (NAD ⁺)	GAPDH	1,3-Bisphosphoglycerate + NAD(P)H + H ⁺ \rightleftharpoons glyceraldehyde 3-phosphate + NAD(P) ⁺ + P _i	N-terminal domain NAD(P) binding Rossmann fold-like domain superfamily; C-terminal glyceraldehyde 3-phosphate dehydrogenase-like C-terminal domain superfamily	<i>Eukarya, Bacteria, Archaea</i>
Triosephosphate isomerase	5.3.1.1	TIM	Glyceraldehyde 3-phosphate \rightleftharpoons dihydroxyacetone phosphate	Triosephosphate isomerase superfamily [(βα) ₈]	<i>Eukarya, Bacteria, Archaea</i>
Fructose-1,6-bisphosphatase	3.1.3.11	FBPase	Fructose 1,6-bisphosphate \rightarrow fructose 6-phosphate + P _i	Carbohydrate phosphatase superfamily	<i>Type I, Eukarya, Bacteria, and a few haloarchaea and methanogens; type II, Bacteria and a few methanogens; type III, Bacteria; type IV, Euryarchaeota, Crenarchaeota, and a few Bacteria (Thermotoga)</i>
Fructose-1,6-bisphosphate aldolase class II	4.1.2.13	FBPA II	Dihydroxyacetone phosphate + glyceraldehyde 3-phosphate \rightleftharpoons fructose 1,6-bisphosphate	Aldolase superfamily [(βα) ₈ barrel fold]	<i>A few halophilic Euryarchaeota, Bacteria, fungi</i>
Archaeal-type class I fructose-1,6-bisphosphate aldolase	4.1.2.13	FBPA IA	Dihydroxyacetone phosphate + glyceraldehyde 3-phosphate \rightleftharpoons fructose 1,6-bisphosphate	Aldolase superfamily [(βα) ₈ barrel fold]	<i>Archaea, Bacteria</i>
Fructose-1,6-bisphosphate aldolase class I	4.1.2.13	FBPA I	Dihydroxyacetone phosphate + glyceraldehyde 3-phosphate \rightleftharpoons fructose 1,6-bisphosphate	Aldolase superfamily [(βα) ₈ barrel fold]	<i>Eukarya</i>

PP _i -dependent phosphofructokinase	2.7.1.90	PP _i -PFK	Fructose 1,6-bisphosphate + P _i ⇌ glucose 6-phosphate + PP _i	Phosphofructokinase family (known as PFK-A) forming a distinct subfamily	Crenarchaeota (<i>Thermoprotius tenax</i>), some <i>Bacteria</i> , <i>Eukarya</i> (protists, plants)
Fructose-1,6-bisphosphate aldolase/phosphatase (type V fructose-1,6-bisphosphatase)	3.1.3.11	FBPA/ase	Dihydroxyacetone phosphate + glyceraldehyde 3-phosphate → fructose 6-phosphate + P _i	Sulfobolus fructose-1,6-bisphosphatase-like protein superfamily (SCOP database) (similarity to the ferredoxin fold in their N-terminal part and to bacterial S-adenosylmethionine decarboxylase in their C-terminal part)	Sulfobolus fructose-1,6-bisphosphatase-like protein superfamily (SCOP database)
Cupin-type phosphoglucose isomerase	5.3.1.9	cPGI	Fructose 6-phosphate ⇌ glucose 6-phosphate	Cupin superfamily	cPGI family
Phosphoglucose isomerase/phosphomannose isomerase	5.3.1.9/5.3.1.8	PGI/PMI	Fructose 6-phosphate ⇌ glucose 6-phosphate/mannose 6-phosphate	PGI superfamily (SIS domain superfamily)	PGI/PMI family
Phosphoglucose isomerase	5.3.1.9	PGI	Fructose 6-phosphate ⇌ glucose 6-phosphate	PGI superfamily (SIS domain superfamily)	PGI family

Eukarya, *Bacteria*, halophilic *Euryarchaeota*, methanogenic *Euryarchaeota* (*Methanococcus*) (*Thermoplasmata*)

whereas the GTP-PCKs are found in mammals and a few *Bacteria* (for literature, see reference 330). Due to significant sequence homology (30 to 35% identity), all archaeal sequences identified so far belong to the GTP-dependent PCK class, like, e.g., GTP-PCK from *Corynebacterium glutamicum*, the crystal structure of which has been reported (331). In contrast to the characterized monomeric PCKs from *Bacteria* and *Eukarya*, the enzyme from *Tco. kodakarensis* has been characterized as a 280-kDa homotetramer (70-kDa subunits) and requires divalent cations (Mg²⁺, Co²⁺, and Mn²⁺) for activity. The enzyme exhibited a higher affinity toward oxaloacetate than toward PEP and was induced at the transcriptional level during growth under gluconeogenic conditions, and also, the specific activities in cells grown on pyruvate or peptides were consistently higher than those in starch-grown cells. This indicates a gluconeogenic function of the enzyme, especially in the conversion of oxaloacetate derived from amino acids such as Asp and Asn during growth on peptides. The higher induction level of the enzyme during growth on pyruvate was discussed to reflect an anaplerotic function of the enzyme in the conversion of excess PEP to oxaloacetate, thus replacing the PEP carboxylase apparently lacking in this organism (330).

Glyceraldehyde-3-Phosphate Dehydrogenase/Phosphoglycerate Kinase

With the exception of the modified EMP and ED pathways reported for halophilic *Archaea* employing the reversible GAPDH/PGK couple in the catabolic direction, all other *Archaea* characterized, particularly hyperthermophiles and anaerobes, utilize irreversible GAPN and/or GAPOR for the oxidation of GAP in the course of their modified EMP and ED pathways (see the section on EMP pathways, above). The absence of GAPN- and GAPOR-encoding genes in some methanogens as well as *Archaeoglobus* strains might reflect the inability of these organisms to metabolize sugars or glycogen, although the GAPDH/PGK couple is present. Thus, the irreversible GAP oxidation in *Archaea* has to be bypassed during gluconeogenic growth. Apparently, all *Archaea*, including the autotrophic organism *Ign. hospitalis*, have been shown to contain the classical GAPDH/PGK couple (30, 36, 316), and mutational analyses have clearly shown that this enzyme couple operates exclusively in the gluconeogenic direction in *Tco. kodakarensis* (175). Also, from the kinetic and regulatory point of view, this could be confirmed, since catabolic GAPN and GAPOR are upregulated in response to glycolytic conditions, whereas the GAPDH/PGK couple is upregulated during gluconeogenic growth in *Tpt. tenax*, *Pyr. furiosus*, and *Tco. kodakarensis* (31, 178, 207, 208). Furthermore, in most cases, PGK and GAPDH show a pronounced preference for the anabolic direction, as deduced from their kinetic properties (176, 178, 185, 198, 200).

Bifunctional Fructose-1,6-Bisphosphate Aldolase/Phosphatase

The classical FBPases (classes I to III) known for *Bacteria* and *Eukarya* are absent in most *Archaea*, as revealed by genome sequence analyses (332). However, FBPase activity was demonstrated in *Archaea* growing under gluconeogenic conditions (198, 333). In *Mca. jannaschii*, a FBPase also showing inositol monophosphatase activity, a so-called class IV phosphatase, was identified through structural comparisons, and orthologs of this protein have also been identified in several other *Archaea* such as *Arc. fulgidus* and *Pyr. furiosus* (334, 335). However, for *Tco. kodakarensis*

ensis, using biochemical and mutational approaches, it was shown that the FBPase activity in this organism is carried out by a further type of FBPase, a class V enzyme (332, 336). Orthologs of such class V FBPases have also been identified in most archaeal as well as deeply branching bacterial genome sequences (336, 337). The enzyme was shown to be essential for gluconeogenesis but not for glycolytic growth, since a deletion strain of *Tco. kodakarensis* grew well on sugars but did not grow under gluconeogenic conditions (332). Furthermore, the regulation pattern at the transcript level, showing gene transcription under gluconeogenic conditions (growth on pyruvate and peptides) but not under glycolytic conditions (growth on starch), confirmed the gluconeogenic function (336). Surprisingly, this class V enzyme was later shown to exhibit bifunctional activity, catalyzing not only the dephosphorylation of F1,6BP to F6P but also the aldol condensation of DHAP and GAP to F1,6BP, which was not recognized initially (337). Its bifunctionality ensures that heat-labile triosephosphates are quickly removed and trapped in stable fructose 6-phosphate, rendering gluconeogenesis unidirectional, and might therefore represent a mechanism of thermodadaptation. Notably, the FBPA/ase has been described to be heat stable even in mesophilic Archaea (e.g., *Cen. symbiosum*). The bifunctional FBPA/ase from several archaeal organisms, i.e., *Ign. hospitalis*, *Met. sedula*, *Thermoproteus neutrophilus*, *Methanothermobacter marburgensis*, and *Cen. symbiosum* (337), as well as from *Sul. solfataricus* (338) was characterized, and it could be identified in nearly all archaeal genomes (except for extreme halophiles and some methanogens) as well as some deeply branching Bacteria (337, 339). The enzyme is a 340-kDa homooctamer composed of 42-kDa subunits and is specific for F1,6BP (for the phosphatase reaction) and DHAP/GAP (for the aldolase reaction), and its activity depends on Mg²⁺ (336, 337). The F1,6BP intermediate is not liberated during catalysis (337). The crystal structures of the enzyme from *Sul. tokodaii* and *Tpt. neutrophilus* have been reported (340–342). The FBPA/ase is composed of a single domain forming an α-β-β-α four-layered sandwich fold, which is completely different from known FBPase structures, which represent the typical α-β-α-β-α five-layered sandwich sugar phosphatase fold, and also has nothing in common with the typical (βα)₈ barrel fold of the classical aldolases (341) (Fig. 14). The bifunctional FBPA/ases form the superfamily of *Sulfolobus* fructose-1,6-bisphosphatase-like proteins (SCOP database) and show similarity to the ferredoxin fold in their N-terminal part and to bacterial S-adenosylmethionine decarboxylase in their C-terminal part (341). Although the structures of the FBPA/ases show no similarity to class I FBPAs, the catalytic mechanism of the aldol condensation of the bifunctional FBPA/ase was also shown to proceed via a Schiff base intermediate (Fig. 7). The Schiff base is formed between the keto group of DHAP and the side-chain amino group of a catalytically essential lysine residue (Lys232 in the *Tpt. neutrophilus* enzyme) facilitated by a tyrosine (Tyr229) (340, 342). In its unliganded state, the enzyme binds 2 Mg²⁺ molecules, and the active site is accessible. Upon DHAP binding, a third Mg²⁺ molecule is bound so that all three oxygen atoms of the phosphate moiety are complexed, and the loop containing the lysine (“aldolase loop”) is redirected in a position to form the Schiff base. A second loop (anchor loop) is retracted from the active site to accommodate this conformational change. The tyrosine then abstracts a proton from the C-3 of the Schiff base DHAP intermediate, resulting in the formation of an enamine intermediate, which in turn carries out a nucleophilic attack

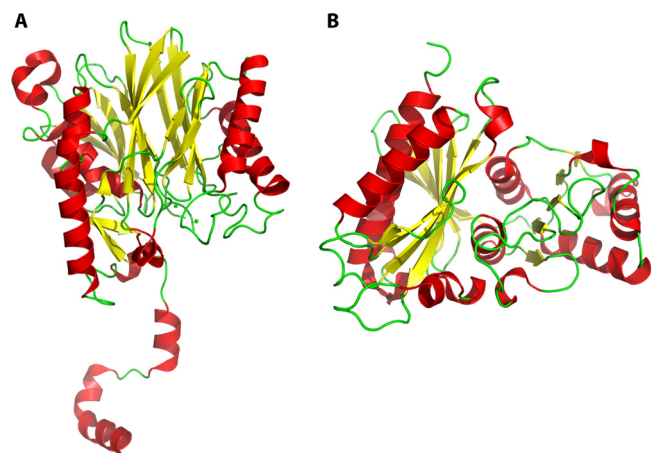


FIG 14 (A) Crystal structure of the monomer of the bifunctional fructose-1,6-bisphosphate aldolase/phosphatase (class V phosphatase) (PDB accession number 3T2B) (342) bypassing the FBPA and PFK reactions in gluconeogenesis of most Archaea and deeply branching Bacteria. The bifunctional FBPA/ase exhibits an α-β-β-α four-layered sandwich fold. (B) However, the class I phosphatase from *E. coli* (PDB accession number 2OX3) (579) shows an α-β-α-β-α five-layered sandwich fold (similar to class II and class IV phosphatases). Class I phosphatase represents the canonical enzyme in gluconeogenesis of Eukarya and Bacteria.

on the C-1 of GAP, forming the Schiff base enzyme intermediate of F1,6BP. After aldol condensation and release of the Schiff base, a fourth Mg²⁺ molecule is bound, facilitated by a conformational change of the aldolase loop, and a third loop (the phosphatase loop) undergoes a conformational change, closing the active site. Hydrolysis of the phosphate at C-1 is enabled by the action of Mg²⁺ activating a water molecule. Hydrolysis of the phosphate group leads to disassembly of the four-Mg²⁺ complex, resulting in a conformational change to the original state of the protein. Thus, the bifunctionality of the FBPA/ase is not achieved by different protein domains but by large conformational changes of different loops upon binding of the substrate, intermediates, and product, altering the structure and function of the active center while keeping the substrates in place (342). From the function and distribution of the enzyme as well as its phylogenetic affiliations, it has been assumed to represent the ancestral “pacemaking” gluconeogenic enzyme (337, 342). The results obtained from these studies have been taken as a further indication for the chemolithotrophic origin of life and that gluconeogenesis is the more ancient pathway preceding the origin of glycolysis.

PENTOSE DEGRADATION PATHWAYS IN ARCHAEA

Pentoses, as constituents of polymers such as nucleic acids (ribose) and hemicelluloses/plant cell wall polysaccharides (arabinose and xylose), are abundant molecules in nature. Many Bacteria and Eukarya, mainly fungi, have been described to utilize these compounds as carbon and energy sources. Pentose catabolism was studied mainly for D,L-arabinose and D-xylose, and so far, three main degradation pathways have been described (for literature, see references 283, 287, 343, and 344) (Fig. 15). In the first pathway, found in many Bacteria such as, e.g., *E. coli* and *Bac. subtilis*, D,L-arabinose and D-xylose are converted to xylulose 5-phosphate (Xu5P) through the action of isomerases, kinases, and epimerases, with D,L-ribulose, D,L-ribulose 5-phosphate, as well as D-xyulose

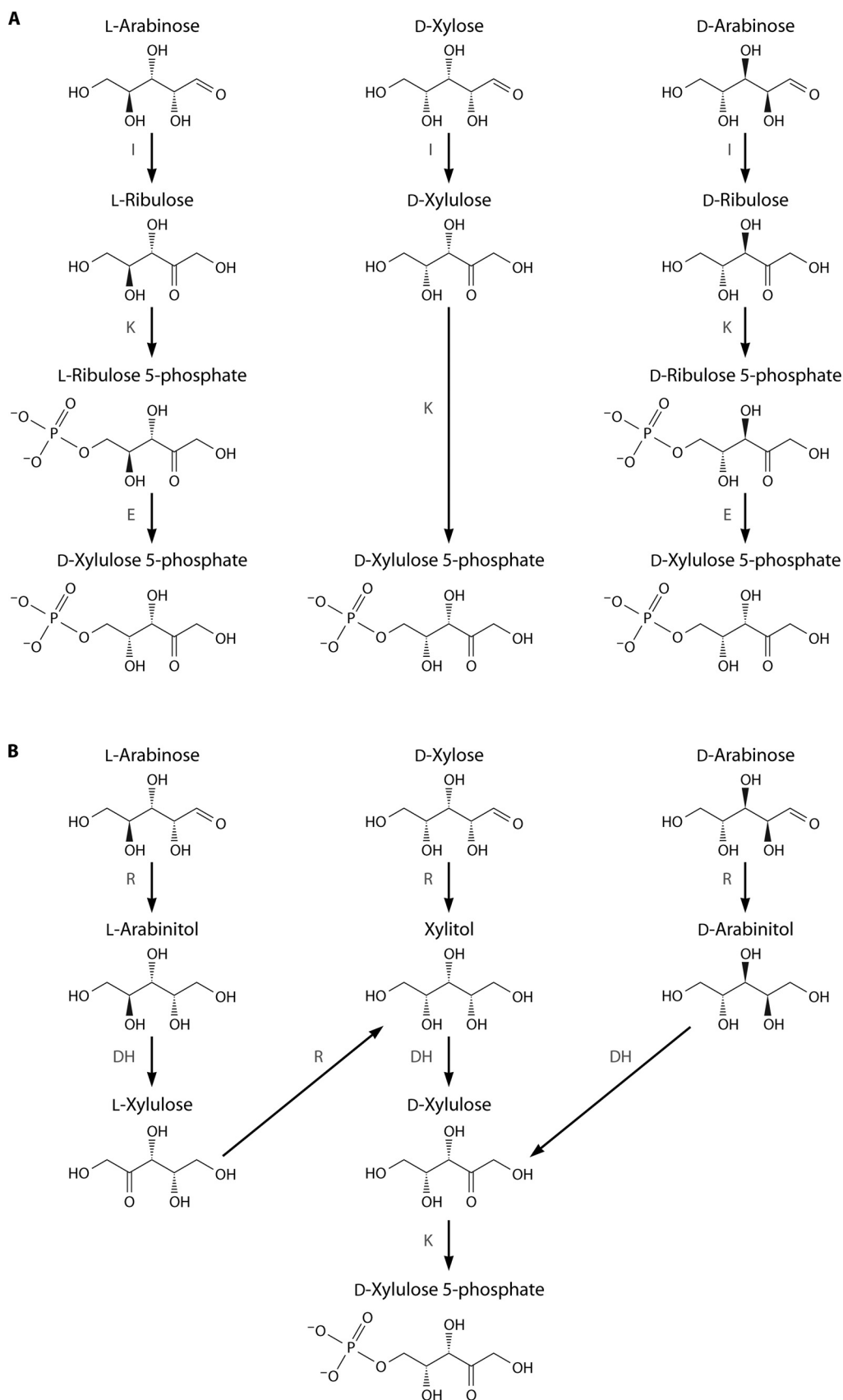


FIG 15 (A) Pentose degradation pathway found in *Bacteria* and *Eukarya* (yeasts, mammals, and fungi), proceeding via isomerases (I), kinases (K), and epimerases (E). (B) In few *Bacteria*, pentose degradation proceeds via reductases (R), dehydrogenases (DH), and kinases (K).

as intermediates, respectively (Fig. 15A). Xylulose 5-phosphate is then further metabolized via the pentose phosphate cycle. In the second pathway, xylulose 5-phosphate is also formed from the C₅ substrates via D,L-arabinitol or xylitol and D-xylulose, catalyzed by reductases, dehydrogenases, and kinases (Fig. 15B). This pathway is known mainly for fungi. The third pathway, reported for some *Bacteria*, degrades pentoses to D,L-2-keto-3-deoxyarabinonate (D,L-KDA) via sugar dehydrogenases, lactonases, and dehydratases. D,L-KDA can be converted via an additional dehydratase and a dehydrogenase either to dioxopentanoate and, finally, α-ketoglutarate or, alternatively, to pyruvate and glycolaldehyde, catalyzed by an aldolase. α-KG then enters the citric acid cycle (CAC) (Fig. 16). Also, glycolaldehyde is shuttled into the CAC after oxidation to glyoxylate via glycolate and further conversion to malate via malate synthase. In *Archaea*, pentose utilization has been reported for some aerobic halophiles and for *Sulfolobus* species (14, 283, 287, 291, 343, 345). For other *Archaea*, including hyperthermophiles from the orders *Thermococcales*, *Archaeoglobales*, *Thermoproteales*, *Desulfurococcales*, and *Pyrodictiales*, no growth on pentoses has been reported, although many of these organisms are able to grow with hexoses or hexose polymers as carbon and energy sources (14). The degradation pathways have been elucidated by using enzyme measurements in crude extracts, ¹³C labeling experiments, transcriptomic and proteomic analyses, mutational analyses, and biochemical characterization of the enzymes involved. So far, neither the first, i.e., isomerase/kinase, pathway nor the second, i.e., reductase/dehydrogenase, pathway have been found in *Archaea*. Instead, all archaeal pentose degradation pathways identified have been described to be similar to the third pathway (Fig. 16 and Table 4).

The first detailed studies on pentose catabolism in *Archaea* were carried out with *Har. marismortui* grown on D-xylose, and the initial step was identified to be catalyzed by a D-xylose dehydrogenase (see below) (343). Based on these results, the complete pathway was later unraveled in a comprehensive study of the close relative *Hfx. volcanii*: Johnsen and coworkers (287) demonstrated that 20 genes were highly upregulated (between 6- and 30-fold) during growth on D-xylose. In *Hfx. volcanii*, these genes include three ATP binding cassette (ABC) transporter clusters (13 genes) as well as eight enzyme-encoding genes. Among these genes, HVO_B0027, HVO_B0028, HVO_B0038A, and HVO_B0039, encoding 2-keto-3-deoxyxylonate dehydratase (KDXD), xylose dehydrogenase (XDH), xylonate dehydratase (XAD), and α-KGSADH, respectively, turned out to be essential for growth on D-xylose rather than on D-glucose. Furthermore, the D-xylose-induced activities of XDH, XAD, and α-KGSADH were detected in crude extracts, and the encoding genes were identified via functional overexpression. From these data, it was concluded that in *Hfx. volcanii*, D-xylose is exclusively degraded to α-KG via xylonate (XA), 2-keto-3-deoxyxylonate (KDX), and KGSA (287) (Fig. 16B). Apart from *Hfx. volcanii*, this pathway was also proposed for the halophiles *Har. marismortui*, *Haloterrigena turmenica*, and *Haloterrigena lacusprofundi* based on comparative genome analysis, although growth of the latter two organisms on D-xylose has not yet been described (287, 346). Conversely, in *Halorhabdus utahensis*, the presence of the classical xylose degradation pathway via xylose isomerase and xylulokinase, as known, e.g., for *E. coli*, has been proposed (346–348).

During growth on L-arabinose, an L-arabinose dehydrogenase (L-AraDH) is induced in *Hfx. volcanii*, which exhibits high sub-

strate specificity in contrast to the promiscuous *Sulfolobus* GDH-1, catalyzing D-xylose, L-arabinose, and also hexose oxidation (see below). The *Haloferax* L-AraDH-encoding gene, HVO_B0032, is part of the same gene cluster described above for the degradation of D-xylose, and it was shown that the same genes/proteins responsible for D-xylonate degradation are also involved in the conversion of L-arabinonate to KGSA, i.e., XAD (HVO_B0038A), KDXD (HVO_B0027), and α-KGSADH (HVO_0039), suggesting that either these enzymes are promiscuous or L-arabinonate is epimerized by a so-far-unknown epimerase. Since promiscuity could not be shown for HfxXAD, a C-4 epimerase seems likely (344).

Growth of *Sul. solfataricus* and *Sul. acidocaldarius* on D-arabinose as well as on D-arabinose and D-xylose has been studied extensively (283). It has been proposed that D-arabinose in *Sul. solfataricus* is degraded via an aldolase-independent pathway very similar to that described for *Hfx. volcanii*; the induction of AraDH, AraD, a novel 2-keto-3-deoxyarabinonate dehydratase (KDAD), and an α-KGSADH at the transcriptional as well as translational levels has been reported; and the recombinant enzymes have been characterized (283) (Fig. 16B). In *Sul. acidocaldarius*, however, [¹³C]xylose labeling experiments demonstrated the coexistence of a similar aldolase-independent pathway together with an aldolase-dependent pathway during D-xylose (and also L-arabinose) degradation (Fig. 16B). D-KDX (same as D-KDA) generated by XDH and XAD is simultaneously converted to equal amounts of α-KG and pyruvate/glyoxylate. In addition, XDH, XAD, KDX aldolase, glycolaldehyde oxidoreductase (OR), glycolate dehydrogenase, malate synthase, as well as α-KGSADH (synonymous with dioxopentanoate dehydrogenase [DOPDH]) activities have been detected in crude extracts from both *Sul. solfataricus* and *Sul. acidocaldarius* cells grown on D-xylose (291). The enzymes from *S. solfataricus*, except for AOR and XAD, were recombinantly produced and biochemically characterized. From these experiments, it was proposed that the same enzymes, i.e., GDH and KD(P)G aldolase (see above), involved in hexose (D-glucose and D-galactose) degradation via the branched ED pathway, are also employed in pentose (D-xylose and L-arabinose) degradation due to their promiscuous properties toward C₆ and C₅ sugars and the corresponding keto sugar acids, respectively (291). Furthermore, the glycolaldehyde OR activity was argued to represent a side activity of GA:OR from the npED branch. Accordingly, all three enzyme activities [GDH, KD(P)A, and glycolaldehyde:OR] were found to be unchanged upon growth on D-glucose and D-xylose, respectively. Conversely, those enzyme activities specific for pentose catabolism, i.e., the conversion of KDX/KDA to α-KG and malate, were found to be induced during growth on D-xylose (291). Dehydratase activities, i.e., XAD/AraD and GAD, which appear to be specific for pentose and hexose breakdown, respectively, seem not to be regulated in response to the growth substrate. However, *Sul. solfataricus* GAD has been described to be subject to regulatory protein phosphorylation, pointing to additional regulation at the protein level.

Pentose Oxidation and Xylose Dehydrogenase/Arabinose Dehydrogenase

The initial step of xylose degradation in halophilic *Archaea*, the NADP⁺-dependent oxidation of D-xylose, is catalyzed by a xylose-inducible XDH (287, 343). NADP⁺-dependent D-glucose-oxidiz-

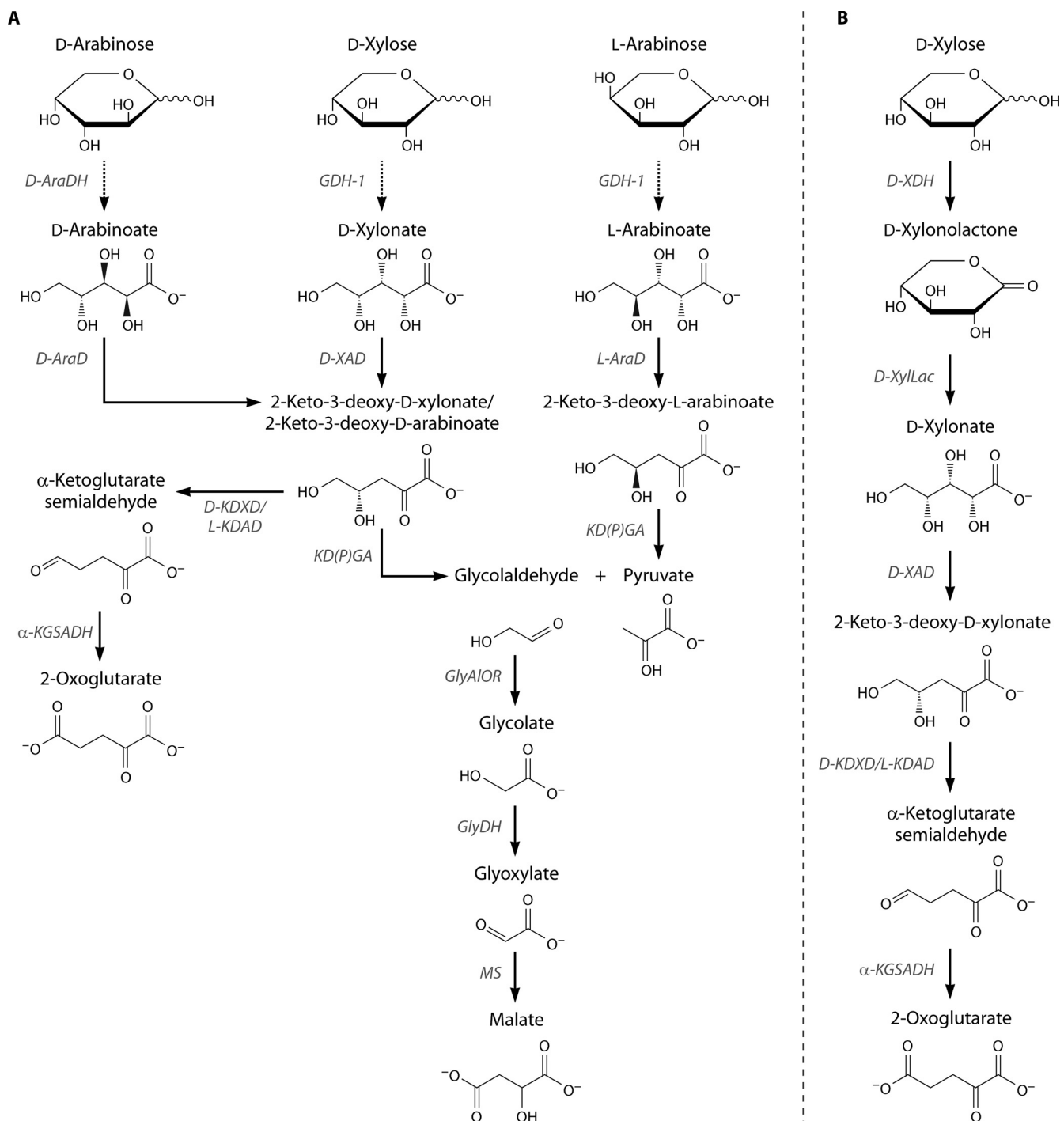


FIG 16 Current understanding of pentose degradation pathways in *Archaea*. The degradation pathways reported for D-arabinose, D-xylose, and L-arabinose in *Sulfolobus* spp. (A) and the D-xylose degradation pathway in *Haloferax volcanii* (B) are depicted. The dashed arrow indicates the presence of lactones as intermediates, which are supposed to be spontaneously transformed to the respective sugar acid at high temperatures. AraDH, D-arabinose dehydrogenase; AraD, D-arabinatoate dehydratase; α -KGSADH, α -ketoglutarate semialdehyde dehydrogenase; GDH-1, glucose dehydrogenase (isozyme 1) (SSO3003); GlyAlOR, glycolaldehyde:ferredoxin oxidoreductase; GlyDH, glycolate dehydrogenase; KD(P)GA aldolase, 2-keto-3-deoxy-(6-phospho)gluconate aldolase; KDAD, 2-keto-3-deoxyarabinato dehydratase; MS, malate synthase; KDXD, 2-keto-3-deoxyxylonate dehydratase; XDH, xylose dehydrogenase; XylLac, xylono-1,4-lactone lactonase; D-XAD, xylonate dehydratase.

TABLE 4 Overview of enzymes involved in pentose degradation in Archaea and some Bacteria

Enzyme	EC no.	Abbreviation	Reaction(s)	Protein superfamily(ies) according to the SCOP database	Protein family(ies)	Distribution
D-Glucose dehydrogenase	1.1.1.47	GDH	D-Glucose + NAD(P) ⁺ → D-glucono-1,5-lactone + NAD(P)H + H ⁺ (also converts D-xylose, D-galactose, and L-arabinose in <i>Sulfolobus</i> spp.)	N-terminal GroES-like superfamily; C-terminal NAD(P) binding Rossmann fold domain superfamily (also known as the MDR superfamily)	Alcohol dehydrogenase N-terminal domain-like and C-terminal domain-like (classical Rossmann fold)	Thermoacidophilic Crenarchaeota (<i>Sulfolobus</i> spp.)
D-Xylose dehydrogenase	1.1.1.175	XDH	D-Xylose + NADP ⁺ → D-xylylalactone + NADPH + H ⁺	N-terminal domain NAD(P) binding Rossmann fold-like domain superfamily; C-terminal glyceraldehyde-3-phosphate dehydrogenase-like, C-terminal domain superfamily (also known as the GFO/IDH/MocA superfamily)	Halophilic Euryarchaeota, Archaea, some Bacteria (e.g., <i>Caulobacter crescentus</i>)	
L-Arabinose dehydrogenase	1.1.1.46	L-AraDH	L-Arabinose + NAD(P) ⁺ → L-arabinolactone + NAD(P)H + H ⁺	Short-chain dehydrogenase/reductase family (SDR family)	Halophilic Euryarchaeota	
D-Arabinose dehydrogenase	1.1.1.116	AraDH	D-Arabinose + NADP ⁺ → D-arabinolactone + NADPH + H ⁺ (also converts L-fucose, L-galactose, and D-ribose in <i>Sulfolobus</i> spp.)	N-terminal GroES-like superfamily; C-terminal NAD(P) binding Rossmann fold domain superfamily (also known as the MDR superfamily)	Alcohol dehydrogenase N-terminal domain-like and C-terminal domain-like (classical Rossmann fold)	Thermoacidophilic Crenarchaeota (<i>Sulfolobus</i> spp.)
D-Xylylone dehydratase	4.2.1.82	XAD	D-Xylylone → 2-keto-3-deoxy-D-xylylate + H ₂ O (also converts L-arabinonate in <i>Sulfolobus</i> spp. and <i>Hfx. volanii</i>)	Endo-lactamase-like N-terminal and C-terminal domain superfamily	Halophilic Euryarchaeota, Archaea, thermoacidophilic Crenarchaeota (<i>Sulfolobus</i> spp.)	
D-Arabinonate dehydratase	4.2.1.5	AraD	D-Arabinonate → 2-keto-3-deoxy-D-arabinonate + H ₂ O	Endo-lactamase-like N-terminal and C-terminal domain superfamily	Thermoacidophilic Crenarchaeota (<i>Sulfolobus</i> spp.)	
2-Keto-3-deoxy-D-arabinonate/xylose dehydratase	4.2.1.43	KDAD/KDXD	2-Keto-3-deoxy-D-arabinonate → α-ketoglutamate semialdehyde + H ₂ O (2-keto-3-deoxy-D-arabinonate and 2-keto-3-deoxy-D-xylose are identical in <i>Hfx. volanii</i> , the enzyme also converts 2-keto-3-deoxy-L-arabinonate)	FAH superfamily (C-terminal domain)	Bacteria, ED pathway-utilizing Archaea	
2-Keto-3-deoxy-(6-phospho)-D-glucuronate aldolase	4.1.2.14/ 4.1.2.18/ 4.1.2.21	KD(P)GA	2-Keto-3-deoxy-(6-phospho)-D-glucuronate-D-galactonate ⇌ glyceraldehyde-3-phosphate + pyruvate, 2-keto-3-deoxy-D-arabinonate/D-xylylate ⇌ glyceraldehyde + pyruvate	Aldolase superfamily [(βα) ₈ barrel fold]	Class I aldolase family (KDG aldolase subfamily distinct from bacterial KDPG aldolases and also from class I Flt1,6BP aldolases and archaeal-type class IA Flt1,6BP aldolases)	Bacteria, halophilic Euryarchaeota, thermoacidophilic Crenarchaeota (<i>Sulfolobus</i> spp.)
α-Ketoglutarate semialdehyde dehydrogenase	1.2.1.26	α-KGSADH	α-Ketoglutarate semialdehyde + NAD(P) ⁺ + H ₂ O → α-ketoglutarate + NAD(P)H + H ⁺	ALDH-like superfamily	Thermoacidophilic Crenarchaeota, halophilic Euryarchaeota	
Glyceraldehydeferredoxin oxidoreductase	1.2.99.B1	GAOR	Glyceraldehyde + Fd _{ox} + H ₂ O → glyceraldehyde + Fd _{red} + H ⁺ ; likely with side activity toward glyceraldehyde yielding glycolate	Aldehyde oxidase/xanthine dehydrogenase superfamily	<i>Sulfolobus</i> spp.	
Glyoxylate reductase	1.1.1.26		Glycolate + NAD ⁺ ⇌ glyoxylate + NADH + H ⁺	Formate/glyoxylate dehydrogenase-like superfamily (NCBI)	Thermoacidophilic Crenarchaeota (<i>Sulfolobus</i> spp.)	
Malate synthase	2.3.3.9	MS	Glyoxylate + acetyl-CoA + H ₂ O → malate + HS-CoA ^a	Malate synthase superfamily (NCBI)	Halophilic Euryarchaeota, Archaea, <i>Sulfolobus</i> spp., Bacteria, Eukarya (plants, fungi)	

^a HS-CoA, free unbound coenzyme A.

ing activity was also detected in xylose-grown cells but with 70-fold-lower activity than with xylose, indicating that xylose oxidation and glucose oxidation in the modified ED pathway are catalyzed by different enzymes. XDH has been characterized in *Har. marismortui* (HarXDH) and *Hfx. volcanii* (HfxXDH; HVO_B0028), exhibiting 59% sequence identity (287, 343). The 160-kDa homotetrameric enzymes (40-kDa subunits) strongly prefer D-xylose as the substrate, and D-glucose is converted only with a highly reduced efficiency. In contrast to HfxXDH, HarXDH additionally converted D-ribose. No activity was detected with D-galactose, D-fructose, or D-arabinose with both halophilic enzymes. Also, the enzyme encoded by HVO_B0029, located directly adjacent in the same gene cluster and possessing high sequence similarity to HarXDH, shows XDH activity but with a highly reduced affinity for D-xylose (specific activity of 10.0 U/mg; K_m of 89 mM) and an even lower affinity for D-glucose, indicating another function of the enzyme (287). Accordingly, the HVO_B0028 enzyme was demonstrated to be essential for growth on D-xylose, as revealed by deletion mutant analyses, whereas the HVO_B0029 enzyme is not.

Halophilic XDHs belong to the GFO (glucose/fructose oxidoreductase)/IDH (isocitrate dehydrogenase)/MocA family (Pfam02894) of proteins and exhibit significant sequence similarity to the glucose-fructose oxidoreductase from *Zymomonas mobilis* comprising an N-terminal classical Rossmann fold and a C-terminal GAPDH-like domain (GAPDH-like, C-terminal domain superfamily [SCOP database]). Interestingly, this enzyme family shows a high degree of structural similarity to glucose 6-phosphate dehydrogenases (G6PDH-like family [SCOP data]) known from the classical ED pathway in *Bacteria* (349). The 130-kDa homotetrameric L-arabinose-specific L-AraDH from *Hfx. volcanii*, exhibiting dual cosubstrate specificity, was shown to be essential for growth on L-arabinose, whereas the deletion of the gene did not affect growth on D-glucose or D-xylose, indicating a specific function in L-arabinose degradation. The enzyme belongs to the short-chain dehydrogenase/reductase (SDR) family but to a subclade other than the pentose dehydrogenase from *Cau. crescentus* (see below) (344). Conversely, as outlined above, the broad-substrate-spectrum SsoGDH-1, proposed to catalyze D-xylose and L-arabinose oxidation in *Sulfolobus* spp. (291), as well as the D-arabinose-oxidizing AraDH from *Sul. solfataricus* belong to the medium-chain dehydrogenase/reductase (MDR) superfamily (350). The pentose dehydrogenases characterized for *Bacteria*, e.g., *Cau. crescentus* and *Azo. brasiliense*, employing the same first steps in pentose degradation, belong to the SDR and the GFO/IDH/MocA families, respectively (285, 351).

As described for the archaeal GDHs (see the ED pathway section, above), SsoAraDH represents a 150-kDa homotetramer (37-kDa subunits) (283, 350). Although only 19% identical, SsoAraDH, as deduced from the solved crystal structure, shows an overall fold very similar to that described for SsoGDH-1 (269, 352) (Fig. 13). The nucleotide binding domain is comprised of a classical Rossmann fold with a six-stranded parallel β sheet flanked by five α helices. The catalytic domain is formed by a seven-stranded mixed β sheet surrounded by two small antiparallel sheets and four α helices (350). The active site is located in a deep cleft between both domains. The catalytic domain contains one structural zinc as well as a catalytic zinc ion near the active site, as described for GDHs (see above) but with slightly modified coordination sites (268, 269, 272, 350). Although only the apo struc-

ture of AraDH has been reported, structural and sequence similarities as well as substrate modeling suggest a reaction mechanism similar to that described for GDH (see above) (269, 272, 350). SsoAraDH converts sugars with the stereoconfiguration of D-arabinose at C-3 and C-4, i.e., L-fucose, L-galactose, D-ribose, and D-arabinose, whereas SsoGDH-1 utilizes D-glucose, D-galactose, D-fucose, L-arabinose, and D-xylose (257, 283, 350). Thus, both enzymes favor those substrates not utilized by the other. Furthermore, none of the amino acid residues forming hydrogen bonds to the substrate hydroxyl groups are conserved between both enzymes. It has also been proposed that SsoAraDH is selective for the opposite chair conformation of the sugar substrate than SsoGDH-1 and that the substrate pyranose ring in the AraDH active site is flipped by 180° compared to GDH (350).

C₅ Sugar Acid Dehydration and Xylonate Dehydratase/Arabinonate Dehydratase

The dehydration of xylonate to 2-keto-3-deoxyxylonate is catalyzed by XAD. XAD activity was induced during growth of *Hfx. volcanii* on xylose, and the encoding *xad* gene (HVO_0038A) was identified by purification of the native enzyme from xylose-grown cells and N-terminal amino acid sequencing (287). The *xad* gene was also found to be induced at the transcript level, and the recombinant enzyme was characterized as a 340-kDa octamer composed of 45-kDa subunits. The enzyme is capable of catalyzing the dehydration of both sugar acids D-xylonate and D-gluconate with similar efficiencies; D-galactonate was not accepted as the substrate. However, analyses of the Δ HVO_B0038A deletion strain showed that XAD is indispensable for growth on D-xylose, whereas growth on D-glucose is not affected by the deletion (287).

The D-xylonate/L-arabinonate dehydratase from *Sul. solfataricus* (SsoXAD) efficiently converted both C₅ sugar acids but not the C₆ sugar acids D-gluconate and D-galactonate (291). Conversely, the D-gluconate dehydratase from the modified ED pathway (see above) converts only the C₆ sugar acids but not D-xylonate or L-arabinonate (290). It has thus been concluded that D-xylose/L-arabinose and D-glucose/D-galactose degradation involves C₅- and C₆-specific dehydratases, respectively, whereas dehydrogenases and aldolases are promiscuous for both C₅ and C₆ sugar degradation intermediates (291). Although specific for C₅ sugar acids, the SsoXAD activity in *Sul. solfataricus* appeared not to be significantly regulated during growth on xylose and glucose. The enzyme was proposed to be encoded by SSO2665, although the coding function has not clearly been demonstrated (291). The D-arabinonate dehydratase (SSO3124) from *Sul. solfataricus* (SsoAraD) seems to be specific for D-arabinose degradation. The enzyme is induced at the transcript as well as the protein levels by D-arabinose and was described to be specific for D-arabinonate not converting gluconate. SsoAraD shows an octameric quaternary structure (43-kDa subunits) very similar to that described for XAD from *Hfx. volcanii*, whereas SsoXAD is active as a tetramer (283, 291).

All archaeal pentanoate dehydratases characterized so far, including XADs from *Hfx. volcanii* and *Sul. solfataricus* as well as AraD from *Sul. solfataricus*, belong to the mandelate racemase/muconate-lactonizing enzyme (MR/MLE) family of the enolase superfamily (see the enolase fold in Fig. 8B). This family also includes the gluconate dehydratases of the modified ED pathways described above. Sequence comparisons revealed that the two typical signature motifs of the family and also the metal ligands are

conserved in the archaeal pentanoate dehydratases. The general base catalyst (His299 in SsoGAD) essential for proton abstraction from C- α in the catalytic cycle of all members of the superfamily is also conserved in XAD and AraD (283, 287, 290, 353) (see above). Also, a second histidine (i.e., His199 in SsoGAD [SSO3198]), the acid catalyst proposed to be involved in the second partial reaction, i.e., water elimination, is conserved in the characterized archaeal pentanoate dehydratases except for SsoAraD, where it is substituted for asparagine (N201). However, the structural and mechanistic implications of this substitution have not been investigated so far. The sequence conservation is in agreement with the dependence of the archaeal pentanoate dehydratase enzymes on divalent metal ions stabilizing the enolic intermediate. For SsoAraD, it has been described that addition of Mg²⁺ to the medium is required for heterologous overexpression of the functional octameric enzyme. In the absence of divalent metal ions, AraD is expressed in its monomeric, inactive state (283). The archaeal XAD, AraD, and GAD enzymes within the MR/MLE family show moderate amino acid sequence identity, in the range of 25%, to each other as well as to the members of the enolase group within the enolase superfamily. Phylogenetic analyses revealed that HfxXAD and SsoAraD, including their homologs identified in other *Archaea*, as well as the characterized archaeal GADs, each form distinct subgroups within the enolase superfamily (287). Notably, the pentanoate dehydratases from the analogous pentose degradation pathways in *Bacteria*, e.g., *Cau. crescentus*, *Azo. brasiliense*, and *Pseudomonas* spp., belong to a different protein superfamily, i.e., the dihydroxy acid dehydratase/6-phosphogluconate dehydratase (IlvD/EDD) superfamily, also including the 6-phosphogluconate dehydratase from the classical ED pathway (285, 354).

2-Keto-3-Deoxyxylonate Dehydratase/2-Keto-3-Deoxyarabinonate Dehydratase

KDXD/KDAD catalyzes the dehydration of KDX (identical to KDA) to KGSA. In *Hfx. volcanii*, the encoding gene, HVO_B0027, is cotranscribed with the *xdh* gene (HVO_B0028), and transcription is upregulated on D-xylose. Deletion of the KDXD-encoding gene resulted in the inability to grow on D-xylose, whereas growth on D-glucose was unaffected (287). Although the coding function has not yet been demonstrated by functional overexpression, HVO_B0027 shows 40% sequence identity to SSO3118, encoding KDAD, catalyzing the dehydration of D-KDA/D-KDX in the course of D-arabinose and D-xylose degradation in *Sul. solfataricus* (290, 291). SSO3118 was found to be induced at the transcriptional as well as protein level in response to growth on D-arabinose (283). Also, the combined α -KG-forming activity from D-arabinonate was found to be highly induced in crude extracts. Recombinant KDAD is essential for the *in vitro* conversion of D-arabinonate to α -KG in addition to purified recombinant AraDH and KGSADH (283). The enzyme was characterized as an Mg²⁺-dependent 132-kDa homotetramer (33-kDa subunits), which was confirmed by the resolution of the crystal structure (355). The four SsoKDAD subunits form a ring-like structure. Each subunit consists of an N-terminal domain with a four-stranded β sheet flanked by two α helices and a C-terminal catalytic domain with a fumarylacetacetate hydrolase (FAH) fold. Also, the bacterial KDXD encoded by the xylose degradation gene cluster in *Cau. crescentus* belongs to the fumarylacetacetate hydrolase superfamily, whereas the characterized KDAD from *Azo. brasiliense* belongs

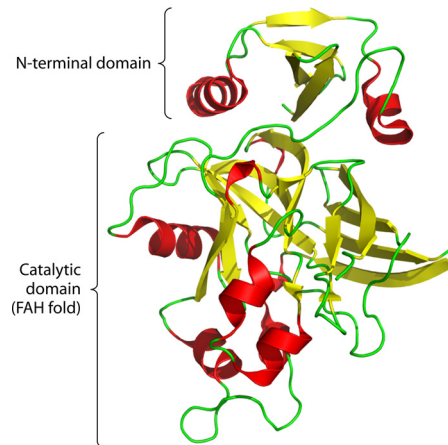


FIG 17 Crystal structure of the KDAD monomer from *Sul. solfataricus* (PDB accession number 3QTG) (355) shown as a ribbon diagram. The enzyme consists of an N-terminal domain and a C-terminal catalytic domain and belongs to the fumarylacetacetate hydrolase (FAH) superfamily.

to the dihydropicoline synthase/neuraminate lyase family (285, 354). The FAH fold in SSO3118 is comprised of two mostly antiparallel β sheets consisting of six and five β strands, respectively (Fig. 17). The two β sheets are flanked by four α helices and four small 3₁₀ helices. The twisted six-stranded β sheet forms a barrel-like structure harboring the active site, which is covered by a flexible loop. At the bottom of the active center, the Mg²⁺ ion is hexacoordinated by the carboxyl groups of two Glu residues (i.e., E143 and E145) and one Asp residue (D164) as well as carboxyl- and carbonyl-oxygens of the substrate and a water molecule. Substrate binding is additionally achieved by interactions with backbone amide groups as well as with three catalytically important residues, i.e., K182, E114, and E171 (355). From the crystal structure, two possible reaction mechanisms have been proposed, both proceeding via an enediolate intermediate. The base function of E114 seems to be enabled on the one hand by the closing of the active site by the flexible loop, which excludes bulk solvent from the active site, and by the binding mode of the substrate chelating both the C-1 carboxyl- and the C-2 carbonyl-oxygens, resulting in enhanced acidity and thus easier abstraction of the C-3 proton.

α -Ketoglutarate Semialdehyde Dehydrogenase

α -KGSADH, catalyzing the NADP⁺-dependent oxidation of α -KGSA to α -KG, was purified from xylose-grown cells of *Hfx. volcanii*, and the encoding gene, HVO_B0039, was identified after N-terminal amino acid sequencing (287). *Hfx. volcanii* KGSADH was characterized as a 215-kDa homotetramer composed of 50-kDa subunits. The enzyme prefers glutaraldehyde as the substrate, followed by succinic semialdehyde and α -KGSA. HVO_B0039 is essential for growth on D-xylose but dispensable for growth on D-glucose, as revealed by deletion mutant analyses. These results suggest that HVO_B0039 is the α -KGSADH involved in D-xylose degradation (287). HfxKG-SADH belongs to the ALDH superfamily and shows 30 to 45% sequence identity to its characterized bacterial counterparts from *Cau. crescentus* and *Azo. brasiliense* and to the characterized KGSADH enzyme from *Sul. solfataricus* (SSO3117) (283–285). In *Cau. crescentus*, the KGSADH-encoding gene (CC_0822) is also located in the xylose gene cluster, as de-

scribed for KDXD (285). SSO3117 from *Sul. solfataricus* shows an oligomeric structure similar that of HfxKGSADH and revealed activity with α -KGSA, GA, and glycolaldehyde as substrates. NADP⁺ is preferred over NAD⁺ as a cosubstrate (283). Also, for *Sul. acidocaldarius*, a KGSADH with similar molecular and catalytic properties was reported (291). In both *Sul. solfataricus* and *Sul. acidocaldarius*, KGSADH activity was detected in crude extracts of pentose-grown cells. In *Sul. solfataricus*, SSO3117 was shown to be induced at the activity level during growth on D-xylose as well as at the transcriptional and protein levels during growth on D-arabinose (283). However, recently, two further ALDHs from *S. solfataricus* (SSO1629 [SSADH-I] and SSO1842 [SSADH-II]) have been identified and characterized, which, in addition to succinic semialdehyde, convert α -KGSA with significant efficiencies (305). From the biochemical properties as well as from bioinformatic reconstructions, a major function of both enzymes in aminobutyrate, polyamine, as well as nitrogen metabolism has been proposed, but due to the significant activities with α -KGSA, an additional function in pentose degradation could not be excluded (305).

2-Keto-3-Deoxyxylonate (KDX)/2-Keto-3-Deoxyarabinonate (KDA) Cleavage

In both *Sul. solfataricus* and *Sul. acidocaldarius*, a second route, operating simultaneously with the conversion of D-KDX/KDA to α -KG, for the conversion of KDX/KDA has been identified, proceeding via aldol cleavage of KDX/KDA to glycolaldehyde and pyruvate. Glycolaldehyde is then further oxidized to glyoxylate via glycolate, catalyzed by glycolaldehyde oxidoreductase and glyoxylate reductase, which is then shuttled into the citric acid cycle (CAC) via malate synthase, catalyzing the condensation of glyoxylate and acetyl coenzyme A (CoA) to malate (291).

SSO3197 was previously characterized as catalyzing the reversible cleavage of 2-keto-3-deoxygluconate/2-keto-3-deoxy-6-phosphogluconate (KDG/KDPG) [KD(P)G] as well as 2-keto-3-deoxygalactonate/2-keto-3-deoxy-6-phosphogalactonate (KDGal/KDPGal) [KD(P)Gal] to pyruvate and GA/GAP lacking facial selectivity (173, 255, 257, 294). The enzyme is thus promiscuous for both hexose C-4 epimers as well as their phosphorylated and non-phosphorylated forms. The homolog of SSO3197 in *Sul. acidocaldarius*, Saci_0226, was shown to also utilize glycolaldehyde for condensation with pyruvate, which is essential for the second proposed route (302). Later, recombinant SSO3197 was shown to catalyze the condensation of glycolaldehyde and pyruvate with a 2-fold-higher V_{max} value than for GA/GAP and pyruvate (291). In addition, the catabolic activity was confirmed by proving pyruvate and glycolaldehyde formation after incubation of SSO3197 with the reaction products generated from D-xylonate or D-arabinonate by using semipurified XAD, converting D-xylonate to KDX (291). Furthermore, very recently, it was directly shown that the KD(P)G aldolase utilizes both D-KDX and L-KDA, converting them to glycolaldehyde and pyruvate (356). Thus, the same single aldolase is involved in the breakdown of both C₆ and C₅ sugars in *Sulfolobus* spp.

Conversion of Glycolaldehyde to Malate

In crude extracts of both *Sul. acidocaldarius* and *Sul. solfataricus*, 2,6-dichlorophenolindophenol (DCPIP)- or NADP⁺-dependent glycolaldehyde-oxidizing activity was detected. The glycolaldehyde:DCPIP oxidoreductase activity was argued to likely reflect a

side activity of the ferredoxin-dependent AOR, operative in the npED branch of glucose degradation, previously characterized by Kardinahl et al. for *Sul. acidocaldarius* (see above) (171). Homologs encoding the three subunits of the enzyme have also been identified in the genome of *Sul. solfataricus* (SSO2636, SSO2637, and SSO2639) (291). According to the proposed function in hexose and pentose degradation, the DCPIP-dependent AOR activity in *Sul. solfataricus* was not found to be significantly regulated in response to glucose and xylose, respectively. However, although the purified *Sul. acidocaldarius* enzyme was shown to be active with a variety of aldehydes, including GA, GAP, formaldehyde, acetaldehyde, and propionaldehyde (171), activity with glycolaldehyde has not yet been shown. Also, α -KGSADH (DOPDH; SSO3117) has been reported to utilize glycolaldehyde as the substrate (283), and the NADP⁺-dependent glycolaldehyde dehydrogenase activity in crude extracts has been attributed to this enzyme (291). The 7- to 10-fold-lower dehydrogenase activity in crude extracts than for AOR, however, suggested that the latter enzyme is the more likely enzyme for glycolaldehyde oxidation to glycolate in *Sulfolobus* spp. (291). NADH-dependent glyoxylate reductase (glycolate dehydrogenase) activity was detected in crude extracts of both *Sulfolobus* strains. The purified, recombinant protein encoded by SSO3187 was shown to catalyze this activity with an affinity for glyoxylate and NADH very similar to that reported for the crude extract. Also, malate synthase activity has been reported in D-glucose- and D-xylose-grown cells of *Sul. acidocaldarius* and *Sul. solfataricus*, with a 2- to 3-fold induction on the pentose sugar (291). The recombinant homodimeric (189-kDa) malate synthase encoded by SSO1334 showed molecular and enzymatic properties comparable to those previously reported for the *Sul. acidocaldarius* enzyme. The affinity of the recombinant enzyme was in the same range as those observed in crude extracts (357). The malate synthase induction on pentoses strongly supports the proposed function of the enzyme in shuttling the glyoxylate formed from KDX/KDA into the CAC via condensation with acetyl-CoA to malate during pentose degradation. Activity of isocitrate lyase, catalyzing the cleavage of isocitrate to succinate and glyoxylate, which is, together with malate synthase, essential for a functional glyoxylate bypass during growth on C₂ compounds like acetate, could not be detected in xylose-grown cells of *Sul. solfataricus*. This differential regulation of both enzymes is in accordance with the genomic organization. Both genes, encoding isocitrate lyase (SSO1333) and malate synthase (SSO1334), are consecutively co-localized in the genome but are separated by >450 bp and each exhibits its own promoter region including an upstream TATA box not forming an operon (291). The presence of the entire glyoxylate shunt in glucose-grown cells might be due to the reutilization of acetate excreted during exponential growth on glucose in the stationary phase, as also described for haloarchaea (357–359).

PENTOSE SYNTHESIS PATHWAYS IN ARCHAEA

Bacteria and *Eukarya* utilize the pentose phosphate pathway (PPP) to generate reducing equivalents (NADPH) and precursors for the biosynthesis of nucleotides and histidine (from ribose 5-phosphate [R5P]) as well as aromatic amino acids (from erythrose 6-phosphate). The PPP is divided into two main parts (Fig. 18). (i) In the oxidative PPP (OPPP), G6P is oxidized to 6-phosphoglucono- δ -lactone (6PGL) by G6PDH, yielding NADPH. After 6-phosphogluconolactonase-mediated cleavage, 6-phosphogluconate (6PG) is oxidatively decarboxylated to ribulose

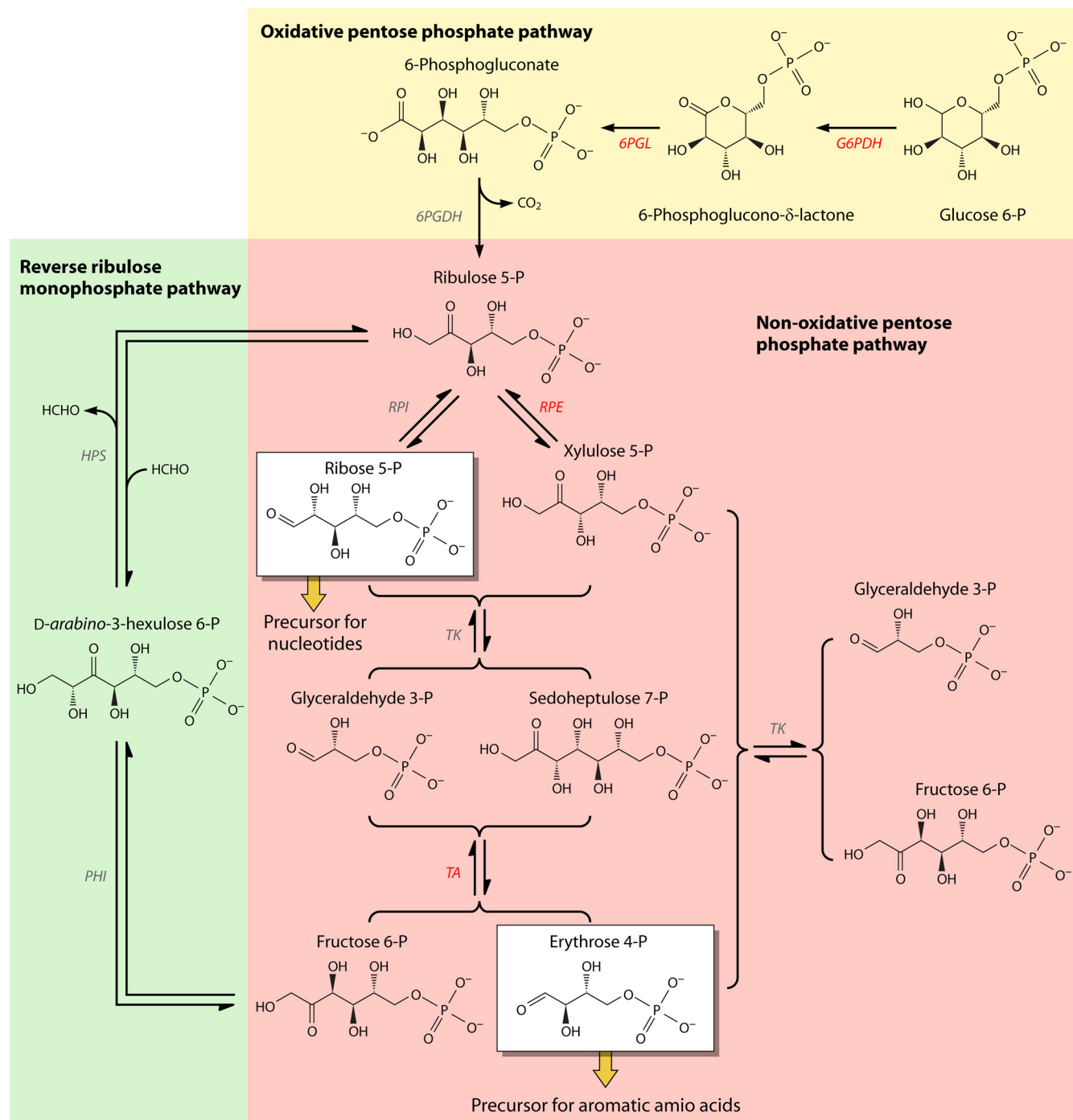


FIG 18 Current understanding of pathways for pentose formation in the three domains of life. Depicted are the reversed ribulose monophosphate pathway, the nonoxidative pentose phosphate pathway, and the oxidative pentose phosphate pathway. Enzymes depicted in red have not been identified in *Archaea* so far. Abbreviations: G6PDH, glucose-6-phosphate dehydrogenase; 6PGL, 6-phosphogluconate- δ -lactonase; 6PGDH 6-phosphogluconate dehydrogenase; RPI, ribose-5-phosphate isomerase; RPE, ribose-5-phosphate-3-epimerase; TK, transketolase; TA, transaldolase; HPS, 3-hexulose-6-phosphate synthase; PHI, 6-phospho-3-hexulioisomerase.

5-phosphate (Ru5P), CO₂, and NADPH via 6PG dehydrogenase (6PGDH) ($3\text{G6P} + 6\text{NADP}^+ + 3\text{H}_2\text{O} \rightarrow 3\text{Ru5P} + 6\text{NADPH} + 6\text{H}^+ + 3\text{CO}_2$). (ii) In the nonoxidative PPP (NOPPP), Ru5P is transformed into either R5P, catalyzed by ribose-5-phosphate isomerase (RPI), or xylulose 5-phosphate (Xu5P), via ribulose

5-phosphate 3-epimerase (RPE). From Xu5P, a C₂ unit is transferred to either R5P or erythrose 4-phosphate (E4P), catalyzed by transketolase (TK), to yield GAP and sedoheptulose 7-phosphate (S7P) or GAP and F6P, respectively. E4P is formed from S7P and GAP through C₃ transfer via transaldolase (TA), also yielding F6P

as a product. Thus, from 3 molecules of Ru5P formed in the OPPP, 2 molecules of the CCM intermediates F6P and 1 molecule of GAP are regenerated.

In *Archaea*, the OPPP seems to be absent, with the exception of 6PGDH orthologs identified in a couple of archaeal, mainly halophilic, genomes (30, 360). Also, a complete NOPPP appears to be rare in *Archaea*. Orthologs of all four of the enzymes RPI, RPE, TK, and TA seem to be restricted to *Methanococci* (e.g., *Mca. jannaschii*) and *Thermoplasmatales* (*Tpl. acidophilum* and *Pic. torridus*), indicating that these organisms are able to synthesize R5P and E4P via the reverse reactions of the NOPPP from F6P and GAP (30). In *Mco. maripaludis*, all NOPPP enzyme activities have been detected in crude extracts of autotrophically grown cells. A TA from *Mca. jannaschii* has been characterized, and the crystal structure of TA from *Tpl. acidophilum* has been reported (127, 361–364). However, in *Mca. jannaschii*, formation of the NOPPP intermediates E4P, S7P, and X5P could not be detected after incubation of labeled G6P with crude extracts (365). Instead, the RuMP pathway intermediate D-arabino-3-hexulose-6-phosphate was demonstrated, indicating that the RuMP pathway is operative instead of the NOPPP. The RuMP pathway (Fig. 18) was first identified as a formaldehyde fixation pathway in methylotrophic *Bacteria*. For nonmethylotrophic *Bacteria*, e.g., *Bac. subtilis*, a role in formaldehyde detoxification has been shown (366). In addition, a function in the metabolism of, e.g., xylose has been suggested (367, 368). The key enzymes of the RuMP pathway, 3-hexulose 6-phosphate synthase (HPS) and 3-hexulose 6-phosphate isomerase (PHI), catalyze the reversible interconversion of Ru5P and formaldehyde to D-arabino-3-hexulose 6-phosphate and further isomerization to F6P, respectively. The genes encoding HPS and PHI have been identified in the *Mca. jannaschii* genome as well as in most other archaeal genomes, indicating the RuMP pathway to be the major pathway for pentose phosphate biosynthesis in *Archaea* (360, 361, 365). However, in some *Archaea*, mainly in halophiles and *Thermoplasmatales*, homologs of RuMP pathway enzymes are missing. Accordingly, haloarchaea have been proposed to utilize a modified version of the OPPP involving the above-mentioned 6PGDH homolog and a so-far-uncharacterized alternative to G6PDH (homologs of classical bacterial G6PDH could not be identified in any archaeon) for Ru5P synthesis. In *Thermoplasmatales*, the complete NOPPP likely provides pentose phosphates for nucleotide and amino acid biosynthesis (360, 369) (the pentose biosynthesis enzymes are summarized in Table 5).

Hexulosephosphate Synthase/Phosphohexulose Isomerase

For *Pyr. horikoshii* and *Tco. kodakarensis*, HPS/PHI fusion enzymes encoded by a single *hps-phi* gene have been characterized (370, 371). As revealed by sequence comparison, such fusion enzymes are widespread in *Euryarchaeota*, particularly in methanogens, *Thermococcales*, as well as *Archaeoglobus* spp. Many of the organisms harboring an *hps-phi* fusion gene (mainly methanogens and *Archaeoglobus*) simultaneously also contain a gene encoding a single PHI homolog, and, especially, methanogens additionally encode an *fae-hps* fusion (*fae* for formaldehyde-activating enzyme [see below]). *Mca. jannaschii* as well as a few other *Methanococcaceae* strains encode only separated PHI and HPS enzymes concomitant with FAE-HPS fusions. However, in *Crenarchaeota*, the separated PHI and HPS enzymes predominate, and FAE-HPS or PHI-HPS fusions appear to be absent. Biochemical

analyses of the *Pyr. horikoshii* and *Tco. kodakarensis* HPS-PHI fusion proteins revealed bifunctional, i.e., HPS and PHI, activity. The continuous Ru5P consumption for nucleotide biosynthesis is supposed to drive the reaction in the Ru5P-forming direction, although both enzymes exhibited a higher catalytic efficiency for the formaldehyde-fixing direction (370, 371). The fusion of both HPS and PHI was shown to enhance catalytic efficiency as well as thermostability compared to the artificially separated HPS and PHI moieties of the protein, as demonstrated for the *Pyr. horikoshii* enzyme (371). For *Mca. jannaschii*, the single PHI, not fused to a HPS, has been crystallized. The protein belongs to the SIS (sugar isomerase) domain superfamily also comprising PGIs (see the section on the EMP pathway, above). The homotetrameric protein shows a three-layered α - β - α sandwich fold comprising a central five-stranded parallel β sheet flanked on both sides by α helices. The active site is made up of residues from three subunits and seems to be at least partly conserved in other PHI homologs. However, the substrate binding site and the catalytic mechanism have not yet been clearly identified (372). HPS structures from *Archaea* have not yet been reported. Only for the *Bacteria Mycobacterium gastri* and *Salmonella Typhimurium* are HPS structures available. The HPS region of the fused *Pyr. horikoshii* and *Tco. kodakarensis* PHI-HPS enzymes shows 42% sequence identity to *Myc. gastri* HPS, which belongs to the ribulose-phosphate binding barrel superfamily (SCOP database) within the orotidine monophosphate decarboxylase-like suprafamily (373). These enzymes show a $(\beta/\alpha)_8$ barrel fold and a characteristic D-x-K-x-x-D motif at the end of the third β strand in the active site. The HPS catalytic mechanism is proposed to involve the Mg^{2+} -assisted formation of an enediolate intermediate (for details, see references 374 and 375). The operation of the RuMP pathway for pentose biosynthesis in *Archaea* is further strongly supported by the constitutive expression of HPS/PHI in *Pyr. horikoshii* and *Tco. kodakarensis* independent of the presence or absence of formaldehyde. This suggests that the RuMP pathway in this organism is involved in a more general metabolic activity rather than in formaldehyde fixation/detoxification (370, 371). Furthermore, deletion of the *phi-hps* fusion gene in *Tco. kodakarensis* resulted in an auxotrophic growth phenotype, with cells being unable to grow on minimal medium in the absence of nucleosides, indicating that the RuMP pathway is essential for nucleotide biosynthesis in providing the Ru5P precursor in this archaeon (370, 371).

Ribose-5-Phosphate Isomerase

The synthesis of nucleotides requires R5P as a precursor, which is formed from Ru5P, the product of the HPS- and PHI-catalyzed reactions, through the action of the R5P isomerase (Fig. 18 and 19). In addition to the key RuMP pathway enzymes PHI and HPS, RPI-encoding genes of the A type (*rpiA*) are also present in nearly all archaeal genomes, again indicating the important function of the RuMP pathway in *Archaea* (30, 36, 360). *RpiA* enzymes are the most abundant RPI enzymes present in all three domains of life, whereas the *RpiB* enzymes, ribose-5-phosphate isomerase isoenzymes unrelated/nonhomologous to *RpiA*, are less widespread and restricted mainly to *Bacteria*. Both isoenzymes are present, e.g., in *E. coli* (376). In *Archaea*, *RpiB* homologs were found only in a few *Desulfurococcus* spp. The recombinant A-type RPI from *Pyr. horikoshii* has been characterized, and the crystal structure was solved (377). Also, a structural description of the enzyme from *Mca. jannaschii* is available (378). *RpiA* enzymes belong the

TABLE 5 Overview of enzymes involved in pentose biosynthesis in Archaea, Bacteria, and Eukarya

Enzyme	EC no.	Abbreviation	Reaction	Protein superfamily(ies) (according to SCOP)	Protein family(ies)	Distribution
Phosphohexulose isomerase	5.3.1.27	PHI	Fructose 6-phosphate \rightleftharpoons D-arabino-3-hexulose 6-phosphate	SIS domain superfamily	Mono-SIS domain family	Archaea (except for some halophiles and <i>Thermoplasmatales</i>), Bacteria (especially methylotrophs)
Hexulose phosphate synthase	4.1.2.43	HPS	D-Arabino-3-hexulose 6-phosphate \rightleftharpoons ribulose 5-phosphate + formaldehyde	Ribulose phosphate binding barrel superfamily	NagB/RpiA/CoA transferase-like superfamily; ribulose 5-phosphate isomerase lid domain superfamily	Archaea (except for some halophiles and <i>Thermoplasmatales</i>), Bacteria (especially methylotrophs)
Ribose-5-phosphate isomerase	5.3.1.6	RPI	Ribulose 5-phosphate \rightleftharpoons ribose 5-phosphate	NagB/RpiA/CoA transferase-like superfamily; ribulose 5-phosphate isomerase lid domain superfamily	D-Ribose-5-phosphate isomerase (RpiA), catalytic domain family; ribulose 5-phosphate isomerase lid domain family	Archaea, Bacteria, Eukarya
Transketolase	2.2.1.1	TK	Sedoheptulose 7-phosphate + D-glyceraldehyde-3-phosphate \rightleftharpoons D-ribose 5-phosphate + D-xylulose 5-phosphate	Thiamine diphosphate binding fold (THDP binding), TK C-terminal domain-like	TK-like Pyr module, transketolase C-terminal domain-like	<i>Mca. jannaschii</i> , <i>Thermoplasmatales</i> , <i>Thermococcales</i> , <i>Sulfobacales</i> , <i>Thermoproteales</i> (not in most haloarchaea, other methanogens, and <i>Archaeoglobales</i>), Bacteria, Eukarya
Transaldolase	2.2.1.2	TA	Sedoheptulose 7-phosphate + D-glyceraldehyde 3-phosphate \rightleftharpoons D-erythrose 4-phosphate + D-fructose 6-phosphate	Aldolase superfamily	Class I aldolase family	<i>Methanococcus</i> spp., <i>Thermoplasmatales</i> (not in most other Archaea), Bacteria, Eukarya
Glucose 6-phosphate dehydrogenase	1.1.1.49	G6PDH	D-Glucose 6-phosphate + NAD(P) ⁺ \rightarrow D-glucono-1,5-lactone 6-phosphate + NAD(P)H + H ⁺	N-terminal domain NAD(P) binding Rossman fold-like domain superfamily; C-terminal glyceraldehyde-3-phosphate dehydrogenase-like, C-terminal domain superfamily	GAPDH N-terminal domain family, glucose-6-phosphate dehydrogenase-like family (C-terminal domain)	Bacteria, Eukarya, some Halarchaea
6-Phosphogluconate dehydrogenase	1.1.1.44	6PGDH	6-Phospho-D-gluconate + NADP ⁺ \rightarrow D-ribulose 5-phosphate + CO ₂ + NADPH + H ⁺	NAD(P) binding Rossman fold domains, 6-phosphogluconate dehydrogenase C-terminal domain-like superfamily	6-Phosphogluconate dehydrogenase-like, N-terminal domain family; hydroxyisobutyrate and 6-phosphogluconate dehydrogenase domain family	Bacteria, Eukarya
Ribose 5-phosphate epimerase	5.1.3.1	RPE	D-Ribulose 5-phosphate \rightleftharpoons D-xylulose 5-phosphate	Ribulose phosphate binding barrel superfamily	D-Ribulose-5-phosphate 3-epimerase family	<i>Methanococcus</i> spp., <i>Thermoplasmatales</i> (not in most other Archaea), Bacteria, Eukarya

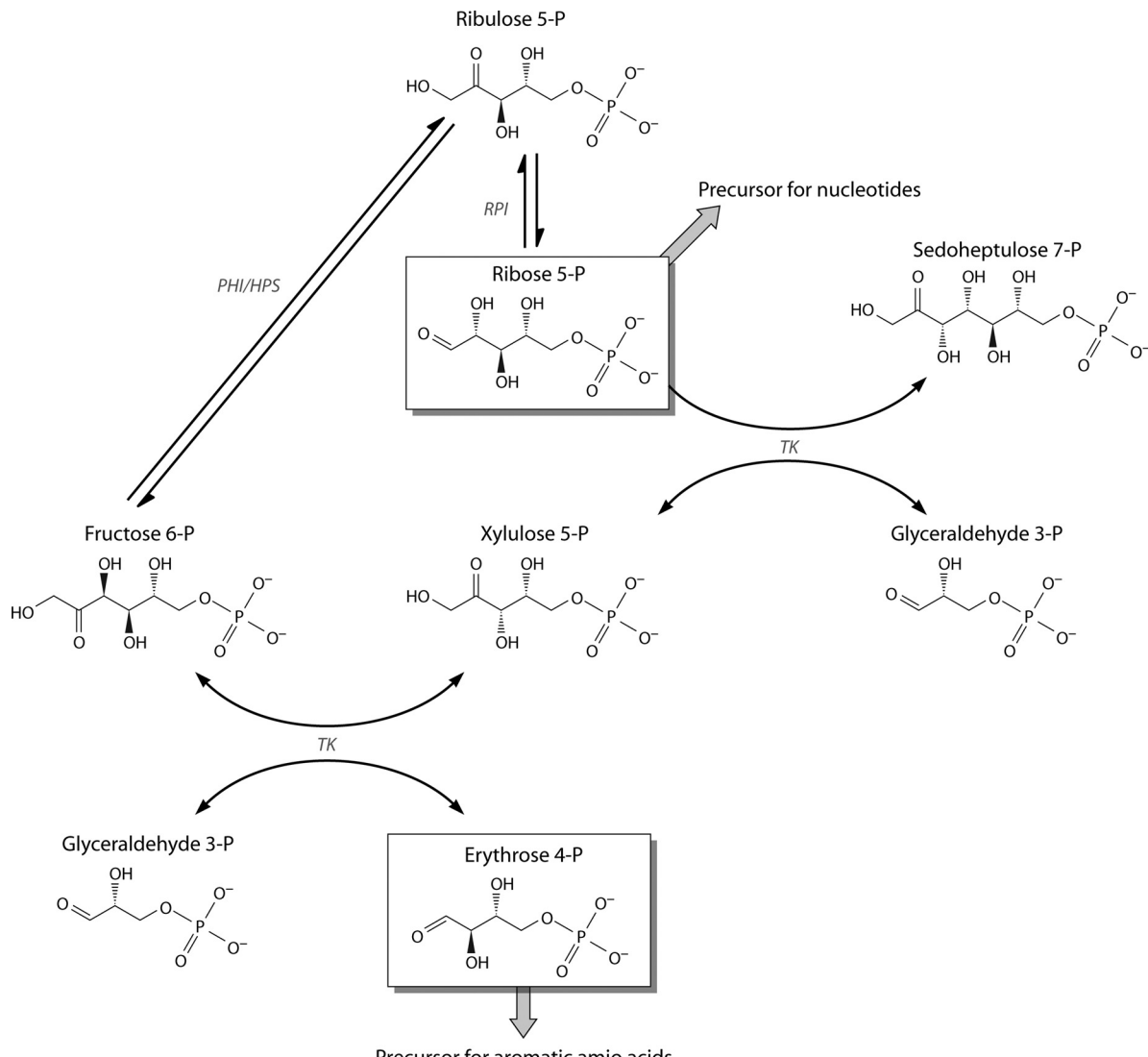


FIG 19 Erythrose 4-phosphate and pentose 5-phosphate synthesis via the incomplete NOPPP, as found in most archaea. All required building blocks, e.g., ribose 5-phosphate for nucleotides and erythrose 4-phosphate for aromatic amino acid synthesis, are formed. The fate of sedoheptulose 7-phosphate is still unclear. Abbreviations: HPS, 3-hexulose-6-phosphate synthase; PHI, 6-phospho-3-hexulose-isomerase; RPI, ribose-5-phosphate isomerase; TK, transketolase.

ribose-5-phosphate isomerase family (Pfam06026). Both enzymes represent 100-kDa homotetramers composed of 25-kDa subunits. Each subunit is comprised of two domains: the first consists of a seven-stranded, mostly parallel β sheet composed of six parallel strands and one antiparallel strand surrounded by five α helices. In the SCOP classification, this domain belongs to the ribulose-5-phosphate isomerase catalytic domain family within the NagB/RpiA/CoA transferase superfamily. The second domain is comprised of a four-stranded antiparallel β sheet and two helices located on the same side of the β sheet. This domain belongs to the ribulose-5-phosphate isomerase lid domain superfamily (SCOP database). Both domains are connected by a short three-stranded β sheet. The active center is located at the interface between the two domains, and the conserved sequence motifs identified for RipA enzymes, e.g., in *E. coli* (379), are also present in the archaeal enzymes (+25GxGxGST, +85DGAD, and +98KGxGxxxxxEK in *Pyr. horikoshii* RPI) and were found to be located at

the entrance of, inside, and at the bottom of the cavity, respectively (380). In RPIs, similar to PGIs, substrate conversion has been suggested to proceed via a ring-opening reaction and a proton transfer between the first and the second carbon atoms of the pentose 5-phosphate involving a *cis*-enediol(ate) intermediate. This is mediated by two acid/base catalysts (E103 and D81 in the *E. coli* enzyme and E107 and D85 in the *Pyr. horikoshii* enzyme from the conserved motifs). The intermediate is stabilized by a conserved lysine (K98 in the *Pyr. horikoshii* enzyme), similarly to TIMs. The catalytic aspartate also seems to be involved in the ring-opening reaction.

In the RuMP pathway, the cytotoxic by-product formaldehyde is formed in the HPS reaction from D-arabino-3-hexulose 6-phosphate to yield Ru5P, and thus, mechanisms are necessary to detoxify this compound. One mechanism of formaldehyde detoxification involves the formaldehyde-activating enzyme (FAE) which catalyzes the condensation of formaldehyde and tetrahy-

dromethanopterin, enabling subsequent oxidation to CO₂ (374, 381). FAE is found in many methanogenic *Archaea* as well as in *Archaeoglobus* spp. and is often fused to HPS, indicating a likely functional association of both enzymes in the detoxification of formaldehyde (381). However, since FAE seems to be restricted to methanogens and *Archaeoglobus*, other detoxification mechanisms must exist in *Archaea*, and the oxidation of formaldehyde via the formaldehyde:Fd OR (see above) characterized for *Pyr. furiosus* has been proposed, even though the efficiency of formaldehyde oxidation of the enzyme appeared to be rather low (K_m of 25 mM) (163, 168). Since not all *Archaea* harbor FAE- or FOR-encoding genes, further mechanisms of formaldehyde detoxification likely exist.

Transketolase

For the synthesis of E4P as the common precursor of aromatic amino acids, many *Archaea*, including, e.g., *Mca. jannaschii*, *Thermoplasmatales*, *Thermococcales*, *Sulfolobales*, and *Thermoproteales*, harbor the genes encoding TK, catalyzing the reversible formation of E4P and Xu5P from F6P and GAP, suggesting that E4P synthesis proceeds via the (in)complete NOPPP (30, 36) (Fig. 19). However, in many other *Archaea* such as, e.g., haloarchaea, other methanogens such as *Methanosarcina* spp., as well as *Archaeoglobales*, TK-encoding sequences seem to be absent (30, 36). Furthermore, as described above, in the NOPPP-containing organism *Mca. jannaschii*, E4P could not be detected, and also, labeling experiments were not consistent with E4P being a precursor for aromatic amino acids (362). Instead, in *Mca. jannaschii* and *Mco. maripaludis*, an E4P-independent pathway for the initial synthesis of 3-dehydrochinate (and further to chorismate) has been identified. The key intermediate of this pathway is 6-deoxy-5-ketofructose 1-phosphate (DKFP), differing from the canonical pathway, which starts with the condensation of E4P and PEP yielding 3-deoxy-arabino-heptulosanate 7-phosphate (382–384). This alternative pathway also appears to be present in other methanogens as well as in halophiles and might also be operative in other TK-negative organisms such as *Arc. fulgidus* (369).

Alternative Pathways for C₅-C₃ Interconversion

In *Tco. kodakarensis*, two further pathways linking the central carbohydrate metabolism to the synthesis/degradation of (deoxy)nucleotides have been identified.

In the first pathway, the reversible interconversion of deoxy-nucleoside-derived deoxyribose 1-phosphate (dR1P) via dR5P to GAP and acetaldehyde is catalyzed by phosphopentomutase (PPM) and 2-deoxyribose-5-phosphate aldolase (DERA); the deoxynucleosides are cleaved by the action of nucleoside phosphorylases into dR1P and the free base. PPM and DERA have been characterized, and they turned out to be specific for dR1P and dR5P, respectively. From the presence of both enzyme activities in crude extracts of starch- and pyruvate-grown cells of *Tco. kodakarensis*, the physiological importance of this pathway was concluded, and a biosynthetic function was proposed (385). However, the pathway seems to be restricted to only a few archaeal species, and the physiological significance remains unclear. The PPM/DERA pathway seems to be unable to compensate for the RuMP pathway in *Δphi-hps* mutants of *Tco. kodakarensis* and apparently also does not permit growth on deoxynucleosides in this deletion strain (370).

In the second pathway, the conversion of nucleoside mono-

phosphates (AMP, CMP, and UMP) to 3PG and the free base involves three steps. AMP phosphorylase (AMPPase) catalyzes base replacement by a phosphate group, yielding ribose 1,5-bisphosphate (R1,5BP). Subsequently, R1,5BP isomerase converts R1,5BP to ribulose 1,5-bisphosphate (Ru1,5BP). Finally, a type III Ru1,5BP carboxylase/oxygenase (RubisCO) forms two molecules of 3PG, an intermediate of central sugar metabolism, from Ru1,5BP, CO₂, and H₂O. This pathway was reported to be widespread among the *Archaea* but is apparently absent from *Bacteria* and *Eukarya* (386, 387). All three enzymes have been studied extensively, and the crystal structures from archaeal R1,5BP isomerase and type III RubisCOs have been reported (386–396). The conversion of nucleoside monophosphates to 3PG was also detected in crude extracts of *Tco. kodakarensis*, and the pathway was shown to be upregulated at the protein level upon supplementation of exogenous nucleosides in the medium (386). The irreversible reaction catalyzed by RubisCO results in the unidirectional formation of 3PG by this pathway, and a function in nucleoside/nucleotide degradation has been discussed. Deletion of the RubisCO-encoding gene (TK2290) showed that the enzyme and, thus, presumably the whole pathway are not essential for growth. However, the mutant strain showed a slightly decreased cell yield when grown on rich medium (387).

METABOLIC AND REGULATORY CHARACTERISTICS OF WELL-STUDIED ARCHAEAL MODEL ORGANISMS

In the last years, major advances in the unraveling of metabolic networks as well as their regulatory properties were achieved by the use of holistic genomics-based technologies, often accompanied by biochemical studies. In addition, a major breakthrough was the invention of genetic tools, especially the construction of knockout mutants for all major classes of *Archaea*, such as halophiles (e.g., *Hfx. volcanii* and *Hbt. salinarium*), methanogens (e.g., *Mco. maripaludis* and *Methanosarcina*), and (hyper)thermophiles (e.g., *Sulfolobus* sp., *Tco. kodakarensis*, and *Pyr. furiosus*) (for review and literature, see references 27 and 28). This exciting progress allowed the unraveling of protein function *in vivo* and qualifies *Archaea* as model organisms for synthetic biology and systems biology (303, 397, 398). Thus, within the last years, the first genome-wide metabolic models, flux balance analysis (FBA), as well as first detailed reaction kinetic models were established for *Archaea* (338, 399–404). These studies also analyzed the responses to different carbon sources and, often performed in combination with biochemical studies, revealed new, exciting, deeper insights into the regulation of metabolic networks at the transcript and protein levels.

Regulation at the Transcript Level

The archaeal transcription apparatus closely resembles the eukaryotic one and comprises a multisubunit RNA polymerase (RNAP) (10 to 13 subunits, homologous to the eukaryotic RNAP II system) and a subset of general transcription factors, i.e., homologs of transcription factor IIB (TFB), TATA binding protein (TBP), and transcription factor IIE-α (TFE) (6–12, 405–407). The archaeal RNA polymerase is recruited to the promoter (similarly to the eukaryotic RNAP II promoter), forming the ternary complex of DNA with TBP and TFB. However, a multiplicity of general transcription factors (TFB and TBP) is commonly found within the *Archaea*, and a function in adaptation to changing environmental conditions has been discussed (408–414). For exam-

ple, *Halobacterium salinarum* NRC-1 possesses six *tbp* genes and seven *tfb* genes (415), *Sul. solfataricus* encompass three TFB proteins and one TBP (416, 417), and *Thermoproteus tenax* harbors four TFB proteins and one TBP (418).

Intriguingly, almost all transcriptional regulators identified in *Archaea* so far are bacterial-type regulators, which interact with the eukaryal-like transcription machinery. The only exception is GvpE, a proposed leucine zipper regulator from haloarchaea (419), and the eukaryal-like multiprotein bridging factor identified in archaeal genomes (420–422).

In recent studies on the control of carbohydrate metabolism, transcriptional changes in response to different carbon sources were analyzed and led to the identification of the respective transcriptional regulators (see below). Further on, first insights into global gene regulation by carbon catabolite repression in *Archaea* were gained. Carbon catabolite repression is well established in the *Bacteria*, where cells select a preferable and quickly metabolizable carbohydrate in a mixture of sugars. One famous example of catabolite repression is the *lac* operon of *E. coli*. The repressor protein LacI binds to the promoter of the *lac* operon to prevent transcription in the presence of glucose. In addition, the cAMP receptor protein (CRP) complex serves as a positive effector that, in conjunction with the phosphoenolpyruvate phosphotransferase system (PTS) for sugar transport, serves as a global regulator in the case of the *lac* operon (423).

Regulation at the Protein Level

Besides regulation at the transcriptional level, changes at the proteome level were also addressed by proteomic studies. There is increasing evidence that posttranscriptional regulation as well as posttranslational modifications (PTMs), e.g., lipid modification, protein glycosylation, methylation, phosphorylation, acetylation, and ubiquitination, also play a significant role within the *Archaea* (for a recent review, see reference 424). Among this great variety of PTMs, reversible protein phosphorylation/dephosphorylation has an important function in signal transduction and allows a rapid cellular response to diverse external and internal signals (425). Protein phosphorylation is well established in *Archaea*. Whereas archaeal two-component systems have been demonstrated in *Euryarchaeota* (i.e., CheA and CheY in *Hbt. salinarum* [426]), they appear to be largely absent in *Crenarchaeota*. However, all *Archaea* harbor eukaryotic-like protein Ser/Thr and Tyr kinases (ePKs) and the respective protein phosphatases (PPs) (for a review, see reference 425). Knowledge about protein phosphorylation in *Archaea* is scarce compared to the achievements with *Bacteria* and *Eukarya*. *Sulfolobus* species, i.e., *Sul. solfataricus*, *Sul. acidocaldarius*, and *Sul. tokodaii*, are the best-studied *Archaea* regarding protein phosphorylation. Four protein phosphatases (427–429) and five protein kinases (430–434) were identified and biochemically investigated. Furthermore, the first signal transduction pathway involved in archaella expression mediated by reversible protein phosphorylation was discovered in *Sul. acidocaldarius* (429, 435) and *Sul. tokodaii* (436).

Only recently, the phosphoproteomes of the euryarchaeon *Hbt. salinarum* R1 and the crenarchaeon *Sul. solfataricus* P2 were analyzed. The phosphoproteomes of two *Hbt. salinarum* strains (wild type and $\Delta serB$ mutant [*serB* is the sole phosphoserine phosphatase]) were investigated by using a genome-wide, gel-free approach (TiO_2) for phosphopeptide (p-peptide) enrichment (437). Overall, 69 p-proteins, with a pS/T/Y ratio of 86%/12%/1%, were

identified in *Hbt. salinarum*. The majority of the identified p-proteins are involved in cellular metabolism, followed by information storage/processing and cellular processes/signaling. The phosphoproteome of *Sul. solfataricus* P2 in response to different carbon sources (glucose versus tryptone) was investigated. The applied gel- and enrichment-free PACIFIC (precursor acquisition independent from ion count) approach (438) revealed an unexpectedly large number of phosphoproteins (540 phosphoproteins) as well as a large amount of p-Tyr (54%) (439). The identified phosphoproteins are located in 21 out of 26 arCOG categories (440), indicating that most of the cellular processes are targeted by protein phosphorylation. For *Sul. solfataricus*, a complex phosphorylation pattern of CCM enzymes with significant changes in response to the offered carbon source was observed (439).

The PACIFIC approach was also used to analyze the phosphoproteomes of three *Sul. acidocaldarius* strains (parental strain MW001 and deletion mutants of both protein phosphatases $\Delta saci_ptp$ and $\Delta saci_pp2a$) (429). In total, 801 phosphoproteins were identified, with an increase in the number of identified phosphoproteins in the deletion mutants. The identified phosphoproteins belong to all processes of the cell, and cellular metabolism was the most targeted process (i.e., especially enzymes of the CAC as well as enzymes located at branching points [e.g., toward amino acid metabolism]). The $\Delta saci_pp2a$ strain also showed an obvious phenotype, with an enhanced doubling time, an altered cell size distribution, and a different motility behavior (hypermotility), resembling the starvation stress response. These results highlight the importance of protein phosphorylation in regulating essential cellular processes in *Sul. acidocaldarius*.

Metabolic Thermoadaptation

Besides the stability of macromolecules such as DNA and proteins, the stability of metabolites/intermediates also offers a great challenge for life at high temperature. In the central carbohydrate metabolism (i.e., EMP and ED pathways), triosephosphates are especially unstable at high temperatures, with half-lives of 12.4 min for GAP, 30.8 min for DHAP (both at 70°C), and 1.6 min for BPG (at 60°C) (338). Due to this metabolic burden, it has been suggested that unique (hyper)thermophilic archaeal enzymes, such as gluconeogenic FBPA/ase and glycolytic GAPN or GAPOR, and the restricted gluconeogenic function of the PGK/GAPDH enzyme couple represent a special adaptation to minimize carbon loss via thermal degradation (153, 337, 338). Glycolytic GAPN and GAPOR catalyze the unidirectional oxidation of GAP to 3PG, omitting the thermolabile 1,3BPG. Both enzymes allow the formation of reducing equivalents [NADP(H) or Fd_{red}] but at the expense of 1 ATP usually gained by substrate-level phosphorylation via PGK. The restricted gluconeogenic function of PGK/GAPDH in (hyper)thermophiles (i.e., *Pyr. furiosus*, *Tco. kodakarensis*, *Tpt. tenax*, and *Sulfolobus* species) was confirmed by detailed enzymatic characterization, indications from regulation at the transcript and protein levels in response to carbon source, and, finally, mutational approaches (see below for a detailed discussion). The bifunctional FBPA/ase enables a unidirectional gluconeogenic pathway and quickly converts thermolabile triosephosphates to heat-stable F6P and thus avoids the formation of toxic methylglyoxal from DHAP and GAP (337). Further evidence for the role of GAPN, GAPOR, and FBPA/ase in metabolic thermoadaptation comes from their phylogenetic distribution, which is, with few exceptions, restricted to (hyper)thermophiles within the

Archaea and, for FBPA/ase, also deep-branching *Bacteria*. Therefore, it is tempting to speculate that the utilization of GAPN, GAPOR, and FBPA/ase represents a general metabolic thermoadaptation strategy in (hyper)thermophilic *Archaea*.

Further insights into important control and thermoadaptive functions of enzymes at the level of GAP conversion came from a recent modeling approach, “cold versus hot design,” which compared GAP to pyruvate conversion in *Saccharomyces cerevisiae* (mesophile) and *Sul. solfataricus* (thermophile) based on the available model of yeast glycolysis (441, 442). For gluconeogenesis via the EMP pathway, the cell relies on the PGK/GAPDH couple, and thus, thermolabile 1,3BPG is formed. At high temperatures, the model predicted futile cycling (ATP loss) at the level of PGK due to the decay of the thermolabile 1,3BPG to 3PG. Furthermore, the model predicted that activating GAPN and thus redirecting flux from GAPDH would be advantageous in order to increase glycolytic flux and, even more importantly, the inhibition of PGK in order to prevent energy loss via futile cycling (441). Some of the predictions were confirmed by a detailed characterization of enzymes involved in thermolabile triosephosphate conversion in *Sul. solfataricus* (338) (see below). In addition, a detailed mathematical model was constructed and combined with an *in vitro*-reconstituted enzyme system for gluconeogenesis (3PG-to-F6P conversion). This approach revealed severe carbon loss at high temperatures due to noncatalyzed reactions, indicating that intermediate instability at high temperatures can significantly affect pathway efficiency. During growth on D-glucose, organisms utilizing the branched ED pathway (e.g., *Sul. solfataricus* and *Tpt. tenax*) might be able to circumvent the formation of 1,3BPG by the utilization of the spED branch (see the sections on the ED pathway, above, and *Sul. solfataricus*, below) (256).

In the following section, after summarizing the general growth conditions (i.e., isolation, growth requirements, and life-style), sugar transport, sugar metabolic pathways, and energetics in the respective model *Archaea*, we particularly focus on recent advances in the field of research on regulation of the archaeal CCM at the transcript and protein level.

Thermococcales (Pyrococcus furiosus and Thermococcus kodakarensis)

Growth conditions. The anaerobic hyperthermophiles *Pyr. furiosus* and *Tco. kodakarensis* are members of the *Thermococcales* within the *Euryarchaeota*. *Pyr. furiosus* was isolated from geothermally heated marine sediments (Porto di Levante, Vulcano, Italy) (443) and grows at temperatures of between 70°C and 103°C, with optimal growth at 100°C and pH 7 (pH range, 5 to 9). *Tco. kodakarensis* was isolated from a solfatara on Kodakara Island, Kagoshima, Japan, and exhibits optimal growth at 85°C (growth range, 60°C to 100°C; pH range, 5 to 9) (444, 445). The genomes of *Pyr. furiosus* and *Tco. kodakarensis* as well as those of several other members of the *Thermococcales* have been sequenced (446, 447), and genetic systems have been established (27, 448–451).

Both organisms grow chemoorganoheterotrophically, gaining energy either by fermentation of peptides or carbohydrates such as starch, pullulan, glycogen, and chitin (452) or by sulfur respiration, as both are able to utilize elemental sulfur (S^0) as the terminal electron acceptor, leading to the formation of H_2S . Growth on maltose is restricted to *Pyr. furiosus*, since *Tco. kodakarensis* is able to utilize only higher maltooligosaccharides (i.e., 3 glucose units [maltotriose] or more), whereas glucose cannot be used. For *Pyr.*

furiosus, it was shown that peptides are the preferred carbon source compared to maltose and that growth on maltose is independent from S^0 and peptides (453). The ability to grow on carbohydrates as the sole carbon and energy source is not commonly found within the *Thermococcales*; e.g., *Pyrococcus abyssi* and *Pyr. horikoshii* require peptides and S^0 for growth (207). During fermentative growth on carbohydrates, the main fermentation products are H_2 , CO_2 , and acetate (via ADP-forming acetyl coenzyme A synthetase [128, 454]). Upon the addition of sulfur during saccharolytic growth of *Pyr. furiosus*, the amount of H_2 produced decreases, and H_2S is formed instead (443, 453). The enzyme complex responsible for H_2 formation in *Pyr. furiosus* and *Tco. kodakarensis* is a unique [NiFe]-hydrogenase (Mbh), which catalyzes the formation of H_2 with reduced ferredoxin as the electron donor. In addition, the enzyme creates an ion gradient across the membrane, which can be used directly for ATP synthesis via ATP synthase (0.3 mol ATP generated per mol H_2 formed) (455) (for a review, see reference 456). The A_1A_o -type ATPase (A_1A_o -ATPase) of *Pyr. furiosus* uses a sodium rather than a proton gradient (457), and there is some evidence that the proton gradient generated by the Mbh hydrogenase module (comprising the subunits MbhH to MbhN) is converted to a sodium gradient by the Mrp system (Mrp-type Na^+/H^+ antiporter homologs, comprising the subunits MbhA to MbhH) of Mbh (456). This has been discussed as a “simple” form of respiration, which enables the organism to improve the limited energy yield during fermentative growth (see below). A genetic approach performed with *Tco. kodakarensis* revealed that Mbh is essential for growth in the absence of elemental sulfur (458). The membrane-bound homologous [NiFe]-hydrogenase (Mbx) complex has been shown to play a major although not essential role in sulfur-dependent growth in *Tco. kodakarensis* and *Pyr. furiosus* (458, 459). It is proposed that Mbx catalyzes the transfer of electrons from reduced ferredoxin to $NADP^+$ and, in conjunction with the cytoplasmic coenzyme A (CoASH)-dependent NADPH elemental sulfur reductase (Nsr), catalyzes sulfur reduction. Structure predictions indicate that Mbx, like Mbh, might be able to accept electrons from ferredoxin and to create an ion gradient (for a review, see reference 460). The produced ion gradient is used for ATP generation via the membrane-bound A_oA_1 -ATPase (446). In addition, *Tco. kodakarensis* possesses one (SHI) and *Pyr. furiosus* possesses two (SHI and SHII) cytosolic [NiFe]-hydrogenases, which provide NADPH from H_2 as the electron donor (for detailed discussion, see references 458 and 460).

Sugar transport. In *Thermococcales*, as in most other *Archaea* with the exception of a few *Halocarchaea*, no homologs of the phosphoenolpyruvate-dependent PTS have been identified. Instead, binding protein-dependent ATP binding cassette (ABC) transporters are utilized for sugar uptake. From the energetic point of view, it is still under discussion if 1 ATP or 2 ATPs are required for sugar uptake; however, since ABC transporters possess 2 ATPases, it is assumed that at least 1 ATP is required to activate the transporter for transport (461, 462). In *Tco. kodakarensis*, an ABC oligosaccharide transporter has been shown to be essential for growth on maltooligosaccharides or polysaccharides, where it represents the only available transporter for carbohydrates, as deduced from the genetic/mutational approach (463). In agreement with the additional growth of *Pyr. furiosus* on maltose, two ABC transporters, specific for trehalose/maltose (TM system [PF1739 to PF1741 and PF1744]) and maltodextrins (MD system [PF1933 and PF1936 to PF1938]), were found in *Pyr. furiosus*. The charac-

terized sugar ABC transporters are associated in gene clusters with sugar-degrading enzymes as well as transcriptional regulators, e.g., in *Pyr. furiosus* with an ADP-glucose-dependent trehalose synthase (glycosyltransferring) (TreT) and the transcriptional regulator TrmB in the TM operon and with an amylopullulanase in the TD operon (464–466) (see Fig. 21). In *Tco. kodakarensis*, the ABC transporter-encoding genes are clustered with the TrmB-like regulator Tgr (*Thermococcales* glycolytic regulator) (208, 463) (see Fig. 21 and below). Later, an ABC transporter (OppA family) for cellobiose and a diverse set of other β-galactosides (e.g., celotrioses to cellopentoses, laminaribiose, laminaritriose, and sophorose) from *Pyr. furiosus* were characterized (467; for a review, see reference 452).

Sugar metabolism. In *Pyr. furiosus* as well as *Tco. kodakarensis*, a great variety of extracellular as well as cytoplasmic α- and β-specific glycoside hydrolases (e.g., α-amylases, α-galactosidase, β-glucosidase [CelB], and chitinase) have been identified, which allow for the complete conversion of polysaccharides to monomers (for a recent review on *Pyr. furiosus*, see reference 452).

(i) **The modified EMP pathway.** So far, studies of *Thermococcales* focused mainly on glucose degradation pathways. ¹³C NMR studies revealed that members of the *Thermococcales*, i.e., *Pyr. furiosus* and *Thermococcus* spp., degrade glucose exclusively (100%) via a modified EMP pathway (40, 110) (Fig. 20). The EMP pathway in *Pyr. furiosus* and *Tco. kodakarensis* has been studied in detail by using enzyme characterization as well as genetic mutational approaches in *Tco. kodakarensis*, which allows for crucial insights into the *in vivo* function of key enzymes. The modified EMP pathway in *Thermococcales* for glucose degradation is characterized by ADP-dependent sugar kinases, i.e., ADP-dependent glucokinase (51, 110) and ADP-dependent phosphofructokinase, which exhibit no allosteric potential (111). An unusual cupin-type glucose-6-phosphate isomerase (cPGI) catalyzes the conversion between glucose 6-phosphate and fructose 6-phosphate (74, 89, 90). FBP cleavage is catalyzed by an archaeal-type class I FBP aldolase that shares no obvious homology to classical class I enzymes (126, 133). Both GAPOR and pyridine nucleotide-dependent nonphosphorylating GAPN are essential for glycolytic growth on maltooligosaccharides, as revealed by a mutational approach (175). Both enzymes catalyze the direct oxidation of GAP, forming 3-phosphoglycerate (3PG), and thus omit substrate-level phosphorylation via PGK. For GAPOR, which forms reduced ferredoxin, an important function for energy generation via the Mbh complex (0.3 mol ATP generated per mol H₂ formed) has been discussed (455, 456). For GAPN, due to its NADP⁺ preference, a role for the generation of NADPH in biosynthesis under glycolytic conditions has been suggested. Because of the absence of the classical pentose phosphate pathway in *Archaea* and the generation of pentoses via the reversed ribulose monophosphate pathway in *Thermococcales* and most other *Archaea*, the generation of NADPH for biosynthesis might be crucial for the cell (see above) (for a detailed discussion, see reference 175). In contrast to the essential GAPN and GAPOR in *Thermococcales*, deletion of the classical enzyme couple comprised of GAPDH and PGK does not have any impact on glycolysis. The authors of that study suggest that the presence of a glycolytic active PGK consuming ADP might be energetically unfavorable since it competes for the cosubstrate of ADP-dependent sugar kinases, which is required for sugar activation (175). The conversion of 3PG to PEP proceeds via 2,3-bisphosphoglycerate-independent phosphoglycerate mutase

(iPGAM), which shows only remote similarity to its bacterial and eukaryotic counterparts (11% amino acid identity to the *E. coli* enzyme) (212), and enolase, which has been purified and characterized for *Pyr. furiosus* (226).

The conversion of PEP to pyruvate by phosphoenolpyruvate synthetase (PEPS) and pyruvate kinase (PK) has been a matter of debate. Whereas the pyruvate kinase reaction is considered to be irreversible (PEP + ADP ↔ pyruvate + ATP; ΔG = -25.5 kJ mol⁻¹), the Gibbs free energy of the PEPS reaction is close to zero (PEP + AMP + P_i ↔ pyruvate + ATP + H₂O; ΔG = 0.17 kJ mol⁻¹), and a glycolytic function of PEPS has been suggested (37, 322, 323, 468). The enzymatic characterization of PEPS from *Pyr. furiosus* confirmed that the enzyme reaction is reversible but showed a clear preference (higher catalytic efficiency) for the gluconeogenic direction of PEP formation (324). A genetic analysis of the function of both the PEPS and PK enzymes in the EMP pathway of *Tco. kodakarensis* revealed unexpected results (323): whereas PEPS was essential for glycolysis, PK was not, and only the disruption of the *pps* gene resulted in a strain that was unable to grow under glycolytic conditions on maltooligosaccharides. In contrast, PK deletion resulted in only a moderately decreased (by 15%) growth rate. These unexpected functions of PEPS and PK are difficult to explain. Imanaka and coworkers suggest that a glycolytic PK (like PGK [discussed above]) would compete with the ADP-dependent sugar kinases for ADP, and thus, the utilization of PEPS forming ATP from AMP, the product of the sugar kinase reactions, would help to maintain the carbon flux. The contribution of PK to glycolysis, in conjunction with adenylate kinase (AMP + ATP ↔ 2 ADP), would increase with higher energy/ADP concentrations in the cell, and a function as a natural valve to maintain the intracellular ADP concentrations has been discussed (323) (for a detailed discussion, see the section on energetics, below).

The pyruvate generated via the modified EMP pathway in *Thermococcales* is then further oxidatively decarboxylated in a ferredoxin-dependent manner via pyruvate:ferredoxin oxidoreductase (POR) to acetyl-CoA. The reduced ferredoxin can then serve as an additional energy source via membrane-bound hydrogenase and ATP synthase (42, 456, 469–473). Acetyl-CoA is converted to acetate in one step involving acetyl-CoA synthetase (ADP forming) coupling the reaction with the formation of ATP from ADP and P_i via substrate-level phosphorylation. The ADP-forming acetyl-CoA synthetase substitutes for the acetate kinase/phosphotransacetylase enzyme couple catalyzing the same reaction in *Bacteria*, with acetylphosphate as an intermediate. Thus, the mechanism of acetate formation in prokaryotes seems to be domain specific, proceeding via ADP-forming acetyl-CoA synthetase in *Archaea* and acetate kinase and phosphotransacetylase in *Bacteria*. However, recently, ADP-forming acetyl-CoA synthetase has been detected in the thermophilic bacterium *Chloroflexus aurantiacus* (454, 474–479).

(ii) **Gluconeogenesis.** For gluconeogenesis in *Tco. kodakarensis*, PEPS was shown to be dispensable, since the deletion strain was still able to grow gluconeogenically on pyruvate, although the growth rate as well as cell yield were reduced (about a 15% decrease). The contribution of alternative metabolic routes, e.g., via PEP carboxykinase, to gluconeogenic growth has been suggested, and the enzyme from *Tco. kodakarensis* has been characterized (323, 330). Unexpectedly, the PK deletion strain also exhibited a decreased growth rate (decreased by about 15%) under gluconeo-

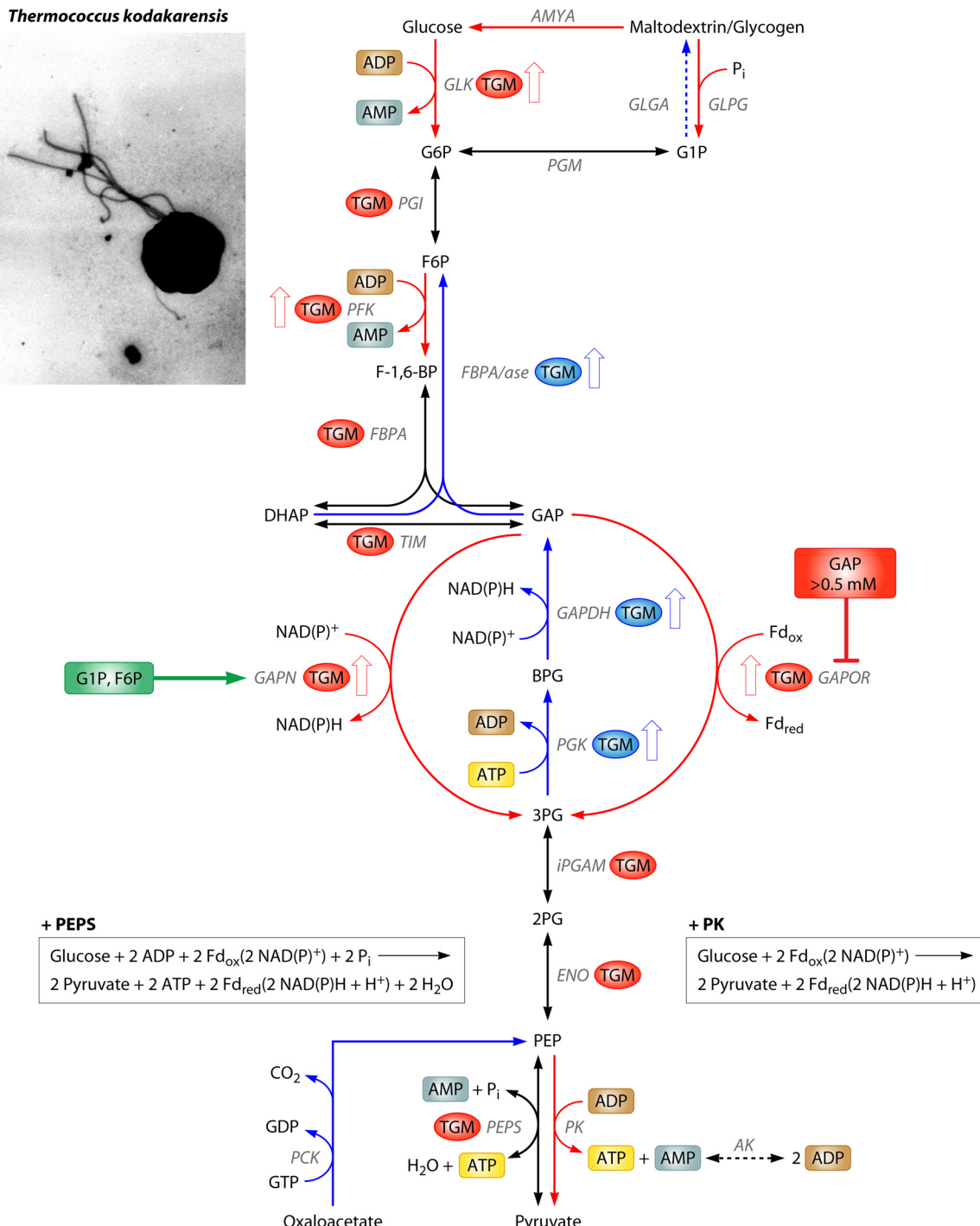


FIG 20 Glycolysis and gluconeogenesis in the anaerobic hyperthermophile *Thermococcus kodakarensis*. *Tco. kodakarensis* utilizes the reversible EMP pathway for glycolysis and gluconeogenesis. The glycolytic pathway is characterized by ADP-dependent sugar kinases, archaeal-type class I FBPA, catabolic irreversible GAPN and GAPOR, and reversible PEPS, besides PK, with preferred glycolytic function. In gluconeogenesis, besides PEPS, alternative reactions, such as those catalyzed by PCK, seem to contribute to PEPS formation. The anabolic direction is characterized by the anabolic PGK/GAPDH enzyme couple as well as FBPA/ase. Enzyme reactions with catabolic function are indicated by red arrows, anabolic reactions are indicated by blue arrows, and reversible reactions are shown as black arrows. Effectors are given in green and red boxes for activators and inhibitors, respectively. Genes comprising the TGM for binding of the transcriptional regulator Tgr (see also Fig. 21) are marked by a blue dot (TGM upstream of the BRE/TATA box, activator binding for genes encoding gluconeogenic proteins) or a red dot (TGM downstream of the BRE/TATA box, repressor binding for genes encoding glycolytic proteins) (208). Transcript levels of genes which are upregulated under glycolytic or gluconeogenic conditions are marked with red or blue open arrows, respectively (208). The net equations of glucose conversion to pyruvate via the modified EMP pathway with utilization of PEP synthetase (+PEPS) and pyruvate kinase (+PK) are indicated in boxes (GLGA, glycogen synthase; GLPG, glycogen phosphorylase; AMYA, α-amylase; PCK, PEP carboxykinase; PGM, phosphoglucomutase; AK, adenylate kinase). (Electron micrograph courtesy of Haruyuki Atomi, Kyoto University, Japan, reproduced with permission.)

genic growth conditions. The reason why PK, from the thermodynamic point of view, operating exclusively in the catabolic direction, affects gluconeogenic growth on pyruvate is still unclear.

In addition to reversible enzymes like enolase and iPGAM, gluconeogenesis in *Thermococcales* involves the GAPDH/PGK couple, which was shown to be essential for gluconeogenic growth on pyruvate for *Tco. kodakarensis* (175). The *gap* deletion strain was unable to grow under these conditions, whereas deletion of the genes encoding GAPOR and GAPN did not affect gluconeogenesis (see above).

Also, the bifunctional FBPA/ase, initially reported as FBPase type V, catalyzing the direct conversion of GAP and DHAP as well as FBP to F6P without a release of reaction intermediates, was shown to be essential for gluconeogenesis (337, 340, 342). The enzyme thus substitutes for the reversible archaeal-type class I FBPA and ADP-PFK in the anabolic direction. The deletion of the FBPA/ase-encoding gene completely abolished growth under gluconeogenic conditions on pyruvate, whereas glycolytic growth on starch was not affected (332, 336).

Energetics. The net energy yield of the modified EMP pathway in *Thermococcales* varies between 0 and 2 ATPs and is difficult to estimate because of the use of unusual ADP-dependent sugar kinases in the preparatory phase and of PEPS and/or PK in the lower part of glycolysis. The use of PK in the modified EMP pathway would result in no net energy gain via substrate-level phosphorylation: in total, 4 ADPs are consumed by both ADP-dependent sugar kinases and PK. These 4 ADPs invested are regenerated from the 2 AMPs (sugar kinases) and 2 ATPs (PK) formed via the adenylyl kinase reaction; therefore, there is no net gain of energy (Fig. 20). From the energetic point of view, the energy conservation via substrate-level phosphorylation utilizing AMP-dependent PEPS is 2 ATPs: 2 ADPs are consumed by sugar kinases in the preparatory phase, and the 2 AMPs produced are used by PEPS, resulting in the formation of 2 ATPs. Hence, per molecule of glucose, 2 energy-rich phosphoanhydride bonds (2 ADP → 2 AMP) are invested, and 4 energy-rich bonds are formed (2 PEP + 2 AMP + 2 P_i → 2 pyruvate + 2 ATP), so that a net of 2 ADPs are converted to 2 ATPs (323). However, sugar uptake via ATP transporters requires additional energy.

The utilization of ADP, which is continuously produced in anabolism, as the phosphoryl donor in the preparatory phase of the modified EMP pathways for *Thermococcales* as well as *Arc. fulgidus* has been discussed as being advantageous under conditions of energy limitation, when the ATP/ADP ratio is low. Thus, the available ADP is used instead of the rare ATP. This would be in line with the anaerobic, fermentative metabolism of *Thermococcales* and *Arc. fulgidus*. Also, the methanogens seem to degrade the internal storage compound glycogen under conditions of energy limitation by using ADP-dependent sugar kinases. Furthermore, most of those *Archaea* using ATP-dependent kinases in the upper part of their modified EMP pathway versions exhibit a respiration metabolism with S⁰, O₂, and NO₃²⁻ as electron acceptors, e.g., *Aeropyrum*, *Pyrobaculum*, and *Thermoproteus*, thus gaining additional or even most of their energy through the CAC and respiratory chains. However, *Des. amyolyticus*, which shows fermentative metabolism similar to that of *Thermococcales*, utilizes ATP-dependent sugar kinases (40, 42, 55, 110, 119). Therefore, the utilization of ADP instead of ATP might also be seen in conjunction with the PEPS reaction, which reutilizes the AMP formed by the ADP-dependent kinases. This concerted mode of action might

coordinate both energy-consuming and energy-gaining steps in glycolysis and therefore help to optimize its energy yield (322, 323). An additional source of energy provided by the modified EMP pathway in *Thermococcales* is the use of ferredoxin-dependent enzymes, i.e., GAPOR and POR (up to 4 reduced ferredoxins per mol glucose); the reduction equivalents formed serve for ATP generation via the hydrogenase complex (Mbh) and ATPase (formation of 1.2 mol ATP from 4 mol Fd_{red} via the hydrogenase complex and ATP synthase) (460). Subsequently, acetyl-CoA is converted to acetate via ADP-forming acetyl-CoA synthetase, yielding a further 2 mol ATP per mol glucose via substrate-level phosphorylation. Further energy, i.e., 1 ADP for glucose phosphorylation, might be saved by the utilization of glycogen-phosphorylase for polysaccharide degradation.

Regulation at the protein level. The three classical points of allosteric control in *Bacteria* and *Eukarya*, i.e., hexokinase, PFK, and PK, are absent in *Thermococcales* (and also generally in *Archaea*). The ADP-dependent kinases and also most archaeal PKs possess no allosteric properties toward classical effectors of bacterial and eukaryotic enzymes (232, 235). Instead, the only allosterically controlled enzyme in the modified EMP pathway of *Thermococcales* identified so far is GAPN. Detailed enzymatic analysis revealed that *Tco. kodakarensis* GAPN is an NADP⁺-dependent enzyme that possesses reduced activity at low GAP concentrations and, like other previously characterized archaeal enzymes, exhibits allosteric potential (175). Glucose 1-phosphate and, to a lesser extent, fructose 6-phosphate are potent activators of the enzyme (addition of 1 mM G1P results in a 15-fold increase of GAPN activity). G1P is a major intermediate of phosphorolytic maltooligosaccharide degradation via glycogen/maltodextrin phosphorylase and phosphohexomutase. The regulation of GAPN by early intermediates of degradation pathways (i.e., G1P and F6P) suggests an enhancement of glycolytic flux via GAPN at high GAP concentrations (175). GAPOR of *Pyr. furiosus* was reported to be significantly inhibited by GAP concentrations above 0.5 mM (160).

Regulation at the gene level. The physiological functions of the respective EMP enzymes in the catabolic or anabolic direction, as deduced from genetic approaches, are also reflected mostly by the transcriptional control of the encoding genes and also the respective enzyme activities in crude extracts. Whole-genome DNA microarray analysis of *Pyr. furiosus* cells grown on carbohydrates (maltose) versus peptides (hydrolyzed casein) revealed significant changes of transcript levels in response to the carbon source. Focused on glucose metabolism, transcripts of genes encoding PGI, ADP-PFK, GAPOR, and TIM in maltose-grown cells and of genes encoding FBPAse (anabolic FBPA/ase), PGK, and GAPDH in peptide-grown cells were upregulated (207). For the highly abundant PEPS (the most abundant enzyme in *Pyr. furiosus*) as well as pyruvate kinase, comparable expression levels were observed under both growth conditions, which was confirmed for PEPS by activity measurements (207). In contrast, a significant increase in PEPS transcription and activity (about 10-fold) was reported for *Pyr. furiosus* cells grown on maltose compared to cells grown in the absence of maltose by Sakuraba and coworkers (322).

An upregulation of GAPOR at the transcriptional level (Northern blot analysis) accompanied by a 5-fold-higher activity was also demonstrated for *Pyr. furiosus* cells grown on pyruvate after addition of cellobiose. In this study, no transcript change and decreased activity were observed for the gene encoding GAPDH, and

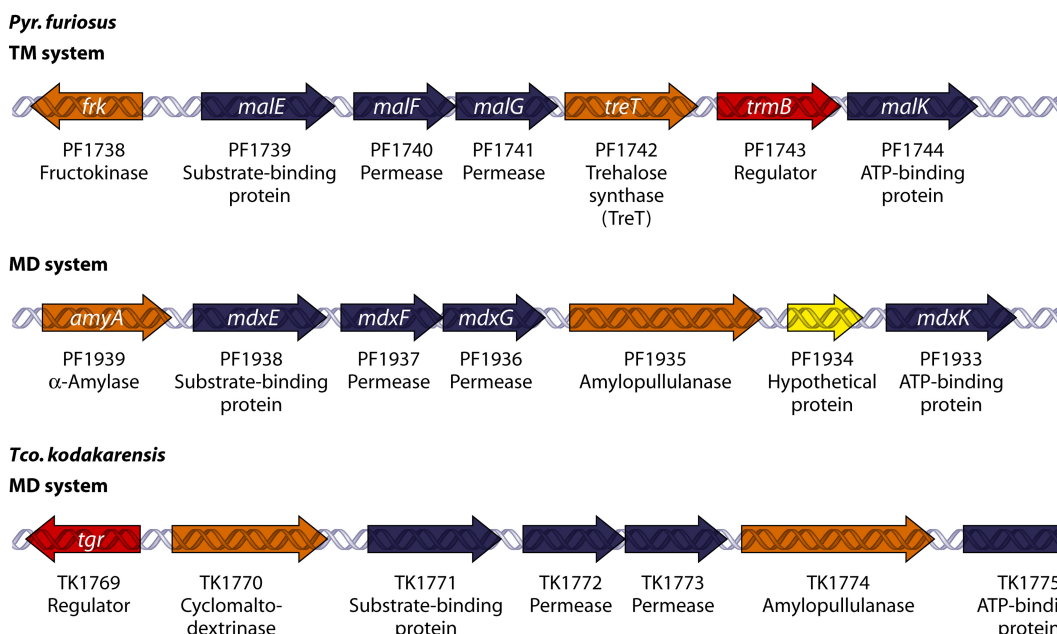


FIG 21 Gene clusters encoding the trehalose/maltose (TM) and maltodextrin (MD) ABC transporters in *Tco. kodakarensis* and *Pyr. furiosus*. Whereas *Pyr. furiosus* possesses the TM and MD systems (481), *Tco. kodakarensis* possesses only the MD system (208) and is not able to utilize maltose or trehalose as a carbon source. In *Tco. kodakarensis*, the gene encoding the *Thermococcales* glycolytic regulator (Tgr; TK1769) is positioned divergently from the gene cluster comprising components of the ABC transporter (i.e., substrate binding protein [TK1771], two permeases [TK1772 and TK1773], and ATP binding protein [TK1775]), and genes encoding enzymes involved in polymer degradation (i.e., amylopullulanase [TK1774] and cyclomaltodextrinase [TK1770]). The TM gene cluster of *Pyr. furiosus* possesses, besides the genes encoding the ABC transporter components, genes encoding fructokinase (PF1738) (divergently oriented), trehalose synthase (TreT; PF1742 involved in trehalose utilization), and the transcriptional regulator TrmB (PF1743). The *Pyr. furiosus* MD gene cluster is also comprised of genes encoding enzymes involved in polymer degradation (i.e., α -amylase [PF1939] and amylopullulanase [PF1935]) and a hypothetical protein (PF1934). Components of the ABC transporter are depicted in gray, enzymes involved in sugar degradation are shown in orange, hypothetical proteins are shown in yellow, and transcriptional regulators are depicted in red.

regulation of GAPOR at the transcript level and of GAPDH at the posttranscriptional level was proposed (161).

In *Tco. kodakarensis*, a microarray analysis of a wild-type strain grown on glycolytic (maltodextrin) versus gluconeogenic (pyruvate or S⁰) carbon sources revealed a significant upregulation of genes encoding enzymes of the modified EMP pathway (e.g., ADP-sugar kinases, GAPN, and GAP:OR [3- to 8-fold]), despite pyruvate kinase, under glycolytic conditions. Under gluconeogenic conditions, upregulation of FBPA/ase, GAPDH, and PGK was observed. According to the higher transcript level, higher activities for GAPDH in peptide-grown cells (7-fold) and for GAPOR in maltose-grown cells (5.4-fold) were determined (208). In another study of *Tco. kodakarensis*, increased transcript levels and enzyme activities of PK and PEPS were reported for cells grown under glycolytic conditions on maltooligosaccharides compared to cells grown with yeast extract and tryptone (YT) (323).

In accordance with its unique gluconeogenic function, the transcript of anabolic FBPA/ase (PF0613) is upregulated 15-fold in peptide-grown cells (336). The reversible archaeal-type class I FBPA has been reported to be upregulated on maltose-grown cells compared to pyruvate-grown cells in another study, suggesting a preferred glycolytic function (126, 133).

Therefore, a sophisticated mode of transcriptional and probably also of posttranslational regulation seems to play a major role in *Thermococcales*, compensating for the reduced allosteric potential of the modified EMP pathway. As outlined below, several global transcriptional regulators important for CCM regulation

(i.e., Tgr in *Tco. kodakarensis* and TrmBL1 and/or TrmB in *Pyr. furiosus* have been identified, which tightly control the expression of genes encoding glycolytic and gluconeogenic enzymes) (208, 464, 480–483).

Transcriptional regulator TrmB in *Thermococcales*. TrmB-dependent repression was reported first for the trehalose/maltose ABC transporter of *Tco. litoralis* and later for *Pyr. furiosus* (464, 484, 485). The transcriptional repressor TrmB (PF1743) is a bi-functional, sugar-sensing regulator which represses transcription of the trehalose/maltose (TM) (*malE*, *malF*, *malG*, *treT*, *trmB*, and *malK*) as well as the maltodextrin (MD) (*mdxE*, *mdxF*, *mdxG*, *pula*, and *mdxK*) ABC transporter operons in *Pyr. furiosus* (Fig. 21). The TM system encodes, in addition to the components of the ABC transport system, TrmB and the reversible trehalose synthase (glycosyltransferring) (TreT), for which a major function in trehalose degradation has been suggested (465). Located divergent from the TM operon is the *frk* gene, which encodes an ATP-dependent fructokinase (465) (Fig. 21). The MD operon comprises, in addition to the ABC transporter, a gene for amylopullulanase (207). Repression of the TM system is relieved by its substrates maltose and trehalose. In contrast, the repression of the MD system is abolished by maltotriose (maltodextrins) and sucrose, which act as inducers, but not by trehalose and maltose (464, 466, 481, 482). Therefore, TrmB is a bifunctional repressor that acts on two different promoters (*malE* [TM] and *mdxE* [MD]) and is differently regulated by the binding of different sugars, as demonstrated by electrophoretic mobility shift assays (EMSA) as well as by *in vitro* transcription studies (481, 482) (see Fig. 23).

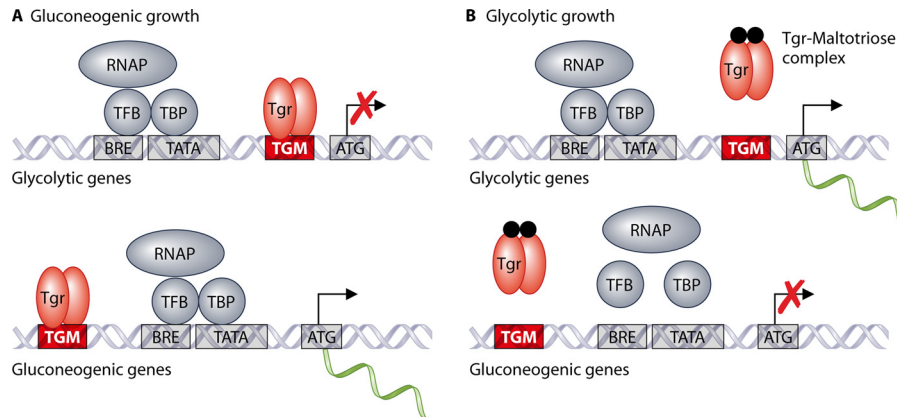


FIG 22 Model for the function of the *Thermococcales* glycolytic regulator (Tgr) in differential expression of glycolytic and gluconeogenic genes in *Tco. kodakarensis* (208). Tgr serves as a repressor for glycolytic genes (*Thermococcales* glycolytic motif [TGM] located downstream of the promoter element [BRE/TATA]) and as an activator for gluconeogenic genes (TGM upstream of the promoter element). (A) Under gluconeogenic growth conditions (absence of the effector maltotriose), Tgr binds to the TGM, inhibits transcription of glycolytic genes, and activates transcription of gluconeogenic genes. (B) Under glycolytic growth conditions, in the presence of the effector (maltotriose) binding of Tgr to DNA is relieved. Abbreviations: RNAP, RNA polymerase; TFB, transcription factor B; TBP, TATA binding protein; BRE, TFB-responsive element; TATA, TATA box; ATG, start codon.

Glucose, which cannot be used as a carbon source by *Pyr. furiosus* but is formed endogenously, was shown to act as an effective corepressor of both the TM and MD systems (481). In addition, maltose (inducer of the TM system) acted as a corepressor of the MD system. Therefore, high cellular levels of glucose will inhibit the uptake of glucose-producing sugars via the TM and MD systems and maltose availability will inhibit the uptake of maltodextrins via the MD system, and similarity to catabolite repression has been discussed (482).

TrmB binds upstream of BRE/TATA elements of the TM promoters and thereby possibly blocks TFB/TBP access to these sites, whereas binding at MD promoter elements overlaps the transcriptional start site and may inhibit RNAP recruitment to the DNA (481). The crystal structure of a truncated TrmB from *Pyr. furiosus* (deletion of residues 2 to 109 [Δ 2-109]) comprising the sugar binding domain but lacking the DNA binding domain was solved (483). Whereas N-terminally truncated TrmB was a monomer in solution, the full-length protein was a dimer. The protein bound maltose, glucose, sucrose, and maltotriose with increasing affinities, and the structure represented a novel sugar binding fold. Cocrystallization with maltose demonstrated that 7 amino acid residues were involved in sugar binding (Ser229, Asn305, Gly320, Met321, Val324, Ile325, and Glu326) (483). Maltose was shown to be bound via the nonreducing glycosyl residue of maltose, and it has been proposed that binding of different sugars may lead to a conformational change of TrmB. The structure of full-length TrmB in complex with sucrose was recently solved (PDB accession number 3QPH) (486). Phylogenetic analyses suggest that the TM system was derived via lateral gene transfer from *Bacteria*, whereas the MD system probably arose within the *Archaea* (487). Sequence comparisons with nonglycolytic promoter regions revealed a “*Thermococcales* glycolytic motif” (TGM) (TATCAC-N₅-GTG ATA) located upstream of genes encoding glycolytic and gluconeogenic enzymes in *Pyr. furiosus* and *Tco. kodakarensis*, which was absent in nonsaccharolytic *Pyr. abyssi* and *Pyr. horikoshii* (488).

TrmB-like regulators in *Thermococcales*. Besides TrmB, three TrmB-like proteins in the genome of *Pyr. furiosus* (TrmBL1

[PF0124], TrmBL2 [PF0496], and TrmBL3 [PF0661]) and no TrmB but two TrmBL homologs in *Tco. kodakarensis* (TK769 [Tgr; TrmBL1 homolog] and TK0471 [TrmBL2]) were identified (482). The role of TrmBL1 homologs (Tgr) in *Pyr. furiosus* and *Tco. kodakarensis* was studied (208, 480).

(i) TrmB-like regulators in *Tco. kodakarensis*. Tgr of *Tco. kodakarensis* exhibits 67% identity to TrmBL1 of *Pyr. furiosus* (PF0124) and 28% identity to *Pyr. furiosus* TrmB (PF1743). The disruption of the *tgr* gene resulted in a significant decrease in growth under gluconeogenic (pyruvate/peptides) conditions, whereas glycolytic growth was not affected in the Δtgr deletion strain compared to the wild-type strain. A whole-genome-wide microarray analysis revealed increased transcript levels for glycolytic genes independent of glycolytic or gluconeogenic growth conditions (i.e., genes encoding enzymes involved in maltodextrin uptake, degradation, as well as glycolysis, such as the maltodextrin ABC transporter [TK1771 to TK1773 and TK1775], maltodextrin phosphorylase [TK1406], ADP-dependent sugar kinases [TK1110 and TK0376], and nonphosphorylating GAP dehydrogenase [TK0705]). In contrast, expression levels of genes encoding gluconeogenic enzymes were reduced (i.e., genes encoding FBPA/ase [TK2164], phosphorylating GAP dehydrogenase [TK0765], and phosphoglycerate kinase [TK1146]), and a dual function of Tgr as an activator and a repressor was proposed (Fig. 22) (208). Interestingly, in agreement with the finding that PEPS and not pyruvate kinase was the major glycolytic enzyme in *Tco. kodakarensis*, no TGM and no significant changes in transcription levels were observed for the gene encoding pyruvate kinase (TK0511) (323). In total, the identified Tgr regulon comprised more than 30 genes (208). EMSAs revealed specific binding of Tgr to genes that harbor the TGM positioned either upstream of the promoter element BRE/TATA in gluconeogenic promoters (e.g., the FBPA/ase-encoding gene TK2164) or downstream of glycolytic promoters (e.g., *pfp* [ADP-PFK]; TK0376) (208). Tgr, like TrmB, possesses the sugar recognition site, and upon addition of maltotriose in EMSAs, complex formation of Tgr and DNA (*pfk* promoter) was inhibited (K_d [dissociation constant] value of ca. 520 μ M), suggesting that maltotriose is the physiological effector

that regulates Tgr-mediated activation or repression. The Tgr promoter itself also exhibits the TGM motif, and autoregulation was demonstrated. The current model suggests that under gluconeogenic growth conditions, Tgr binding to a TGM positioned downstream of the promoter elements (glycolytic genes) blocks recruitment of the RNA polymerase or transcription factors (TBP/TFB) and thus inhibits transcription (repressor), whereas Tgr binding to an upstream-located TGM (gluconeogenic genes) sequence activates transcription (activator) by enhancing recruitment of RNA polymerase and transcription factors (208). In the presence of the physiological effector maltotriose (glycolytic growth conditions), binding of Tgr to DNA and, thus, transcriptional activation or repression are relieved. Thus, Tgr is a global regulator that controls glycolytic (repressor) and gluconeogenic (activator) metabolism by direct binding to the TGM, which is controlled by sugar availability in the cell (Fig. 22).

(ii) **TrmB-like regulators in *Pyrococcus furiosus*.** The dual role of TrmBL1 as a repressor for glycolytic enzymes (TGM located downstream of the BRE/TATA box) and an activator for gluconeogenic enzymes (TGM located upstream of the BRE/TATA box) was also confirmed for *Pyr. furiosus* but with maltose and maltotriose as inducers (480, 482). In addition, regulation in *Pyr. furiosus* seems to be more complex due to the presence of two ABC transport systems (TM and MD) as well as TrmB as an additional repressor (Fig. 23). TrmBL1 of *Pyr. furiosus* was shown to represent a tetramer that is shifted toward a higher octameric oligomerization state in the presence of high concentrations of maltose (5 mM) or maltotriose (1 mM). *In vitro* transcription studies of the *pfp* promoter (PF1784 [ADP-PFK]) revealed transcription only at low maltose concentrations (relieved from repression), whereas in the absence of maltose and at high maltose concentrations, no transcription was observed. A shift from a tightly binding tetrameric repressor in the absence of sugar that can be relieved in the presence of low sugar concentrations to an octamer with high DNA binding affinity at high sugar concentrations, again repressing transcription, was suggested (480, 482). The physiological significance of this phenomenon still remains to be established, but it would allow repression of transcription in response to a high cellular concentration of degradable sugars (i.e., maltose and maltodextrin). Like Tgr, TrmBL1 of *Pyr. furiosus* was shown to bind to promoters that comprise the TGM sequence (e.g., MD and ADP-PFK promoters); however, binding to promoters that lack the TGM sequence, like the TM promoter and the TrmBL1 promoter itself (PF0124), was also observed. Notably, in *Pyr. furiosus*, cross-regulation was observed for TrmB and TrmBL1. In general, the binding affinity for promoter fragments that carry the downstream TGM sequence was higher for TrmBL1 than for TrmB. For the MD promoter, both the TrmB and TrmBL1 (TGM) binding sites (downstream of BRE/TATA) were shown to partially overlap. In contrast, the TM promoter (no TGM sequence) favored TrmB binding, although TrmBL1 binding was still observed. Autoregulation was proposed for the TrmBL1 promoter (no TGM sequence), which was responsive to TrmBL1 but not to TrmB, and unique to this promoter, TrmBL1 repression was relieved by glucose (50 μ M) (480).

In vivo function of TrmB and TrmB-like regulators in *Pyrococcus*. Lee and colleagues suggest that under *in vivo* conditions, the cellular glucose concentration will be the regulatory signal that controls glycolysis, gluconeogenesis, and transport (Fig. 23) (482). At high cellular glucose concentrations (glucose excess), the

TrmBL1 transcription level is high (glucose relieves autorepression of the gene encoding TrmBL1), which in turn represses transcription of glycolytic genes and activates transcription of gluconeogenic genes. The shift from the tetrameric state (responsive to inducers) to the octameric state of TrmBL1 at high cellular maltose and/or maltotriose concentrations might enhance DNA binding affinity and thus further stimulate repression and activation of the respective genes. In addition, uptake of maltose or maltodextrins is also controlled via TrmB (repressor). In the presence of glucose as a corepressor, TrmB represses transcription of both the TM and MD systems. Therefore, at high cellular glucose concentrations, sugar uptake and glycolysis are repressed, whereas gluconeogenesis (e.g., to form glycogen as carbon storage) is activated. In contrast, at low cellular glucose concentrations (glucose depletion) and with the availability of maltose and/or maltodextrin as the carbon source, TrmBL1 transcription is repressed (autoregulation) due to the absence of glucose as an inducer, resulting in low cellular concentrations of TrmBL1. In addition, low concentrations of cellular maltose or maltotriose (tetrameric TrmBL1 responsive to inducers) result in stimulated expression of glycolytic genes (the repressor is relieved by the inducer) and reduced expression of gluconeogenic genes (no activator binding). Further on, transcription of the TM and MD operons is activated by the relief of TrmB (repressor) in the presence of the inducer maltose or maltodextrin (maltotriose-maltopentose or sucrose), respectively, thereby allowing increased sugar uptake. In conclusion, at low cellular concentrations of glucose, sugar uptake via the TM or MD system (depending on the available carbon source) is activated, glycolysis is enhanced, and gluconeogenesis is decreased.

The other TrmBL homolog, TrmBL2 of *Pyr. furiosus*, lacks the sugar binding motif, and initial studies indicated that TrmBL2 recognizes MD promoters, but the way of regulation is still unclear (482). For *Tco. kodakarensis* TrmBL2 (TK0471), a role as an abundant chromosomal protein, which forms fibrous, thick structures with DNA, was reported (489). TrmBL2 binds to coding and intergenic regions of the DNA and thus probably represses transcription by blocking RNAP recruitment.

Sulfolobus solfataricus

Growth conditions. The thermoacidophilic model organism *Sul. solfataricus* (strain P2; DSM1617) is a member of the *Sulfolobales* within the *Crenarchaeota* and was isolated from an acid solfataric field (Pisciarelli) near Naples, Italy (490). The genome sequences of *Sul. solfataricus* strain P2 as well as many other *Sulfolobus* species (e.g., *Sul. tokodaii*, *Sul. acidocaldarius*, and *Sul. islandicus*) have been deciphered (416, 417, 491, 492), and a genetic system was established (for details and literature, see references 27 and 493).

Sul. solfataricus P2 is an aerobic to microaerophilic chemoorganoheterotroph with optimal growth at 80°C (range, 60°C to 92°C) and pH 2 to 4 (32). Also, chemolithoautotrophic growth at the expense of the Knallgas reaction has been reported (494). Heterotrophic growth on various carbon and energy sources, such as many different sugars, like pentoses (e.g., D-arabinose, L-arabinose, and D-xylose), hexoses (e.g., D-glucose, D-galactose, and D-mannose), disaccharides (e.g., maltose and sucrose), polysaccharides (e.g., starch and dextrin); tryptone; peptides; and amino acids, has been reported (345). In *S. solfataricus*, glucose is degraded to pyruvate by the modified branched ED pathway. The pyruvate formed is further oxidized via the action of pyruvate:

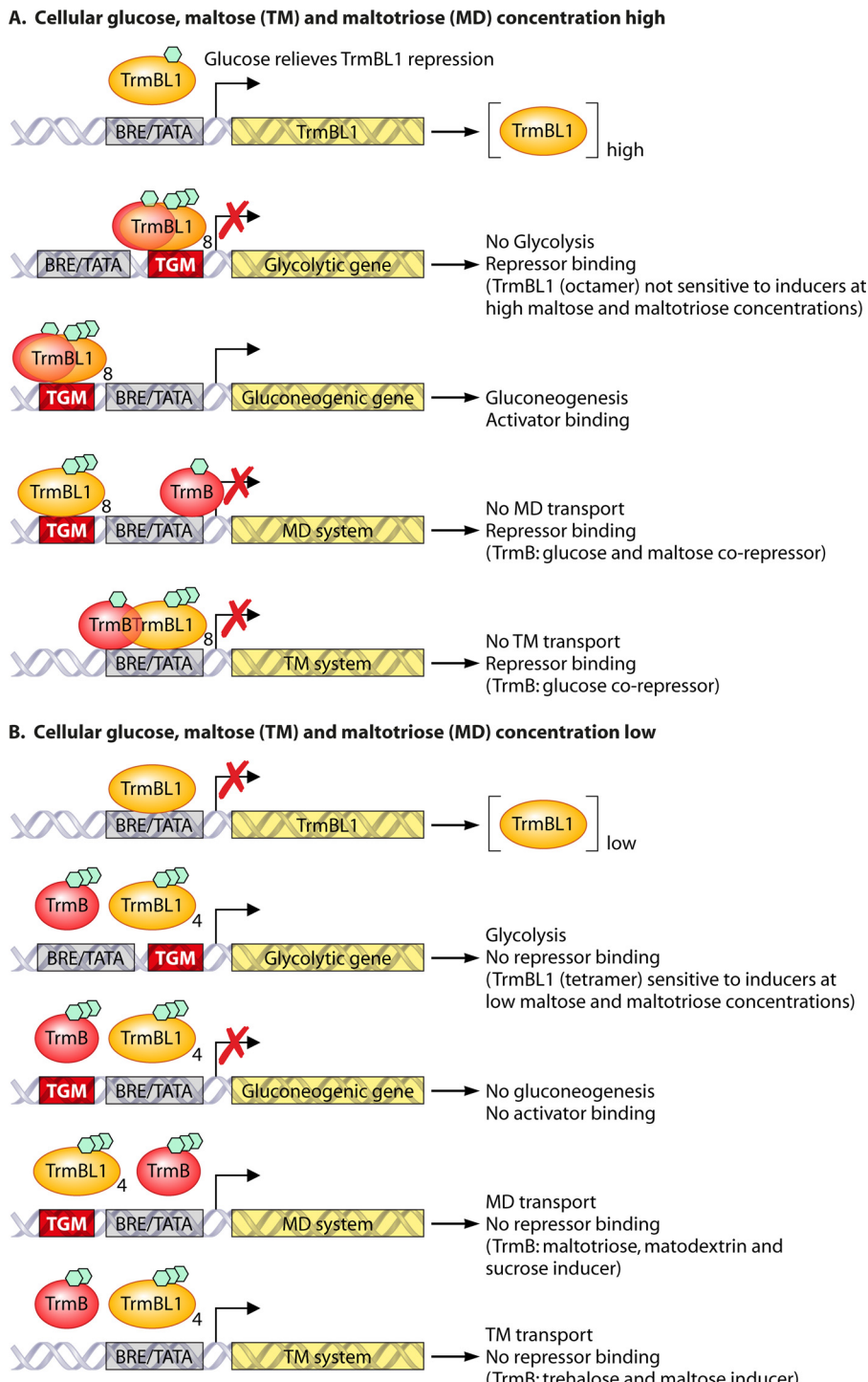


FIG 23 Model for TrmB and TrmBL1 function in differential regulation of genes encoding enzymes catalyzing transport, glycolysis, and gluconeogenesis in *Pyr. furiosus*. Under *in vivo* conditions, the cellular glucose concentration is supposed to be the major regulatory signal (482). (A) At high cellular glucose concentrations, autorepression of the gene encoding TrmBL1 is released, and TrmBL1 is present in high concentrations. High cellular concentrations of TrmBL1 inducers (i.e., maltose and maltotriose) will cause a shift from the tetrameric regulator (inducer sensitive) to the octameric regulator (not responsive to inducers) with high DNA binding affinity. In addition, glucose serves as a corepressor for TrmB, repressing the TM and MD systems. For many promoters tested, cross-regulation was observed for TrmBL1 and TrmB. In general, high cellular glucose concentrations lead to the repression of genes involved in glycolysis and transport (TM and MD systems) and activation of gluconeogenic genes. (B) At low cellular glucose concentrations, TrmBL1 expression is repressed, and low concentrations of the inducers maltose and maltotriose result in the formation of the inducer-responsive tetrameric form of TrmBL1 with a low DNA binding capacity. TrmB repression of the MD system is relieved by maltotriose, maltodextrin, or sucrose (maltose serves as a corepressor), and that of the TM system is relieved by trehalose and maltose, thus enhancing sugar uptake. Therefore, at low cellular glucose concentrations, expression of genes involved in transport (TM and MD systems) and glycolytic genes will be stimulated, whereas the expression of genes involved in gluconeogenic genes will be reduced.

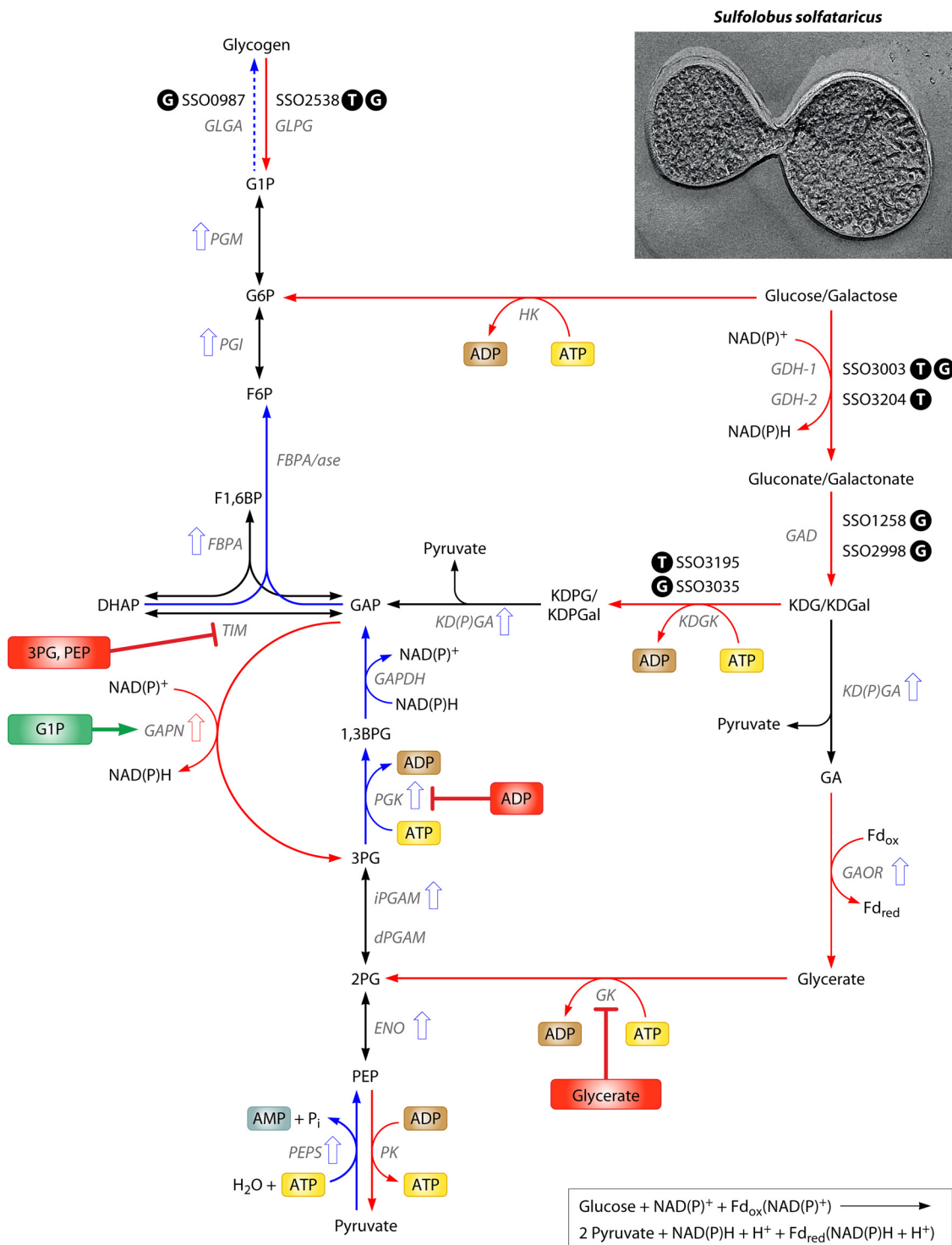


FIG 24 Glycolysis and gluconeogenesis in the aerobic thermoacidophile *Sulfolobus solfataricus*. *Sul. solfataricus* utilizes the branched ED pathway for D-glucose and D-galactose degradation. Gluconeogenesis proceeds via the EMP pathway; for functional glycolysis, only PFK is missing. The ED pathway is characterized by promiscuous enzymes for glucose and galactose degradation up to the level of aldol cleavage. The spED branch is characterized by KDGK, glycolytic, allosterically regulated GAPN, and glycolytic PK, and the npED branch is characterized by GK, which shows substrate inhibition. For gluconeogenesis, the EMP pathway utilizes PEPS, the PGK/GAPDH enzyme couple, as well as FBPA/ase, with PGK and TIM being allosterically regulated. Enzyme reactions with catabolic function are indicated by red arrows, anabolic reactions are indicated by blue arrows, and reversible reactions are indicated by black arrows. Effectors are given in green and red boxes for activators and inhibitors, respectively. Enzymes identified as phosphoproteins under glycolytic (glucose) or gluconeogenic (tryptone) growth conditions are marked by black dots, with T for tryptone and G for glucose (439). Enzymes that were upregulated (>1.5-fold) at the protein level in response to glucose or complex medium (tryptone and yeast extract) are marked with red and blue open arrows, respectively (505). The net equation of glucose conversion to pyruvate via the branched ED pathway is depicted in the box (GLGA, glycogen synthase; GLPG, glycogen phosphorylase; AMYA, α -amylase; PGM, phosphoglucomutase). (Electron micrograph courtesy of Sonja-Verena Albers, Max Planck Institute, Marburg, Germany, reproduced with permission.)

ferredoxin oxidoreductase to acetyl-CoA (473, 495), which enters the oxidative CAC, forming precursor molecules for anabolism as well as CO₂. Reducing equivalents are transferred to a branched electron transfer chain (3 terminal oxidases), with O₂ as the terminal electron acceptor (aerobic respiration) (496, 497). ATP generation proceeds via the archaeal membrane-bound A_iA_o-ATPase (498).

Sugar transport. Studies of sugar transport in *Sul. solfataricus* revealed the predominant utilization of binding protein-dependent ABC transporters (499, 500). Biochemical studies demonstrated the presence of five distinct sugar binding proteins for (i) arabinose/fructose/xylose, (ii) glucose/galactose/mannose, (iii) cellobiose and higher derivatives, (iv) maltose/maltodextrins, and (v) trehalose. Intriguingly, the identified binding proteins are members of two distinct families: monosaccharide transporters and oligopeptide/dipeptide transporters (500). A recent genetic study of celldextrin hydrolysis and transport in a derivative of *Sul. solfataricus* strain 98/2 indicated that the homolog of the maltose transporter (binding protein SSO3053) of strain P2 is required for translocation of celldextrins comprised of three to eight glucose units (G3 to G8) as well as maltose and, to a limited extent, glucose (501). The previously identified glucose transporter (binding protein SSO2847) was not required for glucose transport in this strain, as demonstrated by the unchanged growth of the deletion strain on glucose. If these differences are due to the two strains used in these studies or if there are two glucose transporters that respond to different glucose concentrations remains to be elucidated.

Sugar metabolism. *Sul. solfataricus* and *Sul. acidocaldarius* degrade glucose to 100% via the archaeal-type/modified branched ED pathway, as demonstrated by using ¹³C NMR studies (40) (Fig. 24). Notably, for a functional glycolytic EMP pathway in *Sul. solfataricus*, only phosphofructokinase is missing (32). The central carbohydrate metabolism of *Sul. solfataricus* has been studied in considerable detail by the use of transcriptomic, proteomic, and in-depth biochemical studies. Later, *Sul. solfataricus* was established as a systems biology organism; a genome-scale model was established; and flux balance analysis (FBA) in response to different carbon sources was performed (303, 399).

(i) **The promiscuous branched ED pathway.** In *Sul. solfataricus*, the branched ED variant was shown to be promiscuous, representing an equivalent route for glucose and galactose degradation (255, 257, 290). This pathway promiscuity is established by (i) glucose dehydrogenase isoenzyme 1 (SsoGDH-1) (257, 269), which is active on D-glucose as well as D-galactose; (ii) gluconate dehydratase (GAD), which is active on D-gluconate as well as D-galactonate (290); and (iii) KD(P)G aldolase [KD(P)GA], which catalyzes the cleavage of KDG and KDGal as well as their phosphorylated counterparts KDPG and KDPGal, both yielding GA/pyruvate and GAP/pyruvate, respectively (173, 255, 257). In addition to hexose degradation for SsoGDH-1 and SsoKD(P)GA, a major role of both enzymes in pentose degradation has been suggested (291).

In the common shunt of the ED pathway in *Sul. solfataricus*, the oxidation of D-glucose to D-gluconate is catalyzed by two isoenzymes, SsoGDH-1 (SSO3003) and SsoGDH-2 (SSO3204), which differ in substrate specificity. Biochemical studies indicate that SsoGDH-1 exhibits a dual cosubstrate specificity [NAD(P)⁺] and broad substrate specificity. The highest catalytic efficiency was observed for D-xylose followed by D-galactose, L-arabinose, and D-

glucose. Notably, activity with L-arabinose was observed only in the presence of NADP⁺ (257, 262, 269, 352). In contrast, SsoGDH-2 is specific for D-glucose, and NADP⁺ is the preferred cosubstrate (259). The enzyme exhibited a 27-fold-higher affinity for D-glucose and a 3-fold-increased catalytic efficiency in the presence of NADP⁺ compared to SsoGDH-1. It has been speculated that SsoGDH-1 is involved in different sugar degradation pathways in hexose and pentose metabolism and might thus act as a standby enzyme allowing quick adaptation to different carbon sources and, thus, fine-tuning of metabolism, whereas SsoGDH-2 might function as a sugar- and pathway-specific dehydrogenase in D-glucose degradation (259).

Gluconate dehydratase catalyzes the dehydration of D-gluconate or D-galactonate, forming KDG/KDGal, the characteristic intermediate of the archaeal modified ED pathway (289, 290, 502).

KD(P)G aldolase is one of the key enzymes in the branched ED pathway, which catalyzes aldol cleavage of KDPG/KDPGal and KDG/KDGal in the spED as well as the npED branch, respectively. The enzyme possesses broad substrate specificity and, beside pyruvate, uses GAP, GA, and glycolaldehyde in the direction of aldol condensation (255, 257, 291). In addition, the enzyme was shown to lack facial selectivity, and the two diastereomers D-KDG and D-KDGal are formed from D-pyruvate and D-glyceraldehyde (257, 296). As discussed above for GDH-1, the involvement of KD(P)G aldolase in multiple sugar degradation pathways (D-glucose, D-xylose, and L-arabinose) has been proposed (291) (see also the section on pentose metabolism, above). A detailed characterization of the glycolytic (aldol cleavage) direction revealed a significantly improved catalytic efficiency for the phosphorylated compounds KDPG (585-fold) and KDPGal (296-fold) compared to KDG and KDGal, respectively (255). In addition, the affinities of KDG kinase, the key enzyme of the spED branch, for KDG and, to a lesser extent, for KDGal are significantly higher than those of KD(P)G aldolase [K_m , KDG values of 3.6 and 25.7 mM and K_m , KDGal values of 8.1 and 9.9 mM, for KDGK and KD(P)G aldolase, respectively, at 60°C] (255). Therefore, it was suggested that at least under conditions where the energy charge of the cell is high (K_m , ATP of 2.8 mM for KDGK at 60°C), the spED branch is preferred (255, 256).

In the spED branch, GAP is further converted via GAPN, which is active, in addition to the anabolic enzyme couple GAPDH/PGK. A homolog of ferredoxin-dependent GAPOR is missing in *Sul. solfataricus*. GAPN of *Sul. solfataricus* prefers NADP⁺ as a cosubstrate and, like all other so-far-characterized archaeal GAPNs, exhibits allosteric properties (153, 338). The enzyme is activated by G1P, the product of glycogen phosphorylase-mediated glycogen degradation, which serves as a storage compound in *Sulfolobus* spp. Other reported effectors of *Tpt. tenax* GAPN (i.e., F6P, AMP, and ADP) had only a minor influence (172, 174). The GAPN reaction product 3PG is further metabolized to pyruvate via the common lower shunt of the EMP pathway via PGAM, ENO, and PK.

In the npED branch, GA formed by the KD(P)G aldolase reaction seems to be further oxidized to glyceraldehyde via a ferredoxin-independent aldehyde oxidoreductase, as reported for *Sul. acidocaldarius* (171). There is no evidence for GADH activity in *Sul. solfataricus*, as described for *Tpl. acidophilum* and *Pic. torridus* (248). Glyceraldehyde dehydrogenases are members of the aldehyde dehydrogenase superfamily, like the previously characterized GAPN (SSO3194) (153) and α -KGSADH (2,5-dioxopentanoate dehydrogenase; SSO3117) (283) of *Sul. solfataricus*. A

detailed enzymatic analysis of the three so-far-uncharacterized members of the aldehyde dehydrogenase superfamily from *Sul. solfataricus* (305) combined with phylogenetic analysis confirmed the absence of a glyceraldehyde dehydrogenase, at least of this enzyme family, in *Sul. solfataricus*. Furthermore, the three genes encoding the three subunits of GAOR were identified in the *Sul. solfataricus* genome (SSO2636, SSO2637, and SSO2639) (30, 32, 291). The key enzyme of the npED pathway is glycerate kinase (class II), which catalyzes the phosphorylation of glycerate, forming 2-phosphoglycerate with ATP as the phosphoryl donor. The *Sul. solfataricus* enzyme showed substrate inhibition at low glycerate concentrations as well as positive cooperativity for glycerate and ATP (256). The 2PG formed in the GK reaction is then converted to pyruvate via ENO and PK.

(ii) Significance of both ED branches. The first *in vivo* evidence for the function of the two ED branches and the role of glycerate kinase came from a combined enzymatic/genetic approach (256). A KDG kinase deletion strain was constructed in *Sul. solfataricus* PBL2025, which specifically shuts down the spED pathway. No obvious change in growth rate was observed upon glycolytic growth, indicating that the npED branch is able to compensate for the missing spED branch. However, metabolome analyses revealed that intermediates of the npED branch (glycerate, GA, and KDG) are strongly upregulated. This finding, together with the substrate inhibition of GK by glycerate, indicates an *in vivo* function of GK as a throttle valve: In response to increasing glycolytic activity and the concomitant cellular glycerate concentration, the flux through the npED branch is slowed down by GK, and the flux is redirected to the spED branch, via KDGK and KD(P)GA, to GAP, which can then be degraded further to pyruvate or used for biosynthetic purposes. Accordingly, significant (2-to 4-fold) decreases in the cellular concentrations of hexose and pentose phosphates (i.e., glucose 6-phosphate, fructose 6-phosphate, and xylulose 5-phosphate) as well as trehalose were observed in the KDGK deletion strain, indicating that the spED branch might have an important although not essential role in gluconeogenesis. The utilization of the npED branch, which enters the EMP pathway at the level of 2-phosphoglycerate, for gluconeogenesis is energetically disadvantageous/unfavorable, since it requires additional ATP (PGK reaction) and has to deal with the thermal instability of 1,3BPG. However, the fact that no obvious growth phenotype of the KDGK deletion strain was observed indicated that alternative pathways providing hexose phosphates as building blocks for pentoses, glycogen, and trehalose are present. One such pathway might proceed directly from glucose via hexokinase. Hexokinase activity in *Sul. solfataricus* cell extracts was determined (0.0025 U/mg cell extract [80°C] of strain P2) (256). The enzyme of *Sul. tokodaii*, which exhibits broad substrate specificity, was characterized previously, and the crystal structure was solved (ST2354) (67, 341).

As in all other *Archaea* analyzed so far, in *Sulfolobus* spp., pyruvate derived from the branched ED pathway is also further converted to acetyl-CoA via oxidative decarboxylation by pyruvate-ferredoxin oxidoreductase (POR). Acetyl-CoA is completely oxidized to CO₂ via the oxidative CAC under aerobic growth conditions, generating additional reduced electron carriers [NAD(P)H, Fd_{red}, and reduced flavin adenine dinucleotide (FADH₂)] and energy (for literature, see reference 32).

(iii) Gluconeogenesis. For gluconeogenesis, *Sul. solfataricus* utilizes a unidirectional gluconeogenic PEPS that is replaced by

PK in the catabolic direction (T. Kouril, P. Haferkamp, B. Tjaden, and B. Siebers, unpublished data). Also, in *Sul. solfataricus* as well as *Sul. tokodaii*, as reported for other hyperthermophiles, the GAPDH/PGK couple exhibits an exclusively gluconeogenic function and counteracts glycolytic GAPN (153, 176, 193, 195, 338, 503). In *Sul. solfataricus*, GAPDH is characterized by much higher affinities for its gluconeogenic (K_m values of 0.00041 mM [1,3BPG] and 0.074 mM [NADPH]) than for its glycolytic (K_m values of 0.838 mM [GAP], 0.271 mM [NADP⁺], and 408.5 mM [P_i]) substrates, and cooperativity for its glycolytic substrates was observed. Especially, the low affinity for phosphate dramatically limits the glycolytic function of the enzyme under physiological conditions (338). For the reversible PGK, the glycolytic reaction seems to be preferred with respect to the cosubstrate affinities (K_m values of 0.54 mM [3PG], 9.68 mM [ATP], 5.59 mM [1,3BPG], and 0.085 mM [ADP]), although the strong inhibition of both the glycolytic as well as gluconeogenic reactions at higher ADP concentrations (K_i of 1.14 mM [ADP]) suggests strong regulation by the energy charge of the cell (338). TIM of *Sul. solfataricus* might be regarded as a gluconeogenic enzyme, since it directs fluxes toward anabolic processes (e.g., synthesis of glycerol 3-phosphate [for lipids], pentoses, or glycogen). The enzyme showed a slight preference for the gluconeogenic direction (K_m values of 0.245 mM [GAP] and 0.812 mM [DHAP]), and competitive inhibition with 3PG (K_i , 0.4 mM) and PEP (K_i , 0.661 mM) was observed (338). F6P synthesis proceeds via the unidirectional bifunctional anabolic FBPA/ase (337, 338). The enzyme catalyzes the unidirectional conversion of GAP and DHAP or F1,6BP to F6P. In addition, a gene encoding a so-far-uncharacterized member of the reversible archaeal-type class I FBPA family was identified in the *Sul. solfataricus* genome; however, the enzymatic function still has to be confirmed (32).

Energetics. The utilization of the modified ED pathway with glycolytic GAPN substituting for gluconeogenic GAPDH and PGK in the spED branch results in no net energy gain of both ED branches. In the spED branch, 1 ATP is required for KDG, and in the npED branch, 1 ATP is required for glycerate phosphorylation. The KD(P)G aldolase reaction directly releases 1 molecule of pyruvate, and therefore, only 1 ATP is generated in both branches by the pyruvate kinase reaction. In addition, at least 1 ATP is required for glucose uptake via the ABC transporter (499, 500). Therefore, as in most aerobes, the major source of energy in *Sul. solfataricus* seems to be aerobic respiration via its branched electron transport chain (496, 497) and membrane-bound A₁A_o-ATPase (498). There is evidence that *Sul. solfataricus*, like other thermoacidophiles, possesses a rather low membrane potential (ca. 30 mV) and that mainly the large pH gradient across the membrane (ΔpH) (pH inside, 6.5; pH outside, 2 to 4) maintains the proton motive force. This strict correlation of proton motive force and cellular ATP levels was demonstrated by the use of protonophores, which immediately inhibited ATP synthesis (504; for a review, see reference 496).

Regulation. *Sul. solfataricus* utilizes only the branched ED pathway for glycolysis and the EMP pathway for gluconeogenesis (missing PFK). As in other *Archaea*, the classical control points in *Bacteria* and *Eukarya* at the beginning of the EMP pathway with HK/GK and PFK are missing.

(i) Regulation at the enzyme level by allosteric effectors. As in other (hyper)thermophiles with growth at temperatures close to 80°C, GAPN in the spED branch is so far the only known alloster-

ically regulated enzyme in *Sul. solfataricus* (153, 338). The NADP⁺-dependent *Sul. solfataricus* enzyme is highly activated by G1P (14-fold activation at 0.1 mM G1P), an intermediate in glycogen metabolism and polymer degradation. Other metabolites tested showed only minor (1.1- to 1.3-fold) stimulatory (F6P, AMP, and pyruvate) or inhibitory (ATP, gluconate, and galactonate) effects. No effect was observed with glyceraldehyde and ADP (153). The strong activation at low G1P concentrations suggests that the enzyme is easily activated under physiological conditions in order to drive carbon flux via the catabolic spED branch. The enzyme couple GAPDH/PGK possesses gluconeogenic function (see above). PGK, as predicted by blueprint modeling, is regulated by the energy charge of cell. The enzyme is active only in the gluconeogenic direction at high ATP concentrations, and increasing ADP concentrations (K_i of ADP of 1.14 mM) inhibits the enzyme in both the glycolytic and gluconeogenic directions (338). Thus, in conjunction with the results obtained from a detailed kinetic model, which points to 50% carbon loss through 1,3BPG instability, the regulation of PGK by a low energy charge of the cell, the redirection of carbon flux in the glycolytic direction by activation of GAPN via G1P, and the anabolic function of GAPDH seems to be a unique metabolic adaptation strategy for life at high temperatures in order to circumvent energy and maybe carbon loss due to thermal instability of the intermediates (338, 441). The rationale behind the allosteric regulation of TIM by 3PG and PEP still remains to be elucidated; the enzyme in *Sul. solfataricus* possesses a gluconeogenic/anabolic function, and therefore, the inhibition by early intermediates of gluconeogenesis seems to be inconsistent (338). TIM activity is dramatically high compared to those of other glycolytic/gluconeogenic enzymes, and inhibition might allow a reduction of velocity to levels comparable to those of the other enzymes. Studies on regulation at the level of PEP-pyruvate interconversion by gluconeogenic PEPS and glycolytic PK are under way (Kouril et al., unpublished).

Knowledge of the regulation of the ED pathway is rather scarce, and no allosteric effectors have been reported for the ED-specific enzymes. Kinetic analyses of KD(P)GA and KDGK (see above) indicate that the spED branch is preferred, although it is not essential for growth on glucose. Further on, as also discussed above, the strong inhibition of GK by its substrate glycerate ($K_i = 1$ mM) seems to perform an important physiological role as a throttle valve in order to control fluxes via the two ED branches and suggests an additional gluconeogenic function of the spED branch (256, 441).

(ii) **Regulation at the translational level.** Evidence for regulation by the change of protein synthesis comes from a combined microarray/proteomics study, which was performed for *Sul. solfataricus* P2 cells grown on D-glucose (glycolytic) (defined medium) and yeast extract-tryptone (YT) (complex medium) as the sole carbon source (505; for a recent review, see reference 506). Whereas minor regulation was observed at the gene level (see below), significant upregulation at the protein level (>1.5-fold) was observed for KD(P)GA (SSO3197), AOR (SSO2639, SSO2636, and SSO2637), iPGAM (SSO0417), ENO (SSO0913), PEPS (SSO0883), PGK (SSO0527), FBPA/ase (SSO3226), PGI (SSO2281), and PGM (SSO0207) in complex medium. The upregulation of most enzymes seems to be reasonable in order to drive carbon flux in the gluconeogenic direction. However, the increased level of KD(P)G aldolase synthesis is surprising and might be explained by the utilization of complex medium (i.e., the

presence of complex carbon sources in yeast extract). For GAPN (SSO3194), significant upregulation was observed in the presence of glucose, highlighting its solely glycolytic function. Notably, the highest upregulation (~4.4-fold upregulated [YT plus glucose]) was observed for AOR in response to complex medium. As outlined above, the enzyme is proposed to catalyze the oxidation of GA to glycerate in the npED pathway of *Sul. solfataricus* (171). The physiological relevance is unclear and remains to be elucidated.

(iii) **Regulation at the posttranslational level by protein phosphorylation.** From a study by Snijders et al. (505) based on ¹⁵N labeling, protein separation by two-dimensional gel electrophoresis (2DE), and spot identification via liquid chromatography-tandem mass spectrometry (LC-MS/MS), with the identification of multiple spots for one protein, there was first evidence for the important function of the modulation of enzyme activity by post-translational modifications in *Sul. solfataricus*. Later, the phosphoproteome of *Sul. solfataricus* P2 in response to different carbon sources (glucose versus tryptone) was investigated by using the gel- and enrichment-free PACIFIC approach, revealing an unexpectedly large number of phosphoproteins (540 phosphoproteins) (439). Furthermore, the identified percent pS/T/Y ratio is unique regarding the amount of p-Tyr (54%) compared to those reported for other phosphoproteome studies (1 to 10%). It was shown that the identified phosphoproteins are located in 21 out of 26 arCOG categories (440), indicating that most of the cellular processes are targeted by protein phosphorylation. In response to the offered carbon source, significant changes in the complex phosphorylation pattern were observed, suggesting an important physiological function of reversible protein phosphorylation in the control of central carbohydrate metabolism.

In general, enzymes at the beginning of sugar (hexose and pentose) degradation pathways (i.e., dehydrogenases and dehydratases), gluconeogenesis (PEP carboxykinase [GTP] and malic enzyme), the RuMP pathway (i.e., 3-hexulose-6-phosphate isomerase), glycogen metabolism (i.e., glycogen phosphorylase and glycogen synthase), and trehalose synthesis via the TreY-TreZ pathway (i.e., maltooligosyltrehalose synthase and maltooligosyltrehalose hydrolase) were targeted by reversible protein phosphorylation. Further on, enzymes at branch points such as those between the npED and the spED branches (i.e., KDG kinase and the predicted KDG aldolase) as well as between the CAC and the glyoxylate bypass (i.e., IDH) were detected as p-proteins, suggesting a tight regulation of pathways with respect to different carbon sources and utilization of different branches. The observed significant changes in the phosphorylation pattern in response to the carbon source suggest that sugar degradation pathways are blocked in the presence of tryptone, whereas gluconeogenic enzymes are activated.

Notably, both GDHs have been identified as targets of reversible protein phosphorylation; however, whereas SsoGDH-1 (SSO3003) was found to be phosphorylated in peptide- and glucose-grown cells, SsoGDH-2 (SSO3204) was phosphorylated only in peptide-grown cells (439). The physiological relevance of these results is still unclear, but it has been speculated that SsoGDH-1 is involved in different sugar degradation pathways, whereas SsoGDH-2 might function as a sugar- and pathway-specific dehydrogenase in glucose degradation. Also, KDG kinase (SSO3195), the key enzyme of the spED pathway, was found to be phosphorylated only in tryptone-grown cells, and due to its glycolytic function, an inhibitory effect was suggested (439). Interestingly, phos-

phorylation of KDG kinase, although of another enzyme family, was also demonstrated for the KDG kinase of *Tpl. acidophilum* (293). Although not detected in this study, the only well-established example for regulation of a CCM enzyme by reversible protein phosphorylation in *Sul. solfataricus* is GAD (SSO3198); only phosphorylated GAD was shown to be active (289). The previously reported phosphorylation of iPGAM (SSO0417) (215) on the catalytically important residue Ser59 seems rather to represent a phosphoenzyme intermediate trapped in its catalytic mechanism. Therefore, as outlined above, although numerous phosphoproteins have now been identified in *Sul. solfataricus*, information about the impact of protein phosphorylation on target enzymes and, thus, regulatory function is still rather scarce. Furthermore, the respective protein kinases and phosphatases involved in the respective signal transduction pathways remain to be elucidated. However, the observed complex changes of the phosphorylation pattern in response to the carbon source suggest that reversible protein phosphorylation plays a major role in CCM regulation in *Sul. solfataricus*.

(iv) Regulation at the gene/transcript level. The first evidence for the presence of a branched ED pathway came from the conserved gene organization of ED genes in several *Archaea* (i.e., *Sul. solfataricus*, *Sul. acidocaldarius*, *Sul. tokodaii*, *Tpt. tenax*, and *Hablobacterium* sp.) (153, 173). In *Sul. solfataricus*, the genes encoding gluconate dehydratase, KD(P)G aldolase, and KDG kinase are organized in an operon, and the gene encoding GAPN is located downstream (*gad-kdgA-kdgK* operon; *gapN* gene). Primer extension analysis of RNA samples from cells grown on different carbon sources (i.e., D-glucose, D-arabinose, and tryptone) revealed constitutive expression of the ED operon and the *gapN* gene as well as independent transcription of the *gapN* gene by a separate promoter (153).

Further information for changes at the transcript level in *Sul. solfataricus* in response to the carbon source (D-glucose versus yeast extract and tryptone) came from a combined microarray/proteomics study (505). Intriguingly, although significant regulation was observed at the protein level (see above), only minor changes were observed at the transcript level for CCM genes, pointing to an important role of posttranscriptional and translational modifications. In total, 184 genes were found to be differentially expressed in response to the carbon source; however, most significant changes were observed for genes encoding enzymes involved in amino acid metabolism and transport. No significant changes were observed for CCM genes encoding enzymes of the ED and EMP pathways, the CAC, the glyoxylate shunt, and C₃/C₄ conversions.

Transcriptional regulators of the central carbohydrate metabolism. In *Sul. solfataricus*, several transcriptional regulators have been studied, many of the Lrp (leucine-responsive regulatory protein)/Lrp-like family conserved among *Bacteria* and *Archaea* (for a review, see reference 507). Lrp-like regulators have a divergent function and may act as a repressor or activator, targeting specific genes or complex regulons (feast/famine regulatory proteins). For SsoLrpB, a function in the regulation of genes involved in central carbohydrate metabolism was demonstrated. First, autoregulation of LrpB by binding to the control region of its own gene (508) and, later on, binding to promoter regions of adjacent genes encoding two putative permeases (SSO2126/SSO2127) as well as the first gene (*porD*) of the *porDAB* operon, encoding pyruvate-ferredoxin oxidoreductase, were demonstrated (509). A mutant strain (PBL2025 [510]) lacking LrpB was generated but

showed no effect during growth with tryptone or glucose (509). However, qRT-PCR confirmed that the transcript levels of the putative permeases and the *por* operon were reduced compared to those in wild-type cells, demonstrating a role as an activator (509). Later, in *Sul. solfataricus*, the role of LysM as a positive regulator of an operon encoding enzymes involved in lysine biosynthesis (511) as well as of Lrs14 in regulation of an alcohol dehydrogenase (SSO1108) (i.e., downregulation during the early growth phase) was reported (512–514). Therefore, Lrp-like proteins in *Sul. solfataricus* and *Archaea* in general seem to have an important function as global regulators in central metabolism as well as amino acid metabolism, whereas the role in *Bacteria* is restricted to regulation of genes involved in amino acid metabolism (509).

As in many *Bacteria* and *Eukarya* that utilize multiple carbon sources, a carbon catabolite repression (CCR)-like system has been reported for *Sul. solfataricus*. The system was shown to control the expression of glycosyl hydrolases, i.e., α -amylase (AmyA), α -glucosidase (MalA), and β -glycosidase (LacS), in *Sul. solfataricus* at the transcript level (515–520). Control was shown to be exerted on the one hand via the carbon composition of the medium (519) and on the other hand via the *car* (catabolite repression) gene locus (517, 520). Full expression of genes encoding glycosyl hydrolases was observed in growth medium with sucrose as the sole carbon and energy source, and expression was strongly repressed in the presence of yeast extract, with aspartate and asparagine being the most effective components. In an earlier study, expression of α -amylase (AmyA), which hydrolyzes starch, dextrins, and cyclodextrins, was shown to be inhibited by the addition of glucose to the growth medium (517). The strongest inhibitory effect on *amyA* transcription was observed upon addition of aspartate, whereas glutamate relieved repression (517). Disruption of α -amylase of *Sul. solfataricus* leads to the inability to grow on starch, glycogen, or pullulan as the carbon source, whereas growth was not affected with glucose as the sole carbon source (521). The expression of *lacS* and *amyA* but not *malA* was reduced by spontaneous mutations in the *car* gene locus, and it was suggested by the authors of that study that *car* might encode or modulate a positively *trans*-acting factor that regulates the expression of *lacS* and other genes (515, 520). In 2006, studies by Lubelska and colleagues on the arabinose transporter further supported the assumption of a CCR-like system in *Sul. solfataricus* (522). The arabinose transport operon (*araSTUV*) comprises four genes, encoding the substrate binding protein (AraS), two permeases (AraT and AraU), and one ATPase (AraV). The expression of the transporter was dependent on arabinose in the growth medium, and transcription was downregulated in the presence of glucose. Further on, some amino acids (alanine, aspartate, asparagine, cysteine, leucine, threonine, tyrosine, and valine) affected expression of the ATPase (522). The promoter of the *araS* gene of *Sul. solfataricus* was used for the construction of arabinose-inducible plasmids for overexpression of proteins in *Sul. islandicus* (523).

In contrast to *S. solfataricus*, a CCR-like system seems to be absent in *Sul. acidocaldarius*. It was reported that *Sul. acidocaldarius* metabolized xylose, glucose, and arabinose simultaneously without exhibiting any carbon source preference. Interestingly, transcription patterns greatly differed between D-glucose- and D-xylose-grown cells, whereas cells grown on both carbon sources were more comparable with D-xylose-grown cells (524).

Thermoplasmatales (*Thermoplasma acidophilum* and *Picrophilus torridus*)

Growth conditions. *Tpl. acidophilum* and *Pic. torridus* are members of the *Thermoplasmatales* within the *Euryarchaeota*, and unique to this order, they possess no cell wall but a unique membrane made of lipoglycan. *Tpl. acidophilum* was isolated from a self-heated coal refuse pile, and a relationship to *Mycoplasma* was proposed (525, 526). *Pic. torridus* was first isolated from a dry solfataric field with extremely acidic soil (pH < 0.5) in northern Japan (527, 528). The two thermoacidophiles display heterotrophic growth, preferably on peptides and polymeric sugars. Growth on glucose (and also lactose in *Pic. torridus*) is observed only in the presence of yeast extract (525, 528, 529). Whereas *Pic. torridus* is obligately aerobic (O₂), *Tpl. acidophilum* is facultatively anaerobic with either O₂ or S⁰ (sulfur respiration) as the terminal electron acceptor. *Pic. torridus* is one of the most extreme acidophiles (hyperacidophile), with optimal growth at pH 0.7 (pH range, 0 to 3.5) and 60°C (temperature range, 45°C to 65°C). *Tpl. acidophilum* thrives at similar temperatures (45°C to 63°C; optimal temperature, 59°C) but at higher pH values (optimum, pH 2; pH range, 0 to 3.5). The complete genome sequences of *Pic. torridus* (530) and *Tpl. acidophilum* strain DSM1728 (531) have been deciphered.

Sugar (glucose) metabolism. *Tpl. acidophilum* and *Pic. torridus*, like the aerobe *Sul. solfataricus*, degrade glucose exclusively via the modified ED pathway, as demonstrated by ¹³C NMR analysis (209). However, the utilization of a unique nonphosphorylative or the branched pathway is still a matter of debate, and the ¹³C NMR studies performed do not allow differentiation between the two ED branches (32, 173, 209).

The enzymes of the upper common part of the ED pathway have been characterized in *Pic. torridus* (209) and *Tpl. acidophilum* and revealed, similarly to *Sul. solfataricus*, promiscuous enzymes for D-glucose and D-galactose utilization (209). However, in *Pic. torridus*, besides glucose/galactose dehydrogenase (261) and gluconate/galactonate dehydratase, only a KDG/KDGal-specific aldolase (Pto1279) was reported (209). The enzyme possesses only remote activity with the phosphorylated substrate KDPG (2,225-fold-lower catalytic efficiency than KDG; 371-fold for the recombinant enzyme), and therefore, the presence of a strictly nonphosphorylative ED pathway was suggested. This was also confirmed by using cell extracts of *Pic. torridus* and *Tpl. acidophilum*, where KDG was converted at 25-fold- and 130-fold-higher rates, respectively, than KDPG, whereas in *Sul. acidocaldarius*, which harbors a branched ED pathway, KDG and KDPG were converted at similar rates (209). Despite the unique KDG aldolase, the npED pathway in *Pic. torridus* and *Tpl. acidophilum* is characterized by an NADP⁺-specific GADH (248, 304), a member of the aldehyde dehydrogenase superfamily that is replaced by a ferredoxin-dependent aldehyde oxidoreductase in *Sulfolobus* spp. (171, 305). All enzyme activities of the npED pathway were determined by using cell extracts of *Pic. torridus* (209). In accordance with the thermophilic, aerobic (for *Pic. torridus*, facultative anaerobic) life-style at temperatures of around 60°C, no GAPN or GAPOR homologs, which are found mainly in hyperthermophiles and anaerobes, were identified in *Tpl. acidophilum* and *Pic. torridus* (209, 248, 304, 305).

Intriguingly, a KDG kinase, the key enzyme of the spED branch, from *Tpl. acidophilum* was characterized (Ta0122 [293]),

and additional, so-far-uncharacterized homologs of KDG aldolase with 39 to 40% identity to the KD(P)G aldolase of *Sul. solfataricus* were identified in the genomes of *Pic. torridus* (Pto1026) and *Tpl. acidophilum* (Ta0619) (32, 209). The KDG kinase of *Tpl. acidophilum* is a member of a new enzyme family (BadF/BadG/BcrA/BcrD ATPase family; Pfam01869), is highly specific for KDG, and shows no similarity to the KDG kinase of *Sul. solfataricus*, which belongs to the PFK-B family (see above). Genes encoding homologs of the *Tpl. acidophilum* enzyme are found in all available genomes of *Thermoplasmatales*, with two homologs in *Pic. torridus* (Pto0011 [39% identity] and Pto1094 [33% identity]) (32, 293). As expected for aerobic organisms, the *Thermoplasmatales* also oxidize pyruvate to acetyl-CoA by means of pyruvate:ferredoxin oxidoreductase, which is further completely oxidized to CO₂ via the CAC (32, 33, 532).

Energetics. As in *Sul. solfataricus*, the utilization of the npED pathway results in no net ATP gain. The utilization of a glycolytic spED branch, which is still under debate, in the absence of GAPN and GAPOR with a glycolytic active GAPDH/PGK couple might provide 1 mol ATP per mol glucose.

First insights into regulation at the protein and gene levels. The first evidence for a possible function of protein phosphorylation comes from the work of Jung and Lee (293). KDG kinase, the key enzyme of the predicted spED branch in *Tpl. acidophilum*, was shown to be inactivated upon incubation in the presence of potato acid phosphatase and bacterial alkaline phosphatase. Therefore, those authors suggest that the enzyme is targeted by regulatory protein phosphorylation, with active phosphoprotein being inactivated by dephosphorylation. Notably, the KDG kinase of *Sul. solfataricus*, although of another enzyme family, was also found to be phosphorylated in tryptone-grown cells, and an inhibitory effect due to its glycolytic function was suggested (439).

Further evidence for the use of the branched rather than the npED pathway comes from a combined transcriptome-proteome study of *Tpl. acidophilum*, which revealed significant changes (~30%) at both the mRNA and protein levels in response to aerobic and anaerobic growth conditions with S⁰ as the terminal electron acceptor (533). In accordance with other analyses, only a weak overlap between mRNA and protein level changes was observed (correlation, 0.57), highlighting the significance of post-transcriptional modifications. Remarkably, a significant (3-fold) upregulation of enzymes of the npED branch {except for Ta0619 [KD(P)G aldolase candidate] and Ta0453m (glycerate kinase)}, the lower common EMP shunt, as well as the CAC was observed at the protein level in response to anaerobiosis. In contrast to the significant changes in glucose metabolism at the protein level, the corresponding transcript levels revealed only slight changes, if any. The authors of that study suggest that posttranscriptional regulation of glycolysis plays a major role in enhancing glycolytic flux in order to compensate for the low ATP yield under conditions of anaerobic sulfur respiration compared to aerobic respiration ($\Delta G^{\circ'} = -2,844$ kJ for aerobic respiration with O₂ as the terminal electron acceptor; $\Delta G^{\circ'} = -333$ kJ for anaerobic sulfur respiration with S⁰ as the terminal electron acceptor). However, those authors did not take the spED branch [KDG kinase and KD(P)G aldolase] into account, but this would nicely explain the observed upregulation of enzymes of the lower EMP shunt, particularly of GAP-oxidizing enzymes. The enzymes of the upper EMP branch for C₆ conversion remained unchanged, and the use

of alternative pathways for C₆ carbon conversion via the EMP pathway was suggested. However, for final discussion, the respective enzyme studies are awaited (533).

Thermoproteus tenax

Growth conditions. *Tpt. tenax* is a member of the *Thermoproteales* within the *Crenarchaeota*. The obligate anaerobic, hyperthermophile *Tpt. tenax* (Kra1) was isolated from a terrestrial solfatara in Iceland (Krafla region). The organism grows optimally at 86°C at pH 5.6 and is sulfur dependent; elemental sulfur serves as the terminal electron acceptor, forming H₂S (sulfur respiration). Notably, *Tpt. tenax* is a facultative heterotroph, and besides chemolithoautotrophic growth (CO₂/H₂), chemoorganoheterotrophic growth on a variety of mono-, di-, and polysaccharides; organic acids; and alcohols (e.g., glucose, malate, amylase, starch, glycerate, malate, methanol, or ethanol) was reported (534, 535). Less efficient growth on propionate as well as Casamino Acids has been reported. No fermentative growth was observed, and the universal terminal electron acceptor is elemental sulfur; however, polysulfides and thiosulfate are also utilized (534).

Whereas the pathways for glucose degradation as well as gluconeogenesis have been studied in detail at the enzyme and transcript levels, information on CO₂ fixation and respiration is based mostly on the available genome sequence information (84, 418). Genome sequence analysis suggests that two pathways, the reductive CAC and/or the dicarboxylate/4-hydroxybutyrate cycle, might be involved in CO₂ fixation (84, 321, 418, 536).

Tpt. tenax gains energy under autotrophic growth conditions by anaerobic hydrogen oxidation with sulfur as the terminal electron acceptor (hydrogen-sulfur autotrophy). A short electron transport chain via a single iron-nickel hydrogenase and two sulfur reductases, probably mediated by quinones, has been proposed (418). Under heterotrophic growth conditions, glucose was shown to be completely oxidized to CO₂ via the oxidative CAC (158). Energy conservation seems to proceed via a membrane-bound electron transport chain, and sulfur has been suggested as the final acceptor (sulfur respiration) (418). The respective genes encoding NADH:quinone oxidoreductase (complex I), succinate dehydrogenase (complex II), and the bc₁ complex (complex III) were identified. Only a bona fide terminal oxidase is missing, and therefore, the nature of the terminal electron acceptor still remains elusive. Notably, two copies of complex I were identified, and there is some evidence that NADH and/or reduced ferredoxin might serve as the electron donor. Chemiosmosis in *Tpt. tenax* is mediated via the membrane-bound archaeal A_oA₁-ATP synthase, and the presence of a membrane-bound pyrophosphatase indicates that the hydrolysis of PP_i also contributes, at least partially, to the membrane potential, as demonstrated for the enzyme (V-PPase) of *Pyb. aerophilum*, a close relative of *Tpt. tenax* (418, 537, 538).

Sugar transport. As in other *Archaea*, sugar transport in *Tpt. tenax* seems to be mediated mainly by ABC transporters. Genome analysis revealed the presence of 15 substrate binding proteins, and 4 binding proteins were isolated by concanavalin A (ConA) (lectin) affinity chromatography (418).

Sugar (glucose) metabolism. ¹³C NMR studies ([¹³C]glucose) in *Tpt. tenax* demonstrate that both the modified EMP and the branched ED pathways operate in parallel in *Tpt. tenax* (39, 40; for reviews, see references 31 and 321). The modified EMP pathway represents the main sugar-degrading pathway, converting 85% of glu-

cose. Nevertheless, 15% of glucose is oxidized to pyruvate via the branched ED pathway. *Tpt. tenax* is the only archaeon that has so far been shown to utilize both pathways in parallel (22) (Fig. 25).

(i) The modified EMP pathway. The EMP variant in *Tpt. tenax* operates in both directions and thus represents the major route for glycolysis as well as gluconeogenesis. The pathway in *Tpt. tenax* is characterized by (i) ATP-dependent hexokinase (ROK family), (ii) reversible PP_i-dependent phosphofructokinase, (iii) archaeal-type class I FBPA and FBPA/ase, (iv) three GAP-oxidizing enzymes (GAPDH, GAPN, and GAPOR), and (v) three different enzymes (PEPS, PK, and PPDK) involved in pyruvate/PEP interconversion (for a review, see references 31 and 321).

The first phosphorylation step in the EM variant of *Tpt. tenax* is catalyzed by an ATP-dependent hexokinase (ATP-HK) of the ROK family. The enzyme exhibits broad, hexokinase-like substrate specificity and is active on glucose, fructose, mannose, and 2-deoxyglucose (catalytic efficiency [k_{cat}/K_m] values of 8,179, 1,389, 4,276, and 4,416 mM⁻¹ min⁻¹, respectively) (55). The enzyme revealed no allosteric properties, although inhibition was observed in the presence of G6P, ADP, UDP, AMP, P_i, and PP_i but only at high concentrations (50% inhibition with G6P at >8 mM; UDP, AMP, and P_i at >10 mM; and ADP and PP_i at >1 mM), and therefore, the physiological relevance is still under discussion (55).

The isomerization of G6P to F6P is catalyzed by a bifunctional phosphoglucose isomerase/phosphomannose isomerase (PGI/PMI). Unlike all known PGIs, the enzyme shows similar catalytic efficiencies on G6P and M6P and converts both of them to F6P. The *Tpt. tenax* enzyme has been characterized with respect to G6P conversion and belongs to a new family within the PGI superfamily (83, 84).

The PP_i-dependent phosphofructokinase (PP_i-PFK) catalyzes the reversible phosphorylation of F6P to F1,6BP (F6P + PP_i ↔ F1,6BP + P_i) (107). The enzyme displayed only a slight, if any, preference for the catabolic direction [$V_{max(F6P)} = 2.9$ U/mg protein; $V_{max(F1,6BP)} = 2$ U/mg protein], and similar affinities were observed for PP_i, F6P, and F1,6BP (K_m values of 23, 53, and 33 μM, respectively). Only the affinity toward P_i (K_m value of 1.43 mM) was slightly enhanced, and an adaptation to higher cellular P_i concentrations has been discussed (107). The reversible PP_i-PFK therefore substitutes for the antagonistic enzyme couple ATP-PFK and fructose-1,6-bisphosphatase (FBPase) in *Tpt. tenax*. The enzyme is the only archaeal PP_i-PFK described so far, shows no allosteric properties, and belongs to the PFK-A family, as for the classical ATP-dependent PFKs (107).

As described for *Pyr. furiosus* and *Tco. kodakarensis*, the reversible cleavage of F1,6BP proceeds via the archaeal-type class I FBPA, forming GAP and DHAP (126, 134, 135). The *Tpt. tenax* enzyme uses both F1,6BP and F1P as the substrate, with F1,6BP being the preferred substrate (k_{cat}/K_m values for F1,6BP and F1P of 734.4 and 1.89 mM⁻¹ min⁻¹, respectively). The crystal structure of the *Tpt. tenax* enzyme was solved, revealing some new insights into the basic enzyme mechanism of class I FBP aldolases (134, 135) (see above).

For TIM of *Tpt. tenax*, a preference in the formation of DHAP (anabolic function) was observed (K_m of 0.9 mM and V_{max} of 2,000 U/mg for DHAP; K_m of 0.2 mM and V_{max} of 9,500 U/mg for GAP) (140, 147). The enzyme in solution showed an unusual equilibrium between inactive dimers and active tetramers that was shifted by the specific interaction with glycerol-1-phosphate dehydrogenase toward active tetramers, and a possible physiological

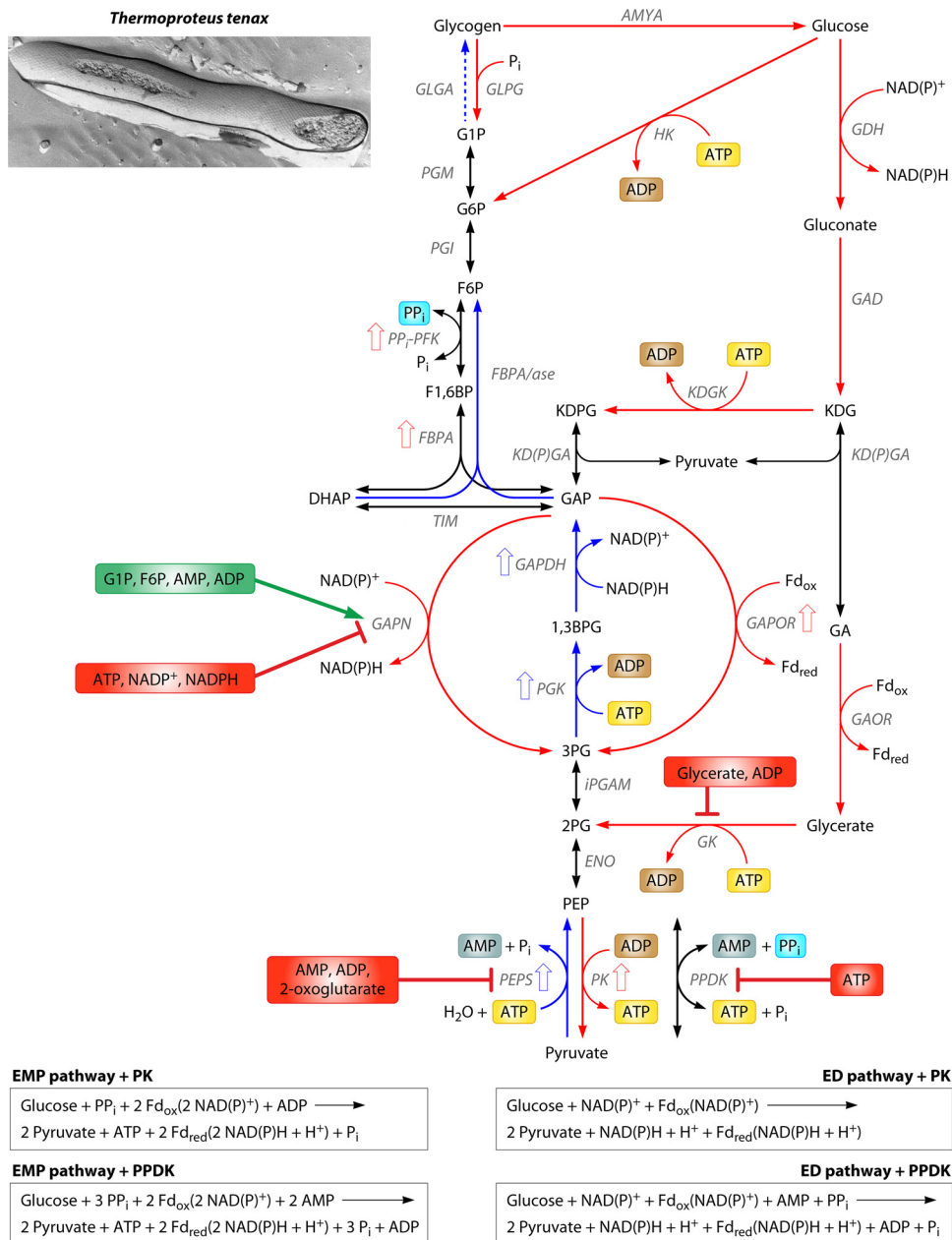


FIG 25 Glycolysis and gluconeogenesis in the anaerobic hyperthermophile *Thermoproteus tenax*. *Tpt. tenax* utilizes both the reversible EMP and branched ED pathways for glycolysis and the EMP pathway for gluconeogenesis. The reversible EMP pathway is characterized by reversible PP_i-PFK, catabolic GAPN and GAPOR, anabolic PGK-GAPDH, catabolic PK, anabolic PEPS, and a reversible PPDK with preferred glycolytic function. Enzyme reactions with catabolic function are indicated by red arrows, anabolic reactions are indicated by blue arrows, and reversible reactions are indicated by black arrows. Effectors are given in green and red boxes for activators and inhibitors, respectively. Enzymes for which the encoding genes were upregulated under heterotrophic/glycolytic (glucose) or autotrophic/gluconeogenic (CO₂/H₂) growth conditions are depicted as open red and blue arrows, respectively (31). The net equations of glucose conversion to pyruvate via the modified EMP pathway and the branched ED pathway are depicted in boxes (GLGA, glycogen synthase; GLPG, glycogen phosphorylase; AMYA, α-amylase; PGM, phosphoglucomutase). (Electron micrograph courtesy of Reinhard Rachel, University of Regensburg, Germany, reproduced with permission.)

function of protein-protein interactions in channeling thermo-labile DHAP toward lipid biosynthesis was discussed (147).

Like *Pyr. furiosus* and *Tco. kodakarensis*, the hyperthermophilic anaerobe *Tpt. tenax* possesses three enzymes involved in GAP conversion: GAPDH, GAPN, and GAPOR. GAPN and GAPDH have been characterized in detail, whereas no biochemical information is available for GAPOR (172, 174, 177, 178, 539).

Studies revealed a gluconeogenic function of the classical reversible GAPDH and a glycolytic function of GAPN (178). Whereas GAPDH exhibits a preferred affinity for its anabolic substrates, glycolytic GAPN of *Tpt. tenax* showed increased affinity (24-fold) and higher activity (2.1-fold) with GAP (*K_m* values and *V_{max}* values with GAP of 20 μM and 36 U/mg for GAPN, respectively, and 45 μM and 17 U/mg for GAPDH, respectively), under-

lining its glycolytic function (172, 174, 178). In addition, TtxGAPN was shown to possess a complex allosteric behavior, which seems to be more sophisticated than that of GAPNs from *Tco. kodakarensis* and *Sul. solfataricus* or *Sul. tokodaii* (153, 175, 176). Also, the interconversion of PEP-pyruvate in *T. tenax* is catalyzed by three different enzymes: PK (235), PEPS, and PPDK (320). Whereas PK and PEPS in *Tpt. tenax* catalyze the unidirectional glycolytic and gluconeogenic reactions, respectively, PPDK catalyzes the reversible interconversion of PEP and pyruvate (pyruvate + ATP + P_i ↔ PEP + AMP + PP_i). Enzymatic characterization of recombinant *Tpt. tenax* PPDK revealed a clear preference for the glycolytic function (2-fold-higher catalytic efficiencies; k_{cat}/K_m values of 141.3 mM⁻¹ min⁻¹ at 70°C for pyruvate and 266 mM⁻¹ min⁻¹ at 55°C for PEP). In addition, PPDK exhibited allosteric properties, and regulation by the energy charge of the cell was reported (320). Like most other archaeal PKs, the *Tpt. tenax* enzyme possesses reduced allosteric properties, and no regulation by effectors (i.e., FBP, AMP, G1P, G6P, ribose 5-phosphate, and P_i) was observed, but the enzyme exhibits positive cooperativity toward PEP (>1 mM) and divalent metal ions (Mg²⁺ and Mn²⁺). Therefore, an increased substrate/PEP concentration will enhance glycolytic flux via PK, and a possible role in metabolic thermoadaptation to reduce the thermolabile PEP pool was discussed (235).

(ii) The branched ED pathway. The catabolic branched ED pathway in *Tpt. Tenax* (Fig. 25) resembles the one of *Sul. solfataricus*; however, the pathway seems to be specific for glucose in *Tpt. tenax* (173). The characterized glucose dehydrogenase (GDH) from *Tpt. tenax* catalyzes the NAD(P)⁺-dependent oxidation of D-glucose (K_m , 0.3 mM; V_{max} , 40 U/mg) and with a significantly lower affinity for D-xylose (K_m , 8 mM; V_{max} , 60 U/mg) (39). The enzyme shows no activity with D-galactose. Also, *Tpt. tenax* GAD is specific for D-gluconate, and no activity with D-galactonate was observed for the recombinant enzyme as well as in *Tpt. tenax* crude extracts (173). In contrast, KD(P)G aldolase of *Tpt. tenax*, like the *Sul. solfataricus* enzyme, lacks facial selectivity, and the diastereomers D-KDG and D-KDGal are formed from D-glyceraldehyde and D-pyruvate (298). The KDG kinase (KDGK) as well as the glycerate kinase (GK) of *T. tenax*, the key enzymes of the semi- and nonphosphorylative ED branches, respectively, have been characterized in detail. Like the *Sul. solfataricus* enzymes, KDGK possesses high affinity for its substrate KDG (K_m of 0.2 mM and V_{max} of 43.3 U/mg for KDG), and GK showed substrate inhibition by glycerate (>0.3 mM). In addition, for GK of *Tpt. tenax*, competitive inhibition by the reaction product ADP (0.1 mM ADP at 50 μM D-glycerate) was observed, which was more pronounced with nonsaturating ATP concentrations (39.1% residual activity at 50 μM ATP) than with saturating ATP concentrations (87.3% at 5 mM ATP). The enzymatic properties of the *Sul. solfataricus* and *Tpt. tenax* GKs suggest a similar function as a throttle valve in order to direct the flux via the two ED branches and, thus, a possible gluconeogenic role of the spED branch in both organisms. The more complex regulation of the *Tpt. tenax* enzyme by additional ADP inhibition (low energy charge of the cell) might be seen with respect to the presence of the reversible EMP pathway.

As a respiring organism (sulfur respiration with S⁰ as the terminal electron acceptor), *Tpt. tenax* oxidizes pyruvate, the product of both the modified EMP pathway as well as the branched ED pathway, to acetyl-CoA via POR and further to CO₂ via the CAC, and the respiratory chain represents the major source of energy in this organism (158, 418).

(iii) Gluconeogenesis. Gluconeogenesis in *Tpt. tenax* is characterized by a gluconeogenic PEPS and the PGK/GAPDH enzyme couple. As in *Bacteria*, PEPS in *Tpt. tenax* catalyzes the unidirectional ATP-dependent formation of PEP (pyruvate + ATP + H₂O → PEP + AMP + P_i), thus representing a true anabolic enzyme. In contrast to PEPS from *Thermococcales*, no glycolytic activity was detected. However, allosteric regulation for the enzyme by the energy charge of the cell was observed (320). In addition to PEPS, reversible PPDK catalyzes the anabolic direction, and due to its allosteric properties, it might enhance gluconeogenesis in the presence of high ATP concentrations. The classical GAPDH, in contrast to glycolytic GAPN, prefers the anabolic reductive direction, which is documented by a 5-fold-increased activity and a 20-fold-higher affinity toward 1,3BPG compared to GAP (K_m of 20 μM and V_{max} of 2 U/mg for GAP; K_m of 10 μM and V_{max} of 10 U/mg for 1,3BPG) (177). Notably, a homolog of the anabolic bifunctional FBPA/ase was also identified in the *Tpt. tenax* genome (31, 321). The enzyme has not been characterized so far, but it might be active, in addition to the reversible FBA and PP_i-PFK couple, or might substitute for both enzymes in the anabolic direction.

Energetics. The net energy gain of the EMP pathway in *Tpt. tenax* is 1 ATP, considering (i) the substitution of the gluconeogenic GAPDH/PGK couple by the utilization of the nonphosphorylating glycolytic GAPN and/or GAPOR omitting substrate-level phosphorylation and (ii) the utilization of a reversible PP_i-dependent PFK, which avoids the consumption of a second ATP. Thus, the net ATP yield in the modified EMP pathway in *Tpt. tenax* is 1 mol ATP per mol glucose. Taking the predicted glucose uptake via ABC transporters into account, at least 1 mol ATP per mol glucose will be required for transport of extracellular glucose, resulting in no net gain of ATP. In contrast, phosphorolytic instead of hydrolytic degradation of the internal carbon storage compound glycogen via glycogen phosphorylase, forming glucose 1-phosphate at the expense of P_i (84), which avoids ATP consumption via ATP-HK, will save 2 mol ATP (1 mol from the transport reaction and 1 mol from the HK reaction) per mol G6P formed, which would result in a net yield of 2 mol ATP from the EMP pathway. However, no net gain of ATP is generated by the utilization of either the npED or spED branch.

PP_i, the phosphoryl donor of the PP_i-PFK as well as the PPDK reactions, is generally regarded as a waste product in the cell and is quickly hydrolyzed by a cytoplasmic soluble pyrophosphatase in order to drive anabolic reactions such as DNA synthesis (418). However, PP_i seems to have a second special function in *Tpt. tenax* in addition to its role as the substrate for PP_i-PFK and PPDK, i.e., a direct contribution to the generation of membrane potential by the presence of a membrane-bound pyrophosphatase, which was shown for the enzyme of the close relative *Pyb. aerophilum* (V-PPase) (537, 538). However, the main energy-gaining process in *Tpt. tenax* appears to be the CAC and the respiratory chain.

Regulation at the protein and gene levels. As generally found in *Archaea*, in *Tpt. tenax*, control at protein level is also shifted to the level of GAP conversion. In addition, a second important control point was identified at the level of PEP-pyruvate conversion.

(i) Regulation at the enzyme level by allosteric effectors. In contrast to the enzymes of *Tco. kodakarensis*, *Sul. solfataricus*, and *Sul. tokodaii*, GAPN of *Tpt. tenax* possesses a complex allosteric behavior, and besides G1P (K_d [dissociation constant] = 1 μM) (intermediate of glycogen metabolism), F6P (K_d = 0.2 mM), as an

early intermediate of the EMP pathway, also activates the enzyme. Further on, TtxGAPN is regulated by the energy charge of the cell, and inhibition by ATP ($K_d = 3$ mM) and activation by ADP or AMP ($K_d = 0.25$ mM and 0.14 mM, respectively) were reported. Strikingly, a strong inhibition was also observed in the presence of NADP⁺ ($K_d = 1$ μ M) and NADPH ($K_d = 0.3$ μ M) (172). However, inhibition by the strongest effector, NADPH, was removed in the presence of activators (10 μ M G1P reduces the affinity for NADPH 200-fold) (172). Later on, it was shown that in the presence of the activator G1P, NADP⁺ is a more efficient cosubstrate than NAD⁺ (K_m values of 0.4 mM for NAD⁺ and 0.1 mM for NADP⁺ in the presence of 0.1 mM G1P [174]). The structural basis for the allosteric regulation and substrate specificity of *Tpt. tenax* GAPN was solved (174). Therefore, the availability of carbohydrates mirrored by activating intermediates as well as the energy charge of the cell (ATP/ADP and AMP ratio) seem to regulate GAPN and, thus, glycolytic flux via the pathway.

At the level of PEP-pyruvate conversion, the reversible PPDK showed significant inhibition of the catabolic reaction by ATP [$K_{i(ATP)} = 75$ μ M] in an AMP-competitive manner, whereas in the anabolic/gluconeogenic direction, positive cooperativity for ATP ($S_{0.5} = 8$ mM) but no allosteric inhibition or activation was observed (320). In contrast, anabolic PEPS was strongly inhibited by AMP [$K_{i(AMP)} = 0.5$ mM], α -ketoglutarate ($K_i = 0.6$ mM), and, to a lesser extent, ADP [$K_{i(ADP)} = 2.6$ mM]), indicating reduced activity at a low energy charge of the cell and under conditions of ammonia limitation (link to amino acid biosynthesis) (320). For glycolytic PK, no allosteric behavior was observed (235). Therefore, at a high energy charge of the cell (increased ATP and reduced ADP and AMP concentrations), anabolic carbon flux via PEPS and PPDK is favored, whereas in the catabolic direction, flux via PPDK is inhibited by the allosteric effector ATP, and flux through the PK reaction is decreased by low ADP concentrations [$K_{m(ADP)} = 0.7$ mM with the cosubstrate PK]. In contrast, at a low energy charge of the cell, anabolic PEPS is allosterically inhibited by AMP and ADP, whereas PK and PPDK will be highly active in the glycolytic direction.

In addition, for FBPA, a slight activation was observed in the presence of citrate (2.2-fold with 10 mM citrate); however, due to the high concentration required for activation, the physiological relevance is unclear (126). Furthermore, as outlined above, in the branched ED pathway, regulatory properties were observed only for glycerate kinase, showing substrate inhibition by glycerate and competitive inhibition by the reaction product ADP (252). Thus, a function similar to that proposed for the *Sul. solfataricus* enzyme as a throttle valve directing flux via the two ED branches and, thus, a possible gluconeogenic role of the spED branch seem likely in *Tpt. tenax*.

The coexistence and utilization of both the modified EMP and the branched ED pathways raise questions about the physiological function of both pathways. Due to the different energy gains (see above), a possible selection between both pathways in response to the energy demand of the cell and/or a possible role in the hydrolytic or phosphorolytic degradation of glycogen, which was identified as a carbon storage compound in *Tpt. tenax* (540), was discussed (321). From the localization of a gene encoding a glucan-1,4- α -glucosidase (glucoamylase [*gaa*]) together with the genes encoding the KD(P)G aldolase and KDG kinase in the *Tpt. tenax* ED operon (*kdgA-kdgK-gaa*) (173), a possible role of the ED pathway in the hydrolytic degradation of glycogen, forming glu-

cose, was deduced. In contrast, the EMP pathway might play a major role in the phosphorolytic degradation of glycogen via glycogen phosphorylase. The glycogen phosphorylase of *Tpt. tenax* has been characterized and forms G1P, which is further converted to G6P via phosphoglucomutase (PGM); the respective homolog (TTX2058) was identified in the *Tpt. tenax* genome (418). Notably, G1P, the key metabolite in glycogen metabolism (synthesis as well as degradation), plays a major role in the regulation of GAPN, the key enzyme in the lower EMP pathway/spED branch.

(ii) Regulation at the gene/transcript level. Information on changes at the transcript level in response to heterotrophic growth on glucose versus autotrophic growth on CO₂/H₂ (glycolytic/gluconeogenic carbon switch) has been derived from Northern blot analyses as well as a focused central carbohydrate metabolism (CCM) microarray study (31, 126, 178, 235, 320; for a review, see reference 321). The focused microarray analysis included 85 identified candidate genes of the reversible EMP pathway, the catabolic branched ED pathway, the reversible CAC, as well as glycogen and pentose metabolism (84). In response to glucose, significant upregulation was observed for the genes encoding the reversible PP_i-PFK (*pfp*) and FBPA (*fba*), which form the *fba-pfp* operon, as well as for catabolic GAPOR (*gor*) and PK (*pyk*) (31, 126, 235). In contrast, the genes encoding PGK (*pgk*) and the classical GAPDH (*gap*) with anabolic function, which form the *pgk-gap* operon, and anabolic PEPS were upregulated under autotrophic growth conditions (31, 178, 320). No regulation at the gene level was observed for the other CCM genes, including those encoding PPDK or GAPN. Therefore, upregulation of the genes encoding PP_i-PFK, FBPA, GAPOR, and PK in glucose-grown cells might allow for an enhancement of carbon flux under glycolytic growth conditions and of GAPDH, PGK, and PEPS under gluconeogenic growth conditions.

From the ED pathway, only the genes encoding glycerate kinase (*garK*) and dihydroxy acid dehydratase (DHAD) (*ilvD*), which seem to form an operon, are upregulated in response to autotrophic growth. The reason for the upregulation of this gene cluster under autotrophic conditions is still unclear, since the ED pathway serves for glycolysis. DHAD from *Sul. solfataricus* has been characterized and possesses similar activity with dihydroxyisovalerate and gluconate, and a function in branched-chain amino acid synthesis as well as the ED pathway has been proposed (289). However, a possible link between the ED pathway and branched amino acid synthesis under autotrophic growth conditions still remains to be elucidated.

For *Tpt. tenax*, there are also first indications for the significance of posttranscriptional processing, as deduced from Northern blot analysis. The gene encoding ATP-HK (*hik*) is cotranscribed with an upstream-located gene (*orfX*), which codes for an 11-kDa protein of unknown function. Microarray analysis revealed that both genes are not regulated in response to the carbon source (glucose/CO₂) (31); however, the presence of mono- and bicistronic transcripts depends on the offered carbon source. The monocistronic *hik* transcript, in addition to the *orfX-hik* transcript, was observed under heterotrophic growth conditions, whereas under autotrophic growth conditions, only the bicistronic transcript was identified (55). Furthermore, evidence for a possible role of small RNAs in the regulation of CCM has been gained for the close relatives *Pyb. aerophilum*, *Pyb. arsenaticum*, *Pyb. calidifontis*, and *Pyb. islandicum* (541), which revealed the presence of a small noncoding RNA (ncRNA) (asR3) targeting the

tpi gene, encoding TIM. This might suggest that in *Tpt. tenax* and other *Crenarchaeota*, small ncRNAs could also be involved in regulation of CCM.

Haloarchaea (*Haloferax volcanii*, *Haloarcula marismortui*, and *Halobacterium salinarum*)

Growth conditions. Haloarchaea belong to the *Euryarchaeota* and thrive in (hyper)saline environments at salt concentrations of at least 12% (2 M) up to saturated concentrations (5.2 M), such as those found in salt lakes (e.g., the Dead Sea) or marine salterns. They are mostly strictly aerobic chemoorganoheterotrophs growing on complex media, with some strains being capable of a facultative anaerobic life-style using alternative electron acceptors like nitrate or fermentative growth on arginine (369, 542, 543). The metabolism of extremely halophilic *Archaea* as well as its diversity have been reviewed recently (369). Some haloarchaea are able to utilize carbohydrates, such as *Hfx. volcanii*, *Hfx. mediterranei*, *Har. marismortui*, *Halococcus saccharolyticus*, and *Hrr. saccharovorum* (for the taxonomy and classification of haloarchaea, see references 542–544), and the pathways for D-glucose, D-fructose, and D-xylose degradation have been analyzed in detail (33, 70, 180, 246, 287, 343). The most detailed studies on sugar metabolism in haloarchaea have been carried out with *Hfx. volcanii* and *Har. marismortui*. Both the moderate halophile *Hfx. volcanii* (optimal NaCl concentration of 1.7 to 2.5 M) and the extreme halophile *Har. marismortui* (optimal NaCl concentration 3.4 to 3.9 M) were originally isolated from the Dead Sea (545–547), and their genome sequences have been deciphered (548, 549). For *Hfx. volcanii*, an efficient genetic system has been established (550, 551). Both organisms grow aerobically with a variety of different sugars and amino acids/peptides as carbon and energy sources, with oxygen as the terminal electron acceptor (aerobic respiration). *Hfx. volcanii* has additionally been described to grow anaerobically by the use of alternative electron acceptors such as nitrate, dimethyl sulfoxide (DMSO), and trimethylamine N-oxide (TMAO).

Sugar transport. Glucose uptake in *Hfx. volcanii* cell suspensions was shown to proceed via an Na^+ -dependent glucose symporter under aerobic growth conditions (552). In accordance with these experimental results, microarray studies identified a 20-fold upregulation of a member of the 12-transmembrane helix transporter (553). However, under anaerobic growth conditions, a glucose-specific ABC transporter was shown to be essential for glucose uptake by using a genetic approach (554).

In addition, fructose uptake as well as degradation in *Hfx. volcanii* were studied recently. Intriguingly, a few haloarchaeal genomes (i.e., *Hfx. volcanii*, *Har. marismortui*, *Haloarcula hispanica*, *Halalkalicoccus jeotgali*, and *Htg. turkmenica*) harbor homologs of the bacterial PEP-dependent phosphotransferase system (PTS). This is unique for the archaeal domain (123, 555), since all other *Archaea* seem to rely on ABC transporters for sugar uptake, and lateral gene transfer from *Bacteria* to *Archaea* has been suggested (123). *Hfx. volcanii* harbors one complete fructose PTS gene cluster (HVO_1495 to HVO_1499 [*ptfB*, *ptfI*, *ptfH1*, *ptfA*, and *ptfC*]). The cluster encodes the soluble components EI (*ptfI*), HPr (*ptfH1*), EIIA (*ptfA*), and EIIB (*ptfB*), which catalyze transient phosphotransfer from PEP to the encoded membrane-bound EIIC (*ptfC*), which is finally responsible for sugar uptake and phosphorylation (Fig. 26). Sequence analysis revealed that *Hfx. volcanii* EIIC is a member of the fructose-specific EII2 type 2 subfamily (TIGR01427) (123). The gene cluster is flanked by an

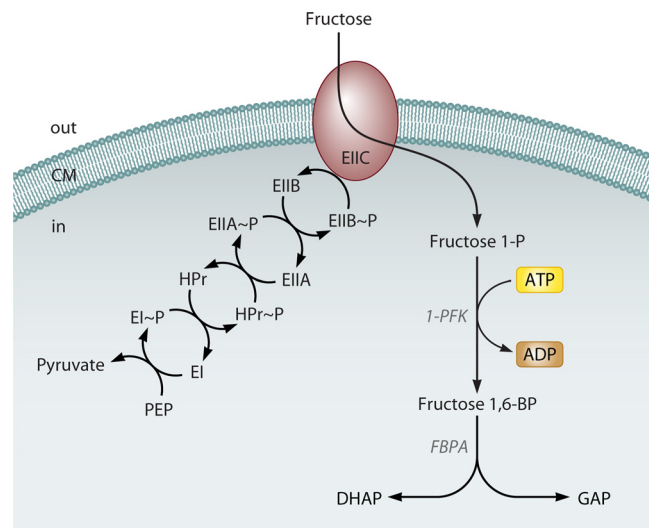


FIG 26 Overview of fructose uptake by the PTS and degradation of fructose 1-phosphate in *Hfx. volcanii* (123). Fructose uptake proceeds via the PEP-dependent PTS; the different PTS components (EI, HPr, EIIA, EIIB, and EIIC) are depicted. The fructose 1-phosphate formed is further converted via fructose-1-phosphate kinase (1-PFK) (*pfkB*) and class II fructose-1,6-bisphosphate aldolase (FBPA) (*fba*), forming dihydroxyacetonephosphate (DHAP) and glyceraldehyde 3-phosphate (GAP). Abbreviations: PEP, phosphoenolpyruvate; CM, cytoplasmic membrane; $\sim\text{P}$, transferred phosphate group.

operon encoding the transcriptional regulator *glpR* (see below) and 1-phosphofructokinase (1-PFK) (*pfkB* gene) (556) and by a downstream-located FBPA (*fba* gene) (123) (Fig. 28). An in-frame deletion of *ptfC* resulted in an inability of the mutant to grow on D-fructose, whereas growth on D-glucose was not affected, demonstrating that the PTS is essential for D-fructose uptake in *Hfx. volcanii* (123).

Sugar metabolism. ^{13}C NMR labeling studies of *Har. marismortui* revealed that glucose was degraded exclusively via the spED pathway and that fructose was degraded predominantly via the modified EMP pathway (96%; 4% spED pathway) (70).

(i) Different degradation pathways for glucose and fructose. The different degradation pathways for glucose and fructose were also confirmed by enzyme studies with crude extracts, identifying GDH, GAD, KDG kinase, and KDPG aldolase activity converting glucose, via gluconate, 2-keto-3-deoxygluconate, and 2-keto-3-deoxy-6-phosphogluconate, finally to pyruvate and GAP, which then enter the common lower shunt of the EMP pathway (Fig. 27). GDH from *Haloferax* spp. has been studied in detail, and the crystal structure is available, as discussed above. The absence of KDG aldolase activity indicated that the npED branch is not operative in haloarchaea. However, a phylogenetic analysis revealed homologs of glycerate kinase, the key enzyme of the npED branch, in almost all haloarchaeal genomes available at that time (except for *Hbt. salinarium*), raising questions about a branched ED pathway also in haloarchaea (252). ^{13}C NMR labeling studies of *Har. marismortui* also confirmed the finding of an EMP variant for fructose degradation reported for several saccharolytic haloarchaea on the basis of crude extract measurements. This modified EMP pathway is characterized by the conversion of fructose to F1P via ketohexokinase (KHK) and 1-PFK. The F1,6BP formed is further converted via FBPA, forming DHAP and GAP, which enter the common lower shunt of the EMP pathway, forming pyruvate (68–70). Py-

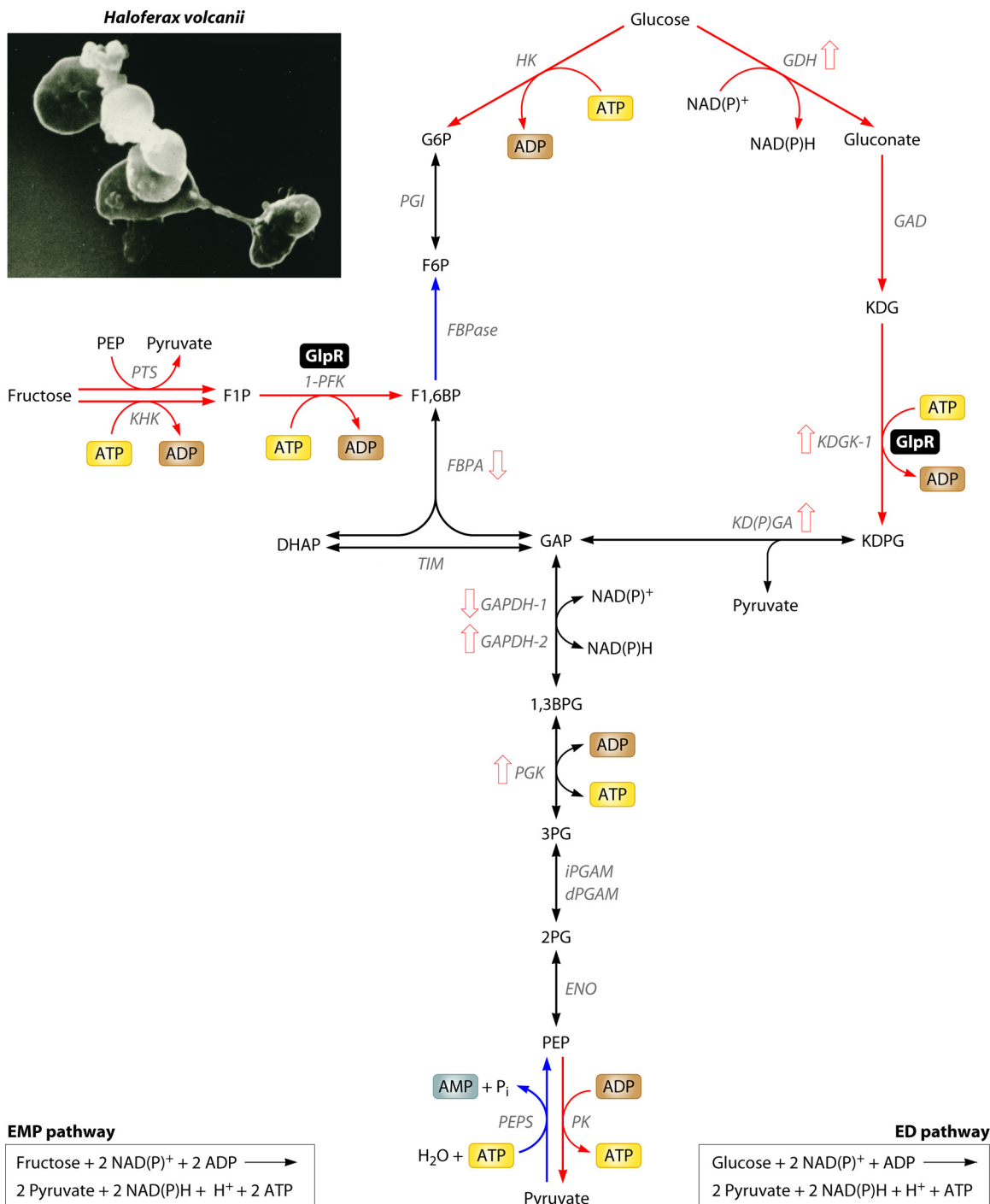


FIG 27 Glycolysis and gluconeogenesis in the mesophilic halophile *Haloferax volcanii*. Glucose is degraded via the spED pathway, and fructose is degraded via the EMP pathway. The pathway for fructose degradation is characterized by 1-PFK and FBPA class II; the common lower EMP shunt is characterized by two GAPDH isoenzymes that are differently regulated in response to the C source (553) as well as catabolic PK and anabolic PEPS. Enzyme reactions with catabolic function are indicated by red arrows, anabolic reactions are shown as blue arrows, and reversible reactions are indicated by black arrows. Enzymes for which the encoding genes are regulated by the transcriptional regulator GlpR are marked (black box). Enzymes for which the encoding genes were up- or downregulated in response to the gluconeogenic (Casamino Acids)/glycolytic (glucose) shift are depicted as red open arrows in the respective direction (553). The net equations of glucose conversion to pyruvate via the modified ED pathway and of fructose conversion to pyruvate via the modified EMP pathway are depicted in boxes (PTS, PEP-dependent phosphotransferase system; KHK, ketohexokinase; 1-PFK, fructose-1-phosphate kinase). (Electron micrograph courtesy of Moshe Mevarech, Tel Aviv University, Israel, reproduced with permission.)

ruvate is further oxidized via acetyl-CoA (POR) finally to CO₂ via the CAC (see reference 369 and references therein).

(ii) **Glucose-fructose diauxie.** *Har. marismortui*, like other *Archaea*, exhibits diauxic growth in the presence of D-glucose and D-fructose. Glucose is used first, and after a lag phase, fructose is degraded, accompanied by an increase in F1P kinase (1-PFK) activity (70). Diauxic growth has also been reported for *Har. vallis-mortis* growing on sucrose (68). However, in resting-cell suspensions, cells pregrown on either glucose or fructose could not metabolize the alternate substrate, i.e., fructose and glucose, respectively. Furthermore, cells pregrown on yeast extract/Casamino Acids medium could not metabolize either sugar. However, after prolonged incubation of the cell suspensions inoculated with glucose-pregrown cells, induction of KHK activity concomitant with fructose uptake from the medium was observed (70). Thus, sugar-specific induction of the respective glycolytic pathway as well as a kind of catabolite repression mechanism well known for *Bacteria* were suggested (70) (see also the section on transcription regulation, below). From labeling studies of *Har. marismortui*, there is no evidence for the utilization of the oxidative pentose phosphate pathway (OPPP) for sugar degradation to pyruvate during growth on glucose or fructose. Enzyme measurements in crude extracts suggest pentose (i.e., ribulose 5-phosphate) formation via a modified OPPP from G6P via glucose 6-phosphate dehydrogenase (G6PDH) and 6-phosphogluconate dehydrogenase (decarboxylating) (6PGDH). The precursor G6P is formed from glucose via HK and from fructose after formation of F1,6BP by ketohexokinase and fructose 1-phosphate kinase, as reported for fructose degradation via FBPAse and glucose-6-phosphate isomerase. All enzyme activities required were detected in crude extracts (70). Such an alternative pathway for pentose phosphate biosynthesis would be consistent with the apparent absence of the RuMP pathway in haloarchaea, and gene homologs encoding 6PGDH have been identified (see above) (360, 369). Notably, *Hfx. volcanii* seems to possess two homologs of phosphorylating GAPDH (HVO_0478 and HVO_0481), and glycolytic as well as gluconeogenic functions, respectively, in response to the carbon source were predicted based on microarray studies (see below) (553).

More enzymatic information is available for fructose degradation via the modified EMP pathway in *Hfx. volcanii*. Threefold and 8-fold inductions of 1-PFK and FBA activity, respectively, in crude extracts were observed in fructose- compared to glucose-grown cells, which are supported by transcript analyses (RT-PCR and Northern blotting) (see below) (123). Characterization of 1-PFK showed a 36-fold-higher catalytic efficiency of the enzyme for F1P than for F6P (k_{cat}/K_m values of $1.2 \times 10^6 \text{ s}^{-1} \text{ M}^{-1}$ for F1P and $0.034 \times 10^6 \text{ s}^{-1} \text{ M}^{-1}$ for F6P). For FBPA, bacterial-like class II activity with Mn²⁺ as the preferred divalent cation was demonstrated (123, 132). The phylogenetic distribution of bacterial-type class II FBPA is restricted to a few haloarchaeal species, and acquisition via lateral gene transfer from *Bacteria* has been suggested (123).

Deletion of the *pfkB* and *fba* genes abolished growth on fructose, whereas growth on glucose was not affected or, in the case of the Δfba mutant, even increased. The genetic approach confirms the essential function of both the 1-PFK and FBPA enzymes in the EMP pathway for fructose degradation, whereas glucose degradation via the spED pathway is not affected. The Δfba mutant also lost its ability to grow with acetate, D-xylose, and Casamino Acids

as the sole carbon source, pointing to an additional important anabolic/gluconeogenic function of class II FBPA in the generation of F1,6BP via the reversed EMP pathway, for example, as a precursor for pentose formation in *Hfx. volcanii*. Notably, class II FBPA is not required for pentose generation during growth on glucose, confirming previous bioinformatics and enzymatic studies with crude extracts pointing to the presence of a modified OPPP in haloarchaea (29, 70, 369).

Energetics. As outlined above, in contrast to most other *Archaea*, haloarchaea utilize the GAPDH/PGK couple for GAP oxidation in the course of the spED and the modified EMP pathways for glucose and fructose breakdown, respectively. Thus, haloarchaea harbor an additional site of substrate-level phosphorylation similar to the classical pathways known for *Bacteria* and *Eukarya*. In the spED pathway, 1 ATP has to be invested for the phosphorylation of KDG to KDGP, which is then cleaved to pyruvate and 1 molecule of GAP. From GAP oxidation in the lower part of the spED pathway, 2 ATPs are gained in PGK and PK reactions, resulting in a net yield of 1 mol ATP per mol glucose. Additionally, 2 moles of NAD(P)H are formed in the GDH and GAPDH reactions, which are reoxidized in the respiratory chain. Glucose transport via an Na⁺ symport or an ABC transport system under anaerobic conditions requires <1 ATP or at least 1 ATP, respectively. Fructose phosphorylation is coupled to its transport via a PTS at the expense of PEP. One ATP additionally has to be invested to phosphorylate F1P to F1,6BP. From F1,6BP, 2 molecules of GAP are formed, which are oxidized via 1,3BPG to 3PG, resulting in 2 ATPs. Of the 2 molecules of PEP finally resulting from 1 molecule of fructose, one has to be invested for transport purposes, and the conversion of the second leads to one further ATP. Thus, 3 molecules of ATP are gained in the lower part of the modified EMP, and 1 ATP has to be invested in the upper part, resulting in a net ATP yield of 2 molecules per molecule of fructose concomitant with 2 moles of NAD(P)H + H⁺ (from the GAP reaction). However, under aerobic conditions, the major source of energy is represented by the CAC, the respiratory chain, and ATP synthesis via A₁A_o-ATPase (496).

Regulation at the gene and protein levels. A transcriptome study (1-fold-coverage shotgun DNA microarray, i.e., PCR product library created from a genomic library) of *Hfx. volcanii* after transition from gluconeogenic/peptolytic (Casamino Acids) to glycolytic (glucose) growth conditions provided the first evidence for regulation at the global gene level in response to a carbon source (553). In total, about 10% of all genes were found to be regulated >2.5-fold. Global analysis revealed the upregulation of glycolytic genes and the downregulation of gluconeogenic genes, but in addition, the downregulation of genes involved in the CAC, electron transport, as well as ATP synthesis was also observed after the shift to glucose. With respect to glucose transport, one of the most highly regulated proteins (20-fold upregulation) was a 12-transmembrane helix transporter, and it was proposed that the protein represents the aerobic Na⁺-dependent glucose symporter reported previously (552). In addition, several ABC transporters were found to be regulated in response to the glycolytic shift; however, the substrate specificity still remains to be elucidated (553). The previously reported glucose-specific ABC transporter was shown to be essential only for glucose uptake under anaerobic conditions by using a genetic approach (554).

With respect to carbohydrate metabolism, significant upregulation of genes encoding enzymes involved in glucose degradation

[i.e., GDH, KDGK-1, KD(P)GA, GAPDH-2, and PGK] as well as downregulation of genes encoding GAPDH-1 and FBPA were observed (553). The upregulation of genes in response to glucose availability is in accordance with the use of the spED branch, and the downregulation of FBPA points to a reduction of gluconeogenesis. In accordance with the different regulations of both GAPDHs, catabolic (GAPDH-2) and anabolic (GAPDH-1) functions have been proposed, highlighting the important role of regulation at the GAP level in *Archaea* (31, 553). In addition, microarray analysis indicated an important role of posttranslational regulation by protein phosphorylation in *Hfx. volcanii*. Genes encoding a serine protein kinase (2 subunits) were highly upregulated, and a gene for phosphoserine phosphatase was quickly repressed upon a glucose shift, suggesting an increased level of protein phosphorylation and thereby possible regulation of target proteins (553). With respect to fructose transport and metabolism, transcript analysis (RT-PCR and Northern blot analysis) of the EIIC-encoding gene (*pftC*) revealed specific upregulation of the fructose PTS operon (cotranscript) as well as of the monocistronic *pftC* transcript in fructose- compared to glucose-grown cells. Furthermore, significant upregulation of the *pfkB* transcript (*glpR-pfkB* operon and monocistronic transcript) as well as the *fba* transcript was observed in the presence of fructose, which was reflected at the enzyme level by 3- and 8-fold-higher 1-PFK and FBA activities, respectively, supporting the function of both enzymes in fructose metabolism (123).

Glycerol-mediated catabolite repression. In *Hfx. volcanii*, glycerol-mediated catabolite repression of glucose metabolism has been reported (557). Glycerol is a preferred carbon source for haloarchaea, because it is highly abundant in high-salt environments. Glycerol is accumulated as a compatible solute in the halotolerant green alga *Dunaliella* to protect the cell from osmotic stress and is released into the environment by leakage and cell lysis (558). Biochemical and genetic studies revealed that glycerol is channeled into the central carbohydrate metabolism via glycerol kinase (*glpK*; HVO_1541) and the glycerol phosphate dehydrogenase complex (*glpA1B1C1*; chromosomal) (556, 557). *Hfx. volcanii* deletion mutants of glycerol kinase ($\Delta glpK$) as well as glycerol phosphate dehydrogenase ($\Delta glpA1$) were incapable of growth on glycerol. In the presence of glycerol, glycerol-mediated catabolite repression of glucose metabolism was more pronounced in the $\Delta glpK$ mutant than in the wild-type strain (557).

Transcriptional regulator GlpR. The involved DeoR/GlpR-type transcriptional regulator GlpR from *Hfx. volcanii* was characterized recently by biochemical and genetic approaches (556). GlpR was shown to control fructose and glucose metabolism in *Hfx. volcanii* by repression of transcription of 1-PFK and KDGK-1 (chromosomal copy) (HVO_0549) in the presence of glycerol. Repression by GlpR was abolished in the presence of glucose and fructose (556). The *glpR* gene (HVO_1501) is cotranscribed with the downstream-positioned 1-PFK gene (*pfkB*; HVO_1500) (located upstream of the fructose PTS gene cluster) (Fig. 28) and therefore serves as an autoregulator for its own transcription, i.e., downregulation in response to glycerol alone. In accordance with the decreased transcription of the *glpR-pfkB* operon and the *kdgK1* gene, 1-PFK and KDGK activities were also significantly reduced upon growth on glycerol compared to growth on fructose and glucose. Deletion of the *glpR* gene resulted in increases of transcript levels and enzyme activity. Therefore, GlpR regulates its own expression and those of 1-PFK and KDGK-1. A binding motif

consisting of an inverted hexameric repeat [TCSnCn₍₃₋₄₎SSnGGA, where S is G/C and n is any nucleotide] was identified (556). In order to analyze the function of GlpR in diauxic growth, a *glpR glpK* double mutant was constructed. Growth studies were performed with single as well as double mutants in comparison to the wild type on glucose and fructose in the presence or absence of glycerol. In the double mutant, in the presence of equimolar amounts of glycerol and fructose, both carbon sources were utilized, supporting a function of GlpR in diauxic growth on fructose. However, no effect on diauxic growth on glucose and glycerol was observed, suggesting that GlpR is not involved in catabolite repression on these carbon sources (556).

Notably, the genes encoding glycerol 3-phosphate dehydrogenase (*glpA1B1C1*) and glycerol kinase (*glpK*), forming DHAP from glycerol, are found in the glycerol metabolic gene cluster (HVO_1538 to HVO_1543 [*glpA1B1C1*, *glpK*, *glpF*, and *ptsH2*]), with the latter two genes encoding a putative glycerol facilitator [*glpF*] and a second homolog of HPr [*ptsH2*] and were cotranscribed (556). Downstream of the *ptsH2* gene but divergently organized, there are three genes putatively encoding a dihydroxyacetone kinase (*dhaMLK*). The encoded proteins represent a cytosolic PTS complex for the phosphorylation of dihydroxyacetone to DHAP (Fig. 28). Glycerol 3-phosphate, the product of the glycerol kinase reaction, was demonstrated to act as a strong inducer of transcription from the *glpA1* promoter; however, GlpR was shown not to be required for the regulation of the glycerol metabolic gene cluster (548, 556). In addition, a second incomplete PTS gene cluster, missing only the EI gene (HVO_2101 to HVO_2104), was identified downstream of the gene encoding triosephosphate isomerase in *Hfx. volcanii*. However, future studies have to be awaited in order to elucidate its function and the underlying regulatory principles.

Halobacterium salinarum. In contrast to *Hfx. volcanii* and *Har. marismortui*, the extremely halophilic *Hbt. salinarum* (optimal growth at 3.5 to 4.5 M NaCl) is a non-carbohydrate utilizer with complex nutritional demands. Genome sequences are available for two strains, i.e., *Hbt. salinarum* NRC-1 (415) and *Hbt. salinarum* R1 (559), and a genetic system has also been developed (560). Some species are able to produce bacteriorhodopsin, one of the best-studied membrane proteins, and use sunlight as an energy source, which is, however, restricted to bright-light and low-oxygen conditions (for more details, see references 542, 543, and 561). Although all genes required for a functional spED pathway as well as gluconeogenesis via the EMP pathway were identified in the genome of *Hbt. salinarum*, no growth with glucose as the sole carbon source has been reported so far (180, 369, 397, 562). For a functional npED pathway, only GK is missing (252). The first evidence for regulation of central carbohydrate metabolism at the protein level via reversible protein phosphorylation in *Hbt. salinarum* was gained from a recent phosphoproteome study (437). Several key metabolic enzymes of glycolysis and gluconeogenesis were identified as p-proteins in the parent and/or phosphatase deletion strain ($\Delta serB$), including, among others, pyruvate kinase, PEPS, 2,3BPG-independent PGAM, and three different phosphoglucomutases (OE2318R, OE4094F, and OE4190F). However, the effect of phosphorylation on the respective enzymes still remains to be elucidated.

(i) TrmB-like transcriptional regulator. Although *Hbt. salinarum* is not able to utilize glucose as the sole carbon source, glucose seems to play an important role in *Hbt. salinarum* cell metabo-

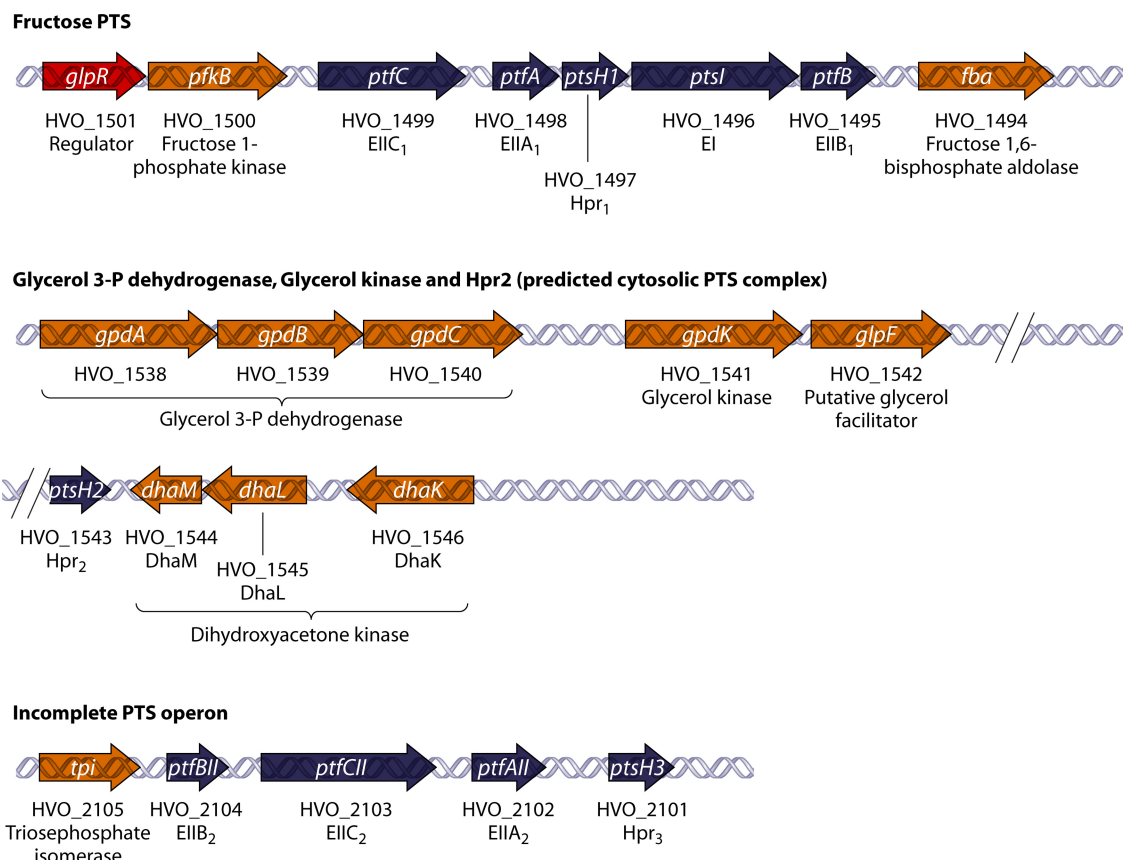


FIG 28 Genomic context of genes encoding components of the PEP-dependent phosphotransferase system (PTS) in *Hfx. volcanii*. Components of the fructose PTS system are colocalized with genes encoding the transcriptional regulator GlpR and enzymes involved in fructose 1-phosphate degradation, i.e., fructose-1-phosphate kinase and fructose-1,6-bisphosphate aldolase. Downstream of genes encoding enzymes for glycerol utilization (i.e., glycerol kinase and glycerol-3-phosphate dehydrogenase) forming dihydroxyacetone phosphate (DHAP), a gene encoding a second single Hpr2 and, in a divergent organization, genes encoding dihydroxyacetone kinase (*dhaM*, *dhal*, and *dhaK*) are found. Hpr2 has been proposed to encode a cytosolic PTS complex, i.e., the dihydroxyacetone kinase (*dhaM*, *dhal*, and *dhaK*) pathway, catalyzing the formation of DHAP from dihydroxyacetone (556). A second incomplete PTS gene cluster is found downstream of the gene encoding triosephosphate isomerase.

lism, as concluded from studies of the TrmB family transcription factor (VNG1451C; TrmBL1 homolog) and its regulatory function by using a systems biology approach (397). A VNG1451C deletion strain was constructed and phenotypically characterized. The mutant revealed a severe growth defect under many different growth conditions tested, and the NAD⁺/NADH ratio in the mid-logarithmic growth phase was significantly reduced. Both effects were complemented by the addition of glucose and, to a lesser extent, glycerol to the growth medium. Transcriptomic studies as well as genome-wide promoter binding studies (chromatin immunoprecipitation with microarray technology [ChIP-chip]) and promoter-reporter fusion assays for selected genes were performed with the Δ trmB mutant in comparison to the parent strain. Finally, computational integration was used to construct transcriptional and metabolic networks regulated by the TrmB family transcription factor (397). In summary, binding of the TrmB-like protein to 113 promoters {cis-regulatory element [TA CT-N₍₇₋₈₎GAGTA]} was found but only in the absence of glucose and glycerol. No binding was observed in the presence of glucose or glycerol. A more detailed analysis confirmed that, in accordance with previous studies of TrmBL1 homologs in *Thermococcales* (see above), a location of the binding site upstream of the

general transcription factor (GTF) binding site of the promoter activated transcription (e.g., the *ppsA* gene, encoding PEP synthetase) and a location downstream repressed transcription (e.g., the *gap* gene, encoding GAPDH). The TrmB-like transcriptional regulator of *Hbt. salinarum* was shown to mediate the control of diverse metabolic pathways, such as glycolysis, gluconeogenesis, the CAC, and amino acid and cofactor (e.g., purine and thiamine) biosynthesis, by repression or activation. Therefore, a major function of the TrmB-like regulator in maintenance of redox and energy balance in response to available carbon sources has been proposed for *Hbt. salinarum* NRC-1 (397).

Methanogens

Growth conditions. Methanogenic Archaea (methanogens) belong to the kingdom *Euryarchaeota*. They thrive in anaerobic habitats and are unique with respect to their ability to produce methane from substrates provided by fermentative organisms from the degradation of organic matter (for recent reviews on methanogenesis, see references 563–565). For methanogens, reports about carbohydrate metabolism are rather scarce, due to their facultative autotrophic life-style with CO₂, H₂, acetate, C₁ compounds like formate, methylamine, and some alcohols. Methane is produced

by two major pathways: (i) by reduction of CO₂ with electrons derived from H₂ or formate and (ii) in the aceticlastic pathway from acetate via cleavage and conversion of the methyl group to methane and of the carbonyl group to CO₂ (564). *Mca. jannaschii* appears to be typical of H₂-utilizing, autotrophic methanogens. These *Archaea* perform anaerobic respiration with CO₂ as the terminal electron acceptor, according to the general equation 4H₂ + CO₂ → CH₄ + 2H₂O. Methanogens do not assimilate carbohydrates or complex organic substrates; however, they rely on gluconeogenesis for carbohydrate formation (e.g., pentoses and hexoses), and some methanogens synthesize glycogen as an internal carbon storage compound and thus possess metabolic pathways for sugar degradation (e.g., *Methanococcus* and *Methanobacter* [127, 398, 566]). Labeling experiments with ¹⁴CO₂ in *Mba. thermautotrophicus* in conjunction with enzyme measurements confirmed the presence of gluconeogenesis via the EMP pathway (PEPS, the only anabolic aldolase) (315, 333).

Mco. maripaludis is a mesophilic hydrogenotrophic methanogen isolated from salt marsh sediments (567). The genome sequence has been deciphered and was used for genome-scale reconstruction (568). Furthermore, the organism is genetically tractable, and numerous genetic tools have been established (569, 570). *Mco. maripaludis* is specialized to reduce CO₂ to methane in the presence of H₂ or formate. During autotrophic growth, CO₂ fixation proceeds via the modified Ljungdahl-Wood pathway (i.e., carbon monoxide dehydrogenase/acetyl coenzyme A synthase), forming acetyl-CoA. In addition, *Mco. maripaludis* is also able to utilize acetate as an alternative carbon source, which is channeled into central metabolic pathways via acetyl-CoA formed by AMP-dependent acetyl-CoA synthetase or by the acetate kinase/phosphotransacetylase enzyme couple (571). Pyruvate is formed from acetyl-CoA by the incorporation of CO₂ catalyzed by anabolic/reversible pyruvate:ferredoxin oxidoreductase (572, 573) and either is used for gluconeogenesis via the EMP pathway or enters the reductive branch of the incomplete CAC after conversion to oxaloacetate by pyruvate carboxylase, leading to 2-oxoglutarate (568). Energy/ATP conservation proceeds via an archaeal-type A₁A_o ATP synthase, which utilizes the proton motive force generated during methanogenesis for ATP synthesis (*Mca. jannaschii*) (574).

Sugar (endogenous glycogen) metabolism. Glycogen metabolism in crude extracts of *Mco. maripaludis* was studied in detail (127), and some additional information is available from detailed enzyme characterizations of the close hyperthermophilic relative *Mca. jannaschii* (363).

Almost all enzymes required for gluconeogenesis as well as glycolysis via the EMP pathway were identified in *Mco. maripaludis* crude extracts (127) (Fig. 29). No enzymes of the classical or modified archaeal ED pathway as well as the OPPP were identified. Pentoses are generated via the NOPPP and the RuMP pathway, as discussed above. For glycogen degradation, glycogen phosphorylase and phosphoglucomutase activity were determined. Regarding the EMP pathway, phosphoglucose isomerase activity in *Mco. maripaludis* crude extracts was reported, and the enzyme from *Mca. jannaschii* was characterized (81). The hyperthermophilic enzyme exhibited a higher catalytic efficiency with F6P (*K_m* values for F6P and G6P were 0.04 mM and 1 mM, respectively; *V_{max}* values were 20 U/mg and 9 U/mg, respectively), and the enzyme was inhibited by 6-phosphogluconate and erythrose 4-phosphate. Furthermore, ATP-dependent PFK activity with ac-

tivation by P_i, AMP, and ADP was identified in *Mco. maripaludis* crude extracts; only later was the ADP-dependent bifunctional glucokinase/phosphofructokinase from *Mca. jannaschii* characterized (58), and a homolog with high similarity was identified in *Mco. maripaludis* (MMP1296). Both *Mca. jannaschii* and *Mco. maripaludis* possess two homologs of the archaeal-type class I FBPA (MOFRL family; MJ1585 and MJ0400, and MMP0293 and MMP0686, respectively). However, only one candidate was shown to exhibit FBPA activity (MJ1585 and MMP0293), as confirmed by gene expression and enzyme measurements of the two *Mca. jannaschii* homologs as well as analysis of the FBPA deletion strain (*ΔaroA'*; MMP0686) in *Mco. maripaludis*, which revealed FBPA activity similar to that of the wild-type strain (384). There is additional experimental evidence that the other FBPA homologs (MJ0400 and MMP0686) have a function in 6-deoxy-5-ketofuctose 1-phosphate (DKFP) formation in *Mca. jannaschii*, a key step in a novel pathway for the formation of aromatic amino acids (382, 384). In the genome, two candidates for the noncanonical phosphoglycerate mutases were identified (MMP0112 and MMP1439); the *Mca. jannaschii* enzymes (MJ0010 and MJ1612) were shown previously to be members of the alkaline phosphatase binuclear metalloenzyme superfamily and exhibit PGAM activity (214).

Notably, *Mco. maripaludis* is the only mesophile that has been reported so far to possess GAPOR and classical GAPDH for GAP conversion (154). Expression studies indicate that the enzyme requires molybdenum (Mo) for activity and, as for other GAPORs, catalyzes only the glycolytic oxidation of GAP to 3PG. GAPOR was irreversibly inhibited by its substrate GAP at concentrations above 0.15 mM (as also observed for the *Pyr. furiosus* enzyme but less pronounced [156]), and significant inhibition by ATP was observed. In contrast to previous crude extract measurements (127), GAPDH activity was detected only in the gluconeogenic direction, and a unidirectional enzyme function was proposed. However, the assay was performed in the presence of 5 mM P_i, and for some archaeal enzymes, a requirement for much higher P_i concentrations was reported, which might explain the missing glycolytic GAPDH activity (154). Therefore, a more detailed characterization is awaited for final discussion.

For the annotated GAPN of *Mca. jannaschii* (MJ1411), lactaldehyde dehydrogenase activity with broad substrate specificity but no activity with GAP was reported (575), which is also supported by a recent phylogenetic analysis of selected members of the aldehyde dehydrogenase superfamily from *Archaea* (305). The enzyme plays an important role in lactate formation for cofactor F420 biosynthesis, and since the *Mco. maripaludis* enzyme (MMP1487) shares 56% amino acid identity, a similar function has been proposed (154). Pyruvate kinase activity in *Mco. maripaludis* crude extracts was shown to be Mn²⁺ dependent.

Energetics. Glycogen degradation via the glycogen phosphorylase requires 1 ADP for F6P phosphorylation by the bifunctional ADP-dependent glucokinase/phosphofructokinase. Assuming the use of glycolytic GAPOR instead of the PGK/GAPDH enzyme couple, 2 ATPs are generated from 2 ADPs by pyruvate kinase. As for *Tco. kodakarensis*, the presence of adenylate kinase has been reported for *Mco. maripaludis* (323, 576). Therefore, assuming the presence of adenylate kinase, 1 ATP is used to regenerate 2 ADPs from AMP and ATP, resulting in a net energy gain of 1 ATP from 1 ADP (Fig. 29).

Regulation at the gene and protein levels. As reported so far for all *Archaea*, no allosteric regulation was observed for the bifunc-

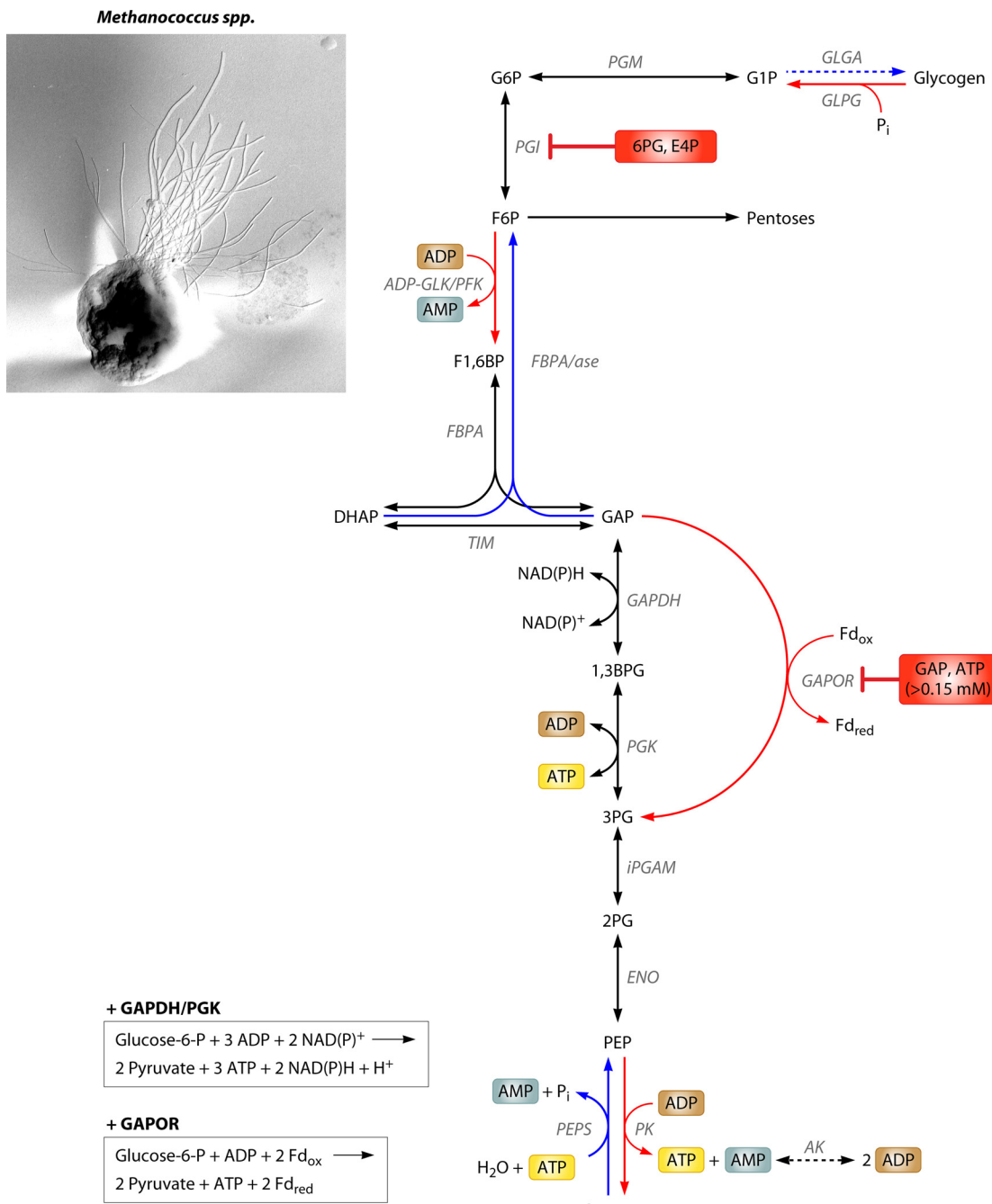


FIG 29 Glycolysis and gluconeogenesis in the autotrophic methanogens *Methanococcus maripaludis* and *Methanocaldococcus jannaschii*. The most extensively studied, *Mco. maripaludis*, for example, is a glycogen-forming methanogen and relies on the EMP pathway for glycolysis and gluconeogenesis. Glycolysis is characterized by a bifunctional ADP-GLK/PFK, archaeal-type class I FBPA, GAPOR, as well as PK, and gluconeogenesis is characterized by PEPS and FBPA/ase. The function of the GAPDH/PGK couple in gluconeogenesis and/or glycolysis still remains to be elucidated. Enzyme reactions with catabolic function are indicated by red arrows, anabolic reactions are indicated by blue arrows, and reversible reactions are indicated by black arrows. Effectors are given in green and red boxes for activators and inhibitors, respectively. The net equation of glucose 6-phosphate conversion to pyruvate via GAPDH/PGK or GAPOR in the modified EMP pathway is indicated in the box (GLGA, glycogen synthase; GLPG, glycogen phosphorylase; PGM, phosphoglucomutase; AK, adenylate kinase; 6PG, 6-phosphogluconate; E4P, erythrose 4-phosphate). (Electron micrograph courtesy of Reinhard Rachel, University of Regensburg, Germany, reproduced with permission.)

tional ADP-dependent glucokinase/phosphofructokinase from *Mca. jannaschii* (58). Only for GAPOR was a dramatic inhibition by ATP observed, which resulted in a total loss of activity at 1 μM ATP (154). Due to this efficient inhibition at ATP concentrations

below the typical intracellular concentrations in other microorganisms, the presence of as-yet-unknown positive effectors was suggested (154). Analysis at the transcript and enzyme levels revealed that GAPOR was expressed constitutively throughout the

different growth phases, whereas GAPDH with predicted gluconeogenic function was observed mainly in the early growth stages of the culture.

Flux balance analysis using the stoichiometric multispecies model established for the syntrophic growth of *Desulfovibrio vulgaris* and *Mco. maripaludis* (577) was performed in order to establish a possible physiological function for GAPOR and to analyze a possible role of cycling by the concerted action of GAPOR, PGK, and GAPDH forming an ATP-dependent NADPH:ferredoxin oxidoreductase reaction (154). The model predicts a metabolic role of GAPOR only under nonoptimal, non-steady-state growth conditions, such as stationary phase or starvation. The authors of that study suggest that the effective inhibition of GAPOR by ATP might allow limiting glycogen degradation to conditions of starvation, resulting in ATP depletion and, thus, GAPOR activation. In addition, a possible role of ATP inhibition in preventing futile cycling, i.e., the ATP-driven NADPH-dependent reduction of ferredoxin via PGK, GAPDH, and GAPOR, was discussed.

In contrast, a recent genetic/transcriptomic study by Costa et al. (578) rather supports the idea that energy spilling (i.e., futile cycling) might play an important physiological role in *Mco. maripaludis* under conditions of H₂ and formate excess. A significant decrease in growth yield relative to methane production was observed under conditions of H₂ and formate excess in a continuous defined culture. Notably, different mutants, including, among others, glycogen synthase (*glgA*) and carbon monoxide dehydrogenase (*cdh*) mutants, showed no obvious effect on growth yields, and it was suggested that intracellular carbon storage (i.e., glycogen formation) or a transcriptional response to methanogenesis plays no obvious role. Those authors proposed common energy spilling in methanogenic *Archaea* driven by ATP-dependent or membrane potential-driven futile cycling to maintain low H₂/formate concentrations, which might be advantageous in regard to competition with other H₂/formate utilizers as well as improved growth of both partners during syntrophic growth (578). A recent genetic study in *Mco. maripaludis* confirmed that the GAPOR-dependent pathway of ferredoxin reduction is able to provide anaplerotic electrons for methanogenesis, and a strain missing the seven hydrogenases capable of H₂-independent growth with formate as the sole electron donor was constructed (580). Therefore, the role of GAPOR is still under debate, and further studies are awaited in order to unravel the regulation at the GAP level in *Mco. maripaludis* and to elucidate a possible role in energy spilling.

CONCLUSION

In this review, we have described the complexity of archaeal carbohydrate metabolism, which is characterized by numerous examples of nonhomologous gene replacement as well as new unusual metabolic pathways.

In accordance with the invention of “new” unusual enzymes, often with different regulatory properties, classical regulation sites well established in *Bacteria* and *Eukarya* are lost. For example, in the EMP pathway, classical control sites, i.e., the irreversible reactions catalyzed by antagonistic enzyme couples (hexokinase/glucose-6-phosphatase [*Eukarya*] and phosphofructokinase/fructose-1,6-bisphosphatase and pyruvate kinase/phosphoenolpyruvate synthetase [*Bacteria* and *Archaea*]) are absent. All archaeal kinases characterized so far, such as ADP- and ATP-dependent glucokinases/hexokinases; ADP-, ATP-, and PP_i-dependent phosphofructokinases; and pyruvate kinases (with the exceptions of *Tpl. acidophilum* AMP-

stimulated PK and the 3PG-stimulated PK from *Pyb. aerophilum*) (244), exhibit no allosteric properties. The predominant enzyme under allosteric control identified so far in different (hyper)thermophilic *Archaea* (e.g., *Sul. solfataricus*, *Sul. tokodaii*, *Tco. kodakarensis*, and *Tpt. tenax*) is GAPN, and an essential glycolytic function was demonstrated. Further evidence for a shift of the control point to the C₃/GAP level in mesophiles also comes from *Hfx. volcanii*, with two antagonistic GAPDHs, and from *Mco. maripaludis*, with GAPOR in addition to the GAPDH/PGK enzyme couple. A second control point in *Archaea* seems to be established at the level of PEP-pyruvate conversion, which is, however, less conserved and seems to be influenced largely by the cosubstrate specificity of the respective sugar kinases (e.g., PP_i-dependent PFK and PPDK in addition to PK and PEPS in *Tpt. tenax*; ADP-GK/PFK and glycolytic PEPS for ATP generation from AMP in *Thermococcales*).

As outlined above, archaeal metabolism is characterized by a fascinating complexity resembling that of *Bacteria* and primitive *Eukarya*. However, it is characterized by many new, unusual pathways and enzymes, often with new regulatory properties. Although the understanding of the regulation of archaeal metabolism is still in its beginning, the third domain of life offers new, exciting resources, such as new enzymes (e.g., extremozymes) for utilization in white biotechnology as well as new enzymes or alternative pathways, “biobricks,” for metabolic engineering and synthetic biology, allowing the combination of unique archaeal and bacterial features. The development of genetic systems in archaeal model organisms now enables metabolic engineering and design of *Archaea* for industrial applications (451).

ACKNOWLEDGMENTS

We are most grateful to all colleagues and friends who contributed to the understanding of archaeal metabolism and share enthusiasm for this fascinating domain of life.

For continuous support of our research by generous grants, we acknowledge the Bundesministerium für Bildung und Forschung (BMBF), the Deutsche Forschungsgemeinschaft (DFG), the European Union Framework 7 Programme, and the Mercator Research Center Ruhr (MERCUR). D. Esser was supported by the DFG (grant SI 642/10-1) and B. Rauch by the DFG GRK 1431 (Transcription, chromatin structure, and DNA repair in development and differentiation [UDE]).

REFERENCES

1. Woese CR, Fox GE. 1977. Phylogenetic structure of the prokaryotic domain: the primary kingdoms. Proc. Natl. Acad. Sci. U. S. A. 74:5088–5090. <http://dx.doi.org/10.1073/pnas.74.11.5088>.
2. Woese CR, Kandler O, Wheelis ML. 1990. Towards a natural system of organisms: proposal for the domains Archaea, Bacteria, and Eucarya. Proc. Natl. Acad. Sci. U. S. A. 87:4576–4579. <http://dx.doi.org/10.1073/pnas.87.12.4576>.
3. DeLong EF. 1998. Everything in moderation: Archaea as ‘non-extremophiles’. Curr. Opin. Genet. Dev. 8:649–654. [http://dx.doi.org/10.1016/S0959-437X\(98\)80032-4](http://dx.doi.org/10.1016/S0959-437X(98)80032-4).
4. DeLong EF, Pace NR. 2001. Environmental diversity of bacteria and archaea. Syst. Biol. 50:470–478. <http://dx.doi.org/10.1080/10635150118513>.
5. DeLong E. 1998. Archaeal means and extremes. Science 280:542–543. <http://dx.doi.org/10.1126/science.280.5363.542>.
6. Bell SD, Jackson SP. 1998. Transcription in archaea. Cold Spring Harb. Symp. Quant. Biol. 63:41–51. <http://dx.doi.org/10.1101/sqb.1998.63.41>.
7. Bell SD, Magill CP, Jackson SP. 2001. Basal and regulated transcription in archaea. Biochem. Soc. Trans. 29:392–395. <http://dx.doi.org/10.1042/BST0290392>.
8. Geiduschek EP, Ouhammou M. 2005. Archaeal transcription and its regulators. Mol. Microbiol. 56:1397–1407. <http://dx.doi.org/10.1111/j.1365-2958.2005.04627.x>.

9. Grohmann D, Werner F. 2011. Recent advances in the understanding of archaeal transcription. *Curr. Opin. Microbiol.* 14:328–334. <http://dx.doi.org/10.1016/j.mib.2011.04.012>.
10. Hickey AJ, Conway de Macario E, Macario AJ. 2002. Transcription in the archaeal basal factors, regulation, and stress-gene expression. *Crit. Rev. Biochem. Mol. Biol.* 37:537–599. <http://dx.doi.org/10.1080/10409230290771555>.
11. Soppa J. 2001. Basal and regulated transcription in archaea. *Adv. Appl. Microbiol.* 50:171–217. [http://dx.doi.org/10.1016/S0065-2164\(01\)50006-4](http://dx.doi.org/10.1016/S0065-2164(01)50006-4).
12. Soppa J. 1999. Transcription initiation in archaea: facts, factors and future aspects. *Mol. Microbiol.* 31:1295–1305. <http://dx.doi.org/10.1046/j.1365-2958.1999.01273.x>.
13. Albers SV, Meyer BH. 2011. The archaeal cell envelope. *Nat. Rev. Microbiol.* 9:414–426. <http://dx.doi.org/10.1038/nrmicro2576>.
14. Schönheit P, Schäfer T. 1995. Metabolism of hyperthermophiles. *World J. Microbiol. Biotechnol.* 11:26–57. <http://dx.doi.org/10.1007/BF00339135>.
15. Bryant DA, Frigaard NU. 2006. Prokaryotic photosynthesis and phototrophy illuminated. *Trends Microbiol.* 14:488–496. <http://dx.doi.org/10.1016/j.tim.2006.09.001>.
16. Melendez-Hevia E, Waddell TG, Heinrich R, Montero F. 1997. Theoretical approaches to the evolutionary optimization of glycolysis—chemical analysis. *Eur. J. Biochem.* 244:527–543. <http://dx.doi.org/10.1111/j.1432-1033.1997.t01-1-00527.x>.
17. Galperin MY, Koonin EV. 1999. Functional genomics and enzyme evolution. Homologous and analogous enzymes encoded in microbial genomes. *Genetica* 106:159–170.
18. Makarova KS, Aravind L, Galperin MY, Grishin NV, Tatusov RL, Wolf YI, Koonin EV. 1999. Comparative genomics of the Archaea (Euryarchaeota): evolution of conserved protein families, the stable core, and the variable shell. *Genome Res.* 9:608–628.
19. Morris BEL, Henneberger R, Huber H, Moissl-Eichinger C. 2013. Microbial syntrophy: interaction for the common good. *FEMS Microbiol. Rev.* 37:384–406. <http://dx.doi.org/10.1111/1574-6976.12019>.
20. Podar M, Makarova K, Graham D, Wolf Y, Koonin E, Reysenbach A-L. 2013. Insights into archaeal evolution and symbiosis from the genomes of a nanoarchaeon and its inferred crenarchaeal host from obsidian pool, Yellowstone National Park. *Biol. Direct* 8:9. <http://dx.doi.org/10.1186/1745-6150-8-9>.
21. Elkins JG, Podar M, Graham DE, Makarova KS, Wolf Y, Randau L, Hedlund BP, Brochier-Armanet C, Kunin V, Anderson I, Lapidus A, Goltsman E, Barry K, Koonin EV, Hugenholtz P, Kyrpides N, Wanner G, Richardson P, Keller M, Stetter KO. 2008. A korarchaeal genome reveals insights into the evolution of the archaea. *Proc. Natl. Acad. Sci. U. S. A.* 105:8102–8107. <http://dx.doi.org/10.1073/pnas.0801980105>.
22. Barns SM, Delwiche CF, Palmer JD, Pace NR. 1996. Perspectives on archaeal diversity, thermophily and monophly from environmental rRNA sequences. *Proc. Natl. Acad. Sci. U. S. A.* 93:9188–9193. <http://dx.doi.org/10.1073/pnas.93.17.9188>.
23. Brochier-Armanet C, Boussau B, Gribaldo S, Forterre P. 2008. Mesophilic crenarchaeota: proposal for a third archaeal phylum, the thaumarchaeota. *Nat. Rev. Microbiol.* 6:245–252. <http://dx.doi.org/10.1038/nrmicro1852>.
24. Schleper C, Nicol GW. 2010. Ammonia-oxidising archaea—physiology, ecology and evolution, p 1–41. In Robert KP (ed), *Advances in microbial physiology*, vol 57. Academic Press, San Diego, CA.
25. Nunoura T, Takaki Y, Kakuta J, Nishi S, Sugahara J, Kazama H, Chee G-J, Hattori M, Kanai A, Atomi H, Takai K, Takami H. 2011. Insights into the evolution of archaea and eukaryotic protein modifier systems revealed by the genome of a novel archaeal group. *Nucleic Acids Res.* 39:3204–3223. <http://dx.doi.org/10.1093/nar/gkq1228>.
26. Brochier-Armanet C, Forterre P, Gribaldo S. 2011. Phylogeny and evolution of the archaea: one hundred genomes later. *Curr. Opin. Microbiol.* 14:274–281. <http://dx.doi.org/10.1016/j.mib.2011.04.015>.
27. Atomi H, Imanaka T, Fukui T. 2012. Overview of the genetic tools in the Archaea. *Front. Microbiol.* 3:337. <http://dx.doi.org/10.3389/fmicb.2012.00337>.
28. Leigh JA, Albers SV, Atomi H, Allers T. 2011. Model organisms for genetics in the domain Archaea: methanogens, halophiles, Thermococcales and Sulfolobales. *FEMS Microbiol. Rev.* 35:577–608. <http://dx.doi.org/10.1111/j.1574-6976.2011.00265.x>.
29. Siebers B, Schönheit P. 2005. Unusual pathways and enzymes of central carbohydrate metabolism in archaea. *Curr. Opin. Microbiol.* 8:695–705. <http://dx.doi.org/10.1016/j.mib.2005.10.014>.
30. Van Der Oost J, Siebers B. 2007. The glycolytic pathways of Archaea: evolution by tinkering, p 247–259. In Garrett RA, Klenk H-P (ed), *Archaea: evolution, physiology and molecular biology*, vol 1. Blackwell Publishing, Singapore.
31. Zaparty M, Zaigler A, Stamme C, Soppa J, Hensel R, Siebers B. 2008. DNA microarray analysis of the central carbohydrate metabolism: glycolytic/gluconeogenic carbon switch in the hyperthermophilic crenarchaeum *Thermoproteus tenax*. *J. Bacteriol.* 190:2231–2238. <http://dx.doi.org/10.1128/JB.01524-07>.
32. Zaparty M, Siebers B. 2010. Physiology, metabolism and enzymology of thermoacidophiles, p 601–639. In Horikoshi K, Antranikian G, Bull AT, Robb FT, Stetter KO (ed), *Extremophiles handbook*, vol 1. Springer, Tokyo, Japan.
33. Danson MJ. 1993. Chapter 1. Central metabolism of the archaea, p 1–24. In Kates M, Kushner DJ, Matheson AT (ed), *New comprehensive biochemistry*, vol 26. *The biochemistry of Archaea (Archaeabacteria)*. Elsevier, Philadelphia, PA.
34. Danson MJ, Hough DW. 2005. Promiscuity in the archaea: the enzymology of their metabolic pathways. *Biochemistry (Lond.)* 27:17–21.
35. Sato T, Atomi H. 2011. Novel metabolic pathways in archaea. *Curr. Opin. Microbiol.* 14:307–314. <http://dx.doi.org/10.1016/j.mib.2011.04.014>.
36. Verhees CH, Kengen SW, Tuininga JE, Schut GJ, Adams MW, De Vos WM, Van Der Oost J. 2003. The unique features of glycolytic pathways in archaea. *Biochem. J.* 375:231–246. <http://dx.doi.org/10.1042/BJ20021472>.
37. Sakuraba H, Goda S, Ohshima T. 2004. Unique sugar metabolism and novel enzymes of hyperthermophilic archaea. *Chem. Rec.* 3:281–287. <http://dx.doi.org/10.1002/tcr.10066>.
38. Bar-Even A, Flamholz A, Noor E, Milo R. 2012. Rethinking glycolysis: on the biochemical logic of metabolic pathways. *Nat. Chem. Biol.* 8:509–517. <http://dx.doi.org/10.1038/nchembio.971>.
39. Siebers B, Wendisch VF, Hensel R. 1997. Carbohydrate metabolism in *Thermoproteus tenax*: in vivo utilization of the non-phosphorylative Entner-Doudoroff pathway and characterization of its first enzyme, glucose dehydrogenase. *Arch. Microbiol.* 168:120–127. <http://dx.doi.org/10.1007/s002030050477>.
40. Selig M, Xavier KB, Santos H, Schönheit P. 1997. Comparative analysis of Embden-Meyerhof and Entner-Doudoroff glycolytic pathways in hyperthermophilic archaea and the bacterium *Thermotoga*. *Arch. Microbiol.* 167:217–232.
41. Reher M, Gebhard S, Schönheit P. 2007. Glyceraldehyde-3-phosphate ferredoxin oxidoreductase (GAPOR) and nonphosphorylating glyceraldehyde-3-phosphate dehydrogenase (GAPN), key enzymes of the respective modified Embden-Meyerhof pathways in the hyperthermophilic crenarchaeota *Pyrobaculum aerophilum* and *Aeropyrum pernix*. *FEMS Microbiol. Lett.* 273:196–205. <http://dx.doi.org/10.1111/j.1574-6968.2007.00787.x>.
42. Labes A, Schönheit P. 2001. Sugar utilization in the hyperthermophilic sulfate-reducing archaeon *Archaeoglobus fulgidus* strain 7324: starch degradation to acetate and CO₂ via a modified Embden-Meyerhof pathway and acetyl-CoA synthetase (ADP-forming). *Arch. Microbiol.* 176:329–338. <http://dx.doi.org/10.1007/s002030100330>.
43. Ronimus RS, Morgan HW. 2003. Distribution and phylogenies of enzymes of the Embden-Meyerhof-Parnas pathway from archaea and hyperthermophilic bacteria support a gluconeogenic origin of metabolism. *Archaea* 1:199–221. <http://dx.doi.org/10.1155/2003/162593>.
44. Kawai S, Mukai T, Mori S, Mikami B, Murata K. 2005. Hypothesis: structures, evolution, and ancestor of glucose kinases in the hexokinase family. *J. Biosci. Bioeng.* 99:320–330. <http://dx.doi.org/10.1263/jbb.99.320>.
45. Fothergill-Gilmore LA, Michels PAM. 1993. Evolution of glycolysis. *Prog. Biophys. Mol. Biol.* 59:105–235. [http://dx.doi.org/10.1016/0079-6107\(93\)90001-Z](http://dx.doi.org/10.1016/0079-6107(93)90001-Z).
46. Hansen T, Reichstein B, Schmid R, Schönheit P. 2002. The first archaeal ATP-dependent glucokinase, from the hyperthermophilic crenarchaeon *Aeropyrum pernix*, represents a monomeric, extremely thermostable ROK glucokinase with broad hexose specificity. *J. Bacteriol.* 184:5955–5965. <http://dx.doi.org/10.1128/JB.184.21.5955-5965.2002>.
47. Aleshin AE, Kirby C, Liu X, Bourenkov GP, Bartunik HD, Fromm HJ, Honzatko RB. 2000. Crystal structures of mutant monomeric hexokinase I reveal multiple ADP binding sites and conformational changes

- relevant to allosteric regulation. *J. Mol. Biol.* 296:1001–1015. <http://dx.doi.org/10.1006/jmbi.1999.3494>.
48. Lunin VV, Li Y, Schrag JD, Iannuzzi P, Cygler M, Matte A. 2004. Crystal structures of *Escherichia coli* ATP-dependent glucokinase and its complex with glucose. *J. Bacteriol.* 186:6915–6927. <http://dx.doi.org/10.1128/JB.186.20.6915-6927.2004>.
 49. Nishimasu H, Fushinobu S, Shoun H, Wakagi T. 2007. Crystal structures of an ATP-dependent hexokinase with broad substrate specificity from the hyperthermophilic archaeon *Sulfolobus tokodaii*. *J. Biol. Chem.* 282:9923–9931. <http://dx.doi.org/10.1074/jbc.M610678200>.
 50. Arora KK, Filburn CR, Pedersen PL. 1991. Glucose phosphorylation. Site-directed mutations which impair the catalytic function of hexokinase. *J. Biol. Chem.* 266:5359–5362.
 51. Kengen SW, Tuininga JE, de Bok FA, Stams AJ, de Vos WM. 1995. Purification and characterization of a novel ADP-dependent glucokinase from the hyperthermophilic archaeon *Pyrococcus furiosus*. *J. Biol. Chem.* 270:30453–30457. <http://dx.doi.org/10.1074/jbc.270.51.30453>.
 52. Kengen SW, Tuininga JE, Verhees CH, van der Oost J, Stams AJ, de Vos WM. 2001. ADP-dependent glucokinase and phosphofructokinase from *Pyrococcus furiosus*. *Methods Enzymol.* 331:41–53. [http://dx.doi.org/10.1016/S0076-6879\(01\)31045-5](http://dx.doi.org/10.1016/S0076-6879(01)31045-5).
 53. Labes A, Schonheit P. 2003. ADP-dependent glucokinase from the hyperthermophilic sulfate-reducing archaeon *Archaeoglobus fulgidus* strain 7324. *Arch. Microbiol.* 180:69–75. <http://dx.doi.org/10.1007/s00203-003-0563-2>.
 54. Koga S, Yoshioka I, Sakuraba H, Takahashi M, Sakasegawa S, Shimizu S, Ohshima T. 2000. Biochemical characterization, cloning, and sequencing of ADP-dependent (AMP-forming) glucokinase from two hyperthermophilic archaea, *Pyrococcus furiosus* and *Thermococcus litoralis*. *J. Biochem.* 128:1079–1085. <http://dx.doi.org/10.1093/oxfordjournals.jbchem.a022836>.
 55. Dorr C, Zaparty M, Tjaden B, Brinkmann H, Siebers B. 2003. The hexokinase of the hyperthermophile *Thermoproteus tenax*. ATP-dependent hexokinases and ADP-dependent glucokinases, two alternatives for glucose phosphorylation in archaea. *J. Biol. Chem.* 278:18744–18753. <http://dx.doi.org/10.1074/jbc.M301914200>.
 56. Cárdenas ML, Cornish-Bowden A, Ureta T. 1998. Evolution and regulatory role of the hexokinases. *Biochim. Biophys. Acta* 1401:242–264. [http://dx.doi.org/10.1016/S0167-4889\(97\)00150-X](http://dx.doi.org/10.1016/S0167-4889(97)00150-X).
 57. Guixe V, Merino F. 2009. The ADP-dependent sugar kinase family: kinetic and evolutionary aspects. *IUBMB Life* 61:753–761. <http://dx.doi.org/10.1002/iub.217>.
 58. Sakuraba H, Yoshioka I, Koga S, Takahashi M, Kitahama Y, Satomura T, Kawakami R, Ohshima T. 2002. ADP-dependent glucokinase/phosphofructokinase, a novel bifunctional enzyme from the hyperthermophilic archaeon *Methanococcus jannaschii*. *J. Biol. Chem.* 277:12495–12498. <http://dx.doi.org/10.1074/jbc.C200059200>.
 59. Ito S, Fushinobu S, Jeong JJ, Yoshioka I, Koga S, Shoun H, Wakagi T. 2003. Crystal structure of an ADP-dependent glucokinase from *Pyrococcus furiosus*: implications for a sugar-induced conformational change in ADP-dependent kinase. *J. Mol. Biol.* 331:871–883. [http://dx.doi.org/10.1016/S0022-2836\(03\)00792-7](http://dx.doi.org/10.1016/S0022-2836(03)00792-7).
 60. Ito S, Fushinobu S, Yoshioka I, Koga S, Matsuzawa H, Wakagi T. 2001. Structural basis for the ADP-specificity of a novel glucokinase from a hyperthermophilic archaeon. *Structure* 9:205–214. [http://dx.doi.org/10.1016/S0969-2126\(01\)00577-9](http://dx.doi.org/10.1016/S0969-2126(01)00577-9).
 61. Tsuge H, Sakuraba H, Kobe T, Kujime A, Katunuma N, Ohshima T. 2002. Crystal structure of the ADP-dependent glucokinase from *Pyrococcus horikoshii* at 2.0 Å resolution: a large conformational change in ADP-dependent glucokinase. *Protein Sci.* 11:2456–2463. <http://dx.doi.org/10.1101/ps.0215602>.
 62. Merino F, Rivas-Pardo JA, Caniuguir A, Garcia I, Guixe V. 2012. Catalytic and regulatory roles of divalent metal cations on the phosphoryl-transfer mechanism of ADP-dependent sugar kinases from hyperthermophilic archaea. *Biochimie* 94:516–524. <http://dx.doi.org/10.1016/j.biochi.2011.08.021>.
 63. Hansen T, Schonheit P. 2003. ATP-dependent glucokinase from the hyperthermophilic bacterium *Thermotoga maritima* represents an extremely thermophilic ROK glucokinase with high substrate specificity. *FEMS Microbiol. Lett.* 226:405–411. [http://dx.doi.org/10.1016/S0378-1097\(03\)00642-6](http://dx.doi.org/10.1016/S0378-1097(03)00642-6).
 64. Nakamura T, Kashima Y, Mine S, Oku T, Uegaki K. 2012. Characterization and crystal structure of the thermophilic ROK hexokinase from *Thermus thermophilus*. *J. Biosci. Bioeng.* 114:150–154. <http://dx.doi.org/10.1016/j.jbiosc.2012.03.018>.
 65. Nocek B, Stein AJ, Jedrzejczak R, Cuff ME, Li H, Volkart L, Joachimiak A. 2011. Structural studies of ROK fructokinase YdhR from *Bacillus subtilis*: insights into substrate binding and fructose specificity. *J. Mol. Biol.* 406:325–342. <http://dx.doi.org/10.1016/j.jmb.2010.12.021>.
 66. Miyazono K, Tabei N, Morita S, Ohnishi Y, Horinouchi S, Tanokura M. 2012. Substrate recognition mechanism and substrate-dependent conformational changes of an ROK family glucokinase from *Streptomyces griseus*. *J. Bacteriol.* 194:607–616. <http://dx.doi.org/10.1128/JB.06173-11>.
 67. Nishimasu H, Fushinobu S, Shoun H, Wakagi T. 2006. Identification and characterization of an ATP-dependent hexokinase with broad substrate specificity from the hyperthermophilic archaeon *Sulfolobus tokodaii*. *J. Bacteriol.* 188:2014–2019. <http://dx.doi.org/10.1128/JB.188.5.2014-2019.2006>.
 68. Altekar W, Rangaswamy V. 1992. Degradation of endogenous fructose during catabolism of sucrose and mannitol in halophilic archaeabacteria. *Arch. Microbiol.* 158:356–363. <http://dx.doi.org/10.1007/BF00245365>.
 69. Altekar W, Rangaswamy V. 1990. Indication of a modified EMP pathway for fructose breakdown in a halophilic archaeabacterium. *FEMS Microbiol. Lett.* 69:139–143. <http://dx.doi.org/10.1111/j.1574-6968.1990.tb04190.x>.
 70. Johnsen U, Selig M, Xavier KB, Santos H, Schonheit P. 2001. Different glycolytic pathways for glucose and fructose in the halophilic archaeon *Halococcus saccharolyticus*. *Arch. Microbiol.* 175:52–61. <http://dx.doi.org/10.1007/s002030000237>.
 71. Altekar W, Rangaswamy V. 1991. Ketohexokinase (ATP:d-fructose 1-phosphotransferase) initiates fructose breakdown via the modified EMP pathway in halophilic archaeabacteria. *FEMS Microbiol. Lett.* 83: 241–246. <http://dx.doi.org/10.1111/j.1574-6968.1991.tb04471.x>.
 72. Rangaswamy V, Altekar W. 1994. Ketohexokinase (ATP:D-fructose 1-phosphotransferase) from a halophilic archaeabacterium, *Haloarcula vallismortis*: purification and properties. *J. Bacteriol.* 176:5505–5512.
 73. Trinh CH, Asipu A, Bonthon DT, Phillips SE. 2009. Structures of alternatively spliced isoforms of human ketohexokinase. *Acta Cryst. Dalton Trans.* 65:201–211. <http://dx.doi.org/10.1107/S090744908041115>.
 74. Hansen T, Schlichting B, Felgendreher M, Schonheit P. 2005. Cupin-type phosphoglucose isomerases (cupin-PGIs) constitute a novel metal-dependent PGI family representing a convergent line of PGI evolution. *J. Bacteriol.* 187:1621–1631. <http://dx.doi.org/10.1128/JB.187.5.1621-1631.2005>.
 75. Watanebe H, Takehana K, Date M, Shinozaki T, Raz A. 1996. Tumor cell autocrine motility factor is the neuregulin/phosphohexose isomerase polypeptide. *Cancer Res.* 56:2960–2963.
 76. Xu W, Seiter K, Feldman E, Ahmed T, Chiao JW. 1996. The differentiation and maturation mediator for human myeloid leukemia cells shares homology with neuregulin or phosphoglucose isomerase. *Blood* 87:4502–4506.
 77. Chou C-C, Sun Y-J, Meng M, Hsiao C-D. 2000. The crystal structure of phosphoglucose isomerase/autocrine motility factor/neuregulin complexed with its carbohydrate phosphate inhibitors suggests its substrate/receptor recognition. *J. Biol. Chem.* 275:23154–23160. <http://dx.doi.org/10.1074/jbc.M002017200>.
 78. Davies C, Muirhead H, Chirgwin J. 2003. The structure of human phosphoglucose isomerase complexed with a transition-state analogue. *Acta Cryst. Dalton Trans.* 59:1111–1113. <http://dx.doi.org/10.1107/S090744903007352>.
 79. Jeffery CJ, Bahnsen BJ, Chien W, Ringe D, Petsko GA. 2000. Crystal structure of rabbit phosphoglucose isomerase, a glycolytic enzyme that moonlights as neuregulin, autocrine motility factor, and differentiation mediator. *Biochemistry* 39:955–964. <http://dx.doi.org/10.1021/bi991604m>.
 80. Read J, Pearce J, Li X, Muirhead H, Chirgwin J, Davies C. 2001. The crystal structure of human phosphoglucose isomerase at 1.6 Å resolution: implications for catalytic mechanism, cytokine activity and haemolytic anaemia. *J. Mol. Biol.* 309:447–463. <http://dx.doi.org/10.1006/jmbi.2001.4680>.
 81. Rudolph B, Hansen T, Schonheit P. 2004. Glucose-6-phosphate isomerase from the hyperthermophilic archaeon *Methanococcus jannaschii*: characterization of the first archaeal member of the phosphoglucose isomerase superfamily. *Arch. Microbiol.* 181:82–87. <http://dx.doi.org/10.1007/s00203-003-0626-4>.
 82. Hansen T, Urbanke C, Schonheit P. 2004. Bifunctional phosphoglu-

- cose/phosphomannose isomerase from the hyperthermophilic archaeon *Pyrobaculum aerophilum*. *Extremophiles* 8:507–512. <http://dx.doi.org/10.1007/s00792-004-0411-6>.
83. Hansen T, Wendorff D, Schonheit P. 2004. Bifunctional phosphoglucose/phosphomannose isomerases from the archaea *Aeropyrum pernix* and *Thermoplasma acidophilum* constitute a novel enzyme family within the phosphoglucose isomerase superfamily. *J. Biol. Chem.* 279:2262–2272. <http://dx.doi.org/10.1074/jbc.M309849200>.
 84. Siebers B, Tjaden B, Michalke K, Dorr C, Ahmed H, Zaparty M, Gordon P, Sensen CW, Zibat A, Klenk HP, Schuster SC, Hensel R. 2004. Reconstruction of the central carbohydrate metabolism of *Thermoproteus tenax* by use of genomic and biochemical data. *J. Bacteriol.* 186:2179–2194. <http://dx.doi.org/10.1128/JB.186.7.2179-2194.2004>.
 85. Swan MK, Hansen T, Schonheit P, Davies C. 2004. Crystallization and preliminary X-ray diffraction analysis of phosphoglucose/phosphomannose isomerase from *Pyrobaculum aerophilum*. *Acta Crystallogr. D Biol. Crystallogr.* 60:1481–1483. <http://dx.doi.org/10.1107/S0907444904014052>.
 86. Swan MK, Hansen T, Schonheit P, Davies C. 2004. A novel phosphoglucose isomerase (PGI)/phosphomannose isomerase from the crenarchaeon *Pyrobaculum aerophilum* is a member of the PGI superfamily: structural evidence at 1.16-A resolution. *J. Biol. Chem.* 279:39838–39845. <http://dx.doi.org/10.1074/jbc.M406855200>.
 87. Swan MK, Hansen T, Schonheit P, Davies C. 2004. Structural basis for phosphomannose isomerase activity in phosphoglucose isomerase from *Pyrobaculum aerophilum*: a subtle difference between distantly related enzymes. *Biochemistry* 43:14088–14095. <http://dx.doi.org/10.1021/bi048608y>.
 88. Hansen T, Oehlmann M, Schonheit P. 2001. Novel type of glucose-6-phosphate isomerase in the hyperthermophilic archaeon *Pyrococcus furiosus*. *J. Bacteriol.* 183:3428–3435. <http://dx.doi.org/10.1128/JB.183.11.3428-3435.2001>.
 89. Verhees CH, Huynen MA, Ward DE, Schiltz E, de Vos WM, van der Oost J. 2001. The phosphoglucose isomerase from the hyperthermophilic archaeon *Pyrococcus furiosus* is a unique glycolytic enzyme that belongs to the cupin superfamily. *J. Biol. Chem.* 276:40926–40932. <http://dx.doi.org/10.1074/jbc.M104603200>.
 90. Jeong JJ, Fushinobu S, Ito S, Jeon BS, Shoun H, Wakagi T. 2003. Characterization of the cupin-type phosphoglucose isomerase from the hyperthermophilic archaeon *Thermococcus litoralis*. *FEBS Lett.* 535:200–204. [http://dx.doi.org/10.1016/S0014-5793\(02\)03900-5](http://dx.doi.org/10.1016/S0014-5793(02)03900-5).
 91. Berrisford JM, Akerboom J, Turnbull AP, de Geus D, Sedelnikova SE, Staton I, McLeod CW, Verhees CH, van der Oost J, Rice DW, Baker PJ. 2003. Crystal structure of *Pyrococcus furiosus* phosphoglucose isomerase. Implications for substrate binding and catalysis. *J. Biol. Chem.* 278:33290–33297. <http://dx.doi.org/10.1074/jbc.M305170200>.
 92. Swan MK, Hansen T, Schonheit P, Davies C. 2003. Crystallization and preliminary X-ray diffraction analysis of phosphoglucose isomerase from *Pyrococcus furiosus*. *Protein Pept. Lett.* 10:517–520. <http://dx.doi.org/10.2174/0929866033478762>.
 93. Hansen T, Schlichting B, Grotzinger J, Swan MK, Davies C, Schonheit P. 2005. Mutagenesis of catalytically important residues of cupin type phosphoglucose isomerase from *Archaeoglobus fulgidus*. *FEBS J.* 272: 6266–6275. <http://dx.doi.org/10.1111/j.1742-4658.2005.05007.x>.
 94. Berrisford JM, Akerboom J, Brouns S, Sedelnikova SE, Turnbull AP, van der Oost J, Salmon L, Hardre R, Murray IA, Blackburn GM, Rice DW, Baker PJ. 2004. The structures of inhibitor complexes of *Pyrococcus furiosus* phosphoglucose isomerase provide insights into substrate binding and catalysis. *J. Mol. Biol.* 343:649–657. <http://dx.doi.org/10.1016/j.jmb.2004.08.061>.
 95. Berrisford JM, Hounslow AM, Akerboom J, Hagen WR, Brouns SJ, van der Oost J, Murray IA, Blackburn GM, Walther JP, Rice DW, Baker PJ. 2006. Evidence supporting a cis-enediol-based mechanism for *Pyrococcus furiosus* phosphoglucose isomerase. *J. Mol. Biol.* 358:1353–1366. <http://dx.doi.org/10.1016/j.jmb.2006.03.015>.
 96. Swan MK, Solomons JT, Beeson CC, Hansen T, Schonheit P, Davies C. 2003. Structural evidence for a hydride transfer mechanism of catalysis in phosphoglucose isomerase from *Pyrococcus furiosus*. *J. Biol. Chem.* 278:47261–47268. <http://dx.doi.org/10.1074/jbc.M308603200>.
 97. Wu R, Xie H, Cao Z, Mo Y. 2008. Combined quantum mechanics/molecular mechanics study on the reversible isomerization of glucose and fructose catalyzed by *Pyrococcus furiosus* phosphoglucose isomerase. *J. Am. Chem. Soc.* 130:7022–7031. <http://dx.doi.org/10.1021/ja710633c>.
 98. Wu LF, Reizer A, Reizer J, Cai B, Tomich JM, Saier MH, Jr. 1991. Nucleotide sequence of the *Rhodobacter capsulatus fruK* gene, which encodes fructose-1-phosphate kinase: evidence for a kinase superfamily including both phosphofructokinases of *Escherichia coli*. *J. Bacteriol.* 173: 3117–3127.
 99. Ronimus R, Morgan H. 2001. The biochemical properties and phylogenies of phosphofructokinases from extremophiles. *Extremophiles* 5:357–373. <http://dx.doi.org/10.1007/s007920100215>.
 100. Shirakihara Y, Evans PR. 1988. Crystal structure of the complex of phosphofructokinase from *Escherichia coli* with its reaction products. *J. Mol. Biol.* 204:973–994. [http://dx.doi.org/10.1016/0022-2836\(88\)90056-3](http://dx.doi.org/10.1016/0022-2836(88)90056-3).
 101. Schirmer T, Evans PR. 1990. Structural basis of the allosteric behaviour of phosphofructokinase. *Nature* 343:140–145. <http://dx.doi.org/10.1038/343140a0>.
 102. Poorman RA, Randolph A, Kemp RG, Heinrikson RL. 1984. Evolution of phosphofructokinase—gene duplication and creation of new effector sites. *Nature* 309:467–469. <http://dx.doi.org/10.1038/309467a0>.
 103. Berger SA, Evans PR. 1992. Site-directed mutagenesis identifies catalytic residues in the active site of *Escherichia coli* phosphofructokinase. *Biochemistry* 31:9237–9242. <http://dx.doi.org/10.1021/bi00153a017>.
 104. Siebers B, Hensel R. 2001. Pyrophosphate-dependent phosphofructokinase from *Thermoproteus tenax*. *Methods Enzymol.* 331:54–62. [http://dx.doi.org/10.1016/S0076-6879\(01\)31046-7](http://dx.doi.org/10.1016/S0076-6879(01)31046-7).
 105. Siebers B, Hensel R. 1993. Glucose catabolism of the hyperthermophilic archaeum *Thermoproteus tenax*. *FEMS Microbiol. Lett.* 111:1–7. <http://dx.doi.org/10.1111/j.1574-6968.1993.tb06353.x>.
 106. Moore SA, Ronimus RS, Roberson RS, Morgan HW. 2002. The structure of a pyrophosphate-dependent phosphofructokinase from the Lyme disease spirochete *Borrelia burgdorferi*. *Structure* 10:659–671. [http://dx.doi.org/10.1016/S0969-6216\(02\)00760-8](http://dx.doi.org/10.1016/S0969-6216(02)00760-8).
 107. Siebers B, Klenk HP, Hensel R. 1998. PPi-dependent phosphofructokinase from *Thermoproteus tenax*, an archaeal descendant of an ancient line in phosphofructokinase evolution. *J. Bacteriol.* 180:2137–2143.
 108. Ding YH, Ronimus RS, Morgan HW. 2000. Sequencing, cloning, and high-level expression of the pfp gene, encoding a PP(i)-dependent phosphofructokinase from the extremely thermophilic eubacterium *Dictyoglomus thermophilum*. *J. Bacteriol.* 182:4661–4666. <http://dx.doi.org/10.1128/JB.182.16.4661-4666.2000>.
 109. Ding YR, Ronimus RS, Morgan HW. 2001. *Thermotoga maritima* phosphofructokinases: expression and characterization of two unique enzymes. *J. Bacteriol.* 183:791–794. <http://dx.doi.org/10.1128/JB.183.2.791-794.2001>.
 110. Kengen SW, de Bok FA, van Loo ND, Dijkema C, Stams AJ, de Vos WM. 1994. Evidence for the operation of a novel Embden-Meyerhof pathway that involves ADP-dependent kinases during sugar fermentation by *Pyrococcus furiosus*. *J. Biol. Chem.* 269:17537–17541.
 111. Tuininga JE, Verhees CH, van der Oost J, Kengen SW, Stams AJ, de Vos WM. 1999. Molecular and biochemical characterization of the ADP-dependent phosphofructokinase from the hyperthermophilic archaeon *Pyrococcus furiosus*. *J. Biol. Chem.* 274:21023–21028. <http://dx.doi.org/10.1074/jbc.274.30.21023>.
 112. Ronimus RS, de Heus E, Morgan HW. 2001. Sequencing, expression, characterisation and phylogeny of the ADP-dependent phosphofructokinase from the hyperthermophilic, euryarchaeal *Thermococcus zilligii*. *Biochim. Biophys. Acta* 1517:384–391. [http://dx.doi.org/10.1016/S0167-4781\(00\)00301-8](http://dx.doi.org/10.1016/S0167-4781(00)00301-8).
 113. Ronimus RS, Koning J, Morgan HW. 1999. Purification and characterization of an ADP-dependent phosphofructokinase from *Thermococcus zilligii*. *Extremophiles* 3:121–129. <http://dx.doi.org/10.1007/s007920050107>.
 114. Hansen T, Schonheit P. 2004. ADP-dependent 6-phosphofructokinase, an extremely thermophilic, non-allosteric enzyme from the hyperthermophilic, sulfate-reducing archaeon *Archaeoglobus fulgidus* strain 7324. *Extremophiles* 8:29–35. <http://dx.doi.org/10.1007/s00792-003-0356-1>.
 115. Verhees CH, Tuininga JE, Kengen SW, Stams AJ, van der Oost J, de Vos WM. 2001. ADP-dependent phosphofructokinases in mesophilic and thermophilic methanogenic archaea. *J. Bacteriol.* 183:7145–7153. <http://dx.doi.org/10.1128/JB.183.24.7145-7153.2001>.
 116. Currie MA, Merino F, Skarina T, Wong AH, Singer A, Brown G, Savchenko A, Caniuguir A, Guixe V, Yakunin AF, Jia Z. 2009. ADP-dependent 6-phosphofructokinase from *Pyrococcus horikoshii* OT3: structure determination and biochemical characterization of PH1645. *J. Biol. Chem.* 284:22664–22671. <http://dx.doi.org/10.1074/jbc.M109.012401>.

117. Merino F, Guixe V. 2008. Specificity evolution of the ADP-dependent sugar kinase family: *in silico* studies of the glucokinase/phosphofructokinase bifunctional enzyme from *Methanocaldococcus jannaschii*. *FEBS J.* 275:4033–4044. <http://dx.doi.org/10.1111/j.1742-4658.2008.06544.x>.
118. Hansen T, Schonheit P. 2001. Sequence, expression, and characterization of the first archaeal ATP-dependent 6-phosphofructokinase, a non-allosteric enzyme related to the phosphofructokinase-B sugar kinase family, from the hyperthermophilic crenarchaeote *Aeropyrum pernix*. *Arch. Microbiol.* 177:62–69. <http://dx.doi.org/10.1007/s00203-001-0359-1>.
119. Hansen T, Schonheit P. 2000. Purification and properties of the first-identified, archaeal, ATP-dependent 6-phosphofructokinase, an extremely thermophilic non-allosteric enzyme, from the hyperthermophile *Desulfurococcus amylolyticus*. *Arch. Microbiol.* 173:103–109. <http://dx.doi.org/10.1007/s002039900114>.
120. Arnfors L, Hansen T, Schonheit P, Ladenstein R, Meining W. 2006. Structure of *Methanocaldococcus jannaschii* nucleoside kinase: an archaeal member of the ribokinase family. *Acta Crystallogr. D Biol. Crystallogr.* 62:1085–1097. <http://dx.doi.org/10.1107/S0907444906024826>.
121. Hansen T, Arnfors L, Ladenstein R, Schonheit P. 2007. The phosphofructokinase-B (MJ0406) from *Methanocaldococcus jannaschii* represents a nucleoside kinase with a broad substrate specificity. *Extremophiles* 11: 105–114. <http://dx.doi.org/10.1007/s00792-006-0018-1>.
122. Potter JA, Kerou M, Lamble HJ, Bull SD, Hough DW, Danson MJ, Taylor GL. 2008. The structure of *Sulfolobus solfataricus* 2-keto-3-deoxygluconate kinase. *Acta Crystallogr. D Biol. Crystallogr.* 64:1283–1287. <http://dx.doi.org/10.1107/S0907444908036111>.
123. Pickl A, Johnsen U, Schonheit P. 2012. Fructose degradation in the haloarchaeon *Haloflexax volcanii* involves a bacterial type phosphoenolpyruvate-dependent phosphotransferase system, fructose-1-phosphate kinase, and class II fructose-1,6-bisphosphate aldolase. *J. Bacteriol.* 194: 3088–3097. <http://dx.doi.org/10.1128/JB.00200-12>.
124. Kornberg HL. 2001. Routes for fructose utilization by *Escherichia coli*. *J. Mol. Microbiol. Biotechnol.* 3:355–359. <http://www.horizonpress.com/backlist/jmmib/v3/v3n3/04.pdf>.
125. Rangaswamy V, Altekar W. 1994. Characterization of 1-phosphofructokinase from halophilic archaeabacterium *Haloarcula vallismortis*. *Biochim. Biophys. Acta* 1201:106–112. [http://dx.doi.org/10.1016/0304-4165\(94\)90158-9](http://dx.doi.org/10.1016/0304-4165(94)90158-9).
126. Siebers B, Brinkmann H, Dorr C, Tjaden B, Lilie H, van der Oost J, Verhees CH. 2001. Archaeal fructose-1,6-bisphosphate aldolases constitute a new family of archaeal type class I aldolase. *J. Biol. Chem.* 276: 28710–28718. <http://dx.doi.org/10.1074/jbc.M103447200>.
127. Yu JP, Ladapo J, Whitman WB. 1994. Pathway of glycogen metabolism in *Methanococcus maripaludis*. *J. Bacteriol.* 176:325–332.
128. Schäfer T, Schonheit P. 1992. Maltose fermentation to acetate, CO₂ and H₂ in the anaerobic hyperthermophilic archaeon *Pyrococcus furiosus*: evidence for the operation of a novel sugar fermentation pathway. *Arch. Microbiol.* 158:188–202. <http://dx.doi.org/10.1007/BF00290815>.
129. Altekar W, Dhar NM. 1988. Archaeabacterial class I and class II aldolases from extreme halophiles. *Orig. Life Evol. Biosph.* 18:59–64. <http://dx.doi.org/10.1007/BF01808780>.
130. Krishnan G, Altekar W. 1991. An unusual class I (Schiff base) fructose-1,6-bisphosphate aldolase from the halophilic archaeabacterium *Haloarcula vallismortis*. *Eur. J. Biochem.* 195:343–350. <http://dx.doi.org/10.1111/j.1432-1033.1991.tb15712.x>.
131. Krishnan G, Altekar W. 1993. Halophilic class I aldolase and glyceraldehyde-3-phosphate dehydrogenase: some salt-dependent structural features. *Biochemistry* 32:791–798. <http://dx.doi.org/10.1021/bi00054a008>.
132. D’Souza SE, Altekar W. 1998. A class II fructose-1,6-bisphosphate aldolase from a halophilic archaeabacterium *Haloflexax mediterranei*. *J. Gen. Appl. Microbiol.* 44:235–241. <http://dx.doi.org/10.2323/jgam.44.235>.
133. Imanaka H, Fukui T, Atomi H, Imanaka T. 2002. Gene cloning and characterization of fructose-1,6-bisphosphate aldolase from the hyperthermophilic archaeon *Thermococcus kodakaraensis* KOD1. *J. Biosci. Bioeng.* 94:237–243. <http://dx.doi.org/10.1263/jbb.94.237>.
134. Lorentzen E, Siebers B, Hensel R, Pohl E. 2005. Mechanism of the Schiff base forming fructose-1,6-bisphosphate aldolase: structural analysis of reaction intermediates. *Biochemistry* 44:4222–4229. <http://dx.doi.org/10.1021/bi048192o>.
135. Lorentzen E, Pohl E, Zwart P, Stark A, Russell RB, Knura T, Hensel R, Siebers B. 2003. Crystal structure of an archaeal class I aldolase and the evolution of (beta alpha)8 barrel proteins. *J. Biol. Chem.* 278:47253–47260. <http://dx.doi.org/10.1074/jbc.M305922200>.
136. Lorentzen E, Siebers B, Hensel R, Pohl E. 2004. Structure, function and evolution of the archaeal class I fructose-1,6-bisphosphate aldolase. *Biochem. Soc. Trans.* 32:259–263. <http://dx.doi.org/10.1042/BST0320259>.
137. Galperin MY, Aravind L, Koonin EV. 2000. Aldolases of the DhnA family: a possible solution to the problem of pentose and hexose biosynthesis in archaea. *FEMS Microbiol. Lett.* 183:259–264. <http://dx.doi.org/10.1111/j.1574-6968.2000.tb08968.x>.
138. Hall DR, Leonard GA, Reed CD, Watt CI, Berry A, Hunter WN. 1999. The crystal structure of *Escherichia coli* class II fructose-1,6-bisphosphate aldolase in complex with phosphoglycolohydroxamate reveals details of mechanism and specificity. *J. Mol. Biol.* 287:383–394. <http://dx.doi.org/10.1006/jmbi.1999.2609>.
139. Kohlhoff M, Dahm A, Hensel R. 1996. Tetrameric triosephosphate isomerase from hyperthermophilic archaea. *FEBS Lett.* 383:245–250. [http://dx.doi.org/10.1016/0014-5793\(96\)00249-9](http://dx.doi.org/10.1016/0014-5793(96)00249-9).
140. Walden H, Taylor G, Lilie H, Knura T, Hensel R. 2004. Triosephosphate isomerase of the hyperthermophile *Thermoproteus tenax*: thermostability is not everything. *Biochem. Soc. Trans.* 32:305. <http://dx.doi.org/10.1042/BST0320305>.
141. Chandrayan SK, Gupta P. 2008. Partial destabilization of native structure by a combination of heat and denaturant facilitates cold denaturation in a hyperthermophile protein. *Proteins* 72:539–546. <http://dx.doi.org/10.1002/prot.22077>.
142. Chandrayan SK, Gupta P. 2009. Attenuation of ionic interactions profoundly lowers the kinetic thermal stability of *Pyrococcus furiosus* triosephosphate isomerase. *Biochim. Biophys. Acta* 1794:905–912. <http://dx.doi.org/10.1016/j.bbap.2009.03.005>.
143. Banerjee M, Gupta K, Balaram H, Balaram P. 2011. Mass spectrometric identification of an intramolecular disulfide bond in thermally inactivated triosephosphate isomerase from a thermophilic organism *Methanocaldococcus jannaschii*. *Rapid Commun. Mass Spectrom.* 25:1915–1923. <http://dx.doi.org/10.1002/rcm.5058>.
144. Schramm A, Kohlhoff M, Hensel R. 2001. Triose-phosphate isomerase from *Pyrococcus woesei* and *Methanothermus fervidus*. *Methods Enzymol.* 331:62–77. [http://dx.doi.org/10.1016/S0076-6879\(01\)31047-9](http://dx.doi.org/10.1016/S0076-6879(01)31047-9).
145. Bell GS, Russell RJ, Kohlhoff M, Hensel R, Danson MJ, Hough DW, Taylor GL. 1998. Preliminary crystallographic studies of triosephosphate isomerase (TIM) from the hyperthermophilic archaeon *Pyrococcus woesei*. *Acta Crystallogr. D Biol. Crystallogr.* 54:1419–1421. <http://dx.doi.org/10.1107/S090744998004910>.
146. Walden H, Bell GS, Russell RJ, Siebers B, Hensel R, Taylor GL. 2001. Tiny TIM: a small, tetrameric, hyperthermostable triosephosphate isomerase. *J. Mol. Biol.* 306:745–757. <http://dx.doi.org/10.1006/jmbi.2000.4433>.
147. Walden H, Taylor GL, Lorentzen E, Pohl E, Lilie H, Schramm A, Knura T, Stubbe K, Tjaden B, Hensel R. 2004. Structure and function of a regulated archaeal triosephosphate isomerase adapted to high temperature. *J. Mol. Biol.* 342:861–875. <http://dx.doi.org/10.1016/j.jmb.2004.07.067>.
148. Gayathri P, Banerjee M, Vijayalakshmi A, Azeez S, Balaram H, Balaram P, Murthy MR. 2007. Structure of triosephosphate isomerase (TIM) from *Methanocaldococcus jannaschii*. *Acta Crystallogr. D Biol. Crystallogr.* 63: 206–220. <http://dx.doi.org/10.1107/S09074490646488>.
149. Schurig H, Beaucamp N, Ostendorp R, Jaenicke R, Adler E, Knowles JR. 1995. Phosphoglycerate kinase and triosephosphate isomerase from the hyperthermophilic bacterium *Thermotoga maritima* form a covalent bifunctional enzyme complex. *EMBO J.* 14:442–451.
150. Knowles JR. 1991. Enzyme catalysis: not different, just better. *Nature* 350:121–124. <http://dx.doi.org/10.1038/350121a0>.
151. Richard JP. 2012. A paradigm for enzyme-catalyzed proton transfer at carbon: triosephosphate isomerase. *Biochemistry* 51:2652–2661. <http://dx.doi.org/10.1021/bi300195b>.
152. Ebel C, Altekar W, Langowski J, Urbanke C, Forest E, Zaccai G. 1995. Solution structure of glyceraldehyde-3-phosphate dehydrogenase from *Haloarcula vallismortis*. *Biophys. Chem.* 54:219–227. [http://dx.doi.org/10.1016/0301-4622\(94\)00137-9](http://dx.doi.org/10.1016/0301-4622(94)00137-9).
153. Ettema TJG, Ahmed H, Geerling ACM, Van Der Oost J, Siebers B. 2008. The non-phosphorylating glyceraldehyde-3-phosphate dehydrogenase (GAPN) of *Sulfolobus solfataricus*: a key-enzyme of the semi-phosphorylative branch of the Entner-Doudoroff pathway. *Extremophiles* 12:75–88. <http://dx.doi.org/10.1007/s00792-007-0082-1>.

154. Park MO, Mizutani T, Jones PR. 2007. Glyceraldehyde-3-phosphate ferredoxin oxidoreductase from *Methanococcus maripaludis*. *J. Bacteriol.* 189:7281–7289. <http://dx.doi.org/10.1128/JB.00828-07>.
155. Reference deleted.
156. Mukund S, Adams MW. 1991. The novel tungsten-iron-sulfur protein of the hyperthermophilic archaeabacterium, *Pyrococcus furiosus*, is an aldehyde ferredoxin oxidoreductase. Evidence for its participation in a unique glycolytic pathway. *J. Biol. Chem.* 266:14208–14216.
157. Heider J, Ma K, Adams MW. 1995. Purification, characterization, and metabolic function of tungsten-containing aldehyde ferredoxin oxidoreductase from the hyperthermophilic and proteolytic archaeon *Thermococcus* strain ES-1. *J. Bacteriol.* 177:4757–4764.
158. Selig M, Schönheit P. 1994. Oxidation of organic compounds to CO₂ with sulfur or thiosulfate as electron acceptor in the anaerobic hyperthermophilic archaea *Thermoproteus tenax* and *Pyrobaculum islandicum* proceeds via the citric acid cycle. *Arch. Microbiol.* 162:286–294. <http://dx.doi.org/10.1007/BF00301853>.
159. Mukund S, Adams MW. 1996. Molybdenum and vanadium do not replace tungsten in the catalytically active forms of the three tungstoenzymes in the hyperthermophilic archaeon *Pyrococcus furiosus*. *J. Bacteriol.* 178:163–167.
160. Mukund S, Adams MW. 1995. Glyceraldehyde-3-phosphate ferredoxin oxidoreductase, a novel tungsten-containing enzyme with a potential glycolytic role in the hyperthermophilic archaeon *Pyrococcus furiosus*. *J. Biol. Chem.* 270:8389–8392. <http://dx.doi.org/10.1074/jbc.270.15.8389>.
161. van der Oost J, Schut G, Kengen SW, Hagen WR, Thomm M, de Vos WM. 1998. The ferredoxin-dependent conversion of glyceraldehyde-3-phosphate in the hyperthermophilic archaeon *Pyrococcus furiosus* represents a novel site of glycolytic regulation. *J. Biol. Chem.* 273:28149–28154. <http://dx.doi.org/10.1074/jbc.273.43.28149>.
162. Johnson MK, Rees DC, Adams MW. 1996. Tungstoenzymes. *Chem. Rev.* 96:2817–2840.
163. Roy R, Mukund S, Schut GJ, Dunn DM, Weiss R, Adams MW. 1999. Purification and molecular characterization of the tungsten-containing formaldehyde ferredoxin oxidoreductase from the hyperthermophilic archaeon *Pyrococcus furiosus*: the third of a putative five-member tungstoenzyme family. *J. Bacteriol.* 181:1171–1180.
164. Roy R, Menon AL, Adams MW. 2001. Aldehyde oxidoreductases from *Pyrococcus furiosus*. *Methods Enzymol.* 331:132–144. [http://dx.doi.org/10.1016/S0076-6879\(01\)31052-2](http://dx.doi.org/10.1016/S0076-6879(01)31052-2).
165. Roy R, Adams MW. 2002. Characterization of a fourth tungsten-containing enzyme from the hyperthermophilic archaeon *Pyrococcus furiosus*. *J. Bacteriol.* 184:6952–6956. <http://dx.doi.org/10.1128/JB.184.24.6952-6956.2002>.
166. Bevers LE, Bol E, Hagedoorn PL, Hagen WR. 2005. WOR5, a novel tungsten-containing aldehyde oxidoreductase from *Pyrococcus furiosus* with a broad substrate specificity. *J. Bacteriol.* 187:7056–7061. <http://dx.doi.org/10.1128/JB.187.20.7056-7061.2005>.
167. Hagedoorn PL, Chen T, Schroder I, Piersma SR, de Vries S, Hagen WR. 2005. Purification and characterization of the tungsten enzyme aldehyde:ferredoxin oxidoreductase from the hyperthermophilic denitrifier *Pyrobaculum aerophilum*. *J. Biol. Inorg. Chem.* 10:259–269. <http://dx.doi.org/10.1007/s00775-005-0637-5>.
168. Hu Y, Faham S, Roy R, Adams MW, Rees DC. 1999. Formaldehyde ferredoxin oxidoreductase from *Pyrococcus furiosus*: the 1.85 Å resolution crystal structure and its mechanistic implications. *J. Mol. Biol.* 286:899–914. <http://dx.doi.org/10.1006/jmbi.1998.2488>.
169. Chan MK, Mukund S, Kletzin A, Adams MW, Rees DC. 1995. Structure of a hyperthermophilic tungstopterin enzyme, aldehyde ferredoxin oxidoreductase. *Science* 267:1463–1469. <http://dx.doi.org/10.1126/science.7878465>.
170. Liao RZ, Yu JG, Himo F. 2011. Tungsten-dependent formaldehyde ferredoxin oxidoreductase: reaction mechanism from quantum chemical calculations. *J. Inorg. Biochem.* 105:927–936. <http://dx.doi.org/10.1016/j.jinorgbio.2011.03.020>.
171. Kardinahl S, Schmidt CL, Hansen T, Anemuller S, Petersen A, Schafer G. 1999. The strict molybdate-dependence of glucose-degradation by the thermoacidophile *Sulfolobus acidocaldarius* reveals the first crenarchaeotic molybdenum containing enzyme—an aldehyde oxidoreductase. *Eur. J. Biochem.* 260:540–548.
172. Brunner NA, Brinkmann H, Siebers B, Hensel R. 1998. NAD+-dependent glyceraldehyde-3-phosphate dehydrogenase from *Thermoproteus tenax*. The first identified archaeal member of the aldehyde dehydrogenase superfamily is a glycolytic enzyme with unusual regulatory properties. *J. Biol. Chem.* 273:6149–6156.
173. Ahmed H, Ettema TJ, Tjaden B, Geerling AC, van der Oost J, Siebers B. 2005. The semi-phosphorylative Entner-Doudoroff pathway in hyperthermophilic archaea: a re-evaluation. *Biochem. J.* 390:529–540. <http://dx.doi.org/10.1042/BJ20041711>.
174. Lorentzen E, Hensel R, Knura T, Ahmed H, Pohl E. 2004. Structural basis of allosteric regulation and substrate specificity of the non-phosphorylating glyceraldehyde 3-phosphate dehydrogenase from *Thermoproteus tenax*. *J. Mol. Biol.* 341:815–828. <http://dx.doi.org/10.1016/j.jmb.2004.05.032>.
175. Matsubara K, Yokooji Y, Atomi H, Imanaka T. 2011. Biochemical and genetic characterization of the three metabolic routes in *Thermococcus kodakarensis* linking glyceraldehyde 3-phosphate and 3-phosphoglycerate. *Mol. Microbiol.* 81:1300–1312. <http://dx.doi.org/10.1111/j.1365-2958.2011.07762.x>.
176. Ito F, Chishiki H, Fushinobu S, Wakagi T. 2012. Comparative analysis of two glyceraldehyde-3-phosphate dehydrogenases from a thermoacidophilic archaeon, *Sulfolobus tokodaii*. *FEBS Lett.* 586:3097–3103. <http://dx.doi.org/10.1016/j.febslet.2012.07.059>.
177. Brunner NA, Hensel R. 2001. Nonphosphorylating glyceraldehyde-3-phosphate dehydrogenase from *Thermoproteus tenax*. *Methods Enzymol.* 331:117–131. [http://dx.doi.org/10.1016/S0076-6879\(01\)31051-0](http://dx.doi.org/10.1016/S0076-6879(01)31051-0).
178. Brunner NA, Siebers B, Hensel R. 2001. Role of two different glyceraldehyde-3-phosphate dehydrogenases in controlling the reversible Embden-Meyerhof-Parnas pathway in *Thermoproteus tenax*: regulation on protein and transcript level. *Extremophiles* 5:101–109. <http://dx.doi.org/10.1007/s007920100181>.
179. Pohl E, Brunner N, Wilmann M, Hensel R. 2002. The crystal structure of the allosteric non-phosphorylating glyceraldehyde-3-phosphate dehydrogenase from the hyperthermophilic archaeum *Thermoproteus tenax*. *J. Biol. Chem.* 277:19938–19945. <http://dx.doi.org/10.1074/jbc.M112244200>.
180. Rawal N, Kelkar SM, Altekar W. 1988. Alternative routes of carbohydrate metabolism in halophilic archaeabacteria. *Indian J. Biochem. Biophys.* 25:674–686.
181. Stines-Chaumeil C, Talfournier F, Branlant G. 2006. Mechanistic characterization of the MSDH (methylmalonate semialdehyde dehydrogenase) from *Bacillus subtilis*. *Biochem. J.* 395:107–115. <http://dx.doi.org/10.1042/BJ20051525>.
182. Habenicht A. 1997. The non-phosphorylating glyceraldehyde-3-phosphate dehydrogenase: biochemistry, structure, occurrence and evolution. *Biol. Chem.* 378:1413–1419.
183. Habenicht A, Hellman U, Cerff R. 1994. Non-phosphorylating GAPDH of higher plants is a member of the aldehyde dehydrogenase superfamily with no sequence homology to phosphorylating GAPDH. *J. Mol. Biol.* 237:165–171. <http://dx.doi.org/10.1006/jmbi.1994.1217>.
184. Jia B, Linh LT, Lee S, Pham BP, Liu J, Pan H, Zhang S, Cheong GW. 2011. Biochemical characterization of glyceraldehyde-3-phosphate dehydrogenase from *Thermococcus kodakarensis* KOD1. *Extremophiles* 15:337–346. <http://dx.doi.org/10.1007/s00792-011-0365-4>.
185. Fabry S, Hensel R. 1987. Purification and characterization of D-glyceraldehyde-3-phosphate dehydrogenase from the thermophilic archaeabacterium *Methanothermus fervidus*. *Eur. J. Biochem.* 165:147–155. <http://dx.doi.org/10.1111/j.1432-1033.1987.tb11205.x>.
186. Zwickl P, Fabry S, Bogedain C, Haas A, Hensel R. 1990. Glyceraldehyde-3-phosphate dehydrogenase from the hyperthermophilic archaeabacterium *Pyrococcus woesei*: characterization of the enzyme, cloning and sequencing of the gene, and expression in *Escherichia coli*. *J. Bacteriol.* 172:4329–4338.
187. Jones CE, Fleming TM, Cowan DA, Littlechild JA, Piper PW. 1995. The phosphoglycerate kinase and glyceraldehyde-3-phosphate dehydrogenase genes from the thermophilic archaeon *Sulfolobus solfataricus* overlap by 8 bp. Isolation, sequencing of the genes and expression in *Escherichia coli*. *Eur. J. Biochem.* 233:800–808.
188. Charron C, Vitoux B, Aubry A. 2002. Comparative analysis of thermo-adaptation within the archaeal glyceraldehyde-3-phosphate dehydrogenases from mesophilic *Methanobacterium bryantii* and thermophilic *Methanothermus fervidus*. *Biopolymers* 65:263–273. <http://dx.doi.org/10.1002/bip.10235>.
189. Dello Russo A, Rullo R, Masullo M, Ianniciello G, Arcari P, Bocchini V. 1995. Glyceraldehyde-3-phosphate dehydrogenase in the hyperther-

- mophilic archaeon *Sulfolobus solfataricus*: characterization and significance in glucose metabolism. *Biochem. Mol. Biol. Int.* 36:123–135.
190. Krishnan G, Altekar W. 1990. Characterization of a halophilic glyceraldehyde-3-phosphate dehydrogenase from the archaeabacterium *Haloarcula vallismortis*. *J. Gen. Appl. Microbiol.* 36:19–32. <http://dx.doi.org/10.2323/jgam.36.19>.
 191. Pruss B, Meyer HE, Holldorf AW. 1993. Characterization of the glyceraldehyde 3-phosphate dehydrogenase from the extremely halophilic archaeabacterium *Haloarcula vallismortis*. *Arch. Microbiol.* 160:5–11.
 192. Charron C, Talfournier F, Isupov MN, Littlechild JA, Branlant G, Vitoux B, Aubry A. 2000. The crystal structure of d-glyceraldehyde-3-phosphate dehydrogenase from the hyperthermophilic archaeon *Methanothermus fervidus* in the presence of NADP(+) at 2.1 Å resolution. *J. Mol. Biol.* 297:481–500. <http://dx.doi.org/10.1006/jmbi.2000.3565>.
 193. Isupov MN, Fleming TM, Dalby AR, Crowhurst GS, Bourne PC, Littlechild JA. 1999. Crystal structure of the glyceraldehyde-3-phosphate dehydrogenase from the hyperthermophilic archaeon *Sulfolobus solfataricus*. *J. Mol. Biol.* 291:651–660. <http://dx.doi.org/10.1006/jmbi.1999.3003>.
 194. Malay AD, Bessho Y, Ellis MJ, Antonyuk SV, Strange RW, Hasnain SS, Shinkai A, Padmanabhan B, Yokoyama S. 2009. Structure of glyceraldehyde-3-phosphate dehydrogenase from the archaeal hyperthermophile *Methanocaldococcus jannaschii*. *Acta Crystallogr. Sect. F Struct. Biol. Cryst. Commun.* 65:1227–1233. <http://dx.doi.org/10.1107/S1744309109047046>.
 195. Littlechild JA, Guy JE, Isupov MN. 2004. Hyperthermophilic dehydrogenase enzymes. *Biochem. Soc. Trans.* 32:255–258. <http://dx.doi.org/10.1042/BST0320255>.
 196. Littlechild JA, Isupov M. 2001. Glyceraldehyde-3-phosphate dehydrogenase from *Sulfolobus solfataricus*. *Methods Enzymol.* 331:105–117. [http://dx.doi.org/10.1016/S0076-6879\(01\)31050-9](http://dx.doi.org/10.1016/S0076-6879(01)31050-9).
 197. Hensel R, Zwickl P, Fabry S, Lang J, Palm P. 1989. Sequence comparison of glyceraldehyde-3-phosphate dehydrogenases from the three eukaryotic domains: evolutionary implication. *Can. J. Microbiol.* 35:81–85. <http://dx.doi.org/10.1139/m89-012>.
 198. Schafer T, Schonheit P. 1993. Gluconeogenesis from pyruvate in the hyperthermophilic archaeon *Pyrococcus furiosus*: involvement of reactions of the Embden-Meyerhof pathway. *Arch. Microbiol.* 159:354–363. <http://dx.doi.org/10.1007/BF00290918>.
 199. Crowhurst G, McHarg J, Littlechild JA. 2001. Phosphoglycerate kinases from bacteria and archaea. *Methods Enzymol.* 331:90–104. [http://dx.doi.org/10.1016/S0076-6879\(01\)31049-2](http://dx.doi.org/10.1016/S0076-6879(01)31049-2).
 200. Fabry S, Heppner P, Dietmaier W, Hensel R. 1990. Cloning and sequencing the gene encoding 3-phosphoglycerate kinase from mesophilic *Methanobacterium bryantii* and thermophilic *Methanothermus fervidus*. *Gene* 91:19–25. [http://dx.doi.org/10.1016/0378-1119\(90\)90157-M](http://dx.doi.org/10.1016/0378-1119(90)90157-M).
 201. Hess D, Kruger K, Knappik A, Palm P, Hensel R. 1995. Dimeric 3-phosphoglycerate kinases from hyperthermophilic archaea. Cloning, sequencing and expression of the 3-phosphoglycerate kinase gene of *Pyrococcus woesei* in *Escherichia coli* and characterization of the protein. Structural and functional comparison with the 3-phosphoglycerate kinase of *Methanothermus fervidus*. *Eur. J. Biochem.* 233:227–237.
 202. Crowhurst GS, Isupov MN, Fleming T, Littlechild JA. 1998. Two glycolytic enzymes from *Sulfolobus solfataricus*. *Biochem. Soc. Trans.* 26: S275.
 203. Fleming T, Littlechild J. 1997. Sequence and structural comparison of thermophilic phosphoglycerate kinases with a mesophilic equivalent. *Comp. Biochem. Physiol. A Physiol.* 118:439–451. [http://dx.doi.org/10.1016/S0300-9629\(97\)00005-4](http://dx.doi.org/10.1016/S0300-9629(97)00005-4).
 204. Hess D, Hensel R. 1996. The 3-phosphoglycerate kinase of the hyperthermophilic archaeum *Pyrococcus woesei* produced in *Escherichia coli*: loss of heat resistance due to internal translation initiation and its restoration by site-directed mutagenesis. *Gene* 172:121–124. [http://dx.doi.org/10.1016/0378-1119\(96\)00176-X](http://dx.doi.org/10.1016/0378-1119(96)00176-X).
 205. Piper PW, Emson C, Jones CE, Cowan DA, Fleming TM, Littlechild JA. 1996. Complementation of a pgk deletion mutation in *Saccharomyces cerevisiae* with expression of the phosphoglycerate-kinase gene from the hyperthermophilic archaeon *Sulfolobus solfataricus*. *Curr. Genet.* 29: 594–596. <http://dx.doi.org/10.1007/s002940050091>.
 206. Zerrad L, Merli A, Schröder GF, Varga A, Grácer É, Pernot P, Round A, Vas M, Bowler MW. 2011. A spring-loaded release mechanism regulates domain movement and catalysis in phosphoglycerate kinase. *J. Biol. Chem.* 286:14040–14048. <http://dx.doi.org/10.1074/jbc.M110.206813>.
 207. Schut GJ, Brehm SD, Datta S, Adams MW. 2003. Whole-genome DNA microarray analysis of a hyperthermophile and an archaeon: *Pyrococcus furiosus* grown on carbohydrates or peptides. *J. Bacteriol.* 185:3935–3947. <http://dx.doi.org/10.1128/JB.185.13.3935-3947.2003>.
 208. Kanai T, Akerboom J, Takedomi S, van de Werken HJ, Blombach F, van der Oost J, Murakami T, Atomi H, Imanaka T. 2007. A global transcriptional regulator in *Thermococcus kodakaraensis* controls the expression levels of both glycolytic and gluconeogenic enzyme-encoding genes. *J. Biol. Chem.* 282:33659–33670. <http://dx.doi.org/10.1074/jbc.M703424200>.
 209. Reher M, Fuhrer T, Bott M, Schönheit P. 2010. The nonphosphorylative Entner-Doudoroff pathway in the thermoacidophilic euryarchaeon *Picrophilus torridus* involves a novel 2-keto-3-deoxygluconate-specific aldolase. *J. Bacteriol.* 192:964–974. <http://dx.doi.org/10.1128/JB.01281-09>.
 210. Fothergill-Gilmore LA, Watson HC. 1989. The phosphoglycerate mutases. *Adv. Enzymol. Relat. Areas Mol. Biol.* 62:227–313.
 211. Jedrzejas MJ. 2000. Structure, function, and evolution of phosphoglycerate mutases: comparison with fructose-2,6-bisphosphatase, acid phosphatase, and alkaline phosphatase. *Prog. Biophys. Mol. Biol.* 73:263–287. [http://dx.doi.org/10.1016/S0079-6107\(00\)00007-9](http://dx.doi.org/10.1016/S0079-6107(00)00007-9).
 212. van der Oost J, Huynen MA, Verhees CH. 2002. Molecular characterization of phosphoglycerate mutase in archaea. *FEMS Microbiol. Lett.* 212:111–120. <http://dx.doi.org/10.1111/j.1574-6968.2002.tb11253.x>.
 213. Lokanath NK, Kunishima N. 2006. Purification, crystallization and preliminary X-ray crystallographic analysis of the archaeal phosphoglycerate mutase PH0037 from *Pyrococcus horikoshii* OT3. *Acta Crystallogr. Sect. F Struct. Biol. Cryst. Commun.* 62:788–790. <http://dx.doi.org/10.1107/S1744309106026121>.
 214. Graham DE, Xu H, White RH. 2002. A divergent archaeal member of the alkaline phosphatase binuclear metalloenzyme superfamily has phosphoglycerate mutase activity. *FEBS Lett.* 517:190–194. [http://dx.doi.org/10.1016/S0014-5793\(02\)02619-4](http://dx.doi.org/10.1016/S0014-5793(02)02619-4).
 215. Potters MB, Solow BT, Bischoff KM, Graham DE, Lower BH, Helm R, Kennelly PJ. 2003. Phosphoprotein with phosphoglycerate mutase activity from the archaeon *Sulfolobus solfataricus*. *J. Bacteriol.* 185:2112–2121. <http://dx.doi.org/10.1128/JB.185.7.2112-2121.2003>.
 216. Johnsen U, Schonheit P. 2007. Characterization of cofactor-dependent and cofactor-independent phosphoglycerate mutases from archaea. *Extremophiles* 11:647–657. <http://dx.doi.org/10.1007/s00792-007-0094-x>.
 217. Bond CS, White MF, Hunter WN. 2002. Mechanistic implications for *Escherichia coli* cofactor-dependent phosphoglycerate mutase based on the high-resolution crystal structure of a vanadate complex. *J. Mol. Biol.* 316:1071–1081. <http://dx.doi.org/10.1006/jmbi.2002.5418>.
 218. Carreras J, Bartrons R, Grisolía S. 1980. Vanadate inhibits 2,3-bisphosphoglycerate dependent phosphoglycerate mutases but does not affect the 2,3-bisphosphoglycerate independent phosphoglycerate mutases. *Biochem. Biophys. Res. Commun.* 96:1267–1273. [http://dx.doi.org/10.1016/0006-291X\(80\)90088-1](http://dx.doi.org/10.1016/0006-291X(80)90088-1).
 219. Bond CS, White MF, Hunter WN. 2001. High resolution structure of the phosphohistidine-activated form of *Escherichia coli* cofactor-dependent phosphoglycerate mutase. *J. Biol. Chem.* 276:3247–3253. <http://dx.doi.org/10.1074/jbc.M007318200>.
 220. Rigden DJ, Walter RA, Phillips SE, Fothergill-Gilmore LA. 1999. Sulphate ions observed in the 2.12 Å structure of a new crystal form of *Saccharomyces cerevisiae* phosphoglycerate mutase provide insights into understanding the catalytic mechanism. *J. Mol. Biol.* 286:1507–1517. <http://dx.doi.org/10.1006/jmbi.1999.2566>.
 221. Galperin MY, Bairoch A, Koonin EV. 1998. A superfamily of metalloenzymes unifies phosphopentomutase and cofactor-independent phosphoglycerate mutase with alkaline phosphatases and sulfatases. *Protein Sci.* 7:1829–1835. <http://dx.doi.org/10.1002/pro.5560070819>.
 222. Galperin MY, Jedrzejas MJ. 2001. Conserved core structure and active site residues in alkaline phosphatase superfamily enzymes. *Proteins* 45: 318–324. <http://dx.doi.org/10.1002/prot.1152>.
 223. Jedrzejas MJ, Chander M, Setlow P, Krishnasamy G. 2000. Structure and mechanism of action of a novel phosphoglycerate mutase from *Bacillus stearothermophilus*. *EMBO J.* 19:1419–1431. <http://dx.doi.org/10.1093/emboj/19.7.1419>.
 224. Jedrzejas MJ, Setlow P. 2001. Comparison of the binuclear metalloenzymes diphosphoglycerate-independent phosphoglycerate mutase and alkaline phosphatase: their mechanism of catalysis via a

- phosphoserine intermediate. *Chem. Rev.* 101:607–618. <http://dx.doi.org/10.1021/cr000253a>.
225. Fraser HI, Kvaratskhelia M, White MF. 1999. The two analogous phosphoglycerate mutases of *Escherichia coli*. *FEBS Lett.* 455:344–348. [http://dx.doi.org/10.1016/S0014-5793\(99\)00910-2](http://dx.doi.org/10.1016/S0014-5793(99)00910-2).
 226. Peak MJ, Peak JG, Stevens FJ, Blamey J, Mai X, Zhou ZH, Adams MW. 1994. The hyperthermophilic glycolytic enzyme enolase in the archaeon, *Pyrococcus furiosus*: comparison with mesophilic enolases. *Arch. Biochem. Biophys.* 313:280–286. <http://dx.doi.org/10.1006/abbi.1994.1389>.
 227. Budgen N, Danson MJ. 1986. Metabolism of glucose via a modified Entner-Doudoroff pathway in the thermoacidophilic archaeabacterium, *Thermoplasma acidophilum*. *FEBS Lett.* 196:207–210. [http://dx.doi.org/10.1016/0014-5793\(86\)80247-2](http://dx.doi.org/10.1016/0014-5793(86)80247-2).
 228. Hosaka T, Meguro T, Yamato I, Shirakihara Y. 2003. Crystal structure of *Enterococcus hirae* enolase at 2.8 Å resolution. *J. Biochem.* 133:817–823. <http://dx.doi.org/10.1093/jb/mvg104>.
 229. Yamamoto H, Kunishima N. 2008. Purification, crystallization and preliminary crystallographic study of the putative enolase MJ0232 from the hyperthermophilic archaeon *Methanococcus jannaschii*. *Acta Crystallogr. Sect. F Struct. Biol. Cryst. Commun.* 64:1087–1090. <http://dx.doi.org/10.1107/S1744309108034180>.
 230. Babbitt PC, Hasson MS, Wedekind JE, Palmer DR, Barrett WC, Reed GH, Rayment I, Ringe D, Kenyon GL, Gerlt JA. 1996. The enolase superfamily: a general strategy for enzyme-catalyzed abstraction of the alpha-protons of carboxylic acids. *Biochemistry* 35:16489–16501. <http://dx.doi.org/10.1021/bi9616413>.
 231. Kuhnel K, Luisi BF. 2001. Crystal structure of the *Escherichia coli* RNA degradosome component enolase. *J. Mol. Biol.* 313:583–592. <http://dx.doi.org/10.1006/jmbi.2001.5065>.
 232. Johnsen U, Hansen T, Schönheit P. 2003. Comparative analysis of pyruvate kinases from the hyperthermophilic archaea *Archaeoglobus fulgidus*, *Aeropyrum pernix*, and *Pyrobaculum aerophilum* and the hyperthermophilic bacterium *Thermotoga maritima*: unusual regulatory properties in hyperthermophilic archaea. *J. Biol. Chem.* 278:25417–25427. <http://dx.doi.org/10.1074/jbc.M210288200>.
 233. Potter S, Fothergill-Gilmore LA. 1992. Purification and properties of pyruvate kinase from *Thermoplasma acidophilum*. *FEMS Microbiol. Lett.* 73:235–239.
 234. Potter S, Fothergill-Gilmore LA. 1992. The pyruvate kinase of *Thermoplasma acidophilum*: purification, kinetic characterisation & use as a phylogenetic marker. *Biochem. Soc. Trans.* 20:11S.
 235. Schramm A, Siebers B, Tjaden B, Brinkmann H, Hensel R. 2000. Pyruvate kinase of the hyperthermophilic crenarchaeote *Thermoproteus tenax*: physiological role and phylogenetic aspects. *J. Bacteriol.* 182:2001–2009. <http://dx.doi.org/10.1128/JB.182.7.2001-2009.2000>.
 236. Oria-Hernández J, Riveros-Rosas H, Ramírez-Silva L. 2006. Dichotomic phylogenetic tree of the pyruvate kinase family: K+-dependent and -independent enzymes. *J. Biol. Chem.* 281:30717–30724. <http://dx.doi.org/10.1074/jbc.M605310200>.
 237. Muirhead H, Clayden DA, Barford D, Lorimer CG, Fothergill-Gilmore LA, Schiltz E, Schmitt W. 1986. The structure of cat muscle pyruvate kinase. *EMBO J.* 5:475–481.
 238. Larsen TM, Laughlin LT, Holden HM, Rayment I, Reed GH. 1994. Structure of rabbit muscle pyruvate kinase complexed with Mn²⁺, K⁺, and pyruvate. *Biochemistry* 33:6301–6309. <http://dx.doi.org/10.1021/bi00186a033>.
 239. Mattevi A, Valentini G, Rizzi M, Speranza ML, Bolognesi M, Coda A. 1995. Crystal structure of *Escherichia coli* pyruvate kinase type I: molecular basis of the allosteric transition. *Structure* 3:729–741. [http://dx.doi.org/10.1016/S0969-2126\(01\)00207-6](http://dx.doi.org/10.1016/S0969-2126(01)00207-6).
 240. Jurica MS, Mesecar A, Heath PJ, Shi W, Nowak T, Stoddard BL. 1998. The allosteric regulation of pyruvate kinase by fructose-1,6-bisphosphate. *Structure* 6:195–210. [http://dx.doi.org/10.1016/S0969-2126\(98\)00021-5](http://dx.doi.org/10.1016/S0969-2126(98)00021-5).
 241. Bollenbach TJ, Mesecar AD, Nowak T. 1999. Role of lysine 240 in the mechanism of yeast pyruvate kinase catalysis. *Biochemistry* 38:9137–9145. <http://dx.doi.org/10.1021/bi990690n>.
 242. Valentini G, Chiarelli L, Fortin R, Speranza ML, Galizzi A, Mattevi A. 2000. The allosteric regulation of pyruvate kinase: a site-directed mutagenesis study. *J. Biol. Chem.* 275:18145–18152. <http://dx.doi.org/10.1074/jbc.M001870200>.
 243. Domrauckas JD, Santarsiero BD, Mesecar AD. 2005. Structural basis for tumor pyruvate kinase M2 allosteric regulation and catalysis. *Biochemistry* 44:9417–9429. <http://dx.doi.org/10.1021/bi0474923>.
 244. Solomons JTG, Johnsen U, Schönheit P, Davies C. 2013. 3-Phosphoglycerate is an allosteric activator of pyruvate kinase from the hyperthermophilic archaeon *Pyrobaculum aerophilum*. *Biochemistry* 52:5865–5875. <http://dx.doi.org/10.1021/bi400761b>.
 245. Flamholz A, Noor E, Bar-Even A, Liebermeister W, Milo R. 2013. Glycolytic strategy as a tradeoff between energy yield and protein cost. *Proc. Natl. Acad. Sci. U. S. A.* 110:10039–10044. <http://dx.doi.org/10.1073/pnas.1215283110>.
 246. Hochstein LI. 1974. The metabolism of carbohydrates by extremely halophilic bacteria: glucose metabolism via a modified Entner-Doudoroff pathway. *Can. J. Microbiol.* 20:1085–1091. <http://dx.doi.org/10.1139/m74-170>.
 247. Andreesen JR, Gottschalk G. 1969. The occurrence of a modified Entner-Doudoroff pathway in *Clostridium aceticum*. *Arch. Mikrobiol.* 69:160–170. <http://dx.doi.org/10.1007/BF00409760>.
 248. Reher M, Schönheit P. 2006. Glyceraldehyde dehydrogenases from the thermoacidophilic euryarchaeota *Picrophilus torridus* and *Thermoplasma acidophilum*, key enzymes of the non-phosphorylative Entner-Doudoroff pathway, constitute a novel enzyme family within the aldehyde dehydrogenase superfamily. *FEBS Lett.* 580:1198–1204. <http://dx.doi.org/10.1016/j.febslet.2006.01.029>.
 249. De Rosa M, Gambacorta A, Nicolaus B, Giardina P, Poerio E, Buonocore V. 1984. Glucose metabolism in the extreme thermoacidophilic archaeabacterium *Sulfolobus solfataricus*. *Biochem. J.* 224:407–414.
 250. Elzainy TA, Hassan MM, Allam AM. 1973. New pathway for nonphosphorylated degradation of gluconate by *Aspergillus niger*. *J. Bacteriol.* 114:457–459.
 251. Reher M, Bott M, Schönheit P. 2006. Characterization of glyceraldehyde kinase (2-phosphoglycerate forming), a key enzyme of the nonphosphorylative Entner-Doudoroff pathway, from the thermoacidophilic euryarchaeon *Picrophilus torridus*. *FEMS Microbiol. Lett.* 259:113–119. <http://dx.doi.org/10.1111/j.1574-6968.2006.00264.x>.
 252. Kehrer D, Ahmed H, Brinkmann H, Siebers B. 2007. Glyceraldehyde kinase of the hyperthermophilic archaeon *Thermoproteus tenax*: new insights into the phylogenetic distribution and physiological role of members of the three different glyceraldehyde kinase classes. *BMC Genomics* 8:301. <http://dx.doi.org/10.1186/1471-2164-8-301>.
 253. Liu B, Hong Y, Wu L, Li Z, Ni J, Sheng D, Shen Y. 2007. A unique highly thermostable 2-phosphoglycerate forming glyceraldehyde kinase from the hyperthermophilic archaeon *Pyrococcus horikoshii*: gene cloning, expression and characterization. *Extremophiles* 11:733–739. <http://dx.doi.org/10.1007/s00792-007-0079-9>.
 254. Liu B, Wu L, Liu T, Hong Y, Shen Y, Ni J. 2009. A MOFRL family glyceraldehyde kinase from the thermophilic crenarchaeon, *Sulfolobus tokodaii*, with unique enzymatic properties. *Biotechnol. Lett.* 31:1937–1941. <http://dx.doi.org/10.1007/s10529-009-0089-z>.
 255. Lamble HJ, Theodosis A, Milburn CC, Taylor GL, Bull SD, Hough DW, Danson MJ. 2005. Promiscuity in the part-phosphorylative Entner-Doudoroff pathway of the archaeon *Sulfolobus solfataricus*. *FEBS Lett.* 579:6865–6869. <http://dx.doi.org/10.1016/j.febslet.2005.11.028>.
 256. Kouril T, Wieloch P, Reimann J, Wagner M, Zaparty M, Albers S-V, Schomburg D, Ruoff P, Siebers B. 2013. Unraveling the function of the two Entner-Doudoroff branches in the thermoacidophilic crenarchaeon *Sulfolobus solfataricus* P2. *FEBS J.* 280:1126–1138. <http://dx.doi.org/10.1111/febs.12106>.
 257. Lamble HJ, Heyer NI, Bull SD, Hough DW, Danson MJ. 2003. Metabolic pathway promiscuity in the archaeon *Sulfolobus solfataricus* revealed by studies on glucose dehydrogenase and 2-keto-3-deoxygluconate aldolase. *J. Biol. Chem.* 278:34066–34072. <http://dx.doi.org/10.1074/jbc.M305818200>.
 258. Ohshima T, Ito Y, Sakuraba H, Goda S, Kawarabayashi Y. 2003. The *Sulfolobus tokodaii* gene ST1704 codes highly thermostable glucose dehydrogenase. *J. Mol. Catal. B Enzym.* 23:281–289. [http://dx.doi.org/10.1016/S1381-1177\(03\)00091-2](http://dx.doi.org/10.1016/S1381-1177(03)00091-2).
 259. Haferkamp P, Kutschki S, Treichel J, Hemeda H, Sewczyk K, Hoffmann D, Zaparty M, Siebers B. 2011. An additional glucose dehydrogenase from *Sulfolobus solfataricus*: fine-tuning of sugar degradation? *Biochem. Soc. Trans.* 39:77–81. <http://dx.doi.org/10.1042/BST0390077>.
 260. Bhaumik SR, Sonawat HM. 1999. Kinetic mechanism of glucose dehydrogenase from *Halobacterium salinarum*. *Indian J. Biochem. Biophys.* 36:143–149.

261. Angelov A, Futterer O, Valerius O, Braus GH, Liebl W. 2005. Properties of the recombinant glucose/galactose dehydrogenase from the extreme thermoacidophile, *Picrophilus torridus*. FEBS J. 272:1054–1062. <http://dx.doi.org/10.1111/j.1742-4658.2004.04539.x>.
262. Giardina P, de Biasi MG, de Rosa M, Gambacorta A, Buonocore V. 1986. Glucose dehydrogenase from the thermoacidophilic archaeabacterium *Sulfolobus solfataricus*. Biochem. J. 239:517–522.
263. Smith LD, Budgen N, Bungard SJ, Danson MJ, Hough DW. 1989. Purification and characterization of glucose dehydrogenase from the thermoacidophilic archaeabacterium *Thermoplasma acidophilum*. Biochem. J. 261:973–977.
264. Bonete MJ, Pire C, Llorca FI, Camacho ML. 1996. Glucose dehydrogenase from the halophilic archaeon *Halofexax mediterranei*: enzyme purification, characterisation and N-terminal sequence. FEBS Lett. 383: 227–229. [http://dx.doi.org/10.1016/0014-5793\(96\)00235-9](http://dx.doi.org/10.1016/0014-5793(96)00235-9).
265. Bright JR, Mackness R, Danson MJ, Hough DW, Taylor GL, Towner P, Byrom D. 1991. Crystallization and preliminary crystallographic study of glucose dehydrogenase from the archaeabacterium *Thermoplasma acidophilum*. J. Mol. Biol. 222:143–144. [http://dx.doi.org/10.1016/0022-2836\(91\)90200-P](http://dx.doi.org/10.1016/0022-2836(91)90200-P).
266. John J, Crennell SJ, Hough DW, Danson MJ, Taylor GL. 1994. The crystal structure of glucose dehydrogenase from *Thermoplasma acidophilum*. Structure 2:385–393. [http://dx.doi.org/10.1016/S0969-2126\(00\)00040-X](http://dx.doi.org/10.1016/S0969-2126(00)00040-X).
267. Ferrer J, Fisher M, Burke J, Sedelnikova SE, Baker PJ, Gilmour DJ, Bonete MJ, Pire C, Esclapez J, Rice DW. 2001. Crystallization and preliminary X-ray analysis of glucose dehydrogenase from *Halofexax mediterranei*. Acta Crystallogr. D Biol. Crystallogr. 57:1887–1889. <http://dx.doi.org/10.1107/S09044901015189>.
268. Esclapez J, Britton KL, Baker PJ, Fisher M, Pire C, Ferrer J, Bonete MJ, Rice DW. 2005. Crystallization and preliminary X-ray analysis of binary and ternary complexes of *Halofexax mediterranei* glucose dehydrogenase. Acta Crystallogr. Sect. F Struct. Biol. Cryst. Commun. 61:743–746. <http://dx.doi.org/10.1107/S1744309105019949>.
269. Milburn CC, Lamble HJ, Theodosis A, Bull SD, Hough DW, Danson MJ, Taylor GL. 2006. The structural basis of substrate promiscuity in glucose dehydrogenase from the hyperthermophilic archaeon *Sulfolobus solfataricus*. J. Biol. Chem. 281:14796–14804. <http://dx.doi.org/10.1074/jbc.M601334200>.
270. Britton KL, Baker PJ, Fisher M, Ruzheinikov S, Gilmour DJ, Bonete MJ, Ferrer J, Pire C, Esclapez J, Rice DW. 2006. Analysis of protein solvent interactions in glucose dehydrogenase from the extreme halophile *Halofexax mediterranei*. Proc. Natl. Acad. Sci. U. S. A. 103:4846–4851. <http://dx.doi.org/10.1073/pnas.0508854103>.
271. Esclapez J, Pire C, Bautista V, Martinez-Espinosa RM, Ferrer J, Bonete MJ. 2007. Analysis of acidic surface of *Halofexax mediterranei* glucose dehydrogenase by site-directed mutagenesis. FEBS Lett. 581:837–842. <http://dx.doi.org/10.1016/j.febslet.2007.01.054>.
272. Baker PJ, Britton KL, Fisher M, Esclapez J, Pire C, Bonete MJ, Ferrer J, Rice DW. 2009. Active site dynamics in the zinc-dependent medium chain alcohol dehydrogenase superfamily. Proc. Natl. Acad. Sci. U. S. A. 106:779–784. <http://dx.doi.org/10.1073/pnas.0807529106>.
273. Edwards KJ, Barton JD, Rossjohn J, Thorn JM, Taylor GL, Ollis DL. 1996. Structural and sequence comparisons of quinone oxidoreductase, ζ -crystallin, and glucose and alcohol dehydrogenases. Arch. Biochem. Biophys. 328:173–183. <http://dx.doi.org/10.1006/abbi.1996.0158>.
274. Pire C, Esclapez J, Ferrer J, Bonete MJ. 2001. Heterologous overexpression of glucose dehydrogenase from the halophilic archaeon *Halofexax mediterranei*, an enzyme of the medium chain dehydrogenase/reductase family. FEMS Microbiol. Lett. 200:221–227. <http://dx.doi.org/10.1111/j.1574-6968.2001.tb10719.x>.
275. Persson B, Zigler JS, Jörnvall H. 1994. A super-family of medium-chain dehydrogenases/reductases (MDR). Eur. J. Biochem. 226:15–22. <http://dx.doi.org/10.1111/j.1432-1033.1994.tb20021.x>.
276. Pauly TA, Ekstrom JL, Beebe DA, Chrunyk B, Cunningham D, Griffor M, Kamath A, Lee SE, Madura R, McGuire D, Subashi T, Wasilko D, Watts P, Mylari BL, Oates PJ, Adams PD, Rath VL. 2003. X-ray crystallographic and kinetic studies of human sorbitol dehydrogenase. Structure 11:1071–1085. [http://dx.doi.org/10.1016/S0969-2126\(03\)00167-9](http://dx.doi.org/10.1016/S0969-2126(03)00167-9).
277. Ying X, Ma K. 2011. Characterization of a zinc-containing alcohol dehydrogenase with stereoselectivity from the hyperthermophilic archaeon *Thermococcus guaymasensis*. J. Bacteriol. 193:3009–3019. <http://dx.doi.org/10.1128/JB.01433-10>.
278. Conway T. 1992. The Entner-Doudoroff pathway: history, physiology and molecular biology. FEMS Microbiol. Lett. 103:1–28. <http://dx.doi.org/10.1111/j.1574-6968.1992.tb05822.x>.
279. Hansen T, Schlichting B, Schönheit P. 2002. Glucose-6-phosphate dehydrogenase from the hyperthermophilic bacterium *Thermotoga maritima*: expression of the g6pd gene and characterization of an extremely thermophilic enzyme. FEMS Microbiol. Lett. 216:249–253. <http://dx.doi.org/10.1111/j.1574-6968.2002.tb11443.x>.
280. Cosgrove MS, Gover S, Naylor CE, Vandepitte-Rutten L, Adams MJ, Levy HR. 2000. An examination of the role of Asp-177 in the His-Asp catalytic dyad of leuconostoc mesenteroides glucose 6-phosphate dehydrogenase: X-ray structure and pH dependence of kinetic parameters of the D177N mutant enzyme. Biochemistry 39:15002–15011. <http://dx.doi.org/10.1021/bi0014608>.
281. Brodie AF, Lipmann F. 1955. Identification of a gluconolactonase. J. Biol. Chem. 212:677–686.
282. Doudoroff M, Palleroni NJ. 1956. Characterization and properties of 2-keto-3-deoxy-D-arabonic acid. J. Biol. Chem. 223:499–508.
283. Brouns SJ, Walther J, Snijders APL, van de Werken HJG, Willemen HLDM, Worm P, de Vos MGJ, Andersson A, Lundgren M, Mazon HFM, van den Heuvel RHH, Nilsson P, Salmon I, de Vos WM, Wright PC, Bernander R, van der Oost J. 2006. Identification of the missing links in prokaryotic pentose oxidation pathways. Evidence for enzyme recruitment. J. Biol. Chem. 281:27378–27388. <http://dx.doi.org/10.1074/jbc.M605549200>.
284. Watanabe S, Kodaki T, Makino K. 2006. A novel alpha-ketoglutaric semialdehyde dehydrogenase: evolutionary insight into an alternative pathway of bacterial L-arabinose metabolism. J. Biol. Chem. 281:28876–28888. <http://dx.doi.org/10.1074/jbc.M602585200>.
285. Stephens C, Christen B, Fuchs T, Sundaram V, Watanabe K, Jenal U. 2007. Genetic analysis of a novel pathway for d-xylose metabolism in *Caulobacter crescentus*. J. Bacteriol. 189:2181–2185. <http://dx.doi.org/10.1128/JB.01438-06>.
286. Chen C-N, Chin K-H, Wang AHJ, Chou S-H. 2008. The first crystal structure of gluconolactonase important in the glucose secondary metabolic pathways. J. Mol. Biol. 384:604–614. <http://dx.doi.org/10.1016/j.jmb.2008.09.055>.
287. Johnsen U, Dambeck M, Zaiss H, Fuhrer T, Soppa J, Sauer U, Schonheit P. 2009. d-Xylose degradation pathway in the halophilic archaeon *Halofexax volcanii*. J. Biol. Chem. 284:27290–27303. <http://dx.doi.org/10.1074/jbc.M109.003814>.
288. Hiblot J, Gotthard G, Chabriere E, Elias M. 2012. Structural and enzymatic characterization of the lactonase SisLac from *Sulfolobus islandicus*. PLoS One 7:e47028. <http://dx.doi.org/10.1371/journal.pone.0047028>.
289. Kim S, Lee SB. 2005. Identification and characterization of *Sulfolobus solfataricus* D-gluconate dehydratase: a key enzyme in the non-phosphorylated Entner-Doudoroff pathway. Biochem. J. 387:271–280. <http://dx.doi.org/10.1042/BJ20041053>.
290. Lamble HJ, Milburn CC, Taylor GL, Hough DW, Danson MJ. 2004. Gluconate dehydratase from the promiscuous Entner-Doudoroff pathway in *Sulfolobus solfataricus*. FEBS Lett. 576:133–136. <http://dx.doi.org/10.1016/j.febslet.2004.08.074>.
291. Nunn CEM, Johnsen U, Schonheit P, Fuhrer T, Sauer U, Hough DW, Danson MJ. 2010. Metabolism of pentose sugars in the hyperthermophilic archaea *Sulfolobus solfataricus* and *Sulfolobus acidocaldarius*. J. Biol. Chem. 285:33701–33709. <http://dx.doi.org/10.1074/jbc.M110.146332>.
292. Kim S, Lee SB. 2006. Characterization of *Sulfolobus solfataricus* 2-keto-3-deoxy-D-gluconate kinase in the modified Entner-Doudoroff pathway. Biosci. Biotechnol. Biochem. 70:1308–1316. <http://dx.doi.org/10.1271/bbb.50566>.
293. Jung JH, Lee SB. 2005. Identification and characterization of *Thermoplasma acidophilum* 2-keto-3-deoxy-D-gluconate kinase: a new class of sugar kinases. Biotechnol. Bioprocess Eng. 10:535–539. <http://dx.doi.org/10.1007/BF02932290>.
294. Buchanan CL, Connaris H, Danson MJ, Reeve CD, Hough DW. 1999. An extremely thermostable aldolase from *Sulfolobus solfataricus* with specificity for non-phosphorylated substrates. Biochem. J. 343:563–570. <http://dx.doi.org/10.1042/0264-6021:3430563>.
295. Hendry EJ, Buchanan CL, Russell RJM, Hough DW, Reeve CD, Danson MJ, Taylor GL. 2000. Preliminary crystallographic studies of an extremely thermostable KDG aldolase from *Sulfolobus solfataricus*. Acta

- Crystallogr. D Biol. Crystallogr. 56:1437–1439. <http://dx.doi.org/10.1107/S0907444900009859>.
296. Theodossis A, Walden H, Westwick EJ, Connaris H, Lamble HJ, Hough DW, Danson MJ, Taylor GL. 2004. The structural basis for substrate promiscuity in 2-keto-3-deoxygluconate aldolase from the Entner-Doudoroff pathway in *Sulfolobus solfataricus*. J. Biol. Chem. 279: 43886–43892. <http://dx.doi.org/10.1074/jbc.M407702200>.
297. Wolterink-van Loo S, van Eerde A, Siemerink MA, Akerboom J, Dijkstra BW, van der Oost J. 2007. Biochemical and structural exploration of the catalytic capacity of *Sulfolobus* KDG aldolases. Biochem. J. 403:421–430. <http://dx.doi.org/10.1042/BJ20061419>.
298. Pauluhn A, Ahmed H, Lorentzen E, Buchinger S, Schomburg D, Siebers B, Pohl E. 2008. Crystal structure and stereochemical studies of KDP(G) aldolase from *Thermoproteus tenax*. Proteins 72:35–43. <http://dx.doi.org/10.1002/prot.21890>.
299. Allard J, Grochulski P, Sygusch J. 2001. Covalent intermediate trapped in 2-keto-3-deoxy-6-phosphogluconate (KDPG) aldolase structure at 1.95-Å resolution. Proc. Natl. Acad. Sci. U. S. A. 98:3679–3684. <http://dx.doi.org/10.1073/pnas.071380898>.
300. Fullerton SW, Griffiths JS, Merkel AB, Cheriyan M, Wymer NJ, Hutchins MJ, Fierke CA, Toone EJ, Naismith JH. 2006. Mechanism of the class I KDPG aldolase. Bioorg. Med. Chem. 14:3002–3010. <http://dx.doi.org/10.1016/j.bmc.2005.12.022>.
301. Bell BJ, Watanabe L, Rios-Steiner JL, Tulinsky A, Lebioda L, Arni RK. 2003. Structure of 2-keto-3-deoxy-6-phosphogluconate (KDPG) aldolase from *Pseudomonas putida*. Acta Crystallogr. D Biol. Crystallogr. 59: 1454–1458. <http://dx.doi.org/10.1107/S0907444903013192>.
302. Wolterink-van Loo S, Siemerink MA, Perrakis G, Kaper T, Kengen SW, van der Oost J. 2009. Improving low-temperature activity of *Sulfolobus acidocaldarius* 2-keto-3-deoxygluconate aldolase. Archaea 2:233–239. <http://dx.doi.org/10.1155/2009/194186>.
303. Albers SV, Birkeland NK, Driessens AJM, Gertig S, Haferkamp P, Klenk HP, Kouril T, Manica A, Pham TK, Ruoff P, Schleper C, Schomburg D, Sharkey KJ, Siebers B, Sierociński P, Steuer R, van der Oost J, Westerhoff HV, Wieloch P, Wright PC, Zaparty M. 2009. SulfoSYS (*Sulfolobus* Systems Biology): towards a silicon cell model for the central carbohydrate metabolism of the archaeon *Sulfolobus solfataricus* under temperature variation. Biochem. Soc. Trans. 37:58–64. <http://dx.doi.org/10.1042/BST0370058>.
304. Jung JH, Lee SB. 2006. Identification and characterization of *Thermoplasma acidophilum* glyceraldehyde dehydrogenase: a new class of NADP⁺-specific aldehyde dehydrogenase. Biochem. J. 397:131–138. <http://dx.doi.org/10.1042/BJ20051763>.
305. Esser D, Kouril T, Talfournier F, Polkowska J, Schrader T, Brasen C, Siebers B. 2013. Unraveling the function of paralogs of the aldehyde dehydrogenase super family from *Sulfolobus solfataricus*. Extremophiles 17:205–216. <http://dx.doi.org/10.1007/s00792-012-0507-3>.
306. Kisker C, Schindelin H, Rees DC. 1997. Molybdenum-cofactor-containing enzymes: structure and mechanism. Annu. Rev. Biochem. 66:233–267. <http://dx.doi.org/10.1146/annurev.biochem.66.1.233>.
307. Noh M, Jung JH, Lee SB. 2006. Purification and characterization of glycerate kinase from the thermoacidophilic archaeon *Thermoplasma acidophilum*: an enzyme belonging to the second glycerate kinase family. Biotechnol. Bioprocess Eng. 11:344–350. <http://dx.doi.org/10.1007/BF03026251>.
308. Schwarzenbacher R, McMullan D, Krishna SS, Xu Q, Miller MD, Canaves JM, Elsliger MA, Floyd R, Grzechnik SK, Jaroszewski L, Klock HE, Koesema E, Kovarik JS, Kreusch A, Kuhn P, McPhillips TM, Morse AT, Quijano K, Spraggan G, Stevens RC, Van Den Bedem H, Wolf G, Hodgson KO, Wooley J, Deacon AM, Godzik A, Lesley SA, Wilson IA. 2006. Crystal structure of a glycerate kinase (TM1585) from *Thermotoga maritima* at 2.70 Å resolution reveals a new fold. Proteins 65:243–248. <http://dx.doi.org/10.1002/prot.21058>.
309. Yang C, Rodionov DA, Rodionova IA, Li X, Osterman AL. 2008. Glycerate 2-kinase of *Thermotoga maritima* and genomic reconstruction of related metabolic pathways. J. Bacteriol. 190:1773–1782. <http://dx.doi.org/10.1128/JB.01469-07>.
310. Hubbard BK, Koch M, Palmer DRJ, Babbitt PC, Gerlt JA. 1998. Evolution of enzymatic activities in the enolase superfamily: characterization of the (D)-glucarate/galactarate catabolic pathway in *Escherichia coli*. Biochemistry 37:14369–14375. <http://dx.doi.org/10.1021/bi981124f>.
311. Cheek S, Ginalski K, Zhang H, Grishin N. 2005. A comprehensive update of the sequence and structure classification of kinases. BMC Struct. Biol. 5:6. <http://dx.doi.org/10.1186/1472-6807-5-6>.
312. Boldt R, Edner C, Kolukisaoglu Ü, Hagemann M, Weckwerth W, Wienkoop S, Morgenthal K, Bauwe H. 2005. D-Glycerate-3-kinase, the last unknown enzyme in the photorespiratory cycle in *Arabidopsis*, belongs to a novel kinase family. Plant Cell 17:2413–2420. <http://dx.doi.org/10.1105/tpc.105.033993>.
313. Smyer JR, Jeter RM. 1989. Characterization of phosphoenolpyruvate synthase mutants in *Salmonella typhimurium*. Arch. Microbiol. 153:26–32. <http://dx.doi.org/10.1007/BF00277536>.
314. Patnaik R, Spitzer RG, Liao JC. 1995. Pathway engineering for production of aromatics in *Escherichia coli*: confirmation of stoichiometric analysis by independent modulation of AroG, TktA, and Pps activities. Biotechnol. Bioeng. 46:361–370. <http://dx.doi.org/10.1002/bit.260460409>.
315. Eyzaguirre J, Jansen K, Fuchs G. 1982. Phosphoenolpyruvate synthetase in Methanobacterium thermoautotrophicum. Arch. Microbiol. 132: 67–74. <http://dx.doi.org/10.1007/BF00690820>.
316. Jahn U, Huber H, Eisenreich W, Hugler M, Fuchs G. 2007. Insights into the autotrophic CO₂ fixation pathway of the archaeon *Ignicoccus hospitalis*: comprehensive analysis of the central carbon metabolism. J. Bacteriol. 189:4108–4119. <http://dx.doi.org/10.1128/JB.00047-07>.
317. Estelmann S, Hugler M, Eisenreich W, Werner K, Berg IA, Ramos-Vera WH, Say RF, Kockelkorn D, Gad'On N, Fuchs G. 2011. Labeling and enzyme studies of the central carbon metabolism in *Metallosphaera sedula*. J. Bacteriol. 193:1191–1200. <http://dx.doi.org/10.1128/JB.01155-10>.
318. Cicicopoli C, Peters J, Lupas A, Cejka Z, Müller SA, Golbik R, Pfeifer G, Lilie H, Engel A, Baumeister W. 1999. Novel molecular architecture of the multimeric archaeal PEP-synthase homologue (MAPS) from *Staphylothermus marinus*. J. Mol. Biol. 290:347–361. <http://dx.doi.org/10.1006/jmbi.1999.2878>.
319. Harauz G, Cicicopoli C, Hegerl R, Cejka Z, Goldie K, Santarius U, Engel A, Baumeister W. 1996. Structural studies on the 2.25-MDa homomultimeric phosphoenolpyruvate synthase from *Staphylothermus marinus*. J. Struct. Biol. 116:290–301. <http://dx.doi.org/10.1006/jbsb.1996.0044>.
320. Tjaden B, Plagens A, Dorr C, Siebers B, Hensel R. 2006. Phosphoenolpyruvate synthetase and pyruvate,phosphate dikinase of *Thermoproteus tenax*: key pieces in the puzzle of archaeal carbohydrate metabolism. Mol. Microbiol. 60:287–298. <http://dx.doi.org/10.1111/j.1365-2958.2006.05098.x>.
321. Zaparty M, Tjaden B, Hensel R, Siebers B. 2008. The central carbohydrate metabolism of the hyperthermophilic crenarchaeote *Thermoproteus tenax*: pathways and insights into their regulation. Arch. Microbiol. 190:231–245. <http://dx.doi.org/10.1007/s00203-008-0375-5>.
322. Sakuraba H, Utsumi E, Schreier HJ, Ohshima T. 2001. Transcriptional regulation of phosphoenolpyruvate synthase by maltose in the hyperthermophilic archaeon, *Pyrococcus furiosus*. J. Biosci. Bioeng. 92:108–113. <http://dx.doi.org/10.1263/jbb.92.108>.
323. Imanaka H, Yamatsu A, Fukui T, Atomi H, Imanaka T. 2006. Phosphoenolpyruvate synthase plays an essential role for glycolysis in the modified Embden-Meyerhof pathway in *Thermococcus kodakarensis*. Mol. Microbiol. 61:898–909. <http://dx.doi.org/10.1111/j.1365-2958.2006.05287.x>.
324. Hutchins AM, Holden JF, Adams MW. 2001. Phosphoenolpyruvate synthetase from the hyperthermophilic archaeon *Pyrococcus furiosus*. J. Bacteriol. 183:709–715. http://dx.doi.org/10.1128/JB.183.2.709-715_2001.
325. Niersbach M, Kreuzaler F, Geerse RH, Postma PW, Hirsch HJ. 1992. Cloning and nucleotide sequence of the *Escherichia coli* K-12 ppsA gene, encoding PEP synthase. Mol. Gen. Genet. 231:332–336.
326. Pocalko DJ, Carroll LJ, Martin BM, Babbitt PC, Dunaway-Mariano D. 1990. Analysis of sequence homologies in plant and bacterial pyruvate phosphate dikinase, enzyme I of the bacterial phosphoenolpyruvate:sugar phosphotransferase system and other PEP-utilizing enzymes. Identification of potential catalytic and regulatory motifs. Biochemistry 29: 10757–10765.
327. Narindrasorasak S, Bridger WA. 1977. Phosphoenolpyruvate synthetase of *Escherichia coli*: molecular weight, subunit composition, and identification of phosphohistidine in phosphoenzyme intermediate. J. Biol. Chem. 252:3121–3127.
328. Herzberg O, Chen CC, Kapadia G, McGuire M, Carroll LJ, Noh SJ, Dunaway-Mariano D. 1996. Swiveling-domain mechanism for enzy-

- matic phosphotransfer between remote reaction sites. Proc. Natl. Acad. Sci. U. S. A. 93:2652–2657. <http://dx.doi.org/10.1073/pnas.93.7.2652>.
329. Lim K, Read RJ, Chen CCH, Tempczyk A, Wei M, Ye D, Wu C, Dunaway-Mariano D, Herzberg O. 2007. Swiveling domain mechanism in pyruvate phosphate dikinase. Biochemistry 46:14845–14853. <http://dx.doi.org/10.1021/bi701848w>.
330. Fukuda W, Fukui T, Atomi H, Imanaka T. 2004. First characterization of an archaeal GTP-dependent phosphoenolpyruvate carboxykinase from the hyperthermophilic archaeon *Thermococcus kodakaraensis* KOD1. J. Bacteriol. 186:4620–4627. <http://dx.doi.org/10.1128/JB.186.14.4620-4627.2004>.
331. Aich S, Prasad L, Delbaere LTJ. 2008. Structure of a GTP-dependent bacterial PEP-carboxykinase from *Corynebacterium glutamicum*. Int. J. Biochem. Cell Biol. 40:1597–1603. <http://dx.doi.org/10.1016/j.biocel.2007.12.002>.
332. Sato T, Imanaka H, Rashid N, Fukui T, Atomi H, Imanaka T. 2004. Genetic evidence identifying the true gluconeogenic fructose-1,6-bisphosphatase in *Thermococcus kodakaraensis* and other hyperthermophiles. J. Bacteriol. 186:5799–5807. <http://dx.doi.org/10.1128/JB.186.17.5799-5807.2004>.
333. Fuchs G, Winter H, Steiner I, Stupperich E. 1983. Enzymes of gluconeogenesis in the autotroph *Methanobacterium thermoautotrophicum*. Arch. Microbiol. 136:160–162. <http://dx.doi.org/10.1007/BF00404793>.
334. Stec B, Yang H, Johnson KA, Chen L, Roberts MF. 2000. MJ0109 is an enzyme that is both an inositol monophosphatase and the ‘missing’ archaeal fructose-1,6-bisphosphatase. Nat. Struct. Biol. 7:1046–1050. <http://dx.doi.org/10.1038/80968>.
335. Verhees CH, Akerboom J, Schiltz E, de Vos WM, van der Oost J. 2002. Molecular and biochemical characterization of a distinct type of fructose-1,6-bisphosphatase from *Pyrococcus furiosus*. J. Bacteriol. 184:3401–3405. <http://dx.doi.org/10.1128/JB.184.12.3401-3405.2002>.
336. Rashid N, Imanaka H, Kanai T, Fukui T, Atomi H, Imanaka T. 2002. A novel candidate for the true fructose-1,6-bisphosphatase in archaea. J. Biol. Chem. 277:30649–30655. <http://dx.doi.org/10.1074/jbc.M202868200>.
337. Say RF, Fuchs G. 2010. Fructose 1,6-bisphosphate aldolase/phosphatase may be an ancestral gluconeogenic enzyme. Nature 464:1077–1081. <http://dx.doi.org/10.1038/nature08884>.
338. Kouril T, Esser D, Kort J, Westerhoff HV, Siebers B, Snoep JL. 2013. Intermediate instability at high temperature leads to low pathway efficiency for an in vitro reconstituted system of gluconeogenesis in *Sulfolobus solfataricus*. FEBS J. 280:4666–4680. <http://dx.doi.org/10.1111/febs.12438>.
339. Berg IA, Kockelkorn D, Ramos-Vera WH, Say RF, Zarzycki J, Hugler M, Alber BE, Fuchs G. 2010. Autotrophic carbon fixation in archaea. Nat. Rev. Microbiol. 8:447–460. <http://dx.doi.org/10.1038/nrmicro2365>.
340. Fushinobu S, Nishimatsu H, Hattori D, Song HJ, Wakagi T. 2011. Structural basis for the bifunctionality of fructose-1,6-bisphosphate aldolase/phosphatase. Nature 478:538–541. <http://dx.doi.org/10.1038/nature10457>.
341. Nishimatsu H, Fushinobu S, Shoun H, Wakagi T. 2004. The first crystal structure of the novel class of fructose-1,6-bisphosphatase present in thermophilic archaea. Structure 12:949–959. <http://dx.doi.org/10.1016/j.str.2004.03.026>.
342. Du J, Say RF, Lu W, Fuchs G, Einsle O. 2011. Active-site remodelling in the bifunctional fructose-1,6-bisphosphate aldolase/phosphatase. Nature 478:534–537. <http://dx.doi.org/10.1038/nature10458>.
343. Johnsen U, Schönenheit P. 2004. Novel xylose dehydrogenase in the halophilic archaeon *Haloarcula marismortui*. J. Bacteriol. 186:6198–6207. <http://dx.doi.org/10.1128/JB.186.18.6198-6207.2004>.
344. Johnsen U, Sutter J-M, Zaiß H, Schönenheit P. 2013. L-Arabinose degradation pathway in the haloarchaeon *Haloferax volcanii* involves a novel type of L-arabinose dehydrogenase. Extremophiles 17:897–909. <http://dx.doi.org/10.1007/s00792-013-0572-2>.
345. Grogan DW. 1989. Phenotypic characterization of the archaeabacterial genus *Sulfolobus*: comparison of five wild-type strains. J. Bacteriol. 171:6710–6719.
346. Anderson I, Scheuner C, Goker M, Mavromatis K, Hooper SD, Porat I, Klenk HP, Ivanova N, Kyprides N. 2011. Novel insights into the diversity of catabolic metabolism from ten haloarchaeal genomes. PLoS One 6:e20237. <http://dx.doi.org/10.1371/journal.pone.0020237>.
347. Schellenberg GD, Sarthy A, Larson AE, Backer MP, Crabb JW, Lidstrom M, Hall BD, Furlong CE. 1984. Xylose isomerase from *Esche-*
richia coli. Characterization of the protein and the structural gene. J. Biol. Chem. 259:6826–6832.
348. Di Luccio E, Petschacher B, Voegeli J, Chou H-T, Stahlberg H, Nideetzky B, Wilson DK. 2007. Structural and kinetic studies of induced fit in xylulose kinase from *Escherichia coli*. J. Mol. Biol. 365:783–798. <http://dx.doi.org/10.1016/j.jmb.2006.10.068>.
349. Kingston RL, Scopes RK, Baker EN. 1996. The structure of glucose-fructose oxidoreductase from *Zymomonas mobilis*: an osmoprotective periplasmic enzyme containing non-dissociable NADP. Structure 4:1413–1428. [http://dx.doi.org/10.1016/S0969-2126\(96\)00149-9](http://dx.doi.org/10.1016/S0969-2126(96)00149-9).
350. Brouns SJ, Turnbull AP, Willemen HLD, Akerboom J, van der Oost J. 2007. Crystal structure and biochemical properties of the d-arabinose dehydrogenase from *Sulfolobus solfataricus*. J. Mol. Biol. 371:1249–1260. <http://dx.doi.org/10.1016/j.jmb.2007.05.097>.
351. Watanabe S, Kodaki T, Makino K. 2006. Cloning, expression, and characterization of bacterial L-arabinose 1-dehydrogenase involved in an alternative pathway of L-arabinose metabolism. J. Biol. Chem. 281:2612–2623. <http://dx.doi.org/10.1074/jbc.M506477200>.
352. Theodosis A, Milburn CC, Heyer NI, Lamble HJ, Hough DW, Danson MJ, Taylor GL. 2005. Preliminary crystallographic studies of glucose dehydrogenase from the promiscuous Entner-Doudoroff pathway in the hyperthermophilic archaeon *Sulfolobus solfataricus*. Acta Crystallogr. Sect. F Struct. Biol. Cryst. Commun. 61:112–115. <http://dx.doi.org/10.1107/S174430910403101X>.
353. Gerlt JA, Babbitt PC, Rayment I. 2005. Divergent evolution in the enolase superfamily: the interplay of mechanism and specificity. Arch. Biochem. Biophys. 433:59–70. <http://dx.doi.org/10.1016/j.abb.2004.07.034>.
354. Watanabe S, Shimada N, Tajima K, Kodaki T, Makino K. 2006. Identification and characterization of L-arabonate dehydratase, L-2-keto-3-deoxyarabonate dehydratase, and L-arabinolactonase involved in an alternative pathway of L-arabinose metabolism. Novel evolutionary insight into sugar metabolism. J. Biol. Chem. 281:33521–33536. <http://dx.doi.org/10.1074/jbc.M606727200>.
355. Brouns SJ, Barends TRM, Worm P, Akerboom J, Turnbull AP, Salmon L, van der Oost J. 2008. Structural insight into substrate binding and catalysis of a novel 2-keto-3-deoxy-d-arabinonate dehydratase illustrates common mechanistic features of the FAH superfamily. J. Mol. Biol. 379:357–371. <http://dx.doi.org/10.1016/j.jmb.2008.03.064>.
356. Archer RM, Royer SF, Mahy W, Winn CL, Danson MJ, Bull SD. 2013. Syntheses of 2-keto-3-deoxy-D-xylonate and 2-keto-3-deoxy-L-arabinonate as stereochemical probes for demonstrating the metabolic promiscuity of *Sulfolobus solfataricus* towards D-xylose and L-arabinose. Chemistry 19:2895–2902. <http://dx.doi.org/10.1002/chem.201203489>.
357. Uhrigshardt H, Walden M, John H, Petersen A, Anemuller S. 2002. Evidence for an operative glyoxylate cycle in the thermoacidophilic crearchaeon *Sulfolobus acidocaldarius*. FEBS Lett. 513:223–229. [http://dx.doi.org/10.1016/S0014-5793\(02\)02317-7](http://dx.doi.org/10.1016/S0014-5793(02)02317-7).
358. Brasen C, Schönenheit P. 2001. Mechanisms of acetate formation and acetate activation in halophilic archaea. Arch. Microbiol. 175:360–368. <http://dx.doi.org/10.1007/s002030100273>.
359. Brasen C, Schönenheit P. 2004. Regulation of acetate and acetyl-CoA converting enzymes during growth on acetate and/or glucose in the halophilic archaeon *Haloarcula marismortui*. FEMS Microbiol. Lett. 241:21–26. <http://dx.doi.org/10.1016/j.femsle.2004.09.033>.
360. Soderberg T. 2005. Biosynthesis of ribose-5-phosphate and erythrose-4-phosphate in archaea: a phylogenetic analysis of archaeal genomes. Archaea 1:347–352. <http://dx.doi.org/10.1155/2005/314760>.
361. Soderberg T, Alver RC. 2004. Transaldolase of *Methanocaldococcus jannaschii*. Archaea 1:255–262. <http://dx.doi.org/10.1155/2004/608428>.
362. Tumbula DL, Teng Q, Bartlett MG, Whitman WB. 1997. Ribose biosynthesis and evidence for an alternative first step in the common aromatic amino acid pathway in *Methanococcus maripaludis*. J. Bacteriol. 179:6010–6013.
363. Selkov E, Maltsev N, Olsen GJ, Overbeek R, Whitman WB. 1997. A reconstruction of the metabolism of *Methanococcus jannaschii* from sequence data. Gene 197:GC11–GC26.
364. Lehwers-Litzmann A, Neumann P, Parthier C, Ludtke S, Golbik R, Ficner R, Tittmann K. 2011. Twisted Schiff base intermediates and substrate locale revise transaldolase mechanism. Nat. Chem. Biol. 7:678–684. <http://dx.doi.org/10.1038/nchembio.633>.
365. Grochowski LL, Xu H, White RH. 2005. Ribose-5-phosphate biosynthesis in *Methanocaldococcus jannaschii* occurs in the absence of a pen-

- tose-phosphate pathway. *J. Bacteriol.* 187:7382–7389. <http://dx.doi.org/10.1128/JB.187.21.7382-7389.2005>.
366. Yasueda H, Kawahara Y, Sugimoto S. 1999. *Bacillus subtilis* yckG and yckF encode two key enzymes of the ribulose monophosphate pathway used by methylotrophs, and yckH is required for their expression. *J. Bacteriol.* 181:7154–7160.
367. Reizer J, Reizer A, Saier MH, Jr. 1997. Is the ribulose monophosphate pathway widely distributed in bacteria? *Microbiology* 143:2519–2520. <http://dx.doi.org/10.1099/00221287-143-8-2519>.
368. Quayle JR, Ferenci T. 1978. Evolutionary aspects of autotrophy. *Microbiol. Rev.* 42:251–273.
369. Falb M, Muller K, Konigsmaier L, Oberwinkler T, Horn P, von Gronau S, Gonzalez O, Pfeiffer F, Bornberg-Bauer E, Oesterhelt D. 2008. Metabolism of halophilic archaea. *Extremophiles* 12:177–196. <http://dx.doi.org/10.1007/s00792-008-0138-x>.
370. Orita I, Sato T, Yurimoto H, Kato N, Atomi H, Imanaka T, Sakai Y. 2006. The ribulose monophosphate pathway substitutes for the missing pentose phosphate pathway in the archaeon *Thermococcus kodakaraensis*. *J. Bacteriol.* 188:4698–4704. <http://dx.doi.org/10.1128/JB.00492-06>.
371. Orita I, Yurimoto H, Hirai R, Kawarabayasi Y, Sakai Y, Kato N. 2005. The archaeon *Pyrococcus horikoshii* possesses a bifunctional enzyme for formaldehyde fixation via the ribulose monophosphate pathway. *J. Bacteriol.* 187:3636–3642. <http://dx.doi.org/10.1128/JB.187.11.3636-3642.2005>.
372. Martinez-Cruz LA, Dreyer MK, Boisvert DC, Yokota H, Martinez-Chantar ML, Kim R, Kim SH. 2002. Crystal structure of MJ1247 protein from *M. jannaschii* at 2.0 Å resolution infers a molecular function of 3-hexulose-6-phosphate isomerase. *Structure* 10:195–204. [http://dx.doi.org/10.1016/S0969-2126\(02\)00701-3](http://dx.doi.org/10.1016/S0969-2126(02)00701-3).
373. Orita I, Kita A, Yurimoto H, Kato N, Sakai Y, Miki K. 2010. Crystal structure of 3-hexulose-6-phosphate synthase, a member of the orotidine 5'-monophosphate decarboxylase superfamily. *Proteins* 78:3488–3492. <http://dx.doi.org/10.1002/prot.22860>.
374. Kato N, Yurimoto H, Thauer RK. 2006. The physiological role of the ribulose monophosphate pathway in bacteria and archaea. *Biosci. Biotechnol. Biochem.* 70:10–21. <http://dx.doi.org/10.1271/bbb.70.10>.
375. Gerlt JA, Raushel FM. 2003. Evolution of function in (β/α) -8-barrel enzymes. *Curr. Opin. Chem. Biol.* 7:252–264. [http://dx.doi.org/10.1016/S1367-5931\(03\)00019-X](http://dx.doi.org/10.1016/S1367-5931(03)00019-X).
376. Essenberg MK, Cooper RA. 1975. Two ribose-5-phosphate isomerases from *Escherichia coli* K12: partial characterisation of the enzymes and consideration of their possible physiological roles. *Eur. J. Biochem.* 55: 323–332. <http://dx.doi.org/10.1111/j.1432-1033.1975.tb02166.x>.
377. Ishikawa K, Matsui I, Payan F, Cambillau C, Ishida H, Kawarabayasi Y, Kikuchi H, Roussel A. 2002. A hyperthermstable D-ribose-5-phosphate isomerase from *Pyrococcus horikoshii* characterization and three-dimensional structure. *Structure* 10:877–886. [http://dx.doi.org/10.1016/S0969-2126\(02\)00779-7](http://dx.doi.org/10.1016/S0969-2126(02)00779-7).
378. Strange RW, Antonyuk SV, Ellis MJ, Bessho Y, Kuramitsu S, Yokoyama S, Hasnain SS. 2009. The structure of an archaeal ribose-5-phosphate isomerase from *Methanocaldococcus jannaschii* (MJ1603). *Acta Crystallogr. Sect. F Struct. Biol. Cryst. Commun.* 65:1214–1217. <http://dx.doi.org/10.1107/S1744390109044923>.
379. Rangarajan ES, Sivaraman J, Matte A, Cygler M. 2002. Crystal structure of D-ribose-5-phosphate isomerase (RpiA) from *Escherichia coli*. *Proteins* 48:737–740. <http://dx.doi.org/10.1002/prot.10203>.
380. Zhang R, Andersson CE, Savchenko A, Skarina T, Evdokimova E, Beasley S, Arrowsmith CH, Edwards AM, Joachimiak A, Mowbray SL. 2003. Structure of *Escherichia coli* ribose-5-phosphate isomerase: a ubiquitous enzyme of the pentose phosphate pathway and the calvin cycle. *Structure* 11:31–42. [http://dx.doi.org/10.1016/S0969-2126\(02\)00933-4](http://dx.doi.org/10.1016/S0969-2126(02)00933-4).
381. Goenrich M, Thauer RK, Yurimoto H, Kato N. 2005. Formaldehyde activating enzyme (Fae) and hexulose-6-phosphate synthase (Hps) in *Methanosarcina barkeri*: a possible function in ribose-5-phosphate biosynthesis. *Arch. Microbiol.* 184:41–48. <http://dx.doi.org/10.1007/s00203-005-0008-1>.
382. White RH. 2004. L-Aspartate semialdehyde and a 6-deoxy-5-ketohexose 1-phosphate are the precursors to the aromatic amino acids in *Methanocaldococcus jannaschii*. *Biochemistry* 43:7618–7627. <http://dx.doi.org/10.1021/bi0495127>.
383. White RH, Xu H. 2006. Methylglyoxal is an intermediate in the biosynthesis of 6-deoxy-5-ketofructose-1-phosphate: a precursor for aromatic amino acid biosynthesis in *Methanocaldococcus jannaschii*. *Biochemistry* 45:12366–12379. <http://dx.doi.org/10.1021/bi061018a>.
384. Porat I, Sieprawska-Lupa M, Teng Q, Bohanon FJ, White RH, Whitman WB. 2006. Biochemical and genetic characterization of an early step in a novel pathway for the biosynthesis of aromatic amino acids and p-aminobenzoic acid in the archaeon *Methanococcus maripaludis*. *Mol. Microbiol.* 62:1117–1131. <http://dx.doi.org/10.1111/j.1365-2958.2006.05426.x>.
385. Rashid N, Imanaka H, Fukui T, Atomi H, Imanaka T. 2004. Presence of a novel phosphopentomutase and a 2-deoxyribose 5-phosphate aldolase reveals a metabolic link between pentoses and central carbon metabolism in the hyperthermophilic archaeon *Thermococcus kodakaraensis*. *J. Bacteriol.* 186:4185–4191. <http://dx.doi.org/10.1128/JB.186.13.4185-4191.2004>.
386. Aono R, Sato T, Yano A, Yoshida S, Nishitani Y, Miki K, Imanaka T, Atomi H. 2012. Enzymatic characterization of AMP phosphorylase and ribose-1,5-bisphosphate isomerase functioning in an archaeal AMP metabolic pathway. *J. Bacteriol.* 194:6847–6855. <http://dx.doi.org/10.1128/JB.01335-12>.
387. Sato T, Atomi H, Imanaka T. 2007. Archaeal type III rubiscos function in a pathway for AMP metabolism. *Science* 315:1003–1006. <http://dx.doi.org/10.1126/science.1135999>.
388. Alonso H, Blayney MJ, Beck JL, Whitney SM. 2009. Substrate-induced assembly of *Methanococcoides burtonii* D-ribulose-1,5-bisphosphate carboxylase/oxygenase dimers into decamers. *J. Biol. Chem.* 284:33876–33882. <http://dx.doi.org/10.1074/jbc.M109.050989>.
389. Ezaki S, Maeda N, Kishimoto T, Atomi H, Imanaka T. 1999. Presence of a structurally novel type ribulose-bisphosphate carboxylase/oxygenase in the hyperthermophilic archaeon, *Pyrococcus kodakaraensis* KOD1. *J. Biol. Chem.* 274:5078–5082. <http://dx.doi.org/10.1074/jbc.274.8.5078>.
390. Kitano K, Maeda N, Fukui T, Atomi H, Imanaka T, Miki K. 2001. Crystal structure of a novel-type archaeal rubisco with pentagonal symmetry. *Structure* 9:473–481. [http://dx.doi.org/10.1016/S0969-2126\(01\)00608-6](http://dx.doi.org/10.1016/S0969-2126(01)00608-6).
391. Kreel NE, Tabita FR. 2007. Substitutions at methionine 295 of *Archaeoglobus fulgidus* ribulose-1,5-bisphosphate carboxylase/oxygenase affect oxygen binding and CO₂/O₂ specificity. *J. Biol. Chem.* 282:1341–1351. <http://dx.doi.org/10.1074/jbc.M609399200>.
392. Maeda N, Kitano K, Fukui T, Ezaki S, Atomi H, Miki K, Imanaka T. 1999. Ribulose bisphosphate carboxylase/oxygenase from the hyperthermophilic archaeon *Pyrococcus kodakaraensis* KOD1 is composed solely of large subunits and forms a pentagonal structure. *J. Mol. Biol.* 293:57–66. <http://dx.doi.org/10.1006/jmbi.1999.3145>.
393. Nishitani Y, Yoshida S, Fujihashi M, Kitagawa K, Doi T, Atomi H, Imanaka T, Miki K. 2010. Structure-based catalytic optimization of a type III rubisco from a hyperthermophile. *J. Biol. Chem.* 285:39339–39347. <http://dx.doi.org/10.1074/jbc.M110.147587>.
394. Tabita FR, Hanson TE, Li H, Satagopan S, Singh J, Chan S. 2007. Function, structure, and evolution of the rubisco-like proteins and their rubisco homologs. *Microbiol. Mol. Biol. Rev.* 71:576–599. <http://dx.doi.org/10.1128/MMBR.00015-07>.
395. Watson GM, Yu JP, Tabita FR. 1999. Unusual ribulose 1,5-bisphosphate carboxylase/oxygenase of anoxic archaea. *J. Bacteriol.* 181: 1569–1575.
396. Nakamura A, Fujihashi M, Aono R, Sato T, Nishiba Y, Yoshida S, Yano A, Atomi H, Imanaka T, Miki K. 2012. Dynamic, ligand-dependent conformational change triggers reaction of ribose-1,5-bisphosphate isomerase from *Thermococcus kodakaraensis* KOD1. *J. Biol. Chem.* 287:20784–20796. <http://dx.doi.org/10.1074/jbc.M112.349423>.
397. Schmid AK, Reiss DJ, Pan M, Koide T, Baliga NS. 2009. A single transcription factor regulates evolutionarily diverse but functionally linked metabolic pathways in response to nutrient availability. *Mol. Syst. Biol.* 5:282. <http://dx.doi.org/10.1038/msb.2009.40>.
398. Simpson PG, Whitman WB. 1993. Anabolic pathways in methanogens, p 445–472. In Ferry JG (ed), *Methanogenesis: ecology, physiology, biochemistry & genetics*. Chapman & Hall, Inc, New York, NY.
399. Ulas T, Riener SA, Zaparty M, Siebers B, Schomburg D. 2012. Genome-scale reconstruction and analysis of the metabolic network in the hyperthermophilic archaeon *Sulfolobus solfataricus*. *PLoS One* 7:e43401. <http://dx.doi.org/10.1371/journal.pone.0043401>.
400. Gonzalez O, Gronau S, Falb M, Pfeiffer F, Mendoza E, Zimmer R, Oesterhelt D. 2008. Reconstruction, modeling & analysis of *Halobacter-*

- rium salinarum* R-1 metabolism. Mol. Biosyst. 4:148–159. <http://dx.doi.org/10.1039/b715203e>.
401. Benedict MN, Gonnerman MC, Metcalf WW, Price ND. 2012. Genome-scale metabolic reconstruction and hypothesis testing in the methanogenic archaeon *Methanosarcina acetivorans* C2A. J. Bacteriol. 194:855–865. <http://dx.doi.org/10.1128/JB.06040-11>.
 402. Feist AM, Scholten JC, Palsson BO, Brockman FJ, Ideker T. 2006. Modeling methanogenesis with a genome-scale metabolic reconstruction of *Methanosarcina barkeri*. Mol. Syst. Biol. 2:2006.0004. <http://dx.doi.org/10.1038/msb4100046>.
 403. Satish Kumar V, Ferry JG, Maranas CD. 2011. Metabolic reconstruction of the archaeon methanogen *Methanosarcina acetivorans*. BMC Syst. Biol. 5:28. <http://dx.doi.org/10.1186/1752-0509-5-28>.
 404. Tsoka S, Simon D, Ouzounis CA. 2004. Automated metabolic reconstruction for *Methanococcus jannaschii*. Archaea 1:223–229. <http://dx.doi.org/10.1155/2004/324925>.
 405. Danner S, Soppa J. 1996. Characterization of the distal promoter element of halobacteria in vivo using saturation mutagenesis and selection. Mol. Microbiol. 19:1265–1276. <http://dx.doi.org/10.1111/j.1365-2958.1996.tb02471.x>.
 406. Bell SD, Jackson SP. 1998. Transcription and translation in archaea: a mosaic of eukaryal and bacterial features. Trends Microbiol. 6:222–228. [http://dx.doi.org/10.1016/S0966-842X\(98\)01281-5](http://dx.doi.org/10.1016/S0966-842X(98)01281-5).
 407. Bell SD, Jackson SP. 2001. Mechanism and regulation of transcription in archaea. Curr. Opin. Microbiol. 4:208–213. [http://dx.doi.org/10.1016/S1369-5274\(00\)00190-9](http://dx.doi.org/10.1016/S1369-5274(00)00190-9).
 408. Baliga NS, Goo YA, Ng WV, Hood L, Daniels CJ, DasSarma S. 2000. Is gene expression in *Halobacterium* NRC-1 regulated by multiple TBP and TFB transcription factors? Mol. Microbiol. 36:1184–1185. <http://dx.doi.org/10.1046/j.1365-2958.2000.01916.x>.
 409. Facciotti MT, Reiss DJ, Pan M, Kaur A, Vuthoori M, Bonneau R, Shannon P, Srivastava A, Donohoe SM, Hood LE, Baliga NS. 2007. General transcription factor specified global gene regulation in archaea. Proc. Natl. Acad. Sci. U. S. A. 104:4630–4635. <http://dx.doi.org/10.1073/pnas.0611663104>.
 410. Turkarslan S, Reiss DJ, Gibbins G, Su WL, Pan M, Bare JC, Plaisier CL, Baliga NS. 2011. Niche adaptation by expansion and reprogramming of general transcription factors. Mol. Syst. Biol. 7:554. <http://dx.doi.org/10.1038/msb.2011.87>.
 411. Coker JA, DasSarma S. 2007. Genetic and transcriptomic analysis of transcription factor genes in the model halophilic archaeon: coordinate action of TbpD and TfbA. BMC Genet. 8:61. <http://dx.doi.org/10.1186/1471-2156-8-61>.
 412. Thompson DK, Palmer JR, Daniels CJ. 1999. Expression and heat-responsive regulation of a TFIIB homologue from the archaeon *Haloflexax volcanii*. Mol. Microbiol. 33:1081–1092. <http://dx.doi.org/10.1046/j.1365-2958.1999.01551.x>.
 413. Shockley KR, Ward DE, Chhabra SR, Conners SB, Montero CI, Kelly RM. 2003. Heat shock response by the hyperthermophilic archaeon *Pyrococcus furiosus*. Appl. Environ. Microbiol. 69:2365–2371. <http://dx.doi.org/10.1128/AEM.69.4.2365-2371.2003>.
 414. Micrescu M, Grunberg S, Franke A, Cramer P, Thomm M, Bartlett M. 2008. Archaeal transcription: function of an alternative transcription factor B from *Pyrococcus furiosus*. J. Bacteriol. 190:157–167. <http://dx.doi.org/10.1128/JB.01498-07>.
 415. Ng WV, Kennedy SP, Mahairas GG, Berquist B, Pan M, Shukla HD, Lasky SR, Baliga NS, Thorsson V, Sbrogna J, Swartzell S, Weir D, Hall J, Dahl TA, Welti R, Goo YA, Leithauer B, Keller K, Cruz R, Danson MJ, Hough DW, Maddocks DG, Jablonski PE, Krebs MP, Angevine CM, Dale H, Isenbarger TA, Peck RF, Pohlshroder M, Spudich JL, Jung KH, Alam M, Freitas T, Hou S, Daniels CJ, Dennis PP, Omer AD, Ebhardt H, Lowe TM, Liang P, Riley M, Hood L, DasSarma S. 2000. Genome sequence of *Halobacterium* species NRC-1. Proc. Natl. Acad. Sci. U. S. A. 97:12176–12181. <http://dx.doi.org/10.1073/pnas.190337797>.
 416. She Q, Singh RK, Confalonieri F, Zivanovic Y, Allard G, Awayez MJ, Chan-Weiher CC, Clausen IG, Curtis BA, De Moors A, Erauso G, Fletcher C, Gordon PM, Heikamp-de Jong I, Jeffries AC, Kozena CJ, Medina N, Peng X, Thi-Ngoi HP, Redder P, Schenk ME, Theriault C, Tolstrup N, Charlebois RL, Doolittle WF, Duguet M, Gaasterland T, Garrett RA, Ragan MA, Sensen CW, Van der Oost J. 2001. The complete genome of the crenarchaeon *Sulfolobus solfataricus* P2. Proc. Natl. Acad. Sci. U. S. A. 98:7835–7840. <http://dx.doi.org/10.1073/pnas.141222098>.
 417. Chen L, Brugger K, Skovgaard M, Redder P, She Q, Torarinsson E, Greve B, Awayez M, Zibat A, Klenk HP, Garrett RA. 2005. The genome of *Sulfolobus acidocaldarius*, a model organism of the Crenarchaeota. J. Bacteriol. 187:4992–4999. <http://dx.doi.org/10.1128/JB.187.14.4992-4999.2005>.
 418. Siebers B, Zaparty M, Raddatz G, Tjaden B, Albers SV, Bell SD, Blomback F, Kletzin A, Kyripides N, Lanz C, Plaggen A, Rampp M, Rosinus A, von Jan M, Makarova KS, Klenk HP, Schuster SC, Hensel R. 2011. The complete genome sequence of *Thermoproteus tenax*: a physiologically versatile member of the crenarchaeota. PLoS One 6:e24222. <http://dx.doi.org/10.1371/journal.pone.0024222>.
 419. Kruger K, Hermann T, Armbruster V, Pfeifer F. 1998. The transcriptional activator GvpE for the halobacterial gas vesicle genes resembles a basic region leucine-zipper regulatory protein. J. Mol. Biol. 279:761–771. <http://dx.doi.org/10.1006/jmbi.1998.1795>.
 420. de Koning B, Blomback F, Wu H, Brouns SJ, van der Oost J. 2009. Role of multiprotein bridging factor 1 in archaea: bridging the domains? Biochem. Soc. Trans. 37:52–57. <http://dx.doi.org/10.1042/BST0370052>.
 421. Marrero Coto J, Ehrenhofer-Murray AE, Pons T, Siebers B. 2011. Functional analysis of archaeal MBF1 by complementation studies in yeast. Biol. Direct 6:18. <http://dx.doi.org/10.1186/1745-6150-6-18>.
 422. Makarova KS, Koonin EV. 2003. Comparative genomics of archaea: how much have we learned in six years, and what's next? Genome Biol. 4:115. <http://dx.doi.org/10.1186/gb-2003-4-8-115>.
 423. Wilson CJ, Zhan H, Swint-Kruse L, Matthews KS. 2007. The lactose repressor system: paradigms for regulation, allosteric behavior and protein folding. Cell. Mol. Life Sci. 64:3–16. <http://dx.doi.org/10.1007/s00018-006-6296-z>.
 424. Eichler J, Adams MW. 2005. Posttranslational protein modification in archaea. Microbiol. Mol. Biol. Rev. 69:393–425. <http://dx.doi.org/10.1128/MMBR.69.3.393-425.2005>.
 425. Kennelly PJ. 2003. Archaeal protein kinases and protein phosphatases: insights from genomics and biochemistry. Biochem. J. 370:373–389. <http://dx.doi.org/10.1042/BJ20021547>.
 426. Rudolph J, Oesterhelt D. 1995. Chemotaxis and phototaxis require a CheA histidine kinase in the archaeon *Halobacterium salinarium*. EMBO J. 14:667–673.
 427. Chu H-M, Wang AH-J. 2007. Enzyme-substrate interactions revealed by the crystal structures of the archaeal *Sulfolobus* PTP-fold phosphatase and its phosphopeptide complexes. Proteins 66:996–1003. <http://dx.doi.org/10.1002/prot.21262>.
 428. Leng J, Cameron AJM, Buckel S, Kennelly PJ. 1995. Isolation and cloning of a protein-serine/threonine phosphatase from an archaeon. J. Bacteriol. 177:6510–6517.
 429. Reimann J, Esser D, Orell A, Amman F, Pham TK, Noirel J, Lindås A-C, Bernander R, Wright PC, Siebers B, Albers S-V. 2013. Archaeal signal transduction: impact of protein phosphatase deletions on cell size, motility, and energy metabolism in *Sulfolobus acidocaldarius*. Mol. Cell. Proteomics 12:3908–3923. <http://dx.doi.org/10.1074/mcp.M113.027375>.
 430. Haile JD, Kennelly PJ. 2011. The activity of an ancient atypical protein kinase is stimulated by ADP-ribose in vitro. Arch. Biochem. Biophys. 511:56–63. <http://dx.doi.org/10.1016/j.abb.2011.04.006>.
 431. Lower BH, Bischoff KM, Kennelly PJ. 2000. The archaeon *Sulfolobus solfataricus* contains a membrane-associated protein kinase activity that preferentially phosphorylates threonine residues in vitro. J. Bacteriol. 182:3452–3459. <http://dx.doi.org/10.1128/JB.182.12.3452-3459.2000>.
 432. Lower BH, Kennelly PJ. 2003. Open reading frame sso2387 from the archaeon *Sulfolobus solfataricus* encodes a polypeptide with protein-serine kinase activity. J. Bacteriol. 185:3436–3445. <http://dx.doi.org/10.1128/JB.185.11.3436-3445.2003>.
 433. Lower BH, Potters MB, Kennelly PJ. 2004. A phosphoprotein from the archaeon *Sulfolobus solfataricus* with protein-serine/threonine kinase activity. J. Bacteriol. 186:463–472. <http://dx.doi.org/10.1128/JB.186.2.463-472.2004>.
 434. Lower BH, Kennelly PJ. 2002. The membrane-associated protein-serine/threonine kinase from *Sulfolobus solfataricus* is a glycoprotein. J. Bacteriol. 184:2614–2619. <http://dx.doi.org/10.1128/JB.184.10.2614-2619.2002>.
 435. Reimann J, Lassak K, Khadouma S, Ettema TJG, Yang N, Driessen AJM, Klingl A, Albers SV. 2012. Regulation of archaella expression by the FHA and von Willebrand domain-containing proteins ArnA and ArnB in *Sulfolobus acidocaldarius*. Mol. Microbiol. 86:24–36. <http://dx.doi.org/10.1111/j.1365-2958.2012.08186.x>.

436. Wang B, Yang S, Zhang L, He ZG. 2010. Archaeal eukaryote-like serine/threonine protein kinase interacts with and phosphorylates a forkhead-associated-domain-containing protein. *J. Bacteriol.* 192:1956–1964. <http://dx.doi.org/10.1128/JB.01471-09>.
437. Aivaliotis M, Macek B, Gnad F, Reichelt P, Mann M, Oesterhelt D. 2009. Ser/Thr/Tyr protein phosphorylation in the archaeon *Halobacterium salinarum*—a representative of the third domain of life. *PLoS One* 4:e4777. <http://dx.doi.org/10.1371/journal.pone.0004777>.
438. Panchaud A, Scherl A, Shaffer SA, Von Haller PD, Kulasekara HD, Miller SI, Goodlett DR. 2009. Precursor acquisition independent from ion count: how to dive deeper into the proteomics ocean. *Anal. Chem.* 81:6481–6488. <http://dx.doi.org/10.1021/ac900888s>.
439. Esser D, Pham KT, Reimann J, Albers S-V, Siebers B, Wright PC. 2012. Change of carbon source causes dramatic effects in the phosphoproteome of the archaeon *Sulfolobus solfataricus*. *J. Proteome Res.* 11: 4823–4833. <http://dx.doi.org/10.1021/pr300190k>.
440. Makarova KS, Sorokin AV, Novichkov PS, Wolf YI, Koonin EV. 2007. Clusters of orthologous genes for 41 archaeal genomes and implications for evolutionary genomics of archaea. *Biol. Direct* 2:33. <http://dx.doi.org/10.1186/1745-6150-2-33>.
441. Kouril T, Kolodkin A, Zaparty M, Steuer R, Ruoff P, Westerhoff HV, Snoep J, Siebers B, SulfoSYS Consortium. 2012. *Sulfolobus* systems biology: cool hot design for metabolic pathways, p 151–168. In Wren B, Robertson B (ed), *Systems biology of microorganisms*. Caister Academic Press, Norwich, United Kingdom.
442. Teusink B, Passarge J, Reijenga CA, Esgalhado E, van der Weijden CC, Schepper M, Walsh MC, Bakker BM, van Dam K, Westerhoff HV, Snoep JL. 2000. Can yeast glycolysis be understood in terms of *in vitro* kinetics of the constituent enzymes? Testing biochemistry. *Eur. J. Biochem.* 267:5313–5329. <http://dx.doi.org/10.1046/j.1432-1327.2000.01527.x>.
443. Fiala G, Stetter K. 1986. *Pyrococcus furiosus* sp. nov. represents a novel genus of marine heterotrophic archaeabacteria growing optimally at 100°C. *Arch. Microbiol.* 145:56–61. <http://dx.doi.org/10.1007/BF00413027>.
444. Atomi H, Fukui T, Kanai T, Morikawa M, Imanaka T. 2004. Description of *Thermococcus kodakaraensis* sp. nov., a well studied hyperthermophilic archaeon previously reported as *Pyrococcus* sp. KOD1. *Archaea* 1:263–267. <http://dx.doi.org/10.1155/2004/204953>.
445. Morikawa M, Izawa Y, Rashid N, Hoaki T, Imanaka T. 1994. Purification and characterization of a thermostable thiol protease from a newly isolated hyperthermophilic *Pyrococcus* sp. *Appl. Environ. Microbiol.* 60: 4559–4566.
446. Fukui T, Atomi H, Kanai T, Matsumi R, Fujiwara S, Imanaka T. 2005. Complete genome sequence of the hyperthermophilic archaeon *Thermococcus kodakaraensis* KOD1 and comparison with *Pyrococcus* genomes. *Genome Res.* 15:352–363. <http://dx.doi.org/10.1101/gr.3003105>.
447. Robb FT, Maeder DL, Brown JR, DiRuggiero J, Stump MD, Yeh RK, Weiss RB, Dunn DM. 2001. Genomic sequence of hyperthermophile, *Pyrococcus furiosus*: implications for physiology and enzymology. *Methods Enzymol.* 330:134–157. [http://dx.doi.org/10.1016/S0076-6879\(01\)30372-5](http://dx.doi.org/10.1016/S0076-6879(01)30372-5).
448. Waegle I, Schmid G, Thumann S, Thomm M, Hausner W. 2010. Shuttle vector-based transformation system for *Pyrococcus furiosus*. *Appl. Environ. Microbiol.* 76:3308–3313. <http://dx.doi.org/10.1128/AEM.01951-09>.
449. Sato T, Fukui T, Atomi H, Imanaka T. 2003. Targeted gene disruption by homologous recombination in the hyperthermophilic archaeon *Thermococcus kodakaraensis* KOD1. *J. Bacteriol.* 185:210–220. <http://dx.doi.org/10.1128/JB.185.1.210-220.2003>.
450. Sato T, Fukui T, Atomi H, Imanaka T. 2005. Improved and versatile transformation system allowing multiple genetic manipulations of the hyperthermophilic archaeon *Thermococcus kodakaraensis*. *Appl. Environ. Microbiol.* 71:3889–3899. <http://dx.doi.org/10.1128/AEM.71.3889-3899.2005>.
451. Keller MW, Schut GJ, Lipscomb GL, Menon AL, Iwuchukwu IJ, Leuko TT, Thorgeresen MP, Nixon WJ, Hawkins AS, Kelly RM, Adams MW. 2013. Exploiting microbial hyperthermophilicity to produce an industrial chemical, using hydrogen and carbon dioxide. *Proc. Natl. Acad. Sci. U. S. A.* 110:5840–5845. <http://dx.doi.org/10.1073/pnas.1222607110>.
452. Vanfosson AL, Lewis DL, Nichols JD, Kelly RM. 2008. Polysaccharide degradation and synthesis by extremely thermophilic anaerobes. *Ann. N. Y. Acad. Sci.* 1125:322–337. <http://dx.doi.org/10.1196/annals.1419.017>.
453. Adams MW, Holden JF, Menon AL, Schut GJ, Grunden AM, Hou C, Hutchins AM, Jenney FE, Jr, Kim C, Ma K, Pan G, Roy R, Sapra R, Story SV, Verhagen MF. 2001. Key role for sulfur in peptide metabolism and in regulation of three hydrogenases in the hyperthermophilic archaeon *Pyrococcus furiosus*. *J. Bacteriol.* 183:716–724. <http://dx.doi.org/10.1128/JB.183.2.716-724.2001>.
454. Glasemacher J, Bock AK, Schmid R, Schönheit P. 1997. Purification and properties of acetyl-CoA synthetase (ADP-forming), an archaeal enzyme of acetate formation and ATP synthesis, from the hyperthermophile *Pyrococcus furiosus*. *Eur. J. Biochem.* 244:561–567. <http://dx.doi.org/10.1111/j.1432-1033.1997.00561.x>.
455. Sapra R, Bagramyan K, Adams MW. 2003. A simple energy-conserving system: proton reduction coupled to proton translocation. *Proc. Natl. Acad. Sci. U. S. A.* 100:7545–7550. <http://dx.doi.org/10.1073/pnas.1331436100>.
456. Schut GJ, Boyd ES, Peters JW, Adams MW. 2013. The modular respiratory complexes involved in hydrogen and sulfur metabolism by heterotrophic hyperthermophilic archaea and their evolutionary implications. *FEMS Microbiol. Rev.* 37:182–203. <http://dx.doi.org/10.1111/j.1574-6976.2012.00346.x>.
457. Pisa KY, Huber H, Thomm M, Müller V. 2007. A sodium ion-dependent AIAO ATP synthase from the hyperthermophilic archaeon *Pyrococcus furiosus*. *FEBS J.* 274:3928–3938. <http://dx.doi.org/10.1111/j.1742-4658.2007.05925.x>.
458. Kanai T, Matsuoka R, Beppu H, Nakajima A, Okada Y, Atomi H, Imanaka T. 2011. Distinct physiological roles of the three [NiFe]-hydrogenase orthologs in the hyperthermophilic archaeon *Thermococcus kodakaraensis*. *J. Bacteriol.* 193:3109–3116. <http://dx.doi.org/10.1128/JB.01072-10>.
459. Bridger SL, Clarkson SM, Stirrett K, DeBarry MB, Lipscomb GL, Schut GJ, Westpheling J, Scott RA, Adams MW. 2011. Deletion strains reveal metabolic roles for key elemental sulfur-responsive proteins in *Pyrococcus furiosus*. *J. Bacteriol.* 193:6498–6504. <http://dx.doi.org/10.1128/JB.05445-11>.
460. Schut GJ, Nixon WJ, Lipscomb GL, Scott RA, Adams MW. 2012. Mutational analyses of the enzymes involved in the metabolism of hydrogen by the hyperthermophilic archaeon *Pyrococcus furiosus*. *Front. Microbiol.* 3:163. <http://dx.doi.org/10.3389/fmicb.2012.00163>.
461. Albers SV, Koning SM, Konings WN, Driessens AJ. 2004. Insights into ABC transport in archaea. *J. Bioenerg. Biomembr.* 36:5–15. <http://dx.doi.org/10.1023/B:JOBB.0000019593.84933.e6>.
462. Lee SJ, Bohm A, Krug M, Boos W. 2007. The ABC of binding-protein-dependent transport in archaea. *Trends Microbiol.* 15:389–397. <http://dx.doi.org/10.1016/j.tim.2007.08.002>.
463. Matsumi R, Manabe K, Fukui T, Atomi H, Imanaka T. 2007. Disruption of a sugar transporter gene cluster in a hyperthermophilic archaeon using a host-marker system based on antibiotic resistance. *J. Bacteriol.* 189:2683–2691. <http://dx.doi.org/10.1128/JB.01692-06>.
464. Lee SJ, Engelmann A, Horlacher R, Qu Q, Vierke G, Hebbeln C, Thomm M, Boos W. 2003. TrmB, a sugar-specific transcriptional regulator of the trehalose/maltose ABC transporter from the hyperthermophilic archaeon *Thermococcus litoralis*. *J. Biol. Chem.* 278:983–990. <http://dx.doi.org/10.1074/jbc.M210236200>.
465. Qu Q, Lee SJ, Boos W. 2004. TreT, a novel trehalose glycosyltransferring synthase of the hyperthermophilic archaeon *Thermococcus litoralis*. *J. Biol. Chem.* 279:47890–47897. <http://dx.doi.org/10.1074/jbc.M404955200>.
466. Lee SJ, Moulakakis C, Koning SM, Hausner W, Thomm M, Boos W. 2005. TrmB, a sugar sensing regulator of ABC transporter genes in *Pyrococcus furiosus* exhibits dual promoter specificity and is controlled by different inducers. *Mol. Microbiol.* 57:1797–1807. <http://dx.doi.org/10.1111/j.1365-2958.2005.04804.x>.
467. Koning SM, Elferink MG, Konings WN, Driessens AJ. 2001. Cellobiose uptake in the hyperthermophilic archaeon *Pyrococcus furiosus* is mediated by an inducible, high-affinity ABC transporter. *J. Bacteriol.* 183: 4979–4984. <http://dx.doi.org/10.1128/JB.183.17.4979-4984.2001>.
468. Sakuraba H, Utsumi E, Kujo C, Ohshima T. 1999. An AMP-dependent (ATP-forming) kinase in the hyperthermophilic archaeon *Pyrococcus furiosus*: characterization and novel physiological role. *Arch. Biochem. Biophys.* 364:125–128. <http://dx.doi.org/10.1006/abbi.1999.1121>.
469. Blamey JM, Adams MW. 1993. Purification and characterization of pyruvate ferredoxin oxidoreductase from the hyperthermophilic archaeon *Pyrococcus furiosus*. *Biochim. Biophys. Acta* 1161:19–27. [http://dx.doi.org/10.1016/0167-4838\(93\)90190-3](http://dx.doi.org/10.1016/0167-4838(93)90190-3).

470. Hopkins RC, Sun J, Jenney FE, Jr, Chandrayan SK, McTernan PM, Adams MW. 2011. Homologous expression of a subcomplex of *Pyrococcus furiosus* hydrogenase that interacts with pyruvate ferredoxin oxidoreductase. *PLoS One* 6:e26569. <http://dx.doi.org/10.1371/journal.pone.0026569>.
471. Kletzin A, Adams MW. 1996. Molecular and phylogenetic characterization of pyruvate and 2-ketoisovalerate ferredoxin oxidoreductases from *Pyrococcus furiosus* and pyruvate ferredoxin oxidoreductase from *Thermotoga maritima*. *J. Bacteriol.* 178:248–257.
472. Kunow J, Linder D, Thauer RK. 1995. Pyruvate:ferredoxin oxidoreductase from the sulfate-reducing *Archaeoglobus fulgidus*: molecular composition, catalytic properties, and sequence alignments. *Arch. Microbiol.* 163:21–28. <http://dx.doi.org/10.1007/BF00262199>.
473. Ma K, Hutchins A, Sung SJ, Adams MW. 1997. Pyruvate ferredoxin oxidoreductase from the hyperthermophilic archaeon, *Pyrococcus furiosus*, functions as a CoA-dependent pyruvate decarboxylase. *Proc. Natl. Acad. Sci. U. S. A.* 94:9608–9613. <http://dx.doi.org/10.1073/pnas.94.18.9608>.
474. Brasen C, Schmidt M, Grotzinger J, Schonheit P. 2008. Reaction mechanism and structural model of ADP-forming acetyl-CoA synthetase from the hyperthermophilic archaeon *Pyrococcus furiosus*: evidence for a second active site histidine residue. *J. Biol. Chem.* 283:15409–15418. <http://dx.doi.org/10.1074/jbc.M710218200>.
475. Musfeldt M, Selig M, Schönheit P. 1999. Acetyl coenzyme A synthetase (ADP forming) from the hyperthermophilic archaeon *Pyrococcus furiosus*: identification, cloning, separate expression of the encoding genes, acdAI and acdBI, in *Escherichia coli*, and in vitro reconstitution of the active heterotetrameric enzyme from its recombinant subunits. *J. Bacteriol.* 181:5885–5888.
476. Schafer T, Selig M, Schonheit P. 1993. Acetyl-CoA synthetase (ADP forming) in archaea, a novel enzyme involved in acetate formation and ATP synthesis. *Arch. Microbiol.* 159:72–83. <http://dx.doi.org/10.1007/BF00244267>.
477. Schmidt M, Schönheit P. 2013. Acetate formation in the photoheterotrophic bacterium *Chloroflexus aurantiacus* involves an archaeal type ADP-forming acetyl-CoA synthetase isoenzyme I. *FEMS Microbiol. Lett.* 349:171–179. <http://dx.doi.org/10.1111/1574-6968.12312>.
478. Mai X, Adams MW. 1996. Purification and characterization of two reversible and ADP-dependent acetyl coenzyme A synthetases from the hyperthermophilic archaeon *Pyrococcus furiosus*. *J. Bacteriol.* 178:5897–5903.
479. Bock AK, Glasemacher J, Schmidt R, Schönheit P. 1999. Purification and characterization of two extremely thermostable enzymes, phosphate acetyltransferase and acetate kinase, from the hyperthermophilic eubacterium *Thermotoga maritima*. *J. Bacteriol.* 181:1861–1867.
480. Lee SJ, Surma M, Seitz S, Hausner W, Thomm M, Boos W. 2007. Characterization of the TrmB-like protein, PF0124, a TGM-recognizing global transcriptional regulator of the hyperthermophilic archaeon *Pyrococcus furiosus*. *Mol. Microbiol.* 65:305–318. <http://dx.doi.org/10.1111/j.1365-2958.2007.05780.x>.
481. Lee SJ, Surma M, Seitz S, Hausner W, Thomm M, Boos W. 2007. Differential signal transduction via TrmB, a sugar sensing transcriptional repressor of *Pyrococcus furiosus*. *Mol. Microbiol.* 64:1499–1505. <http://dx.doi.org/10.1111/j.1365-2958.2007.05737.x>.
482. Lee SJ, Surma M, Hausner W, Thomm M, Boos W. 2008. The role of TrmB and TrmB-like transcriptional regulators for sugar transport and metabolism in the hyperthermophilic archaeon *Pyrococcus furiosus*. *Arch. Microbiol.* 190:247–256. <http://dx.doi.org/10.1007/s00203-008-0378-2>.
483. Krug M, Lee SJ, Diederichs K, Boos W, Welte W. 2006. Crystal structure of the sugar binding domain of the archaeal transcriptional regulator TrmB. *J. Biol. Chem.* 281:10976–10982. <http://dx.doi.org/10.1074/jbc.M512809200>.
484. Xavier KB, Peist R, Kossmann M, Boos W, Santos H. 1999. Maltose metabolism in the hyperthermophilic archaeon *Thermococcus litoralis*: purification and characterization of key enzymes. *J. Bacteriol.* 181:3358–3367.
485. Horlacher R, Xavier KB, Santos H, DiRuggiero J, Kossmann M, Boos W. 1998. Archaeal binding protein-dependent ABC transporter: molecular and biochemical analysis of the trehalose/maltose transport system of the hyperthermophilic archaeon *Thermococcus litoralis*. *J. Bacteriol.* 180:680–689.
486. Krug M, Lee SJ, Boos W, Diederichs K, Welte W. 2013. The three-dimensional structure of TrmB, a transcriptional regulator of dual function in the hyperthermophilic archaeon *Pyrococcus furiosus* in complex with sucrose. *Protein Sci.* 22:800–808. <http://dx.doi.org/10.1002/pro.2263>.
487. Noll KM, Lapierre P, Gogarten JP, Nanavati DM. 2008. Evolution of mal ABC transporter operons in the *Thermococcales* and *Thermotogales*. *BMC Evol. Biol.* 8:7. <http://dx.doi.org/10.1186/1471-2148-8-7>.
488. van de Werken HJ, Verhees CH, Akerboom J, de Vos WM, van der Oost J. 2006. Identification of a glycolytic regulon in the archaea *Pyrococcus* and *Thermococcus*. *FEMS Microbiol. Lett.* 260:69–76. <http://dx.doi.org/10.1111/j.1574-6968.2006.00292.x>.
489. Maruyama H, Shin M, Oda T, Matsumi R, Ohnawa RL, Itoh T, Shirahige K, Imanaka T, Atomi H, Yoshimura SH, Takeyasu K. 2011. Histone and TK0471/TrmBL2 form a novel heterogeneous genome architecture in the hyperthermophilic archaeon *Thermococcus kodakarensis*. *Mol. Biol. Cell* 22:386–398. <http://dx.doi.org/10.1091/mbc.E10-08-0668>.
490. Zillig W, Stetter KO, Wunderl S. 1980. The Sulfolobus-“Caldariella” group: taxonomy on the basis of the structure of DNA-dependent RNA polymerases. *Arch. Microbiol.* 125:259–269. <http://dx.doi.org/10.1007/BF00446886>.
491. Guo L, Brugger K, Liu C, Shah SA, Zheng H, Zhu Y, Wang S, Lillestol RK, Chen L, Frank J, Prangishvili D, Paulin L, She Q, Huang L, Garrett RA. 2011. Genome analyses of Icelandic strains of *Sulfolobus islandicus*, model organisms for genetic and virus-host interaction studies. *J. Bacteriol.* 193:1672–1680. <http://dx.doi.org/10.1128/JB.01487-10>.
492. Kawarabayasi Y, Hino Y, Horikawa H, Jin-no K, Takahashi M, Sekine M, Baba S, Ankai A, Kosugi H, Hosoyama A, Fukui S, Nagai Y, Nishijima K, Otsuka R, Nakazawa H, Takamiya M, Kato Y, Yoshizawa T, Tanaka T, Kudoh Y, Yamazaki J, Kushida N, Oguchi A, Aoki K, Masuda S, Yanagii M, Nishimura M, Yamagishi A, Oshima T, Kikuchi H. 2001. Complete genome sequence of an aerobic thermoacidophilic crenarchaeon, Sulfolobus tokodaii strain7. *DNA Res.* 8:123–140. <http://dx.doi.org/10.1093/dnare/8.4.123>.
493. Wagner M, Berkner S, Ajon M, Driessens AJM, Lipps G, Albers SV. 2009. Expanding and understanding the genetic toolbox of the hyperthermophilic genus *Sulfolobus*. *Biochem. Soc. Trans.* 37:97–101. <http://dx.doi.org/10.1042/BST0370097>.
494. Huber G, Drobner E, Huber H, Stetter KO. 1992. Growth by aerobic oxidation of molecular hydrogen in archaea—a metabolic property so far unknown for this domain. *Syst. Appl. Microbiol.* 15:502–504. [http://dx.doi.org/10.1016/S0723-2020\(11\)80108-6](http://dx.doi.org/10.1016/S0723-2020(11)80108-6).
495. Kerscher L, Nowitzki S, Oesterhelt D. 1982. Thermoacidophilic archaeabacteria contain bacterial-type ferredoxins acting as electron acceptors of 2-oxacid:ferredoxin oxidoreductases. *Eur. J. Biochem.* 128:223–230.
496. Schafer G, Engelhard M, Muller V. 1999. Bioenergetics of the archaea. *Microbiol. Mol. Biol. Rev.* 63:570–620.
497. Simon G, Walther J, Zabeti N, Combet-Blanc Y, Auria R, van der Oost J, Casalot L. 2009. Effect of O₂ concentrations on *Sulfolobus solfataricus* P2. *FEMS Microbiol. Lett.* 299:255–260. <http://dx.doi.org/10.1111/j.1574-6968.2009.01759.x>.
498. Hochstein LI, Stan-Lotter H. 1992. Purification and properties of an ATPase from *Sulfolobus solfataricus*. *Arch. Biochem. Biophys.* 295:153–160. [http://dx.doi.org/10.1016/0003-9861\(92\)90501-M](http://dx.doi.org/10.1016/0003-9861(92)90501-M).
499. Albers SV, Elferink MG, Charlebois RL, Sensen CW, Driessens AJ, Konings WN. 1999. Glucose transport in the extremely thermoacidophilic Sulfolobus solfataricus involves a high-affinity membrane-integrated binding protein. *J. Bacteriol.* 181:4285–4291.
500. Elferink MG, Albers SV, Konings WN, Driessens AJ. 2001. Sugar transport in *Sulfolobus solfataricus* is mediated by two families of binding protein-dependent ABC transporters. *Mol. Microbiol.* 39:1494–1503. <http://dx.doi.org/10.1046/j.1365-2958.2001.02336.x>.
501. Lalithambika S, Peterson L, Dana K, Blum P. 2012. Carbohydrate hydrolysis and transport in the extreme thermoacidophile *Sulfolobus solfataricus*. *Appl. Environ. Microbiol.* 78:7931–7938. <http://dx.doi.org/10.1128/AEM.01758-12>.
502. Zaparty M, Esser D, Gertig S, Haferkamp P, Kouril T, Manica A, Pham TK, Reimann J, Schreiber K, Sierociński P, Teichmann D, van Wolferen M, von Jan M, Wieloch P, Albers SV, Driessens AJM, Klenk HP, Schleper C, Schomburg D, van der Oost J, Wright PC, Siebers B. 2010. “Hot standards” for the thermoacidophilic archaeon *Sulfolobus solfataricus*. *Extremophiles* 14:119–142.
503. Fleming TM, Jones CE, Piper PW, Cowan DA, Isupov MN, Littlechild JA. 1998. Characterization, crystallization and preliminary X-ray investigation of glyceraldehyde-3-phosphate dehydrogenase from the hyperthermophilic archaeon *Sulfolobus solfataricus*. *Acta Crystallogr. D Biol. Crystallogr.* 54:671–674. <http://dx.doi.org/10.1107/S090744997018076>.
504. Moll R, Schäfer G. 1988. Chemiosmotic H⁺ cycling across the

- plasma membrane of the thermoacidophilic archaeabacterium *Sulfolobus acidocaldarius*. FEBS Lett. 232:359–363. [http://dx.doi.org/10.1016/0014-5793\(88\)80769-5](http://dx.doi.org/10.1016/0014-5793(88)80769-5).
505. Snijders APL, Walther J, Peter S, Kinnman I, De Vos MGJ, Van De Werken HJG, Brouns SJ, Van Der Oost J, Wright PC. 2006. Reconstruction of central carbon metabolism in *Sulfolobus solfataricus* using a two-dimensional gel electrophoresis map, stable isotope labelling and DNA microarray analysis. Proteomics 6:1518–1529. <http://dx.doi.org/10.1002/pmic.200402070>.
 506. Kort JC, Esser D, Pham TK, Noirel J, Wright PC, Siebers B. 2013. A cool tool for hot and sour Archaea: proteomics of *Sulfolobus solfataricus*. Proteomics 13(18–19):2831–2850. <http://dx.doi.org/10.1002/pmic.201300088>.
 507. Peeters E, Charlier D. 2010. The Lrp family of transcription regulators in archaea. Archaea 2010:750457. <http://dx.doi.org/10.1155/2010/750457>.
 508. Peeters E, Thia-Toong TL, Gigot D, Maes D, Charlier D. 2004. Ss-LrpB, a novel Lrp-like regulator of *Sulfolobus solfataricus* P2, binds cooperatively to three conserved targets in its own control region. Mol. Microbiol. 54:321–336. <http://dx.doi.org/10.1111/j.1365-2958.2004.04274.x>.
 509. Peeters E, Albers SV, Vassart A, Driessens AJ, Charlier D. 2009. Ss-LrpB, a transcriptional regulator from *Sulfolobus solfataricus*, regulates a gene cluster with a pyruvate ferredoxin oxidoreductase-encoding operon and permease genes. Mol. Microbiol. 71:972–988. <http://dx.doi.org/10.1111/j.1365-2958.2008.06578.x>.
 510. Schelert J, Dixit V, Hoang V, Simbahan J, Drozda M, Blum P. 2004. Occurrence and characterization of mercury resistance in the hyperthermophilic archaeon *Sulfolobus solfataricus* by use of gene disruption. J. Bacteriol. 186:427–437. <http://dx.doi.org/10.1128/JB.186.2.427-437.2004>.
 511. Brinkman AB, Bell SD, Lebbink RJ, de Vos WM, van der Oost J. 2002. The *Sulfolobus solfataricus* Lrp-like protein LysM regulates lysine biosynthesis in response to lysine availability. J. Biol. Chem. 277:29537–29549. <http://dx.doi.org/10.1074/jbc.M203528200>.
 512. Fiorentino G, Cannio R, Rossi M, Bartolucci S. 2003. Transcriptional regulation of the gene encoding an alcohol dehydrogenase in the archaeon *Sulfolobus solfataricus* involves multiple factors and control elements. J. Bacteriol. 185:3926–3934. <http://dx.doi.org/10.1128/JB.185.13.3926-3934.2003>.
 513. Napoli A, van der Oost J, Sensen CW, Charlebois RL, Rossi M, Ciaramella M. 1999. An Lrp-like protein of the hyperthermophilic archaeon *Sulfolobus solfataricus* which binds to its own promoter. J. Bacteriol. 181:1474–1480.
 514. Bell SD, Jackson SP. 2000. Mechanism of autoregulation by an archaeal transcriptional repressor. J. Biol. Chem. 275:31624–31629. <http://dx.doi.org/10.1074/jbc.M00542200>.
 515. Haseltine C, Montalvo-Rodriguez R, Bini E, Carl A, Blum P. 1999. Coordinate transcriptional control in the hyperthermophilic archaeon *Sulfolobus solfataricus*. J. Bacteriol. 181:3920–3927.
 516. Haseltine C, Montalvo-Rodriguez R, Carl A, Bini E, Blum P. 1999. Extragenic pleiotropic mutations that repress glycosyl hydrolase expression in the hyperthermophilic archaeon *Sulfolobus solfataricus*. Genetics 152:1353–1361.
 517. Haseltine C, Rolfsmeier M, Blum P. 1996. The glucose effect and regulation of alpha-amylase synthesis in the hyperthermophilic archaeon *Sulfolobus solfataricus*. J. Bacteriol. 178:945–950.
 518. Rolfsmeier M, Haseltine C, Bini E, Clark A, Blum P. 1998. Molecular characterization of the alpha-glucosidase gene (*malA*) from the hyperthermophilic archaeon *Sulfolobus solfataricus*. J. Bacteriol. 180:1287–1295.
 519. Bini E, Blum P. 2001. Archaeal catabolite repression: a gene regulatory paradigm. Adv. Appl. Microbiol. 50:339–366. [http://dx.doi.org/10.1016/S0065-2164\(01\)0009-X](http://dx.doi.org/10.1016/S0065-2164(01)0009-X).
 520. Hoang V, Bini E, Dixit V, Drozda M, Blum P. 2004. The role of cis-acting sequences governing catabolite repression control of lacS expression in the archaeon *Sulfolobus solfataricus*. Genetics 167:1563–1572. <http://dx.doi.org/10.1534/genetics.103.024380>.
 521. Worthington P, Hoang V, Perez-Pomares F, Blum P. 2003. Targeted disruption of the alpha-amylase gene in the hyperthermophilic archaeon *Sulfolobus solfataricus*. J. Bacteriol. 185:482–488. <http://dx.doi.org/10.1128/JB.185.2.482-488.2003>.
 522. Lubelska J, Jonascheit M, Schleper C, Albers S-V, Driessens A. 2006. Regulation of expression of the arabinose and glucose transporter genes in the thermophilic archaeon *Sulfolobus solfataricus*. Extremophiles 10:383–391. <http://dx.doi.org/10.1007/s00792-006-0510-7>.
 523. Peng N, Deng L, Mei Y, Jiang D, Hu Y, Awayez M, Liang Y, She Q. 2012. A synthetic arabinose-inducible promoter confers high levels of recombinant protein expression in hyperthermophilic archaeon *Sulfolobus islandicus*. Appl. Environ. Microbiol. 78:5630–5637. <http://dx.doi.org/10.1128/AEM.00855-12>.
 524. Joshua CJ, Dahl R, Benke PI, Keasling JD. 2011. Absence of diauxie during simultaneous utilization of glucose and xylose by *Sulfolobus acidocaldarius*. J. Bacteriol. 193:1293–1301. <http://dx.doi.org/10.1128/JB.01219-10>.
 525. Darland G, Brock TD, Samsonoff W, Conti SF. 1970. A thermophilic, acidophilic mycoplasma isolated from a coal refuse pile. Science 170:1416–1418. <http://dx.doi.org/10.1126/science.170.3965.1416>.
 526. Langworthy TA. 1982. Lipids of *Thermoplasma*. Methods Enzymol. 88:396–406.
 527. Schleper C, Puhler G, Kuhlmann B, Zillig W. 1995. Life at extremely low pH. Nature 375:741–742. <http://dx.doi.org/10.1038/375741b0>.
 528. Schleper C, Puhler G, Holz I, Gambacorta A, Janečković D, Santarius U, Kleink HP, Zillig W. 1995. *Picrophilus* gen. nov., fam. nov.: a novel aerobic, heterotrophic, thermoacidophilic genus and family comprising archaea capable of growth around pH 0. J. Bacteriol. 177:7050–7059.
 529. Smith PF, Langworthy TA, Smith MR. 1975. Polypeptide nature of growth requirement in yeast extract for *Thermoplasma acidophilum*. J. Bacteriol. 124:884–892.
 530. Futterer O, Angelov A, Liesegang H, Gottschalk G, Schleper C, Schepers B, Dock C, Antranikian G, Liebl W. 2004. Genome sequence of *Picrophilus torridus* and its implications for life around pH 0. Proc. Natl. Acad. Sci. U. S. A. 101:9091–9096. <http://dx.doi.org/10.1073/pnas.0401356101>.
 531. Ruepp A, Graml W, Santos-Martinez ML, Korette KK, Volker C, Mewes HW, Frishman D, Stocker S, Lupas AN, Baumeister W. 2000. The genome sequence of the thermoacidophilic scavenger *Thermoplasma acidophilum*. Nature 407:508–513. <http://dx.doi.org/10.1038/35035069>.
 532. Danson MJ. 1989. Central metabolism of the archaeabacteria: an overview. Can. J. Microbiol. 35:58–64. <http://dx.doi.org/10.1139/m89-009>.
 533. Sun N, Pan C, Nickell S, Mann M, Baumeister W, Nagy I. 2010. Quantitative proteome and transcriptome analysis of the archaeon *Thermoplasma acidophilum* cultured under aerobic and anaerobic conditions. J. Proteome Res. 9:4839–4850. <http://dx.doi.org/10.1021/pr100567u>.
 534. Zillig W, Stetter KO, Schaefer W. 1981. *Thermoproteales*: a novel type of extremely thermoacidophilic anaerobic archaeabacteria isolated from Icelandic softwaters. Zentralbl. Bakteriol. Allg. Angew. Okol. Microbiol. Abt. 1 Orig. C Hyg. 2:205–227.
 535. Fischer F, Zillig W, Stetter KO, Schreiber G. 1983. Chemolithoautotrophic metabolism of anaerobic extremely thermophilic archaeabacteria. Nature 301:511–513. <http://dx.doi.org/10.1038/301511a0>.
 536. Huber H, Gallenberger M, Jahn U, Eylert E, Berg IA, Kockelkorn D, Eisenreich W, Fuchs G. 2008. A dicarboxylate/4-hydroxybutyrate autotrophic carbon assimilation cycle in the hyperthermophilic archaeum *Ignicoccus hospitalis*. Proc. Natl. Acad. Sci. U. S. A. 105:7851–7856. <http://dx.doi.org/10.1073/pnas.0801043105>.
 537. Drozdowicz YM, Lu YP, Patel V, Fitz-Gibbon S, Miller JH, Rea PA. 1999. A thermostable vacuolar-type membrane pyrophosphatase from the archaeon *Pyrobaculum aerophilum*: implications for the origins of pyrophosphate-energized pumps. FEBS Lett. 460:505–512. [http://dx.doi.org/10.1016/S0014-5793\(99\)01404-0](http://dx.doi.org/10.1016/S0014-5793(99)01404-0).
 538. Drozdowicz YM, Rea PA. 2001. Vacuolar H⁺ pyrophosphatases: from the evolutionary backwaters into the mainstream. Trends Plant Sci. 6:206–211. [http://dx.doi.org/10.1016/S1360-1385\(01\)01923-9](http://dx.doi.org/10.1016/S1360-1385(01)01923-9).
 539. Hensel R, Laumann S, Lang J, Heumann H, Lottspeich F. 1987. Characterization of two D-glyceraldehyde-3-phosphate dehydrogenases from the extremely thermophilic archaeabacterium *Thermoproteus tenax*. Eur. J. Biochem. 170:325–333. <http://dx.doi.org/10.1111/j.1432-1033.1987.tb13703.x>.
 540. König H, Skorko R, Zillig W, Reiter W-D. 1982. Glycogen in thermoacidophilic archaeabacteria of the genera *Sulfolobus*, *Thermoproteus*, *Desulfurococcus* and *Thermococcus*. Arch. Microbiol. 132:297–303. <http://dx.doi.org/10.1007/BF00413378>.
 541. Bernick DL, Dennis PP, Lui LM, Lowe TM. 2012. Diversity of antisense and other non-coding RNAs in archaea revealed by comparative small RNA sequencing in four *Pyrobaculum* species. Front. Microbiol. 3:231. <http://dx.doi.org/10.3389/fmicb.2012.00231>.
 542. Garrity G, Holt J. 2001. Phylum AII. Euryarchaeota ph. nov, p 211–

355. In Boone D, Castenholz R (ed), Bergey's manual of systematic bacteriology. Springer, New York, NY.
543. Oren A, Arahal DR, Ventosa A. 2009. Emended descriptions of genera of the family *Halobacteriaceae*. Int. J. Syst. Evol. Microbiol. 59:637–642. <http://dx.doi.org/10.1099/ij.s.0.008904-0>.
544. Kamekura M. 1998. Diversity of extremely halophilic bacteria. Extremophiles 2:289–295. <http://dx.doi.org/10.1007/s007920050071>.
545. Mullakhambai MF, Larsen H. 1975. *Halobacterium volcanii* spec. nov., a Dead Sea halobacterium with a moderate salt requirement. Arch. Microbiol. 104:207–214. <http://dx.doi.org/10.1007/BF00447326>.
546. Torreblanca M, Rodriguez-Valera F, Juez G, Ventosa A, Kamekura M, Kates M. 1986. Classification of non-alkaliphilic halobacteria based on numerical taxonomy and polar lipid composition, and description of *Haloarcula* gen. nov. and *Haloferax* gen. nov. Syst. Appl. Microbiol. 8:89–99. [http://dx.doi.org/10.1016/S0723-2020\(86\)80155-2](http://dx.doi.org/10.1016/S0723-2020(86)80155-2).
547. Oren A, Ginzburg M, Ginzburg BZ, Hochstein LI, Volcani BE. 1990. *Haloarcula marismortui* (Volcani) sp. nov., nom. rev., an extremely halophilic bacterium from the Dead Sea. Int. J. Syst. Bacteriol. 40:209–210. <http://dx.doi.org/10.1099/00207713-40-2-209>.
548. Hartman AL, Norais C, Badger JH, Delmas S, Haldenby S, Madupu R, Robinson J, Khouri H, Ren Q, Lowe TM, Maupin-Furlow J, Pohlschroder M, Daniels C, Pfeiffer F, Allers T, Eisen JA. 2010. The complete genome sequence of *Haloferax volcanii* DS2, a model archaeon. PLoS One 5:e9605. <http://dx.doi.org/10.1371/journal.pone.0009605>.
549. Baliga NS, Bonneau R, Facciotti MT, Pan M, Glusman G, Deutsch EW, Shannon P, Chiu Y, Weng RS, Gan RR, Hung P, Date SV, Marcotte E, Hood L, Ng WV. 2004. Genome sequence of *Haloarcula marismortui*: a halophilic archaeon from the Dead Sea. Genome Res. 14:2221–2234. <http://dx.doi.org/10.1101/gr.2700304>.
550. Allers T, Ngo HP, Mevarech M, Lloyd RG. 2004. Development of additional selectable markers for the halophilic archaeon *Haloferax volcanii* based on the leuB and trpA genes. Appl. Environ. Microbiol. 70: 943–953. <http://dx.doi.org/10.1128/AEM.70.2.943-953.2004>.
551. Bitan-Banin G, Ortenberg R, Mevarech M. 2003. Development of a gene knockout system for the halophilic archaeon *Haloferax volcanii* by use of the pyrE gene. J. Bacteriol. 185:772–778. <http://dx.doi.org/10.1128/JB.185.3.772-778.2003>.
552. Tarawa E, Kamo N. 1991. Glucose transport of *Haloferax volcanii* requires the Na⁺-electrochemical potential gradient and inhibitors for the mammalian glucose transporter inhibit the transport. Biochim. Biophys. Acta 1070:293–299. [http://dx.doi.org/10.1016/0005-2736\(91\)90069-K](http://dx.doi.org/10.1016/0005-2736(91)90069-K).
553. Zaigler A, Schuster SC, Soppa J. 2003. Construction and usage of a one-fold-coverage shotgun DNA microarray to characterize the metabolism of the archaeon *Haloferax volcanii*. Mol. Microbiol. 48:1089–1105. <http://dx.doi.org/10.1046/j.1365-2958.2003.03497.x>.
554. Wanner C, Soppa J. 1999. Genetic identification of three ABC transporters as essential elements for nitrate respiration in *Haloferax volcanii*. Genetics 152:1417–1428.
555. Comas I, Gonzalez-Candelas F, Zuniga M. 2008. Unraveling the evolutionary history of the phosphoryl-transfer chain of the phosphoenol-pyruvate:phosphotransferase system through phylogenetic analyses and genome context. BMC Evol. Biol. 8:147. <http://dx.doi.org/10.1186/1471-2148-8-147>.
556. Rawls KS, Yacovone SK, Maupin-Furlow JA. 2010. GlpR represses fructose and glucose metabolic enzymes at the level of transcription in the haloarchaeon *Haloferax volcanii*. J. Bacteriol. 192:6251–6260. <http://dx.doi.org/10.1128/JB.00827-10>.
557. Sherwood KE, Cano DJ, Maupin-Furlow JA. 2009. Glycerol-mediated repression of glucose metabolism and glycerol kinase as the sole route of glycerol catabolism in the haloarchaeon *Haloferax volcanii*. J. Bacteriol. 191:4307–4315. <http://dx.doi.org/10.1128/JB.00131-09>.
558. Elevi Bardavid R, Khristo P, Oren A. 2008. Interrelationships between *Dunalillales* and halophilic prokaryotes in saltern crystallizer ponds. Extremophiles 12:5–14. <http://dx.doi.org/10.1007/s00792-006-0053-y>.
559. Pfeiffer F, Schuster SC, Broicher A, Falb M, Palm P, Rodewald K, Ruepp A, Soppa J, Tittor J, Oesterhelt D. 2008. Evolution in the laboratory: the genome of *Halobacterium salinarum* strain R1 compared to that of strain NRC-1. Genomics 91:335–346. <http://dx.doi.org/10.1016/j.genbo.2008.01.001>.
560. Peck RF, DasSarma S, Krebs MP. 2000. Homologous gene knockout in the archaeon *Halobacterium salinarum* with ura3 as a counterselectable marker. Mol. Microbiol. 35:667–676. <http://dx.doi.org/10.1046/j.1365-2958.2000.01739.x>.
561. Oren A. 2002. Molecular ecology of extremely halophilic archaea and bacteria. FEMS Microbiol. Ecol. 39:1–7. <http://dx.doi.org/10.1111/j.1574-6941.2002.tb00900.x>.
562. Gochnauer MB, Kushner DJ. 1969. Growth and nutrition of extremely halophilic bacteria. Can. J. Microbiol. 15:1157–1165. <http://dx.doi.org/10.1139/m69-211>.
563. Ferry JG. 2010. How to make a living by exhaling methane. Annu. Rev. Microbiol. 64:453–473. <http://dx.doi.org/10.1146/annurev.micro.112408.134051>.
564. Ferry JG. 2011. Fundamentals of methanogenic pathways that are key to the biomethanation of complex biomass. Curr. Opin. Biotechnol. 22: 351–357. <http://dx.doi.org/10.1016/j.copbio.2011.04.011>.
565. Thauer RK, Kaster AK, Seedorf H, Buckel W, Hedderich R. 2008. Methanogenic archaea: ecologically relevant differences in energy conservation. Nat. Rev. Microbiol. 6:579–591. <http://dx.doi.org/10.1038/nrmicro1931>.
566. König H, Nusser E, Stetter KO. 1985. Glycogen in *Methanolobus* and *Methanococcus*. FEMS Microbiol. Lett. 28:265–269. <http://dx.doi.org/10.1111/j.1574-6968.1985.tb00803.x>.
567. Jones WJ, Paynter MJB, Gupta R. 1983. Characterization of *Methanococcus maripaludis* sp. nov., a new methanogen isolated from salt marsh sediment. Arch. Microbiol. 135:91–97. <http://dx.doi.org/10.1007/BF00408015>.
568. Hendrickson EL, Kaul R, Zhou Y, Bovee D, Chapman P, Chung J, Conway de Macario E, Dodsworth JA, Gillett W, Graham DE, Hackett M, Haydock AK, Kang A, Land ML, Levy R, Lie TJ, Major TA, Moore BC, Porat I, Palmeira A, Rouse G, Saenphimmachak C, Soll D, Van Dien S, Wang T, Whitman WB, Xia Q, Zhang Y, Larimer FW, Olson MV, Leigh JA. 2004. Complete genome sequence of the genetically tractable hydrog-enotrophic methanogen *Methanococcus maripaludis*. J. Bacteriol. 186: 6956–6969. <http://dx.doi.org/10.1128/JB.186.20.6956-6969.2004>.
569. Porat I, Kim W, Hendrickson EL, Xia Q, Zhang Y, Wang T, Taub F, Moore BC, Anderson IJ, Hackett M, Leigh JA, Whitman WB. 2006. Disruption of the operon encoding Ehb hydrogenase limits anabolic CO₂ assimilation in the archaeon *Methanococcus maripaludis*. J. Bacteriol. 188: 1373–1380. <http://dx.doi.org/10.1128/JB.188.4.1373-1380.2006>.
570. Moore BC, Leigh JA. 2005. Markerless mutagenesis in *Methanococcus maripaludis* demonstrates roles for alanine dehydrogenase, alanine racemase, and alanine permease. J. Bacteriol. 187:972–979. <http://dx.doi.org/10.1128/JB.187.3.972-979.2005>.
571. Shieh JS, Whitman WB. 1987. Pathway of acetate assimilation in autotrophic and heterotrophic methanococci. J. Bacteriol. 169:5327–5329.
572. Lin WC, Yang YL, Whitman WB. 2003. The anabolic pyruvate oxidoreductase from *Methanococcus maripaludis*. Arch. Microbiol. 179: 444–456. <http://dx.doi.org/10.1007/s00203-003-0554-3>.
573. Lin W, Whitman WB. 2004. The importance of porE and porF in the anabolic pyruvate oxidoreductase of *Methanococcus maripaludis*. Arch. Microbiol. 181:68–73. <http://dx.doi.org/10.1007/s00203-003-0629-1>.
574. Lingl A, Huber H, Stetter KO, Mayer F, Kellermann J, Muller V. 2003. Isolation of a complete A1AO ATP synthase comprising nine subunits from the hyperthermophile *Methanococcus jannaschii*. Extremophiles 7:249–257. <http://dx.doi.org/10.1007/s00792-003-0318-7>.
575. Grochowski LL, Xu H, White RH. 2006. Identification of lactaldehyde dehydrogenase in *Methanocaldococcus jannaschii* and its involvement in production of lactate for F420 biosynthesis. J. Bacteriol. 188:2836–2844. <http://dx.doi.org/10.1128/JB.188.8.2836-2844.2006>.
576. Davlieva M, Shamoo Y. 2010. Crystal structure of a trimeric archaeal adenylate kinase from the mesophile *Methanococcus maripaludis* with an unusually broad functional range and thermal stability. Proteins 78:357–364. <http://dx.doi.org/10.1002/prot.22549>.
577. Stolyar S, Van Dien S, Hillesland KL, Pinel N, Lie TJ, Leigh JA, Stahl DA. 2007. Metabolic modeling of a mutualistic microbial community. Mol. Syst. Biol. 3:92. <http://dx.doi.org/10.1038/msb4100131>.
578. Costa KC, Yoon SH, Pan M, Burn JA, Baliga NS, Leigh JA. 2013. Effects of H₂ and formate on growth yield and regulation of methanogenesis in *Methanococcus maripaludis*. J. Bacteriol. 195:1456–1462. <http://dx.doi.org/10.1128/JB.02141-12>.
579. Hines JK, Fromm HJ, Honzatko RB. 2007. Structures of activated fructose-1,6-bisphosphatase from *Escherichia coli*: coordinate regulation of bacterial metabolism and the conservation of the r-state. J. Biol. Chem. 282:11696–11704. <http://dx.doi.org/10.1074/jbc.M611104200>.
580. Costa KC, Lie TJ, Jacobs MA, Leigh JA. 2013. H₂-independent growth of the hydrogenotrophic methanogen *Methanococcus maripaludis*. mBio 4(2):e00062–13. <http://dx.doi.org/10.1128/mBio.00062-13>.